AD-787 656

TAKEOFF AND LANDING ANALYSIS (TOLA) COMPUTER PROGRAM. PART II. PROBLEM FORMULATION.

Urban H. D. Lynch, et al

Air Force Flight Dynamics Laboratory
Wright-Patterson Air Force Base, Ohio

May 1974

DISTRIBUTED BY:

NTIS
National Technical Information Service
U. S. DEPARTMENT OF COMMERCE

NOTICE

When Government drawings, specifications, or other data are used for any purpose other than in connection with a definitely related Government procurement operation, the United States Government thereby incurs no responsibility nor any obligation whatsoever; and the fact that the government may have formulated, furnished, or in any way supplied the said drawings, specifications, or other data, is not to be regarded by implication or otherwise as in any manner licensing the holder or any other person or corporation, or conveying any rights or permission to manufacture, use, or sell any patented invention that may in any way be related thereto.

ACCESSION for
NTIS White Section
DDC Buff Section
UNANNOUNCED
JUSTIFICATION
BY
DISTRIBUTION/AVAILABILITY CODES
Dist. AVAIL. and/or SPECIAL

Copies of this report should not be returned unless return is required by security considerations, contractual obligations, or notice on a specific document.

AIR FORCE/56780/16 September 1974 — 200

AFFDL-TR-71-155
Part II

TAKEOFF AND LANDING ANALYSIS (TOLA) COMPUTER PROGRAM

Part II. Problem Formulation

Urban H. D. Lynch, Major, USAF

John J. Dueweke

Approved for public release; distribution unlimited.

FOREWORD

This report was prepared by personnel of the Flight Mechanics Division, Air Force Flight Dynamics Laboratory, and the Digital Computation Division, Aeronautical Systems Division. The report was prepared under Project 1431, "Flight Path Analysis," Task 143109, "Trajectory and Motion Analysis of Flight Vehicles." The formulation and interim documentation were completed by Major Urban H. D. Lynch. Programming was accomplished by Mr. Fay O. Young of the Digital Computation Division (ASVCP) of the Aeronautical Systems Division Computer Science Center (ASV). This report, prepared by Mr. John J. Dueweke of the High Speed Aero Performance Branch (FXG), combines the applicable portions of FDL-TDR-64-1, Part I, Volume 1, with the interim documentation prepared by Major Lynch.

This report is divided into four parts:

Part I: Capabilities of the Takeoff and Landing Analysis Computer Program

Part II: Problem Formulation

Part III: User's Manual

Part IV: Programmer's Manual

This document was submitted by the authors September 1971.

This report has been reviewed and is approved.

Philip P. Antonatos

PHILIP P. ANTONATOS
Chief, Flight Mechanics Division
Air Force Flight Dynamics Laboratory

ABSTRACT

A well-defined integration of the various aspects of the aircraft takeoff and landing problem is presented in the form of a generalized computer program. Total aircraft system performance is evaluated during the glide slope, flare, landing roll, and takeoff.

The flight dynamics of a generalized, rigid body, aerospace vehicle are formulated in six degrees of freedom; a flat, nonrotating Earth is assumed. The independent equations of motion of up to five oleo-type landing gears are also formulated.

A control management formulation is developed to automatically adjust control variables to correct errors in the vehicle's dynamic state. Stability in the small is used to maintain stability in the large.

The equations of motion are integrated using a generalized variable-step Runge-Kutta technique.

The formulation is programmed for the CDC 6000 and Cyber 70 Computer Systems. The program is programmed in Fortran Extended using the Scope 3.4 operating system.

TABLE OF CONTENTS

SECTION		PAGE
I	INTRODUCTION	1
II	TAKEOFF AND LANDING ANALYSIS COMPUTER PROGRAM	3
	1. Original SDF-2 Formulation	3
	2. Landing Gear and Ground Reaction Formulation	3
	3. Control Management Formulation	6
	a. Maneuver Logic	6
	b. Autopilots	8
	c. Control Variable Response	9
	d. Summary	9
III	SUMMARY AND DISCUSSION	10
APPENDIX I	- ORIGINAL SDF-2 EQUATIONS	15
APPENDIX II	- LANDING GEAR EQUATIONS	70
APPENDIX III	- CONTROL MANAGEMENT EQUATIONS	143
REFERENCES		223

Preceding page blank

LIST OF ILLUSTRATIONS

FIGURE		PAGE
1.	SDF-2 Summary	4
2.	Landing Gear Summary	7
3.	Control Management Formulation Summary	9
4.	Takeoff and Landing Analysis	11
5.	Dynamics Summary	12
6.	Generalized Inertial and Body-Axes Coordinate Systems	16
7.	Unit Sphere for Yaw-Pitch-Roll Sequence of Rotation	34
8.	Unit Sphere for Pitch-Yaw-Roll Sequence of Rotation	36
9.	Unit Sphere for Pitch-Roll Yaw Sequence of Rotation	38
10.	Functional Flow Diagram - Platform Angles for Six-Degree-of-Freedom Flat-Planet Option	43
11.	Accelerometer With Sensitive Axis Aligned With Local-Geocentric Vertical	44
12.	Curve Fit Nonlinear Aerodynamic Characteristics	48
13.	Solution of Aerodynamic Forces and Moments Subprogram	49
14.	Thrust Forces and Moments Subprogram	51
15.	Vehicle Physical Characteristics Subprogram	53
16.	Functional Flow Diagram - Wind-Aloft Subprogram	63
17.	Drag Chute Forces and Moments	69
18.	SDF-2 Coordinate Systems	72
19.	Strut Configuration	73
20.	Coordinate Systems	77
21.	Strut Coordinate System	79
22.	Runway Coordinate System	85
23.	Strut Displacements	86

LIST OF ILLUSTRATIONS (Contd)

FIGURE		PAGE
24.	Orifice Drag	91
25.	Ground Reaction Forces	101
26.	Autopilot - SDF-2 Interface	145
27.	Glide Slope Geometry	147
28.	Vertical Plane Glide Slope	148
29.	Horizontal Plane Glide Slope	149
30.	Nominal Forces in Glide Slope	152
31.	Glide Slope Logic	158
32.	Flare Coordinate System	162
33.	Flare Forces	168
34.	Flare Logic	170
35.	Hold-Decrab Logic	175
36.	Landing Roll Logic	177
37.	Takeoff Roll Logic	178
38.	Problem Phase Logic	179
39.	Engine Failure Logic	181
40.	Brake Failure Logic	182
41.	Pitch Autopilot Logic	186
42.	Yaw Autopilot Logic	190
43.	Roll Autopilot Logic	192
44.	Number of Engines Logic	193
45.	Single-Engine Logic	195
46.	Common-Engine Logic	197
47.	Function ENGREV	198

LIST OF ILLUSTRATIONS (Contd)

FIGURE		PAGE
48.	Two-Engine Logic	200
49.	Common Two-Engine Logic	202
50.	Fixed Three-Engine Logic	204
51.	Three-Engine Logic	205
52.	Fixed Four-Engine Logic	207
53.	Four-Engine Logic	208
54.	Brake Autopilot	213
55.	Control Response	218
56.	Problem Organization	222

LIST OF SYMBOLS

$\bar{A}$	Vector sum of platform accelerometer outputs; $\ddot{\bar{R}} - \bar{g}$
A_{GF}	An aerodynamic coefficient for full ground effect
A_{hG}	An aerodynamic coefficient at altitude at h_G
A_{hR}	Flare acceleration required normal to runway - ft/sec^2
A_k	Main piston area of kth strut - ft^2
A_{k2}	Secondary piston area in k^{th} strut - ft^2
A_{Pk}	Footprint area for one tire on k^{th} strut - ft^2
A_{X_p}, A_{Y_p}, A_{Z_p}	Inertial axes components of the vector $\bar{A}$ - ft/sec^2
A_{xR}	Flare acceleration required parallel to runway - ft/sec^2
A_o	An aerodynamic coefficient for no ground effect
a	Body axes system aerodynamic axial force, in the $(-\bar{1}_x)$ direction
a_k	Component in the negative $\bar{1}_{zk}$ direction of the vector difference between the inertial acceleration of the kth strut mass center and its gravitational acceleration; $(\ddot{\bar{R}}_{kc} - \bar{g}) \cdot (-\bar{1}_{zk})$ - ft/sec^2
a_x, a_y, a_z	Body axes components of the vector $\bar{A}$ - ft/sec^2
b	Wing span - ft
C	Coefficient of proportionality between an orifice drag force and the square of the piston speed relative to the orifice - lb - sec^2/ft^2
C_A	Aerodynamic axial force coefficient (body axes system)

LIST OF SYMBOLS (Contd)

C_{A_α}	$\partial C_A/\partial\alpha$ - per degree
$C_{A_{\alpha^2}}$	$\partial^2 C_A/\partial\alpha^2$ - per degree^2
$C_{A_{\alpha\beta}}$	$\partial^2 C_A/\partial\alpha\partial\beta$ - per degree^2
$C_{A_{\alpha\delta q}}$	$\partial^2 C_A/\partial\alpha\partial\delta q$ - per degree^2
C_{A_β}	$\partial C_A/\partial\beta$ - per degree
$C_{A_{\beta^2}}$	$\partial^2 C_A/\partial\beta^2$ - per degree^2
$C_{A_{\beta\delta q}}$	$\partial^2 C_A/\partial\beta\partial\delta q$ - per degree^2
$C_{A_{\delta q}}$	$\partial C_A/\partial\delta q$ - per degree
$C_{A_{\delta q^2}}$	$\partial^2 C_A/\partial\delta q^2$ - per degree^2
C_{A_o}	C_A at $\alpha = \beta = 0°$
C_D	Aerodynamic drag force coefficient
C_{D_α}	Aerodynamic drag force slope at $\beta = 0°$-per degree
$C_{D_{\alpha^2}}$	Aerodynamic drag force slope at $\beta = 0°$-per degree^2
C_{D_o}	Drag force coefficient for $\alpha = \beta = 0°$
C_{DCH}	Parachute drag coefficient (assumed constant)
C_{DR}	Required drag coefficient in glide slope
C_k	Main orifice coefficient of proportionality for k^{th} strut - lb-sec^2/ft^2
C_{k2}	Secondary orifice coefficient of proportionality for k^{th} strut - lb-sec^2/ft^2
C_{k2L}	Secondary piston linear friction drag coefficient for k^{th} strut - lb-sec^2/ft^2

LIST OF SYMBOLS (Contd)

C_L	Aerodynamic lift force coefficient
C_{L_α}	Aerodynamic lift force slope at $\beta = \delta q = 0^\circ$-per degree
$C_{L_{\alpha^2}}$	Aerodynamic lift force slope at $\beta = \delta q = 0^\circ$-per degree^2
$C_{L_{\delta q}}$	Aerodynamic lift force slope at $\alpha = \beta = 0^\circ$-per degree
$C_{L_{\delta q^2}}$	Aerodynamic lift force slope at $\alpha = \beta = 0^\circ$-per degree^2
C_{L_o}	Lift force coefficient at $\delta = \beta = \delta q = 0^\circ$
C_{LR}	Required lift coefficient in glide slope
C_ℓ	Aerodynamic rolling moment coefficient (body axes system)
C_{ℓ_o}	C_ℓ at $\alpha = \beta = 0^\circ$
C_{ℓ_p}	$\partial C_\ell / \partial (pd_2/2V_a)$ - per radian
C_{ℓ_r}	$\partial C_\ell / \partial (rd_2/2V_a)$ - per radian
$C_{\ell_{r_x}}$	$\partial^2 C_\ell / \partial (rd_2/2V_a)\, \partial x_{CG}$ - per radian per foot
C_{ℓ_α}	$\partial C_\ell / \partial \alpha$ - per degree
$C_{\ell_{\alpha^2}}$	$\partial^2 C_\ell / \partial \alpha^2$ - per degree^2
$C_{\ell_{\alpha\beta}}$	$\partial^2 C_\ell / \partial \alpha \partial \beta$ - per degree^2
$C_{\ell_{\alpha\delta p}}$	$\partial^2 C_\ell / \partial \alpha \partial \delta p$ - per degree^2
C_{ℓ_β}	$\partial C_\ell / \partial \beta$ - per degree
$C_{\ell_{\beta^2}}$	$\partial^2 C_\ell / \partial \beta^2$ - per degree^2
$C_{\ell_{\beta\delta p}}$	$\partial^2 C_\ell / \partial \beta \partial \delta p$ - per degree^2

LIST OF SYMBOLS (Contd)

$C_{\ell_{\delta p}}$	$\partial C_\ell/\partial\delta p$ - per degree
$C_{\ell_{\delta p^2}}$	$\partial^2 C_\ell/\partial\delta p^2$ - per degree^2
C_m	Aerodynamic pitching moment coefficient (body axes system).
C_{m_q}	Aerodynamic coefficient of damping in pitch; $\partial C_m/\partial\ (q\ _1/2V_a)$ - per radian
$C_{m_{q_x}}$	$\partial^2 C_m/\partial(qd_1/2V_a)\partial x_{C.G.}$ - per radian per foot
C_{m_α}	Aerodynamic pitching moment slope at $\beta = \delta q = 0°$-per degree
$C_{m_{\alpha^2}}$	Aerodynamic pitching moment slope at $\beta = \delta q = 0°$-per degree^2
$C_{m_{\dot\alpha}}$	$\partial C_m/\partial(\dot\alpha d_1/2V_a)$ - per radian
$C_{m_{\dot\alpha_x}}$	$\partial^2 C_m/\partial(\dot\alpha d_1/2V_a)\partial x_{C.G.}$ - per radian per foot
$C_{m_{\alpha\beta}}$	$\partial^2 C_m/\partial\alpha\partial\beta$ - per degree^2
$C_{m_{\alpha\delta q}}$	$\partial^2 C_m/\partial\alpha\partial\delta q$ - per degree
C_{m_β}	$\partial C_m/\partial\beta$ - per degree
$C_{m_{\beta^2}}$	$\partial^2 C_m/\partial\beta^2$ - per degree
$C_{m_{\beta\delta q}}$	$\partial^2 C_m/\partial\beta\partial\delta q$ - per degree^2
$C_{m_{\delta q}}$	Aerodynamic pitching moment slope at $\alpha = \beta = 0°$ - per degree
$C_{m_{\delta q^2}}$	Aerodynamic pitching moment slope at $\alpha = \beta = 0°$ - per degree
C_{m_o}	Pitching moment coefficient at $\alpha = \beta = \delta q = 0°$
C_N	Aerodynamic normal force coefficient (body axes system)

UNCLASSIFIED
Security Classification

AD787656

DOCUMENT CONTROL DATA - R & D

(Security classification of title, body of abstract and indexing annotation must be entered when the overall report is classified)

1. ORIGINATING ACTIVITY *(Corporate author)*

Air Force Flight Dynamics Laboratory
Wright-Patterson Air Force Base, Ohio

2a. REPORT SECURITY CLASSIFICATION

UNCLASSIFIED

2b. GROUP

3. REPORT TITLE

TAKEOFF AND LANDING ANALYSIS (TOLA) COMPUTER PROGRAM. PART II. PROBLEM FORMULATION

4. DESCRIPTIVE NOTES *(Type of report and inclusive dates)*

5. AUTHOR(S) *(First name, middle initial, last name)*

Urban H. D. Lynch, Major, USAF
John J. Dueweke

6. REPORT DATE

May 1974

7a. TOTAL NO. OF PAGES

~~272~~ 271

7b. NO. OF REFS

26

8a. CONTRACT OR GRANT NO

b. PROJECT NO 1431

c. Task No. 143109

d.

9a. ORIGINATOR'S REPORT NUMBER(S)

AFFDL-TR-71-155, Part II

9b. OTHER REPORT NO(S) *(Any other numbers that may be assigned this report)*

10. DISTRIBUTION STATEMENT

Approved for public release; distribution unlimited.

11. SUPPLEMENTARY NOTES

12. SPONSORING MILITARY ACTIVITY

Air Force Flight Dynamics Laboratory
Air Force Systems Command
Wright-Patterson Air Force Base, Ohio

13. ABSTRACT

A well-defined integration of the various aspects of the aircraft takeoff and landing problem is presented in the form of a generalized computer program. Total aircraft system performance is evaluated during the glide slope, flare, landing roll, and takeoff.

The flight dynamics of a generalized, rigid body, aerospace vehicle are formulated in six degrees of freedom; a flat, nonrotating Earth is assumed. The independent equations of motion of up to five oleo-type landing gears are also formulated.

A control management formulation is developed to automatically adjust control variables to correct errors in the vehicle's dynamic state. Stability in the small is used to maintain stability in the large.

The equations of motion are integrated using a generalized variable-step Runge-Kutta technique.

The formulation is programmed for both the IBM 7094/7044 II Direct Couple Computer System in the FORTRAN IV Computer Language and the CDC 6400/6500/6600 SCOPE 3.3 Computer System in the FORTRAN EXTENDED Computer Language.

271

DD FORM 1473

UNCLASSIFIED
Security Classification

Reproduced by
NATIONAL TECHNICAL
INFORMATION SERVICE
U S Department of Commerce
Springfield VA 22151

UNCLASSIFIED
Security Classification

14 KEY WORDS	LINK A ROLE	LINK A WT	LINK B ROLE	LINK B WT	LINK C ROLE	LINK C WT
Takeoff and Landing Analysis						
Computer Program						
Glide Slope						
Flare						
Landing Roll						
Takeoff Roll						
Landing Gear Loads and Dynamics						
Vehicle Control						

UNCLASSIFIED
Security Classification

*U.S.Government Printing Office: 1974 - 657-013/65

LIST OF SYMBOLS (Contd)

C_{N_q}	$\partial C_N/\partial(qd_1/2V_a)$ - per radian
$C_{N_{q_x}}$	$\partial^2 C_N/\partial(qd_1/2V_a)\partial x_{C.G.}$ - per radian per foot
C_{N_α}	$\partial C_N/\partial\alpha$ - per degree
$C_{N_{\alpha^2}}$	$\partial^2 C_N/\partial\alpha^2$ - per degree^2
$C_{N_{\dot\alpha}}$	$\partial C_N/\partial(\dot\alpha d_1/2V_a)$ - per radian
$C_{N_{\dot\alpha_x}}$	$\partial^2 C_N/\partial(\dot\alpha d_1/2V_a)\partial x_{C.G.}$ - per radian per foot
$C_{N_{\alpha\beta}}$	$\partial^2 C_N/\partial\alpha\partial\beta$ - per degree^2
$C_{N_{\alpha\delta q}}$	$\partial^2 C_N/\partial\alpha\partial\delta q$ - per degree^2
C_{N_β}	$\partial C_N/\partial\beta$ - per degree
$C_{N_{\beta^2}}$	$\partial^2 C_N/\partial\beta^2$ - per degree^2
$C_{N_{\beta\delta q}}$	$\partial^2 C_N/\partial\beta\partial\delta q$ - per degree^2
$C_{N_{\delta q}}$	$\partial C_N/\partial\delta q$ - per degree
$C_{N_{\delta q^2}}$	$\partial^2 C_N/\partial\delta q^2$ - per degree^2
C_{N_o}	C_N at $\alpha = \beta = 0°$
C_n	Aerodynamic yawing moment coefficient (body axes system)
C_{n_r}	$\partial C_n/\partial(rd_2/2V_a)$ - per radian
$C_{n_{r_x}}$	$\partial^2 C_n/\partial(rd_2/2V_a)\partial x_{C.G.}$ - per radian per foot
C_{n_α}	$\partial C_n/\partial\alpha$ - per degree
$C_{n_{\alpha^2}}$	$\partial^2 C_n/\partial\alpha^2$ - per degree^2
$C_{n_{\alpha\beta}}$	$\partial^2 C_n/\partial\alpha\partial\beta$ - per degree^2

LIST OF SYMBOLS (Contd)

$C_{n_{\alpha\delta r}}$	$\partial^2 C_n/\partial\alpha\partial\delta r$ - per degree^2
C_{n_β}	Aerodynamic yawing moment slope at $\alpha = \delta r = 0°$ - per degree
$C_{n_{\beta^2}}$	Aerodynamic yawing moment slope at $\alpha = \delta r = 0°$ - per degree^2
C_{n_β}	$\partial C_n/\partial(\beta d_2/2V_a)$ - per radian
$C_{n_{\beta_x}}$	$\partial^2 C_n/\partial(\beta d_2/2V_a)\partial x_{C.G.}$ - per radian per foot
$C_{n_{\beta\delta r}}$	$\partial^2 C_n/\partial\beta\partial\delta r$ - per degree^2
$C_{n_{\delta r}}$	Aerodynamic yawing moment slope at $\alpha = \beta = 0°$ - per degree
$C_{n_{\delta r^2}}$	Aerodynamic yawing moment slope at $\alpha = \beta = 0°$ - per degree^2
C_{n_o}	C_n at $\alpha = \beta = 0°$
C_p	Specific heat at constant pressure - BTU/(lb - °R)
C_v	Specific heat at constant volume - BTU/(lb - °R)
C_y	Aerodynamic force coefficient (body axes system)
C_{y_r}	$\partial C_y/\partial(rd_2/2V_a)$ - per radian
$C_{y_{r_x}}$	$\partial^2 C_y/\partial(rd_2/2V_a)\partial x_{C.G.}$ - per radian per foot
C_{y_α}	$\partial C_y/\partial\alpha$ - per degree
$C_{y_{\alpha^2}}$	$\partial^2 C_y/\partial\alpha^2$ - per degree^2
$C_{y_{\alpha\beta}}$	$\partial^2 C_y/\partial\alpha\partial\beta$ - per degree^2
$C_{y_{\alpha\delta r}}$	$\partial^2 C_y/\partial\alpha\partial\delta r$ - per degree^2
C_{y_β}	Aerodynamic side force slope at $\alpha = \delta r = 0°$ - per degree
$C_{y_{\beta^2}}$	Aerodynamic side force slope at $\alpha = \delta r = 0°$ - per degree^2
$C_{y_{\dot\beta}}$	$\partial C_y/\partial(\dot\beta d_2/2V_a)$ - per radian

LIST OF SYMBOLS (Contd)

$C_{y_{\dot{\beta}_x}}$	$\partial^2 C_y/\partial(\dot{\beta}d_2/2V_a)\partial x_{C.G.}$ - per radian per foot
$C_{y_{\beta\delta r}}$	$\partial^2 C_y/\partial\beta\partial\delta r$ - per degree^2
$C_{y_{\delta r}}$	$\partial C_y/\partial\delta r$ - per degree
$C_{y_{\delta r^2}}$	$\partial^2 C_y/\partial\delta r^2$ - per degree^2
C_{y_o}	C_y at $\alpha = \beta = 0°$
$\overline{D}$	Drag force vector
D_a	Increment size in flare α search - degrees
D_m	Increase of touchdown point past x_{TD} - ft
D_R	Required drag force in glide slope - lbs
D_{xk}, D_{yk}, D_{zk}	Runway axes components of the vector $\overline{R}_{rk}$ - ft
d_1	Pitch reference length (usually mean aerodynamic chord) - ft
d_2	Yaw reference length (usually wing span) - ft
E_R	Runway elevation angle - degrees
E_{sk}	Error allowed in integrating s_k around the positions zero and s_{kb} - ft
E_{sk2}	Error allowed in integrating s_{k2} around the positions zero and S_{k2T} - ft
$\overline{F}$	Total applied vector force
F_{ck2}	Secondary piston stop contact force for the kth strut-lbs
F_{cx}, F_{cy}, F_{cz}	Body axes components of the vector $\overline{F}_{DC}$ - lbs
$\overline{F}_{DC}$	Parachute drag force vector
F_{DC}	Magnitude of the vector $\overline{F}_{DC}$ - lbs

LIST OF SYMBOLS (Contd)

F_{dxk}	$\bar{1}_{xk}$ component of the vector $\bar{F}_{TRk}$ - lbs
F_{dyk}	$\bar{1}_{yk}$ component of the vector $\bar{F}_{TRk}$ - lbs
F_{fk}	Friction force at wing gear root for the k strut - lbs
$\bar{F}_{GPk}$	Friction force vector between runway and tires on k^{th} strut - lbs
F_{GPk}	Magnitude of the vector $\bar{F}_{GPk}$ - lbs
$\bar{F}_k$	Total applied vector force on the kth body
$\bar{F}_k$	One of many vector forces applied to the kth strut
$\bar{F}_{kg}$	Gravity force vector acting on k^{th} strut
F_{kgz}	$\bar{1}_{zk}$ component of the vector $\bar{F}_{kg}$ - lbs
F_{kz}	$\bar{1}_{zk}$ component of a vector $\bar{F}_k$ - lbs
$\bar{F}_{k2}$	Applied vector force on secondary piston in k^{th} strut
F_{k2z}	$\bar{1}_{zk}$ component of the vector $\bar{F}_{k2}$ - lbs
$\bar{F}_T$	Total applied vector force to the system of K + 1 bodies, namely the vehicle
F_{Tk}	Ground reaction component along the negative 1_{zk} direction - lbs
$\bar{F}_{TR}$	Total ground reaction vector, summed over all k gears from k = 1 to k = K
F_{TRA}, F_{TRB}, F_{TRC}	Body axes components of the vector $\bar{F}_{TR}$ - lbs
$\bar{F}_{TRk}$	Total ground reaction force vector acting on k^{th} strut
F_{TRxk}	Runway axes component of the vector $\bar{F}_{GPk}$ - lbs
F_{TRyk}	Runway axes component of the vector $\bar{F}_{GPk}$ - lbs
$\bar{F}_{TRzk}$	Ground reaction force vector normal to the runway
F_{TRzk}	Magnitude of the vector $\bar{F}_{TRzk}$ - lbs
F_v	Orifice drag force - lbs

LIST OF SYMBOLS (Contd)

F_x, F_y, F_z	Body axes components of the vector $\overline{F}_T$ - lbs
F_{xm}, F_{ym}, F_{zm}	Body axes components of that portion of total ground reaction force vector, $\overline{F}_{TR}$, which is transmitted to the main airframe - lbs
$f_k(\delta_k)$	Force deflection curve for a single tire on k^{th} strut - lbs/tire
$\overline{g}$	Vector acceleration due to gravity
g	Magnitude of the vector $\bar{g}$; 32.174 ft/sec^2 = 1 "g"
g_x, g_y, g_z	Body axes components of the vector $\bar{g}$ - ft/sec^2
g_{zk}	$\bar{I}_{zk}$ component of the vector $\bar{g}$ - ft/sec
$\overline{H}$	Rigid body angular momentum about mass center
$\overline{H}_{k\oplus}$	Vector moment of linear momentum of kth body about k^{th} body mass center - ft-lb-sec
H_x, H_y, H_z	Body axes components of the vector $\bar{H}$ - ft-lb-sec
h	Altitude of vehicle mass center above runway origin - ft
h_{CG}	Altitude of glide slope origin above runway origin, namely, the height of the CG above the runway at impact - ft
h_e	Vertical glide slope position error - ft
$\dot{h}_e$	Rate of vertical glide slope position error - ft/sec
h_{ea}	Allowed glide slope position error in the vertical plane - ft

LIST OF SYMBOLS (Contd)

h_{eT}	Total vertical glide slope position error - ft
h_F	Flare initiation altitude - ft
h_G	Mass center altitude above ground - ft
h_{GS}	Nominal glide slope altitude - ft
h_{Pa}	Allowed glide slope position error in the horizontal plane - ft
h_{PT}	Total horizontal glide slope position error - ft
h_R	Mass center altitude above and perpendicular to runway, positive upward - ft/sec
$\dot{h}_R$	Mass center altitude rate perpendicular to runway, positive upward - ft/sec
h_{RF}	Mass center altitude normal to runway for touchdown - ft
$\dot{h}_{RF}$	Altitude rate normal to runway for touchdown - ft/sec
h_{R1}	First altitude above runway for sequencing engine conditions in flare - ft
h_{R2}	Second altitude above runway for sequencing engine conditions in flare - ft
h_s	Altitude above runway at which takeoff is terminated - ft
h_{TD}	Initial value of h_{RF} in flare - ft
h_1	First altitude above runway for sequencing engine conditions in glide slope - ft
h_2	Second altitude above runway for sequencing engine conditions in glide slope - ft
$\bar{I}$	Moment of inertia matrix about mass center
I	Indicator for number of gears on aircraft
I_B, $I_B(I)$,	
I_{Bi}	Brake condition indication array
I_{Bk1}	First change in I_B array after impact
I_{Bk2}	Second change in I_B array after impact
I_i, I_k	Moment of inertia of a tire, wheel and anything else constrained to rotate with that tire about the axle on the kth strut - slug-ft^2

LIST OF SYMBOLS (Contd)

I_{xr}, I_{yr}, I_{zr}	Moments of inertia of rotating machinery within the body about machinery axes - slug-ft^2
I_{xx}, I_{yy}, I_{zz}	Moments of Inertia of all aircraft mass about body - fixed axes - slug-ft^2
I_{xy}, I_{xz}, I_{yz}	Products of inertia of all aircraft masses about body - fixed axes - slug-ft^2
IAP	Autopilot phase indicator
K_A, K_B	Thrust fractions for engines A and B in Common Two Engine Logic
KE(IN)	Kill engine indicator array
KKA, KKB	Kill engine indicators for engines A and B in common two engine logic
KP	Impact indicator
KT	Kill engine indicator in Common Engine Logic
k	Polytropic exponent
k	Symbol signifying a given body or strut
$k_{(\ )___x}$	Engine fractional load indicator; the first subscript ( ) indicates the number of engines on the aircraft; the last subscript indicates the engine to which this load indicator applies; the subscipts in between indicate the engines not failed

LIST OF SYMBOLS (Contd)

$k_{(2)121}$	Engine fractional load indicator for engine number 1, 2-engine aircraft, both engines assumed working
$k_{(3)131}$	Engine fractional load indicator for engine number 1, 3-engine aircraft, middle engine failed
$k_{(3)232}$	Engine fractional load indicator for engine number 2, 3-engine aircraft, engine number 1 failed
$k_{(3)121}$	Engine fractional load indicator for engine number 1, 3-engine aircraft, engine number 3 failed
$k_{(3)1231}$	Engine fractional load indicator for engine number 1, 3-engine aircraft, all engines working
$k_{(3)1232}$	Engine fractional load indicator for engine number 2, 3-engine aircraft, all engines working
$k_{(4)141}$	Engine fractional load indicator for engine number 1, 4-engine aircraft, engines 2 and 3 failed (both inboard)
$k_{(4)232}$	Engine fractional load indicator for engine number 2, 4-engine aircraft, engines 1 and 4 failed (both outboard)
$k_{(4)343}$	Engine fractional load indicator for engine number 3, 4-engine aircraft, engines 1 and 2 failed (both on same side)
$k_{(4)242}$	Engine fractional load indicator for engine number 2, 4-engine aircraft, engines 1 and 3 failed (one inboard, opposite outboard)
$k_{(4)2342}$	Engine fractional load indicator engine number 2, 4-engine aircraft, engine 1 failed (one outboard)
$k_{(4)2343}$	Engine fractional load indicator for engine number 3, 4-engine aircraft, engine 1 failed (one outboard)
$k_{(4)1341}$	Engine fractional load indicator for engine number 1, 4-engine aircraft, engine 2 failed (one inboard)
$k_{(4)1343}$	Engine fractional load indicator for engine number 3, 4-engine aircraft, engine 2 failed (one inboard)
$k_{(4)12341}$	Engine fractional load indicator for engine number 1, 4-engine aircraft, all engines working
$k_{(4)12342}$	Engine fractional load indicator for engine number 2, 4-engine aircraft, all engines working
$k_{(4)12343}$	Engine fractional load indicator for engine number 3, 4-engine aircraft, all engines working

LIST OF SYMBOLS (Contd)

$\bar{L}$	Lift Vector
L, M, N	Body axes components of the vector M_o - ft-lbs
L_D	Required landing distance to stop aircraft - ft
L_m, M_m, N_m	Body axes components of that portion of total ground reaction moment vector, $\bar{M}_{TR}$ which is transmitted to the main airframe - ft-lbs
L_R	Required lift force in glide slope - lbs
L_T	Net engine roll moment - ft-lbs
ℓ, m, n	Body axes components of aerodynamic moments - ft lbs
ℓ_ℓ, ℓ_m, ℓ_n	Characteristic distances for jet - damping moments-ft
ℓ_y, ℓ_z	Characteristic distances for jet - damping forces - ft
ℓ_2, m_2, n_2	Direction cosines of the inertial $\bar{i}_{yg}$ unit vector relative to the body axes system

LIST OF SYMBOLS (Contd)

$\dot{l}_2$, $\dot{m}_2$, $\dot{n}_2$	Direction cosine rates of the inertial $\bar{I}_{yg}$ unit vector relative to the body axes system - per second
m	Aircraft mass - slug
m_o	Initial mass of the vehicle - slug
$\bar{M}$	Total applied vector moment
$\bar{M}_{Ak}$	Vector moment of the ground reaction about the kth strut axle
M_{Ai}, M_{Ak}	Magnitude of the vector $\bar{M}_{Ak}$ - ft-lbs
$M_{BCi}, M_{BC}(I)$	Constant braking moment array, the use of which is determined in brake autopilot - ft-lbs
M_{Bi}, M_{Bk}	Braking moment applied along k^{th} strut axle - ft-lbs
$M_{BLi}, M_{BL}(I)$	Braking moment lower limit array - ft-lbs
$M_{BUi}, M_{BU}(I)$	Braking moment upper limit array - ft-lbs
$\bar{M}_{CH}$	Vector moment of the parachute drag force $\bar{F}_{DC}$ about the aircraft mass center
M_{Dx}, M_{Dy}, M_{Dz}	Body axes components of the vector $\bar{M}_{CH}$ - ft-lbs
M_k	Applied moment about k^{th} strut axle - ft-lbs
M_N	Mach number (not V/a_o or V/a^*)
M_T	Net engine pitch moment - ft-lbs
$M_T(IN)$	Engine pitch moment array - ft-lbs

LIST OF SYMBOLS (Contd)

$\bar{M}_{TR}$	Total vector moment of all gear ground reactions about the aircraft mass center
$\bar{M}_{TRk}$	Vector moment of the kth strut ground reaction $\bar{F}_{TRk}$ about the aircraft mass center
M_{TRxk}, M_{TRyk}, M_{TRzk}	Runway axes components of the vector $\bar{M}_{TRk}$ - ft-lbs
M_{Tx}, M_{Ty}, M_{Tz}	Body axes components of the vector $\bar{M}_{TR}$ - ft-lbs
$\bar{M}_o$	Total vector moment about the nominal mass center of all the forces applied to the vehicle
m	Total mass - slugs
m_k	Total mass of kth body - slugs
$\bar{m}_{ko}$	Total vector moment of applied forces to k^{th} body about o^{th} body reference point
m_{k2}	Secondary piston mass in k^{th} strut - slug
m_T	Total mass of K + 1 bodies - slug
N	Throttle setting
$\dot{N}(I)$	Actual throttle setting rate array - per second
$N(IN), N_i$	Actual throttle setting array
N_A, N_B	Actual throttle settings for engines A and B in Common Two Engine Logic
$N_B(IN)$	Engine reverse throttle constraint array

LIST OF SYMBOLS (Contd)

N_{BA}, N_{BB}	Engine reverse throttle constraints for engines A and B in Common Two Engine Logic
N_{BC}	Engine reverse throttle constraint in Common Engine Logic
N_C	Actual throttle setting in Common Engine Logic
$N_d(IN)$, N_{di}	Desired throttle setting array
N_{dA}, N_{dB}	Desired throttle settings for engines A and B in Common Two Engine Logic
N_{dC}	Desired throttle setting in Common Engine Logic
$N_{dF}(IN)$	Fixed throttle setting array
$\dot{N}_E$	Constant engine throttle setting rate magnitude used in control response - per second
N_{fk}	Component of ground reaction normal to axis of ^{ch} strut-pounds
$N_{LR}(IN)$	Landing reverse throttle setting array
N_{LRA}, N_{LRB}	Landing reverse throttle settings for engines A and B in Common Two Engine Logic
N_{LRC}	Landing reverse throttle setting in Common Engine Logic
N_T	Net engine yaw moment - ft-lbs
$N_T(IN)$	Engine yaw moment array - ft-lbs
$N_{TO}(IN)$	Takeoff throttle setting array
N_{TOA}, N_{TOB}	Takeoff throttle settings for engines A and B in Common Two Engine Logic
N_{TOC}	Takeoff throttle settings in Common Engine Logic
NF	No Flare indicator - used to stop program after glide slope

LIST OF SYMBOLS (Contd)

NLRI	No landing roll indicator - used to stop program at impact
n_F	Body axes system aerodynamic normal force, in the $(-\bar{1}_z)$ direction-lbs
n_i, n_k	Number of tires on k^{th} strut axle
P	Pressure - lbs/ft^2
$P(x,y,z)$	A point located by the vector $\bar{\rho}$
P_{Ak}	Air compression force acting on the kth strut - lbs
P_D	Desired "percent skid" - %/(100%) (i.e., nondimensional)
P_k	Upper air chamber pressure - lbs/ft^2
P_{k2}	Lower air chamber pressure - lbs/ft^2
P_m	Landing tail-down constraint angle - maximum pitch angle relative to the runway - degrees
P_{Pk}	Nominal tire foot print pressure - lbs/ft^2
P_{si}, P_{skdk}	Actual "percent skid" - %/(100%) (i.e., nondimensional)
P_{ok}	Preload pressure of upper air chamber - lbs/ft^2
P_{ok2}	Preload pressure of lower air chamber - lbs/ft^2
PG_s	Phugoid control sensitivity - deg/ft
PS_A	Roll (aileron) overcontrol constant - deg/deg
PS_H	Angle of attack overcontrol constant in glide slope - deg/deg
PS_{H2}	Angle of attack overcontrol constant for LAP ≥ 2 -deg/deg
PS_R	Sideslip (rudder) overcontrol constant - deg/deg
PS_ψ	Euler yaw angle overcontrol constant - deg/deg
p, q, r	Body axes components of the vector $\bar{\omega}$ - rad/sec
Q_R	Required dynamic pressure in glide slope - lbs/ft^2

LIST OF SYMBOLS (Contd)

q^*	Dynamic pressure - lbs/ft^2
q_d	Pitch rate in flare based on $\dot{\alpha}_d$ and flare acceleration - rad/sec
$\bar{R}$	Vector displacement of aircraft mass center from origin of the inertial axes system
$\ddot{\bar{R}}$	Inertial acceleration of the platform origin - ft/sec^2
R_{Axk}, R_{Ayk}, R_{Azk}	Inertial axes components of the vector sum $(\bar{R}_k)_o + \bar{r}_k$ - ft
$\bar{R}_{CH}$	Vector displacement of parachute attachment point measured from aircraft mass center
R_{Dxk}, R_{Dyk}, R_{Dzk}	Body axes components of the vector sum $(\dot{\bar{R}}_k)_o + \dot{\bar{r}}_k$ - ft/sec
R_{DXGk}, R_{DYGk}, R_{DZGk}	Inertial axes components of the vector sum $\dot{\bar{R}} - \dot{\bar{R}}_{gR} + (\dot{\bar{R}}_{ko}) + \dot{\bar{r}}_k$, the velocity of the kth strut axle as seen by the runway axes origin - ft/sec
$R_{F\alpha}$	Angle of attack rate feedback constant in glide slope - sec
$R_{F\alpha 2}$	Angle of attack rate feedback constant for IAP $\geq$ 2 - sec
$R_{F\beta}$	Sideslip angle rate feedback constant - sec
$R_{F\phi}$	Euler roll angle rate feedback constant - sec
$R_{F\Psi}$	Euler yaw angle rate feedback constant - sec
R_g	Range from the starting point - nautical miles
$\bar{R}_{gR}$	Displacement vector of runway origin from origin of inertial axes system
R_{gR}	Magnitude of the vector $\bar{R}_{gR}$; the component of the vector $\bar{R}_{gR}$ in the $\bar{I}_{xg}$ direction (there are no other components) - ft

LIST OF SYMBOLS (Contd)

$\bar{R}_{kc}$	Total vector displacement of the kth strut mass center from the origin of the inertial axes system
$\ddot{\bar{R}}_{k2c}$	Inertial vector acceleration of the secondary piston
$(\bar{R}_{ko})$	Vector position of the kth body reference point from the oth body reference point
R_{kx}, R_{ky}, R_{kz}	Body axes components of the vector $(\bar{R}_{ko})$ - ft
R_L	Runway length - ft
$\bar{R}_{Pk}$	Vector displacement from the aircraft mass center to the point of application (i.e., the tire footprint) of the kth strut ground reaction force
$\bar{R}_R$	Vector displacement of the aircraft mass center from the origin of the runway axes system
$\bar{R}_{Rk}$	Vector displacement of the kth strut axle from the origin of the runway axes system
R_{RICGx}, R_{RICGy}, R_{RICGz}	k^{th} strut axes components of the vector sum $(\bar{R}_{ko}) + \bar{r}_{kc}$, the vector displacement of the kth strut mass center from the aircraft mass center
$\dot{\bar{R}}_{Tk}$	Total vector velocity of the bottom surface of the kth strut tires as seen by the origin of the runway axes system
RF_h	Vertical plane glide slope position rate feedback constant - sec
RF_Y	Horizontal plane glide slope position rate feedback constant - sec
$\bar{r}$	Vector displacement of the point P(x,y,z) from the origin of the body - fixed axes system

LIST OF SYMBOLS (Contd)

$\bar{r}_c$	Vector position of mass center of the K + 1 bodies from the oth body reference point
r_{Fk}	Fully extended position of kth strut axle from origin of kth strut axle system - ft
$\bar{r}_k$	Instantaneous vector displacement of kth strut axle from origin of kth strut axes system
$\bar{r}_{kc}$	Vector displacement of kth strut mass center from origin of kth strut axes system
$\bar{r}_{k2c}$	Vector displacement of kth strut secondary piston upper surface from origin of kth strut axes system
r_{oi}, r_{ok}	Undeflected tire outer radius - ft
S	Aircraft reference area - ft^2
S_{Fk}	Sum of the forces resisting the kth strut movement(that portion of the kth strut ground reaction transmitted to the main airframe) - lbs
S_{SH}	Parachute reference area - ft^2
s	A scalar variable
$\ddot{s}$	Constant acceleration of s
s_f	Final value of s
$\dot{s}_f$	Final value of $\dot{s}$
s_i	Initial value of s
$\dot{s}_i$	Initial value of $\dot{s}$
s_k	Displacement of kth strut from fully extended axle position - ft
s_{kb}	Maximum allowable displacement of kth strut - ft
s_{kc}	Distance between k^{th} strut axle and k^{th} strut mass center - ft
s_{k2}	Displacement of kth strut secondary piston from its extension stop - ft
s_{k2e}	Distance between k^{th} strut axle and k^{th} strut secondary piston extension stop - ft

LIST OF SYMBOLS (Contd)

s_{k2STOP}	The kth secondary piston acceleration as seen by the kth axes system which would exist if the secondary piston were against either of its stops (i.e., the value of Equation (58 of Appendix II with Γ_{ck2} removed, used to obtain the stop contact force, F_{ck2})
s_{k2T}	Maximum displacement of kth strut secondary piston (distance between secondary piston compression and extension stops less piston height) - ft
s_{Rk}	$\bar{1}_{zk}$ component of inertial acceleration of kth strut axes system - ft/sec^2
$\bar{T}$	Thrust vector in flare
T	Magnitude of the vector $\bar{T}$ - lbs
T(IN)	Actual thrust array - lbs
T_c	Desired thrust in Common Engine Logic - lbs
$\bar{T}_d$	Desired thrust vector in glide slope
T_d	Desired thrust - lbs
T_d(IN)	Desired thrust array - lbs
T_{dA}, T_{dB}	Desired thrust for engines A and B in Common Two Engine Logic - lbs
T_{dx}	Total thrust required in Common Two Engine Logic - lbs
T_e	Engine thrust obtained from TFFS subprogram - lbs
T_I	Impact time - sec
T_L	Lower thrust limit allowed in flare - lbs
T_s	Time after impact to stop landing roll - sec
T_U	Upper thrust limit allowed in flare - lbs
T_x, T_y, T_z	Body axes components of net thrust vector - lbs

LIST OF SYMBOLS (Contd)

TF(I),TF(IN)	Fixed throttle indicator array
t	Time - sec
t_{bk}	Time after impact to start braking - sec
t_{bk1}	First time after impact to change I_B array - sec
t_{bk2}	Second time after impact to change I_B array - sec
t_{ch}	Time after impact to deploy parachute - sec
t_h	Time required to perform the h_R state change in flare - sec
t_r	Time after impact - sec
t_{rv}	Time after impact to reverse engines - sec
t_{r1}	First time after impact for sequencing engine conditions in landing roll - sec
t_{r2}	Second time after impact for sequencing engine conditions in landing roll - sec
t_s	Elapsed time to perform constant acceleration change from initial state (s_i, $\dot{s}_i$) to final state (s_f, $\dot{s}_f$) of a scalar variable, s - sec
t_{sp}	Time after impact to set spoiler aerodynamics staging indicator - sec
t_{st}	Time after impact at which nose over begins - sec
t_x	Time required to perform the x_R state change in flare - sec
u	Body x-axis component of inertial velocity of aircraft mass center - ft/sec
$\dot{u}$	Body x-axis component of the vector $\dot{\bar{V}}$ - ft/sec^2
u, v, w	Body axes components of the vector $\bar{V}$ - ft/sec
$\dot{u}$, $\dot{v}$, $\dot{w}$	Body axes components of the vector $\dot{\bar{V}}$ - ft/sec^2

LIST OF SYMBOLS (Contd)

u_w	
v_w	Body axes components of the vector $\overline{V}_w$ - ft/sec
w_w	
$\overline{V}$	Inertial velocity vector of mass center (in body fixed axes system)
$\dot{\overline{V}}$	Velocity vector rate as seen from the body fixed axes system
V	Volume - ft^3
$\overline{V}$	Velocity of piston pushing fluid through an orifice
$\overline{V}_a$	Airspeed vector
V_a	Magnitude of the vector $\overline{V}_a$ - ft/sec
$\overline{V}_{ad}$	Desired airspeed vector
V_{ai}, V_{ak}	Component parallel to runway of kth strut axle inertial velocity - ft/sec
V_{aTO}	Airspeed for takeoff - ft/sec
$\overline{V}_d$	Desired inertial vector velocity down the glide slope
V_d	Magnitude of the vector $\overline{V}_d$ - ft/sec
V_e	Inertial velocity magnitude error in glide slope - ft/sec
$\overline{V}_g$	Inertial velocity vector
V_g	Magnitude of the vector $\overline{V}_g$ - ft/sec
$\overline{V}_{GPTk}$	Component parallel to runway of velocity of kth strut tire footprint as seen by the runway coordinate system
V_{hTD}	Initial value of h_{RF} in flare - ft/sec
V_s	Speed parallel to runway to stop landing roll - ft/sec
V_{stall}	Aircraft stall speed - ft/sec

LIST OF SYMBOLS (Contd)

V_{Ti}	Tire footprint velocity of ith wheel - ft/sec
V_{TXk}, V_{TYk}	Runway axes component of the vector $\bar{V}_{GPTk}$ - ft/sec
V_{TXk}, V_{TYk}, V_{TZk}	Runway axes components of the vector $\dot{\bar{R}}_{Tk}$ - ft/sec
$\bar{V}_w$	Wind vector
V_{xTD}	Initial value of $\dot{x}_{RF}$ in flare - ft/sec
V_{ok}	Preload volume of upper air chamber - ft^3
V_{ok2}	Preload volume of lower air chamber - ft^3
VSRK	Variable-step Runge-Kutta(integration technique)
$\bar{W}, \bar{W}_T$	Weight vector
w_k	Width of a tire on the kth strut - ft
X_g, Y_g, Z_g	Inertial axes components of the vector $\bar{R}$ - ft
$\dot{X}_{gw}$, $\dot{Y}_{gw}$, $\dot{Z}_{gw}$	Inertial axes components of the vector $\bar{V}_w$ - ft/sec
X_{go}, Y_{go}	Inertial axes components of the starting point of the vehicle center of mass - ft
X_p, Y_p, Z_p	Components of the vector $\bar{\rho}$ in a platform coordinate system (in this formulation identical to the inertial frame - ft)

LIST OF SYMBOLS (Contd)

X_s	Distance down runway to stop landing roll - ft
x, y, z	Body axes components of the vector $\bar{r}$ - ft
$x_{C.G.}$	Center-of-gravity position from the body axes origin in the 1_x direction - ft
$x_{C.G._{Ref}}$	Reference center-of-gravity position from the body axes origin in the $\bar{1}_x$ direction - ft
X_{CH}, Y_{CH}, Z_{CH}	Body axes components of the vector $\bar{R}_{CH}$ - ft
X_R	Aircraft scalar distance down runway - ft
x_R, y_R, z_R	Runway axes components of the vector $(\bar{R}-\bar{R}_{gR})$ - ft
$\dot{x}_R$, $\dot{y}_R$, $\dot{z}_R$	Runway axes components of vector $(\dot{\bar{R}}-\dot{\bar{R}}_{gR})$ - ft/sec
x_{RF}	Distance down runway for touchdown - ft
$\dot{x}_{RF}$	Landing speed parallel to runway for touchdown - ft/sec
x_{RF1}	First distance down runway for sequencing engine conditions in takeoff roll - ft
x_{RF2}	Second distance down runway for sequencing engine conditions in takeoff roll - ft
x_{Rk}, y_{Rk}, z_{ok}	Runway axes components of the vector $\bar{R}_{Rk}$ - ft

LIST OF SYMBOLS (Contd)

x_{TD}	Initial value of x_{RF} in flare; distance down runway before which the aircraft must not touch down - ft
y	Body axes system aerodynamic side force, in the $\bar{I}_y$ direction - lbs
$y_N(IN)$	Body y-axis component engine position array - ft
$z_N(IN)$	Body z-axis component engine position array - ft

LIST OF SYMBOLS (Contd)

α	Angle of attack - deg
$\dot{\alpha}$	Angle of attack rate - rad/sec
α_d	Desired angle of attack - deg
$\dot{\alpha}_d$	Desired angle of attack rate - deg/sec
α_{d-1}	Preceding value of desired angle of attack - deg
$\dot{\alpha}_{d_{max}}$	Maximum allowed value of $\dot{\alpha}_d$ - deg/sec
α_{dL}	Upper limit on angle of attack - deg
α_{dS}	Lower limit on angle of attack - deg
α_e	Angle of attack position error - deg
α_{eT}	Total angle of attack error - deg
α_{Re}	Angle of attack rate error - deg/sec
α_{TO}	Angle of attack for takeoff - deg
β	Sideslip angle - deg
$\dot{\beta}$	Sideslip angle rate - rad/sec
β_d	Desired sideslip angle - deg
β_e	Sideslip angle position error - deg
β_{eT}	Total sideslip angle error - deg
γ	Elevation angle of $\bar{V}_g$ relative to Earth; flight path angle - deg
γ_a	Elevation angle of $\bar{V}_a$ relative to earth - deg
$\gamma_{a'}$	Elevation angle of $\bar{V}_a$ relative to runway - deg
γ_g	Elevation angle of $\bar{V}_g$ relative to runway - deg
$\gamma_{g'}$	Desired flight path angle of $\bar{V}_{ad}$ -deg

LIST OF SYMBOLS (Contd)

ΔF_x, ΔF_y, ΔF_z	Generalized force input (body axes system) - lbs
ΔL_r, ΔM_r, ΔN_r	Gyroscopic moments due to rotation rates p,q,r and angular momentum of rotating machinery (body axes system) - ft-lbs
ΔL_T, ΔM_T, ΔN_T	Generalized moment input (body axes system) - ft-lbs
$\overline{\Delta M}_D$	Jet damping moment vector
Δt	Current integration interval determined by VSRK - sec
ΔV_a	Allowed glide slope inertial velocity magnitude error - ft/sec
Δx	Distance from aerodynamic reference station to aircraft mass center - ft
$\Delta x_{C.G.}$	Center-of-gravity position from the reference center of gravity in the $\bar{1}_x$ direction; $(x_{C.G.} - x_{C.G._{ref}})$
$\Delta\alpha_a$	Allowed magnitude of total angle of attack error, α_{eT}-deg
$\Delta\beta_a$	Allowed magnitude of total sideslip angle error, β_{eT} - deg
$\Delta\phi$	Allowed magnitude of total Euler roll angle error, ϕ_{eT} - deg
$\Delta\psi_a$	Allowed magnitude of total Euler yaw angle error, ψ_{eT} - deg

LIST OF SYMBOLS (Contd)

$\Delta\omega$	Allowed percentage of ω_{TRi} magnitude for wheel angular speed error, ω_{TEi} - %/(100%) (i.e., nondimensional)
$\dot{\delta}_A$	Roll control surface (aileron) deflection rate magnitude used in control response - deg/sec
$\dot{\delta}_F$	Pitch control surface (elevator) deflection rate from δ_{qI} to δ_{qF} in landing roll - deg/sec
$\dot{\delta}_{HS}$	Pitch control surface (elevator) deflection rate magnitude used in control response - deg/sec
δ_h	Altitude normal to runway above h_{RF} to begin "hold" mode - ft
δ_i, δ_k	Sum of the quantities r_{ok}, z_{ok} and $\varepsilon(x_{Rk})$ - ft
$+\delta_k$	Tire deflection of a tire on the kth strut - ft
δ_p	Actual roll control surface (aileron) deflection - deg
$\dot{\delta}_p$	Actual roll control surface (aileron) deflection rate deg/sec
δp_d	Desired roll control surface (aileron) deflection - deg
δp_L	Lower limit on roll control surface (aileron) deflection - deg
δp_N	Nominal roll control surface (aileron) deflection - deg
δp_U	Upper limit on roll control surface (aileron) deflection - deg
δq	Actual pitch control surface (elevator) deflection - deg
$\dot{\delta}_q$	Actual pitch control surface (elevator) deflection rate - deg/sec
δq_c	Pitch control surface (elevator) deflection for "bang-bang" control in glide slope - degrees
δq_{c2}	Pitch control surface (elevator) deflection for "bang-bang" control for IAP $\geq$ 2 - deg
δq_F	Final value of pitch control surface (elevator) deflection in landing roll - deg

LIST OF SYMBOLS (Contd)

δq_I	Initial (impact) value of pitch control surface (elevator) deflection in landing roll - deg
δq_L	Lower limit on pitch control surface (elevator) deflection deg
δq_N	Nominal pitch control surface (elevator) deflection - deg
δq_{TO}	Takeoff pitch control surface (elevator) deflection - deg
δq_u	Upper limit on pitch control surface (elevator) deflection - deg
$\delta^{\bullet}_{RD}$	Yaw control surface (rudder) deflection rate magnitude used in control response - deg/sec
δr	Actual yaw control surface (rudder) deflection - deg
$\dot{\delta} r$	Actual yaw control surface (rudder) deflection rate - deg/sec
δr_d	Desired yaw control surface (rudder) deflection - deg
δr_L	Lower limit on yaw control surface (rudder) deflection - deg
δr_N	Nominal yaw control surface (rudder) deflection - deg
δr_U	Upper limit on yaw control surface (rudder) deflection - deg
$\delta\epsilon$	Fixed angular perturbation of glide slope in vertical plane - rad
$\delta\sigma$	Fixed angular perturbation of glide slope in horizontal plane - rad
$\epsilon(x_{Rk})$	Arbitrary runway profile - ft
ϵ_{GS}	Nominal glide slope angle - deg
ϵ_1	Error multiplier for C_N
ϵ_2	Incremental error in C_N
ϵ_3	Error multiplier for C_A
ϵ_4	Incremental error in C_A
ϵ_5	Error multiplier for C_y

LIST OF SYMBOLS (Contd)

ϵ_6	Incremental error in C_y
ϵ_7	Error multiplier for C_ℓ
ϵ_8	Incremental error in C_ℓ
ϵ_9	Error multiplier for C_m
ϵ_{10}	Incremental error in C_m
ϵ_{11}	Error multiplier for C_n
ϵ_{12}	Incremental error in C_n
ϵ_{18}	Incremental error in C.G. location - ft
ϵ_{19}	Incremental error in I_{xx} - slug-ft^2
ϵ_{20}	Incremental error in I_{yy} - slug-ft^2
ϵ_{21}	Incremental error in I_{zz} - slug-ft^2
ϵ_{22}	Incremental error in I_{xy} - slug-ft^2
ϵ_{23}	Incremental error in I_{xz} - slug-ft^2
ϵ_{24}	Incremental error in I_{yz} - slug-ft^2
ζ	Intermediate z-axis direction
η	Intermediate y-axis direction
θ', ψ', ϕ'	Pitch-yaw-roll sequence of rotation angles
θ'', ϕ'', ψ''	Pitch-roll-yaw sequence of rotation angles

LIST OF SYMBOLS (Contd)

θ_k	Pitch angle of kth strut axes relative to body axes - deg
θ_p	Actual Euler pitch angle (based on pitch-yaw-roll direction cosine sequence) - deg
θ_p', ψ_p', ϕ_p'	Pitch-yaw-roll sequence of rotation angles for body axes relative to inertial platform (in this formulation programmed as θ_p, ψ_p and ϕ_p) - deg
θ_p'', ϕ_p'', ψ_p''	Pitch-roll-yaw sequence of rotation angles for body axes relative to inertial platform (not programmed) - deg
θ_R	Pitch angle of aircraft from horizon - deg
θ_r	Pitch angle of rotating machinery axis relative to body x-axis-deg
$\dot{\theta}_r$	Pitch rate of rotating machinery axis relative to body x-axis-rad/sec
$\mu_k(P_{si})$	Coefficient of friction between a tire on the kth strut and the runway
μ_{sk}	Coefficient of friction at wing gear support for k^{th} strut
ξ	Intermediate x-axis direction
$\bar{\rho}$	Radius vector from origin of inertial axes system to the point P(x,y,z)
ρ	Atmospheric density - slug/ft^3
ϕ_c	Magnitude of desired roll angle in glide slope - deg
ϕ_d	Desired Euler roll angle in glide slope & flare - deg
ϕ_e	Euler roll angle position error - deg
ϕ_{eT}	Total Euler roll angle error - deg
ϕ_p	Actual Euler roll angle (based on pitch-yaw-roll direction cosine sequence) - deg
$\dot{\phi}_p$	Actual Euler roll angle rate (based on pitch-yaw-roll direction cosine sequence) - rad/sec

LIST OF SYMBOLS (Contd)

σ	Horizontal flight-path angle; heading angle - deg
Ψ_e	Euler yaw angle position error - deg
Ψ_{eT}	Total Euler yaw angle error - deg
Ψ_p	Actual Euler yaw angle (based on pitch-yaw-roll direction cosine sequence) - deg
Ψ, θ, ϕ	Yaw-pitch-roll sequence of rotation angles
Ψ_p, θ_p, ϕ_p	Yaw-pitch-roll sequence of rotation angles for body axes relative to inertial platform (not programmed as such - used as names for Ψ'_p, θ'_p, ϕ'_p) - deg
$\dot{\Psi}_p$	Actual Euler yaw angle rate (based on pitch-yaw-roll direction cosine sequence) rad/sec
$\bar{\omega}$	Inertial rotation rate vector of body axes
$\dot{\bar{\omega}}$	Rate of ch[illegible] of $\bar{\omega}$ vector; inertial angular acceleration vector of [illegible] axes
$\dot{\omega}_c$	Absolute magnitude of constant control angular acceleration for any wheel - rad/sec^2
$\bar{\omega}_k$	Inertial rotation rate vector of kth body axes
ω_r	Rotation rate of machinery within the body; about the machinery spin axis - revolutions per minute (R.P.M.)
$\omega_{TR}(I), \omega_{TRi}$	Wheel angular speed error array - rad/sec
$\bar{\omega}_{Tk}$	Rotational vector velocity of the tires on the kth strut
ω_{Tk}, ω_{Ti}	Magnitude of the vector $\bar{\omega}_{Tk}$; T_{yk} component of the vector $\bar{\omega}_{Tk}$ (there are no other components) - rad/sec
$\dot{\omega}_{Tk}, \dot{\omega}_{Ti}$	Wheel angular acceleration on k^{th} strut axle - rad/sec^2
$\omega_{TR}(I), \omega_{TRi}$	Desired (required) wheel speed array to obtain desired "percent skid" - rad/sec

LIST OF SYMBOLS (Contd)

$\dot{\omega}_{TR}(I), \dot{\omega}_{TRi}$	Desired (required) wheel acceleration array to maintain desired "percent skid" - rad/sec^2
$\left.\begin{matrix}\omega_x \\ \omega_y \\ \omega_z\end{matrix}\right\}$	Body axes components of the vector $\bar{\omega}$ - rad/sec
$\bar{\omega}_o$	Inertial rotation rate vector of oth body; inertial rotation rate vector of body axes system
$\bar{1}_{VGPk}$	Unit vector in the direction of the vector $\bar{V}_{GPTk}$ for the kth strut

Notational Conventions

$(\ )_k$	"as seen by the kth coordination system"
$(\dot{\ })$	First derivative of ( ) with respect to time
$(\ddot{\ })$	Second derivative of ( ) with respect to time
$\frac{d(\ )}{dt}$	Total derivative of ( ) with respect to time
$(\bar{\ })$	The vector ( )
$(\bar{\bar{\ }})$	The tensor ( ); the matrix ( )
[ ]	A matrix
$\sum_k$	Summation over all the gears of the vehicle; $\sum_{k=1}^{K}$
$(\dot{\bar{\ }})$	Total derivative of the vector ($\bar{\ }$)
$(\bar{\dot{\ }})$	( ) vector rate as seen from a rotating axes system

Axes System

$$\begin{bmatrix} \bar{1}_x \\ \bar{1}_y \\ \bar{1}_z \end{bmatrix}, \begin{bmatrix} \bar{1}_{xo} \\ \bar{1}_{yo} \\ \bar{1}_{zo} \end{bmatrix}$$

Body-fixed axes system, origin at vehicle nominal mass center (Also, coordinate system of oth body)

$$\begin{bmatrix} \bar{1}_{Xg} \\ \bar{1}_{Yg} \\ \bar{1}_{Zg} \end{bmatrix}, \begin{bmatrix} \bar{1}_{xg} \\ \bar{1}_{yg} \\ \bar{1}_{zg} \end{bmatrix}$$

Earth-fixed axes system, origin at sea level (Inertial frame), 1_{zg} normal to flat-Earth, positive down

$$\begin{bmatrix} \bar{1}_{xk} \\ \bar{1}_{yk} \\ \bar{1}_{zk} \end{bmatrix}$$

Body-fixed strut axes system, directed downward along k^{th} strut, origin along this line of action

$$\begin{bmatrix} \bar{1}_{xR} \\ \bar{1}_{yR} \\ \bar{1}_{zR} \end{bmatrix}$$

Runway axes system, origin at sea level, axes system fixed relative to inertial frame in present formulation

Direction Cosines

$$\begin{bmatrix} \ell_1 \ell_2 \ell_3 \\ m_1 m_2 m_3 \\ n_1 n_2 n_3 \end{bmatrix}$$

Matrix of direction cosines. Used to transfer quantities from Earth-fixed (Inertial Axes System to Body-fixed Axes System

$$\begin{bmatrix} a_{k11} & 0 & a_{k13} \\ 0 & 1 & 0 \\ a_{k31} & 0 & a_{k33} \end{bmatrix}$$

Matrix of direction cosines. Used to transfer quantities from Body-fixed Axes System to k^{th} Strut Axes System

$$\begin{bmatrix} R_{G11} & 0 & R_{G13} \\ 0 & 1 & 0 \\ R_{G31} & 0 & R_{G33} \end{bmatrix}$$

Matrix of direction cosines. Used to transfer quantities from Earth-fixed Axes System to Runway Axes System

Direction Cosines (Contd)

$$\begin{bmatrix} R_{L11} & R_{L12} & R_{L13} \\ R_{L21} & R_{L22} & R_{L33} \\ R_{L31} & R_{L32} & R_{L33} \end{bmatrix}$$

Matrix of direction cosines. Used to transfer quantities from Runway Axes System to Body-fixed Axes System

$$\begin{bmatrix} R_{I11k} & R_{I12k} & R_{I13k} \\ R_{I21k} & R_{I22k} & R_{I23k} \\ R_{I31k} & R_{I32k} & R_{I33k} \end{bmatrix}$$

Matrix of direction cosines. Used to transfer quantities from Runway Axes System to k^{th} Strut Axes System

SECTION I

INTRODUCTION

In the design of an aircraft, the engineer is confronted with the problem of takeoff and landing and the design of aircraft systems and techniques to perform this function. The final evaluation of these systems lies in the answer to the question: How does the aircraft and its system perform as a unit? The Takeoff and Landing Analysis (TOLA) Computer Program is the result of an attempt to generalize the aircraft, the main aircraft control systems, and the landing-takeoff situation into a single comprehensive calculation to answer this question.

Various analyses and simulations have been developed which are rigorous and thorough on a particular aspect of the landing-takeoff situation (e.g., References 20 through 24). Other are cited in Reference 25, which covers virtually every aspect of the problem.

The TOLA simulation answers the above question in the form of a well-defined integration of the various aspects of takeoff and landing. In the equations of motion the assumption is made that the main aircraft frame is rigid; however, the dynamic effects of up to five independent landing gears are included in the equations. The position and velocity of each strut and secondary piston are obtained by numerical integration subject to position constraints (for example, the main strut must move within the limits of the fully extended position and strut bottoming position). The same form of solution applies to the aircraft itself.

The purpose of this report is to unify and summarize the complete formulation of the TOLA Computer Program. TOLA is a FORTRAN IV modification to Option 2 (SDF-2) of the Six-Degree-of-Freedom Flight Path Study Generalized Computer Program of References 1 and 2.

The SDF-2 modification resulting in the TOLA Computer Program was undertaken in two parts which are documented in FDMG TM 68-5, "Derivation of the Equations of Motion for the Landing Gear and Ground Reaction Modification to SDF-2," and in FDMG TM 68-11, "Autopilot Equations and Logic for the Takeoff and Landing Analysis Modification of SDF-2."

SECTION II

TAKEOFF AND LANDING ANALYSIS COMPUTER PROGRAM

This section presents a general description of the Takeoff and Landing Analysis (TOLA) Computer Program formulation. The following will be discussed in order: the original six degree of freedom equations, the landing gear and ground reaction equations, and the autopilot equations.

1. ORIGINAL SDF-2 FORMULATION

The Takeoff and Landing Analysis (TOLA) Computer Program is based on two modifications to SDF-2, which is the second calculation option of References 1 and 2. SDF-2 has six degrees of freedom, but assumes a flat, nonrotating earth. Those portions of the original SDF-2 formulation retained by TOLA are presented in Appendix I. Figure 1 contains a summary of the steps performed by SDF-2 in TOLA, and most of the equations used to perform these steps are found in Appendix I. The exceptions are the equations for the landing gear forces and moments which are discussed in Appendix II.

2. LANDING GEAR AND GROUND REACTION FORMULATION

When each landing gear of a moving aircraft comes in contact with the runway, it is subjected to a force, $\bar{F}_{TRk}$, which is the ground reaction between the tire and the runway. The point of application of this force, namely the tire footprint, is located by a vector $\bar{R}_{Pk}$ from the aircraft center of gravity (cg). Therefore, $\bar{F}_{TRk}$ generates a moment about the cg, $\bar{M}_{TRk} = \bar{R}_{Pk} \times \bar{F}_{TRk}$. Summing over the k struts from 1 to K,

$$F_{TR} = \sum_k \bar{F}_{TRk} = F_{TRA}\bar{i}_{xo} + F_{TRB}\bar{i}_{yo} + F_{TRC}\bar{i}_{zo} \tag{1}$$

$$\bar{M}_{TR} = \sum_k \bar{M}_{TRk} = M_{Tx}\bar{i}_{xo} + M_{Ty}\bar{i}_{yo} + M_{Tz}\bar{i}_{zo} \tag{2}$$

in the body-fixed axes system.

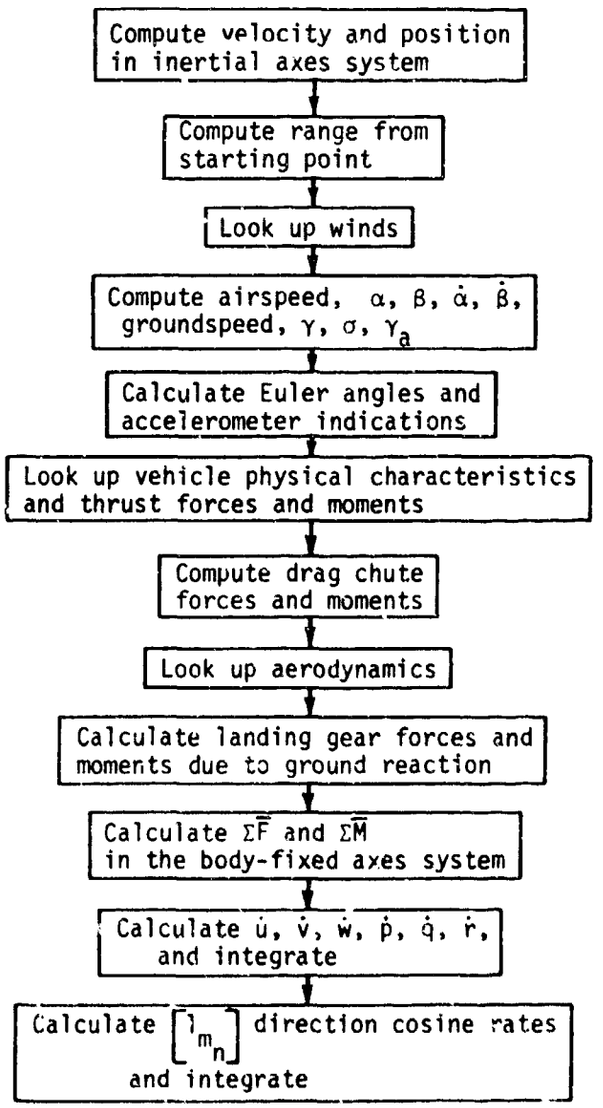

Figure 1. SDF-2 Summary

If the strut were a rigid portion of the total airframe, then $\overline{F}_{TR}$ and $\overline{M}_{TR}$ would be the total ground reaction force and moment transmitted to the airframe. However, the strut is able to telescope, with the result that part of each $\overline{F}_{TRk}$ is used to accelerate the strut relative to the airframe; the remainder of $\overline{F}_{TRk}$ is transmitted to (or "felt" by) the airframe.

Likewise, since $\overline{M}_{TRk} = \overline{R}_{Pk} \times \overline{F}_{TRk}$, then part of each $\overline{M}_{TRk}$ will be evident as a moment of the inertia force portion of $\overline{F}_{TRk}$; the remainder of $\overline{M}_{TRk}$ is transmitted to the airframe.

Let F_{xm}, F_{ym}, and F_{zm} be the body-axes components of that portion of the total ground reaction force transmitted to the main airframe, and L_m, M_m, and N_m be the body-axes components of that portion of the total ground reaction moment transmitted to the main airframe.

Then,

$$\begin{bmatrix} F_{xm} \\ F_{ym} \\ F_{zm} \end{bmatrix} = \begin{bmatrix} F_{TRA} \\ F_{TRB} \\ F_{TRC} \end{bmatrix} + \begin{bmatrix} \sum_k m_k \ddot{S}_k a_{k31} \\ 0 \\ \sum_k m_k \ddot{S}_k d_{k33} \end{bmatrix} \tag{3}$$

and

$$\begin{bmatrix} L_m \\ M_m \\ N_m \end{bmatrix} = \begin{bmatrix} M_{Tx} \\ M_{Ty} \\ M_{Tz} \end{bmatrix} + \begin{bmatrix} \sum_k m_k \ddot{S}_k a_{k11} R_{ky} \\ -\sum_k m_k \ddot{S}_k R_{RkCGx} \\ \sum_k m_k \ddot{S}_k a_{k13} R_{ky} \end{bmatrix} \tag{4}$$

where m_k is the strut mass, $\ddot{S}_k$ is the strut acceleration relative to the main airframe, a_{kij} are direction cosines relating the strut orientation to the body axes system, and R_{ky} and R_{RkCGx} are moment arms of the strut inertia forces.

Equations 3 and 4 are included in the summation of forces and moments as follows:

$$\begin{bmatrix} F_x \\ F_y \\ F_z \end{bmatrix} = \begin{bmatrix} T_x - a + Mg_x + \Delta F_x \\ T_y + y + Mg_y + \Delta F_y \\ T_z + N_F + Mg_z + \Delta F_z \end{bmatrix} + \begin{bmatrix} F_{xm} \\ F_{ym} \\ F_{zm} \end{bmatrix} \tag{5}$$

and

$$\begin{bmatrix} L \\ M \\ N \end{bmatrix} = \begin{bmatrix} L_T + \Delta L_T + \ell \\ M_T + \Delta M_T + m \\ N_T + \Delta N_T + n \end{bmatrix} + \begin{bmatrix} L_m \\ M_m \\ N_m \end{bmatrix} \tag{6}$$

The derivation of the strut acceleration, $\ddot{S}_k$, requires the definition and analysis of the forces internal to the strut. A detailed derivation of the various terms in Equations 3 and 4 will be found in Appendix II of this report. The flow charts in Appendix II are summarized in Figure 2, where the circled letters correspond to those found in the flow charts. The basic equations of motion used in Appendix II are derived in Reference 6.

3. CONTROL MANAGEMENT FORMULATION

The purpose of the TOLA control management formulation is to determine appropriate values for δq, δr, δp, N(IN), and $M_B(I)$, which are the control variables for pitch, yaw, roll, throttle, and braking, respectively. This determination is made in three major steps called the maneuver logic, the autopilots, and the control variable response. The respective tasks of these steps is to determine what needs to be done, how to do it, and how much can be accomplished within a given time step.

a. Maneuver Logic

The maneuver logic is that portion of the control management formulation that is specifically oriented toward the takeoff and landing problem. It determines what needs to be done in two steps.

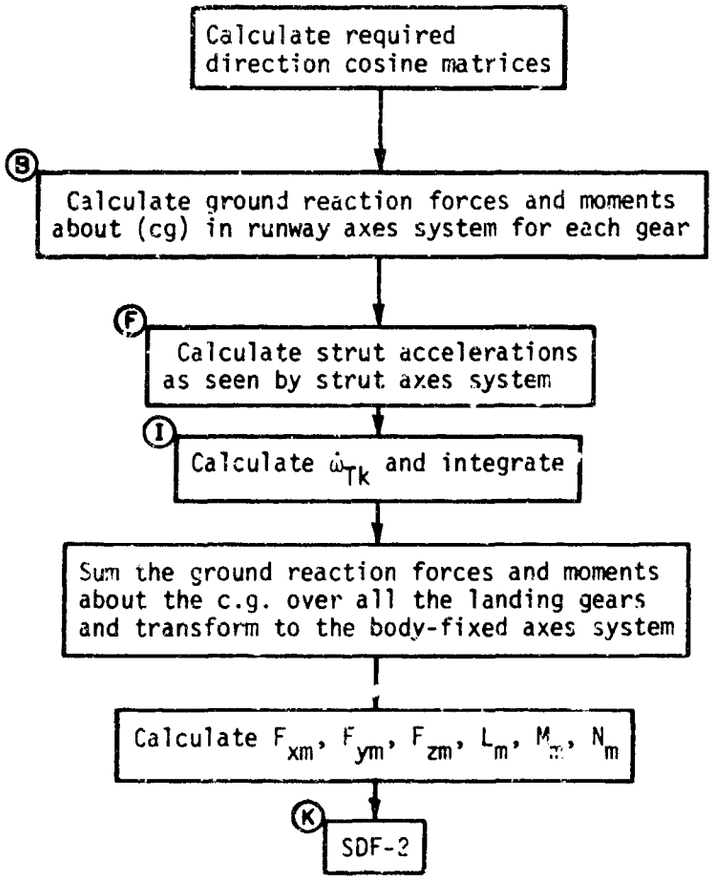

Figure 2. Landing Gear Summary

The first step is the determination of which phase of the analysis is to be examined at the present time step. This is done in the problem phase logic in which a sequence of tests is performed on the present position of the aircraft relative to the runway. In this manner, it is determined whether the aircraft is in the glide slope, flare, landing roll, or takeoff roll phase. Each phase has its own logic for determining the desired state of the aircraft.

The second step performed in the maneuver logic is to determine if an error exists in the present position, velocity, or acceleration of the aircraft relative to the runway. If so, the required dynamics are solved for the desired angle of attack, α_d, the desired roll angle, ϕ_d, and the desired thrust, T_d.

The values of α_d, ϕ_d, and T_d obtained in the above two steps determine what needs to be done in terms of aircraft orientation and thrust to correct kinematic state errors which may exist, depending on the problem phase. This accomplishes the main purpose of the maneuver logic; however, prior to entry into the autopilots, checks are made for possible input system failures. If the aircraft is in the landing roll phase, the condition of the brakes is determined at the present time step for later use in the Brake Autopilot. The final step for all phases in the maneuver logic is to determine the condition of all engines in the engine failure logic. This is done at the present time step for later use in the Throttle Autopilot.

b. Autopilots.

The purpose of the autopilots is to determine the means by which the desired vehicle orientation, thrust, and braking are to be accomplished. The results are obtained in the form of δq_d, δr_d, δp_d, $N_d(IN)$ and $M_B(I)$, which are, respectively, the desired pitch, yaw, and roll control surface deflections, the desired throttle setting array, and the actual braking moment array. These variables are determined in the Pitch, Yaw, Roll, Throttle, and Brake Autopilots, respectively, which are discussed in detail in Appendix III.

c. Control Variable Response

The purpose of the control variable response is to get a first order approximation of the effects of control surface and engine lags on aircraft performance. Constant time rates of change are used to determine the measure of δq_d, δr_d, δp_d, and $N_d(IN)$ attainable within a given time step. The results are the actual control variables δq, δr, δp, and $N(IN)$.

d. Control Management Formulation Summary

A detailed development of the logic and equations for the control management formulation is presented in Appendix III. The basic steps in the control management development are summarized in Figure 3.

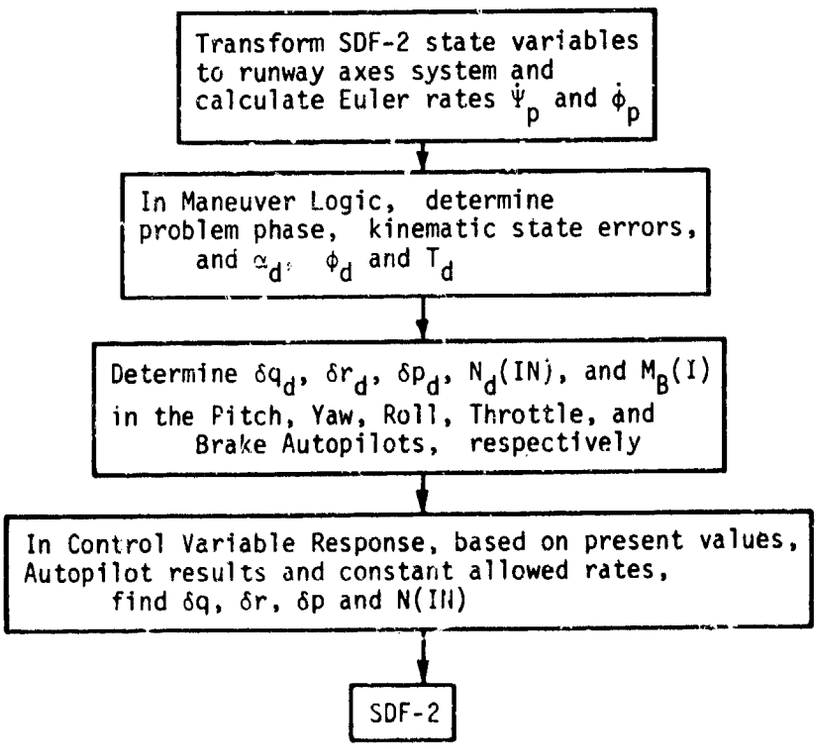

Figure 3. Control Management Formulation Summary

SECTION III

SUMMARY AND DISCUSSION

The Takeoff and Landing Analysis (TOLA) Computer Program is summarized in Figures 4 and 5. Figure 4 shows the various capabilities of TOLA as depicted in a perspective view of an inclined runway. TOLA can simulate aircraft control and performance during glide slope, flare, landing roll, and takeoff subject to changing winds, engine failures, aerodynamic ground effect, runway limitations, and control variable limitations and lags. The (cg) oscillation seen in the landing roll represents the multiple landing gear dynamics. Runway perturbations may be input as a function of distance down the runway, as exemplified by the "bump." The capabilities to cut power; to actuate spoilers and/or drag chute; to have brakes locked, off, or on with constant or controlled braking, and to reverse engines are shown as functions of time. This demonstrates how the TOLA simulation allows the order of these effects to be changed. The takeoff is accomplished as an acceleration run to a predetermined airspeed, at which a desired angle of attack is sent to the pitch autopilot. The above versatility is maintained in as generalized a manner as possible.

Figure 5 is a block diagram summarizing the flight mechanics performed in TOLA. The instantaneous dynamic state of the vehicle is determined by the six-degree-of-freedom routine, which determines the accelerations caused by the aerodynamic, thrust, and landing gear forces and moments. These accelerations are integrated twice by the executive routine, which then sends the kinematic state information in terms of position and velocity to the control management routine. In the Maneuver Logic, errors in kinematic state determine the desired angle of attack, thrust, and roll angle. These are processed as forcing functions by the Autopilots, which determine the desired control settings. The Control Variable Response then determines the actual control settings attainable during a given time step.

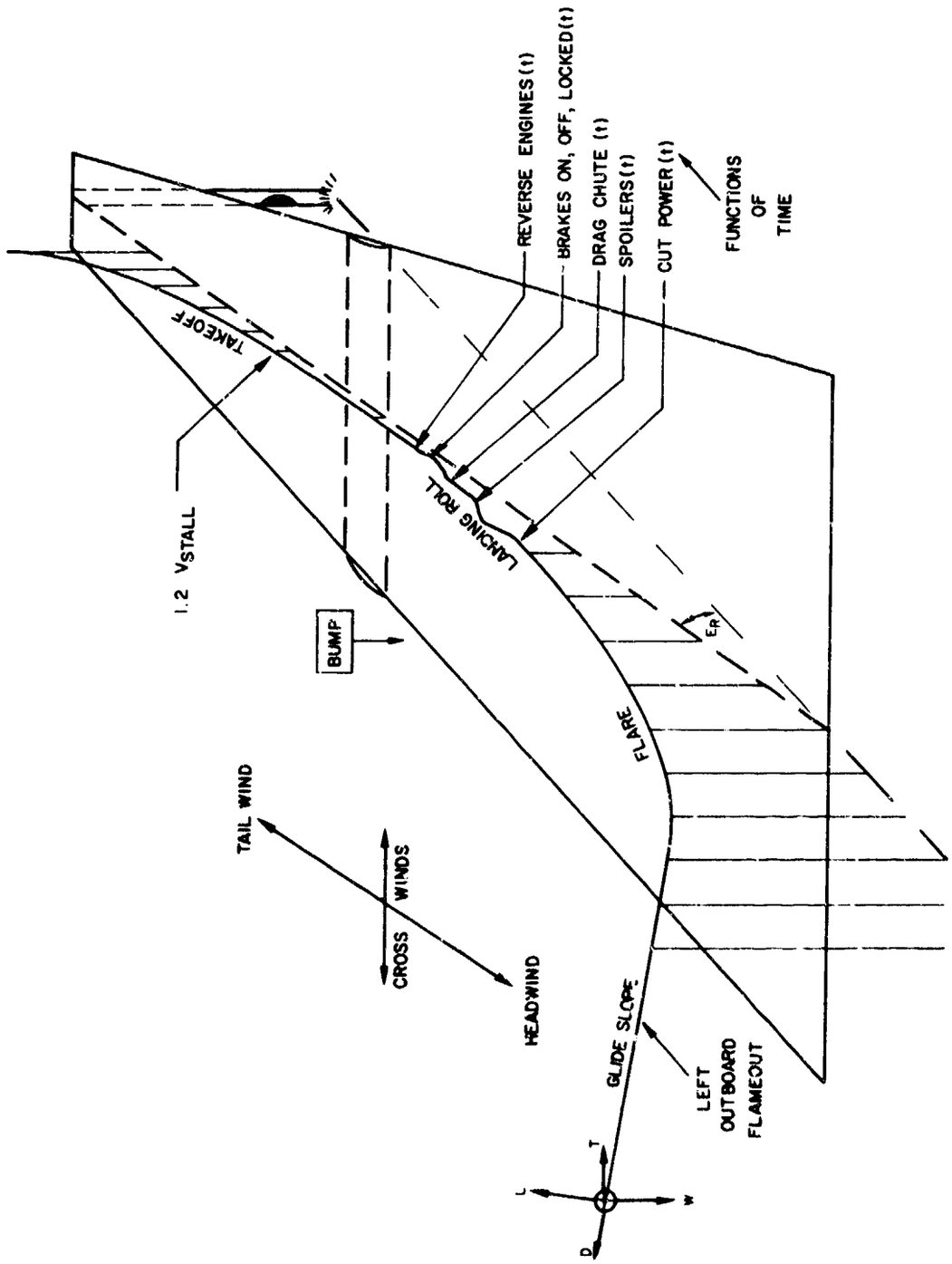

Figure 4. Takeoff and Landing Analysis

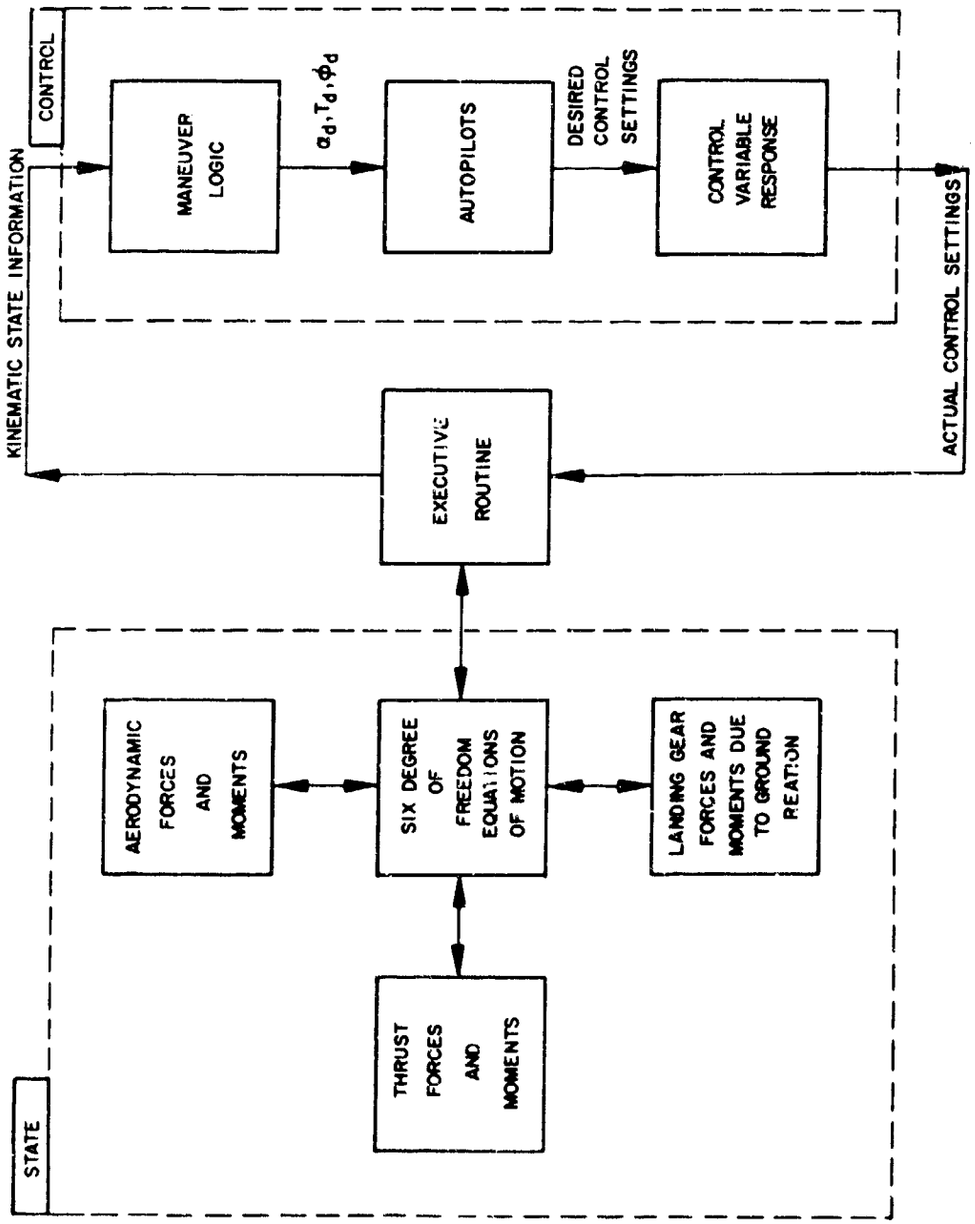

Figure 5. Dynamics Summary

TOLA development grew out of a need for comprehensive, quantitative analysis of aircraft takeoff and landing performance. The simulation attempts to generalize conventional powered aircraft, the main control systems, and the landing takeoff situation into a single comprehensive calculation. The simulation does not perform the design function; it simply takes input data and evaluates performance.

The concept a single, comprehensive, quantitative simulation of total system performance has yielded very promising results (see paper, "Capabilities of the TOLA Simulation," presented July 1969 at the AIAA Aircraft Design and Operations Meeting, L. A., Calif.) for the takeoff and landing problem. To date, the capability of the program as a design tool to do tradeoff studies in major system component design has only just begun. Even with the cursory results received so far, many questions come to mind:

(a) What effect does limited runway length, changing winds, and engine failure have on a go-around decision for a particular situation?

(b) How does a change in the control schedule for the landing roll affect maximum gear loads?

(c) What limitations would have to be placed on the landing if one strut failed to brake or failed to extend from the fuselage?

(d) With multiple-engine aircraft and a reverse capability, is it safe to have some engines in reverse during landing in view of possible engine failure?

These are just a few of the questions that are within the capability of study by the TOLA simulation. In its interest to develop better technology, the Air Force Flight Dynamics Laboratory will continue to improve the TOLA simulation and use it as a tool to study the takeoff and landing problem.

APPENDIX I

ORIGINAL SDF-2 EQUATIONS

1. DERIVATION OF EQUATIONS OF MOTION

This section presents the derivation of the equations of motion, of a body in "inertial" space, as required for use in the Takeoff and Landing Analysis computer program. The equations of motion will form a portion of the computation loop which is unaffected by the libraries of interchangeable subprograms describing alternate control systems: airframe aerodynamics, atmospheres, and geophysical parameters, or the data-monitoring subprograms to be incorporated. The several coordinate transformations and velocity and angle resolutions, which complete this central portion of the problem, are described later in this appendix.

Since the equations involving the moments of inertia, aerodynamic forces, and thrust forces are greatly simplified if expressed in body coordinates, this system of body reference will be used. The two basic equations which define the motion of a body are:

$$\bar{F} = \frac{d}{dt}(m\bar{V}) \tag{7}$$

$$M = \frac{d}{dt}(\bar{H}) \tag{8}$$

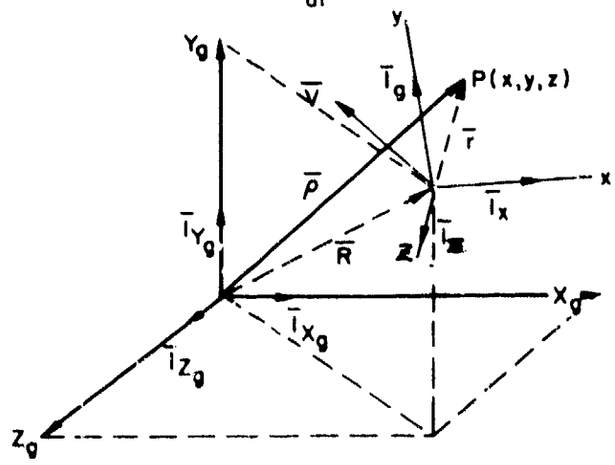

Figure 6. Generalized Inertial and Body-Axes Coordinate Systems

Pages 14 & 15 are Blank.

Numerical analyses of these vector equations require their resolution into vector components and definition of the scalar coefficients. These manipulations are discussed in detail in many texts in mechanics (e.g., References 7 through 14. The essential steps of the derivation are reviewed here, however, for completeness.

To determine the displacement accelerations, consider a point P displaced from the origin of coordinate system x-y-z such that the vector $\bar{r}$ designates the point. Figure 1 illustrates the system.

Let the origin of the coordinate system x-y-z be displaced from the origin of a space-fixed coordinate system X_g-Y_g-Z_g by an amount and direction given by $\bar{R}$. Further, let the coordinate system x-y-z rotate in the X_g-Y_g-Z_g space such that the vector, $\bar{\omega}$, defines the rotation.

Then

$$\begin{aligned} \bar{r} &= x\bar{i}_x + y\bar{i}_y + z\bar{i}_z \\ \bar{R} &= X_g\bar{i}_{xg} + Y_g\bar{i}_{yg} + Z_g\bar{i}_{zg} \\ \bar{\omega} &= \omega_x\bar{i}_x + \omega_y\bar{i}_y + \omega_z\bar{i}_z \end{aligned} \tag{9}$$

The coordinate system x-y-z will be recognized as the body axes and the coordinate system X_g-Y_g-Z_g are the nonmoving "inertial" or Newtonian axes. The total velocity of the point is given by

$$\begin{aligned} \dot{\bar{P}} = \dot{\bar{R}} + \dot{\bar{r}} = \dot{X}_g\bar{i}_{xg} + \dot{Y}_g\bar{i}_{yg} + \dot{Z}_g\bar{i}_{zg} + (\dot{x} - y\omega_z + z\omega_y)\bar{i}_x \\ + (\dot{y} + x\omega_z - z\omega_x)\bar{i}_y + (\dot{z} - x\omega_y + y\omega_x)\bar{i}_z \end{aligned} \tag{10}$$

It is more convenient to express the velocity of the body-axes origin in body-velocity components than in velocity components coincident with the "inertial" reference coordinates. The vector $\bar{R}$ can be written in any coordinate system, so

$$\dot{\bar{R}} = \bar{V} = \dot{X}_g\bar{i}_{xg} + \dot{Y}_g\bar{i}_{yg} + \dot{Z}_g\bar{i}_{zg} = \dot{x}_o\bar{i}_x + \dot{Y}_o\bar{i}_y + \dot{Z}_o\bar{i}_z$$

and Equation 10 may be rewitten as

$$\dot{\bar{p}} = \bar{V} + \dot{\bar{r}} = \dot{x}_o \bar{i}_x + \dot{y}_o \bar{i}_y + \dot{z}_o \bar{i}_z + (\dot{x}_p - y_p \omega_z + z_p \omega_y)\bar{i}_x + (\dot{y}_p + x_p \omega_z - z_p \omega_x)\bar{i}_y + (\dot{z}_p - x_p \omega_y + y_p \omega_x)\bar{i}_z \tag{11}$$

where the subscripts o and p have been added to distinguish between the velocity components of the origin and the relative movement of the point P with respect to the origin of the x-y-z coordinate system, respectively. Differentiating Equation 11 gives the relation for the total acceleration to be

$$\begin{aligned}\ddot{\bar{p}} = {} & \left[\ddot{x}_o - \dot{y}_o \omega_z + \dot{z}_o \omega_y\right]\bar{i}_x + \left[\ddot{y}_o + \dot{x}_o \omega_z - \dot{z}_o \omega_x\right]\bar{i}_y + \left[\ddot{z}_o - \dot{x}_o \omega_y + \dot{y}_o \omega_x\right]\bar{i}_z \\ & + \left[\ddot{x}_p - 2\dot{y}_p \omega_z + 2\dot{z}_p \omega_y - x_p(\omega_z^2 + \omega_y^2) + y_p(\omega_x \omega_y - \dot{\omega}_z) + z_p(\dot{\omega}_y + \omega_x \omega_z)\right]\bar{i}_x \\ & + \left[\ddot{y}_p + 2\dot{x}_p \omega_z - 2\dot{z}_p \omega_x - y_p(\omega_x^2 + \omega_z^2) + z_p(\omega_y \omega_z - \dot{\omega}_x) + x_p(\dot{\omega}_z + \omega_x \omega_y)\right]\bar{i}_y \\ & + \left[\ddot{z}_p - 2\dot{x}_p \omega_y + 2\dot{y}_p \omega_x - z_p(\omega_y^2 + \omega_x^2) + x_p(\omega_z \omega_x - \dot{\omega}_y) + y_p(\dot{\omega}_x + \omega_y \omega_z)\right]\bar{i}_z\end{aligned} \tag{12}$$

This acceleration relation is completely general and applies to any point on the body. In developing the equations of motion, the point of interest, P (x,y,z), is the center of gravity. If the center of gravity is assumed to move, relative to the body, along the x-axis only, the following simplification can be made.

$$y_p = z_p = 0 \quad ; \quad \dot{y}_p = \dot{z}_p = \ddot{y}_p = \ddot{z}_p = 0$$

The components $\dot{x}_o$, $\dot{y}_o$, $\dot{z}_o$ and w_x, w_y, w_z are more commonly known as u, v, w and p, q, r, respectively. The components u, v, and w are the velocities of the reference point on the body. Making the above substitutions gives

$$\begin{aligned} F_x &= M\left[\dot{u} - vr + wq + \ddot{x}_p - x_p(r^2 + q^2)\right] \\ F_y &= M\left[\dot{v} + ur - wp + 2\dot{x}_p r + x_p(\dot{r} + pq)\right] \\ F_z &= M\left[\dot{w} - uq + vp - 2\dot{x}_p q + x_p(rp - \dot{q})\right] \end{aligned} \tag{13}$$

Since most vehicles are designed to have small center-of-gravity travel, the acceleration and velocity of the center of gravity are both very small quantities and may be omitted from the problem formulation. If the reference point is further restricted to be the center of gravity, then x_p and its derivatives may be omitted from the equations and the components u, v, and w are the velocities of the center of gravity. In matrix form the equations reduce to the following:

$$\begin{bmatrix} F_x \\ F_y \\ F_z \end{bmatrix} = \mathcal{M} \left[\begin{bmatrix} \dot{u} \\ \dot{v} \\ \dot{w} \end{bmatrix} + \begin{bmatrix} 0 & -r & q \\ r & 0 & p \\ -q & p & 0 \end{bmatrix} \begin{bmatrix} u \\ v \\ w \end{bmatrix} \right] \tag{14}$$

Note that in the analysis of flight-test data, where the output of accelerometers mounted away from the center of gravity are used to record the motion of the body, the complete form of Equation 13 must be used. Note also that, although Equation 7 states Newton's Law as the time derivative of the momentum, a formal differentiation of $\mathcal{M}\bar{V}$, assuming $\mathcal{M}$ to be a function of time, has not been performed in the derivation of Equation 14. Such a formal differentiation gives

$$\bar{F} = \mathcal{M} \frac{d\bar{V}}{dt} + \frac{d\mathcal{M}}{dt} \bar{V}$$

This differentiation leads to erroneous results, however, since the residual momentum of the expelled gases has not been accounted for by this procedure (see References 6 and 14). The equation should be

$$\bar{F} = \mathcal{M} \frac{d\bar{V}}{dt} + \frac{d\mathcal{M}}{dt} \bar{C}$$

when the residual momentum of the expelled mass is properly considered. Here, $\bar{c}$ is the velocity of the expelled mass with respect to the continuing body. The contribution $\dot{\mathcal{M}}\bar{c}$ is the momentum-change portion of the thrust and is included in the summation of external forces.

There are additional accelerations produced which are unique to configurations which have very large fuel flow rates and which have the thrust nozzle located a considerable distance from the center of gravity. These accelerations, linear and angular, are the so-called jet-damping contributions. The term is a correction to accelerations computed on the basis of only the externally applied forces (or moments) and accounts for the moment of momentum which is imparted to the fuel by the pitching velocity of the body. The derivation of this contribution is considered in greater detail in Reference 1. The principal contribution to the equations for linear acceleration are in the y- and z-directions and have been added to the expressions of Equation 14 to give the following result.

$$\begin{bmatrix} F_x \\ F_y \\ F_z \end{bmatrix} = m \left[\begin{bmatrix} \dot{u} \\ \dot{v} \\ \dot{w} \end{bmatrix} + \begin{bmatrix} 0 & -r & q \\ r & 0 & -p \\ -q & p & 0 \end{bmatrix} \begin{bmatrix} u \\ v \\ w \end{bmatrix} \right] + \begin{bmatrix} 0 \\ -2\dot{m} r \ell_y \\ +2\dot{m} q \ell_z \end{bmatrix} \tag{15}$$

The relations expressing the rotational motion are obtained in a straightforward manner. The components considered in this anslysis come from three basic sources: the time rate of change of the moment of momentum, the gyroscopic moments which arise from the rotating machinery of the vehicle, and the externally applied moments. The moment of momentum of a body (or angular momentum) about its center of gravity, in terms of its components, is given by

$$\begin{bmatrix} H_x \\ H_y \\ H_z \end{bmatrix} = \begin{bmatrix} I_{xx} & -I_{xy} & -I_{xz} \\ -I_{xy} & I_{yy} & -I_{yz} \\ -I_{xz} & -I_{yz} & I_{zz} \end{bmatrix} \begin{bmatrix} w_x \\ w_y \\ w_z \end{bmatrix}$$

or, since w_x, w_y, and w_z are p, q, and r, respectively:

$$\bar{H} = \left[I_{xx}p - I_{xy}q - I_{xz}r \right] \bar{i}_x + \left[-I_{xy}p + I_{yy}q - I_{yz}r \right] \bar{i}_y + \left[-I_{xz}p - I_{yz}q + I_{zz}r \right] \bar{i}_z \tag{16}$$

The required differentiation* of the moment of momentum gives

$$
\begin{aligned}
\dot{\bar{H}} = & \Big[I_{xx}\dot{p} + \dot{I}_{xx}p + (I_{zz} - I_{yy})qr - I_{yz}(q^2 - r^2) - I_{xz}(\dot{r} + pq) \\
& - I_{xy}(\dot{q} - pr) - \dot{I}_{xz}r - \dot{I}_{xy}q \Big] \bar{i}_x \\
& + \Big[I_{yy}\dot{q} + \dot{I}_{yy}q + (I_{xx} - I_{zz})pr - I_{xz}(r^2 - p^2) - I_{xy}(\dot{p} + qr) \\
& - I_{yz}(\dot{r} - pq) - \dot{I}_{xy}p - \dot{I}_{yz}r \Big] \bar{i}_y \\
& + \Big[I_{zz}\dot{r} + \dot{I}_{zz}r + (I_{yy} - I_{xx})pq - I_{xy}(p^2 - q^2) - I_{yz}(\dot{q} + pr) \\
& - I_{xz}(\dot{p} - qr) - \dot{I}_{xz}p - \dot{I}_{yz}q \Big] \bar{i}_z
\end{aligned}
\tag{17}
$$

It is general practice at this point in the derivation of the equations of motion to assume that the reference axes of the aircraft are principal axes and that the moments of inertia do not vary with time. This conveniently elimates the products of inertia and the time derivatives of the moments and products of inertia, respectively. However, it is desired to have a more general applicability than this for the computer program being developed, and these terms will be retained. The inclusion of the time derivatives of the inertia implies that all moment of momentum has been removed from the mass being lost by the body. This assumes that the gases have no swirl after they have left the body. Staging and dropping of discrete masses from the body introduce discontinuities in the mass and inertia properties of the body. The solution must not proceed across these discontinuities. Therefore, the integration of the equations of motion will be interrupted when mass is dropped and automatically reestablished immediately thereafter (see Section 3, Stages and Staging).

---

*The time rate of change of inertia noted here refers to that change occurring at constant mass only.

The jet damping contribution to the expressions for angular acceleration (from Appendix I of Reference 1) is:

$$\Delta\bar{M}_D = -p\dot{m}\ell_\ell^2\,\bar{I}_x - q\dot{m}\,\ell_m^2\,\bar{I}_y - r\dot{m}\ell_n^2\bar{I}_z \tag{18}$$

The expression for the total angular acceleration due to the time rate of change of the moment of momentum, including jet damping, is conveniently given in matrix form:

$$\begin{bmatrix} L \\ M \\ N \end{bmatrix} = \begin{bmatrix} I_{xx} & -I_{xy} & -I_{xz} \\ -I_{xy} & I_{yy} & -I_{yz} \\ -I_{xz} & -I_{yz} & I_{zz} \end{bmatrix} \begin{bmatrix} \dot{p} \\ \dot{q} \\ \dot{r} \end{bmatrix} + \begin{bmatrix} \dot{I}_{xx} - \dot{m}\ell_\ell^2 & -\dot{I}_{xy} & -\dot{I}_{xz} \\ -\dot{I}_{xy} & \dot{I}_{yy} - \dot{m}\ell_m^2 & -\dot{I}_{yz} \\ -\dot{I}_{xz} & -\dot{I}_{yz} & \dot{I}_{zz} - \dot{m}\ell_n^2 \end{bmatrix} \begin{bmatrix} p \\ q \\ r \end{bmatrix}$$

$$+ \begin{bmatrix} 0 & -r & q \\ r & 0 & -p \\ -q & p & 0 \end{bmatrix} \begin{bmatrix} I_{xx} & -I_{xy} & -I_{xz} \\ -I_{xy} & I_{yy} & -I_{zz} \\ -I_{xz} & -I_{yz} & I_{zz} \end{bmatrix} \begin{bmatrix} p \\ q \\ r \end{bmatrix} \tag{19}$$

The torques due to precession and changes in rotational speed of rotating machinery abroad a vehicle which is free to gyrate in space can contribute significantly to the angular accelerations which the vehicle experiences. Appendix II of Reference 1 derives the torques generated by the precession of rotating machinery in general terms and simplifies these relations as required for the solution of the following problems:

(a) The motion of an aircraft powered by an engine with a rotating mass which is fixed in its orientation with respect to the reference axis of the aircraft.

(b) The motion of an aircraft powered by a rotating-mass engine which can be rotated in a plane parallel to the plane of symmetry (e.g., convertiplane which is in the transition from vertical flight to forward motion, or vice versa).

(c) The motion of a satellite in which motors are being operated (by the proper selection of reference axes).

The gyroscopic moments due to the rotational rates p, q, and r and the angular momentum of the rotating machinery are approximated as follows:

$$\begin{aligned} \Delta L_r &= -I_{xr}\omega_r(q+\dot{\theta}_r)\sin\theta_r \\ \Delta M_r &= I_{xr}\omega_r(p\sin\theta_r + r\cos\theta_r) \\ \Delta N_r &= -I_{xr}(q+\dot{\theta}_r)\omega_r\cos\theta_r) \end{aligned} \tag{20}$$

The complete rotational equations of motion are, therefore, from Equations 17, 18, and 19

$$\bar{M} = L\bar{T}_x + M\bar{T}_y + N\bar{T}_z$$

in which

$$\begin{aligned} L = {} & I_{xx}\dot{p} + \dot{I}_{xx}p + (I_{zz}-I_{yy})qr - I_{yz}(q^2-r^2) \\ & - I_{xz}(\dot{r}+pq) - I_{xy}(\dot{q}-pr) - \dot{I}_{xz}r - \dot{I}_{xy}q \\ & - p\dot{m}\ell_\ell^2 - I_{xr}\omega_r(q+\dot{\theta}_r)\sin\theta_r \end{aligned}$$

$$\begin{aligned} M = {} & I_{yy}\dot{q} + \dot{I}_{yy}q + (I_{xx}-I_{zz})pr - I_{xz}(r^2-p^2) \\ & - I_{xy}(\dot{p}+qr) - I_{yz}(\dot{r}-pq) - \dot{I}_{xy}p - \dot{I}_{yz}r \\ & - q\dot{m}l_m^2 + I_{xr}\omega_r(p\sin\theta_r + r\cos\theta_r) \end{aligned}$$

$$\begin{aligned} N = {} & I_{zz}\dot{r} + \dot{I}_{zz}r + (I_{yy}-I_{xx})pq - I_{xy}(p^2-q^2) \\ & - I_{xz}(\dot{p}-qr) - I_{yz}(\dot{q}+pr) - \dot{I}_{xz}p - \dot{I}_{yz}q \\ & - r\dot{m}l_n^2 - I_{xr}(q+\dot{\theta}_r)\omega_r\cos\theta_r \end{aligned}$$

These relations, written in matrix form, are:

$$\begin{bmatrix} L \\ M \\ N \end{bmatrix} = \begin{bmatrix} I_{xx} & -I_{xy} & -I_{xz} \\ -I_{xy} & I_{yy} & -I_{yz} \\ -I_{xz} & -I_{yz} & I_{zz} \end{bmatrix} \begin{bmatrix} \dot{p} \\ \dot{q} \\ \dot{r} \end{bmatrix} + \begin{bmatrix} \dot{I}_{xx} - \dot{m} l_l^2 & -\dot{I}_{xy} & -\dot{I}_{xz} \\ -\dot{I}_{xy} & \dot{I}_{yy} - \dot{m} l_m^2 & -\dot{I}_{yz} \\ -\dot{I}_{xz} & -\dot{I}_{yz} & \dot{I}_{zz} - \dot{m} l_n^2 \end{bmatrix} \begin{bmatrix} p \\ q \\ r \end{bmatrix}$$

$$+ \begin{bmatrix} 0 & -r & q \\ r & 0 & -p \\ -q & p & 0 \end{bmatrix} \begin{bmatrix} I_{xx} & -I_{xy} & -I_{xz} \\ -I_{xy} & I_{yy} & -I_{yz} \\ -I_{xz} & -I_{yz} & I_{zz} \end{bmatrix} \begin{bmatrix} p \\ q \\ r \end{bmatrix} + \begin{bmatrix} -I_{xr}\omega_r(q + \dot{\theta}_r) \sin\theta_r \\ I_{xr}\omega_r(p \sin\theta_r + r \cos\theta_r) \\ -I_{xr}\omega_r(q + \dot{\theta}_r) \cos\theta_r \end{bmatrix} \quad (21)$$

Equations 15 and 21 constitute the general six-degree-of-freedom equations of motion which will be used in the computer program. The program instructions will provide for the removal of certain combinations of terms, as follows:

(a) All product of inertia terms for the case where the body is inertially symmetrical about the x-axis.

(b) The product of inertia terms I_{xy} and I_{yz} which are zero when the x-z plane is a plane of symmetry.

(c) The terms containing the time rates of change of inertia, products of inertia, and mass.

(d) The gyroscopic contributions of rotating machinery.

(e) The jet damping terms, both forces and moments.

2. COORDINATE SYSTEMS AND COORDINATE TRANSFORMATIONS

This section presents a description of the reference coordinate systems chosen for the Takeoff and Landing Analysis computer program. The coordinate transformations required to relate the various parameters of the computation to the several coordinate systems are also derived.

The coordinate transformations required in the program may be categorized as follows:

(1) Transformations inherent in solving the basic equations of motion.

(2) Transformations to provide input data to the guidance and autopilot.

(3) Transformations to present readout data in the most desirable form and auxiliary transformations which may be required for the definition of certain special parameters. These transformations may be deleted from the program when they are not required.

a. Coordinate Transformations for Basic Equations of Motion. The coordinate systems and transformations required to describe the rigid airframe motion in six degrees of freedom and the coordinate transformations which relate the aerodynamic angles and velocities to ground-referenced velocities in the presence of winds are presented.

(1) Body-Axes Coordinates

The equations of motion (Section 4) are solved in a body coordinate system (see Figure 6). The origin of this system is at the center of gravity of the aircraft, with the x-axis along the geometric longitudinal axis of the body. The positive direction of the x-axis is from the center of gravity to the front of the body.

The y-axis is positive to the right, extending from the center of gravity in a water-line plane. The z-axis forms a right-hand orthogonal system. This coordinate system was chosen because inertial characteristics are thus made independent of attitude.

Accelerations and velocities computed in the x-y-z body axis must be related to velocities and accelerations referenced to a fixed point on the surface of the planet to (a) describe the motion which a fixed

observer would sense, and (b) compute the aerodynamic forces on the body immersed in an atmosphere with winds which are referenced to a point on the surface of the planet.

(2) Inertial Coordinates. The inertial coordinates used in this analysis are the X_g-Y_g-Z_g axes. X_g and Y_g lie in the plane tangent to the earth's surface, and Z_g is the inward or downward normal vector to this plane. The effects of the earth's curvature and rotation rate are truly negligible in the takeoff and landing phases of aircraft flight. Thus, the inertial coordinates defines a flat, nonrotating earth.

(3) Direction Cosines. The direction cosines relating the body x-y-z axes to the inertial coordinate system X_g-Y_g-Z_g are obtained in the following manner. Let $\bar{i}_x$, $\bar{i}_y$, $\bar{i}_z$ be unit vectors along the body axes, x, y, z, respectively, and let $\bar{i}_{Xg}$, $\bar{i}_{Yg}$, $\bar{i}_{Zg}$ be unit vectors along the inertial axes, X_g, Y_g, Z_g, respectively. The direction cosine matrix relating these two sets of unit vectors will be:

$$\begin{bmatrix} \bar{i}_x \\ \bar{i}_y \\ \bar{i}_z \end{bmatrix} = \begin{bmatrix} \ell_1 & \ell_2 & \ell_3 \\ m_1 & m_2 & m_3 \\ n_1 & n_2 & n_3 \end{bmatrix} \begin{bmatrix} \bar{i}_{xg} \\ \bar{i}_{yg} \\ \bar{i}_{zg} \end{bmatrix} \tag{22}$$

Performing the matrix multiplication indicated gives:

$$\begin{aligned} \bar{i}_x &= \ell_1 \bar{i}_{Xg} + \ell_2 \bar{i}_{Yg} + \ell_3 \bar{i}_{Zg} \\ \bar{i}_y &= m_1 \bar{i}_{Xg} + m_2 \bar{i}_{Yg} + m_3 \bar{i}_{Zg} \\ \bar{i}_z &= n_1 \bar{i}_{Xg} + n_2 \bar{i}_{Yg} + n_3 \bar{i}_{Zg} \end{aligned} \tag{23}$$

The derivatives of $\bar{1}_x$, $\bar{1}_y$, $\bar{1}_z$ with respect to time in terms of their components in the inertial system are found by differentiating Equation 23. These derivatives are:

$$\begin{aligned} \dot{\bar{1}}_x &= \dot{\ell}_1 \bar{1}_{Xg} + \dot{\ell}_2 \bar{1}_{Yg} + \dot{\ell}_3 \bar{1}_{Zg} \\ \dot{\bar{1}}_y &= \dot{m}_1 \bar{1}_{Xg} + \dot{m}_2 \bar{1}_{Yg} + \dot{m}_3 \bar{1}_{Zg} \\ \dot{\bar{1}}_z &= \dot{n}_1 \bar{1}_{Xg} + \dot{n}_2 \bar{1}_{Yg} + \dot{n}_3 \bar{1}_{Zg} \end{aligned} \tag{24}$$

The derivatives of $\bar{1}_x$, $\bar{1}_y$, $\bar{1}_z$ with respect to time are dependent only on the change in direction of the unit vectors. Therefore,

$$\begin{aligned} \dot{\bar{1}}_x &= \bar{\omega} \times \bar{1}_x = r\bar{1}_y - q\bar{1}_z \\ \dot{\bar{1}}_y &= \bar{\omega} \times \bar{1}_y = p\bar{1}_z - r\bar{1}_x \\ \dot{\bar{1}}_z &= \bar{\omega} \times \bar{1}_z = q\bar{1}_x - p\bar{1}_y \end{aligned} \tag{25}$$

where

$$\bar{\omega} = p\bar{1}_x + q\bar{1}_y + r\bar{1}_z$$

Equating the relations for $\dot{\bar{1}}_x$ from Equations 24 and 25:

$$\dot{\ell}_1 \bar{1}_{Xg} + \dot{\ell}_2 \bar{1}_{Yg} + \dot{\ell}_3 \bar{1}_{Zg} = r\bar{1}_y - q\bar{1}_z$$

Substituting the relationships for $\bar{1}_y$ and $\bar{1}_z$, respectively, gives the relation:

$$\begin{aligned} \dot{\ell}_1 \bar{1}_{Xg} + \dot{\ell}_2 \bar{1}_{Yg} + \dot{\ell}_3 \bar{1}_{Zg} = {} & r(m_1 \bar{1}_{Xg} + m_2 \bar{1}_{Yg} + m_3 \bar{1}_{Zg}) \\ & - q(n_1 \bar{1}_{Xg} + n_2 \bar{1}_{Yg} + n_3 \bar{1}_{Zg}) \end{aligned} \tag{26}$$

By using the component properties of a vector, the relations

$$\dot{\ell}_1 = rm_1 - qn_1 \tag{27}$$

$$\dot{\ell}_2 = rm_2 - qn_2 \tag{28}$$

$$\dot{\ell}_3 = rm_3 - qn_3 \tag{29}$$

are obtained from Equation 26.

Performing the same operation for the $\dot{\bar{1}}_y$ and $\dot{\bar{1}}_z$ components defines the time derivatives of the remaining direction cosines. These are:

$$\dot{m}_1 = pn_1 - r\ell_1 \tag{30}$$

$$\dot{m}_2 = pn_2 - r\ell_2 \tag{31}$$

$$\dot{m}_3 = pn_3 - r\ell_3 \tag{32}$$

$$\dot{n}_1 = q\ell_1 - pm_1 \tag{33}$$

$$\dot{n}_2 = q\ell_2 - pm_2 \tag{34}$$

$$\dot{n}_3 = q\ell_3 - pm_3 \tag{35}$$

Equations 27 through 35 are integrated to obtain the instantaneous values of the direction cosines. This method of calculating the direction cosines has been selected instead of the usual evaluation by means of the Euler angles because, regardless of the order of rotation selected, there are points at which certain Euler angles become undefined. The direction cosines evaluated by this method are always defined (Reference 1). The method by which the orthogonality of the direction cosines is maintained is described in Appendix III of Reference 1. The Euler angles may be calculated from the direction cosines if desired; however, they are not required for component resolution.

(4) Inertial Velocity

The components of inertial velocity in the body coordinate system, u, v, and w, will be resolved into velocity components X_g, Y_g, and Z_g in the inertial coordinates. Since components of inertial velocity are known in body coordinates, a resolution of components using the direction cosines given in Equations (27-35) will give

components of inertial velocity in the inertial coordinate system, as follows:

$$\begin{bmatrix} \dot{X}_g \\ \dot{Y}_g \\ \dot{Z}_g \end{bmatrix} = \begin{bmatrix} \ell_1 & m_1 & n_1 \\ \ell_2 & m_2 & n_2 \\ \ell_3 & m_3 & n_3 \end{bmatrix} \begin{bmatrix} u \\ v \\ w \end{bmatrix} \tag{36}$$

The planet-referenced velocity may be calculated from its components:

$$V_g = \sqrt{\dot{X}_g^2 + \dot{Y}_g^2 + \dot{Z}_g^2} \tag{37}$$

(a) Nine integrations are involved in the present method of computation, instead of the three that are normally required when the Euler-angle rates are integrated to give the Euler angles. However, a coordinate transformation is required to obtain the rates, and the sines and cosines of the angles must also be computed in the usual direction cosine computation. The machine time required for the two methods of computation is comparable.

The flight-path angles are computed in the takeoff and landing problem:

$$\sigma = \sin^{-1}\left(\frac{\dot{Y}_g}{\sqrt{\dot{X}_g^2 + \dot{Y}_g^2}}\right) \tag{38}$$

$$\gamma = \sin^{-1}\left(\frac{-\dot{Z}_g}{V_g}\right) \tag{39}$$

The three inertial components of winds will be introduced in a tabular listing with altitude as the independent variable. Let the three components of wind be written as follows:

$$\overline{V}_w = \dot{X}_{g_w}\,\overline{i}_{x_g} + \dot{Y}_{g_w}\,\overline{i}_{y_g} + \dot{Z}_{g_w}\,\overline{i}_{z_g} \tag{40}$$

The airspeed vector is given by:

$$\overline{V}_a = \overline{V}_g - \overline{V}_w \tag{41}$$

where V_a is the velocity relative to the atmosphere. The three inertial components of airspeed are:

$$\overline{V}_a = (\dot{X}_g - \dot{X}_{g_w})\,\overline{i}_{x_g} + (\dot{Y}_g - \dot{Y}_{g_w})\,\overline{i}_{y_g} + (\dot{Z}_g - \dot{Z}_{g_w})\,\overline{i}_{z_g} \tag{42}$$

The elevation flight path angle of the airspeed vector is:

$$\gamma_a = \sin^{-1}\left(\frac{-(\dot{Z}_g - \dot{Z}_{g_w})}{V_a}\right) \tag{43}$$

Resolving inertial wind components to body-axis components requires the same direction-cosine matrix used in Equation 22, and the body components of winds are:

$$\begin{bmatrix} u_w \\ v_w \\ w_w \end{bmatrix} = \begin{bmatrix} \ell_1 & \ell_2 & \ell_3 \\ m_1 & m_2 & m_3 \\ n_1 & n_2 & n_3 \end{bmatrix} \begin{bmatrix} \dot{X}_{gw} \\ \dot{Y}_{gw} \\ \dot{Z}_{gw} \end{bmatrix} \tag{44}$$

The body components of airspeed are determined by substracting the body components of wind from the body components of velocity.

The body components of airspeed will be used to compute the angle of attack and sideslip.

$$\alpha = \mathrm{Tan}^{-1}\left(\frac{w - w_w}{u - u_w}\right) \tag{45}$$

$$\beta = \mathrm{Tan}^{-1}\left(\frac{v - v_w}{u - u_w}\right) \tag{46}$$

The definitions of angle of attack and sideslip are consistent with the aerodynamic data normally obtained from wind tunnel tests of sting-mounted models because of the manner in which the sting may be moved. If aerodynamic data as obtained from turntable-and-strut mounted models are used, an alternate definition may be required depending upon the procedure used in data reduction.

b. Guidance and Autopilot Coordinate Transformations

The vehicle attitude information taken from the gimbals of a stabilized platform and the outputs of platform-mounted accelerometers may be required in certain autopilot and guidance-system computations in the Takeoff and Landing Analysis computer program. This section presents the derivation of the equations relating accelerometer and attitude information to data computed in the central program. The method for deriving coordinate transformations for any gimbal arrangement is presented for reference.

(1) Gimbal Arrangements and Rotation Sequences

Three frequently used gimbal arrangements will be considered in this section. Each gimbal is equivalent to an intermediate coordinate system in a series of Euler-angle rotations. Reading from the outer gimbal to the inner gimbal (and neglecting redundant gimbals) the arrangements considered are:

(a) Yaw-Pitch-Roll

(b) Pitch-Yaw-Roll (only this sequence is programmed in TOLA)

(c) Pitch-Roll-Yaw

where the analogy between coordinate system rotations and gimbal movement is used. Other gimbal arrangements are possible but the three discussed in this section are the ones most frequently used.

Transformations for the alternate arrangements can be obtained with these same techniques.

(2) Euler Angles. In the central program, the direction cosines relating the vehicle body-coordinate system to a fixed inertial system are calculated by integrating functions of the body angular velocities, p, q, and r. The direction cosines relating the body and inertial systems are determined by the cosines of the angles between the various axes of the coordinate systems and are dependent only upon the position of the body coordinates referenced to inertial coordinates. That is, the order of rotation selected to arrive at a certain orientation does not alter the numerical values of the direction cosines for that orientation.

Each individual direction cosine may, therefore, be defined in terms of the Euler angles from a given sequence of rotations. These definitions will provide the Euler angles of the body with respect to the platform coordinate system for the three rotational sequences selected.

The direction cosines, in terms of three sets of Euler angles, will be derived using the method of Reference 15. The technique used is to find the direction cosines for each individual rotation in a sequence and determine the complete transformation by multiplying the individual direction cosine matrices. The overall picture of the rotations is best observed on a unit sphere diagram. The points on the unit sphere represent the intersections of the coordinate axes with the surface of the sphere.

The order of rotation and the axis about which rotation occurs can be described using the following diagram.

AXIS AND ROTATION			ORDER
X	Y	Z	
		Ψ	1.
ξ	η	Z	
	Θ		2.
x	η	ζ	
ϕ			3.
x	y	z	

This diagram indicates that the first rotation is about the inertial Z-axis through the Euler angle Ψ. The second rotation is about the intermediate axis η through the angle Θ. The final rotation is about the body x-axis through the angle ϕ.

The derivation of each sequence of rotations will proceed in the following manner: (a) the order of rotation will be defined; (b) the unit sphere showing all three rotations will be presented; (c) the individual rotations will be shown in three separate diagrams that contain the plane perpendicular to the appropriate axis of rotation; (d) the direction cosines for each individual rotation will be written in this manner:

$$\begin{vmatrix} \xi \\ \eta \\ \zeta \end{vmatrix} = \begin{vmatrix} C_{\xi X} & C_{\xi Y} & C_{\xi Z} \\ C_{\eta X} & C_{\eta Y} & C_{\eta Z} \\ C_{\zeta X} & C_{\zeta Y} & C_{\zeta Z} \end{vmatrix} \begin{vmatrix} X \\ Y \\ Z \end{vmatrix}$$

where C_{ij} is the cosine of the angle between the i and j axes; and (e) the matrix of direction cosines relating the inertial and body coordinates will be determined by matrix multiplication.

(a) Yaw-Pitch-Roll Rotation

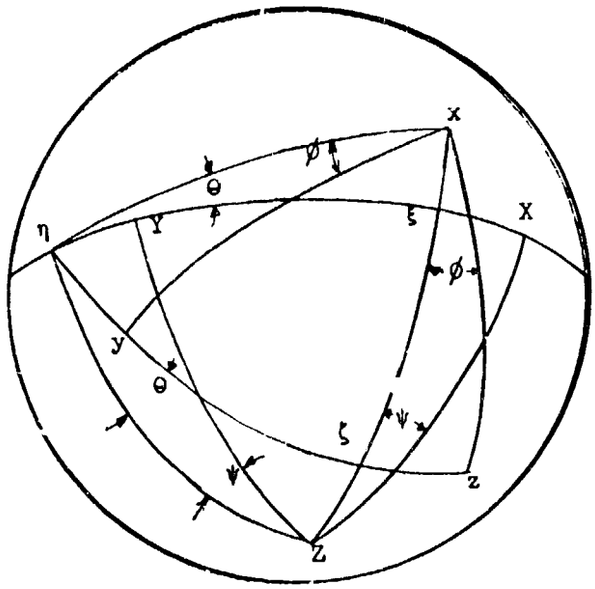

AXIS AND ROTATION			ORDER
X	Y	Z ↕ ψ	1.
ξ	η ↕ Θ	Z	2.
x ↕ ϕ	η	ζ	3.
x	y	z	

Figure 7. Unit Sphere for Yaw-Pitch-Roll Sequence of Rotation

FIRST ROTATION

$$\begin{vmatrix} \xi \\ \eta \\ z \end{vmatrix} = \begin{vmatrix} \cos\psi & \sin\psi & 0 \\ -\sin\psi & \cos\psi & 0 \\ 0 & 0 & 1 \end{vmatrix} \begin{vmatrix} X \\ Y \\ Z \end{vmatrix}$$

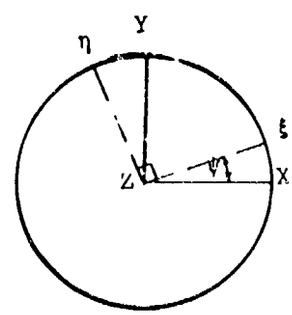

SECOND ROTATION

$$\begin{vmatrix} x \\ \eta \\ \zeta \end{vmatrix} = \begin{vmatrix} \cos\Theta & 0 & -\sin\Theta \\ 0 & 1 & 0 \\ \sin\Theta & 0 & \cos\Theta \end{vmatrix} \begin{vmatrix} \xi \\ \eta \\ Z \end{vmatrix}$$

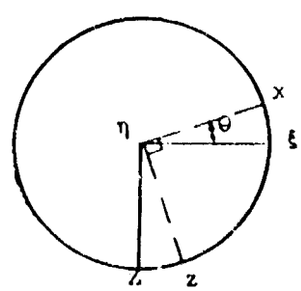

THIRD ROTATION

$$\begin{vmatrix} x \\ y \\ z \end{vmatrix} = \begin{vmatrix} 1 & 0 & 0 \\ 0 & \cos\phi & \sin\phi \\ 0 & -\sin\phi & \cos\phi \end{vmatrix} \begin{vmatrix} x \\ \eta \\ \zeta \end{vmatrix}$$

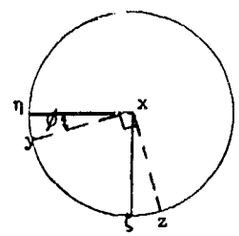

The transformation matrix is given by

$$\begin{vmatrix} x \\ y \\ z \end{vmatrix} = \begin{vmatrix} \phi \end{vmatrix} \begin{vmatrix} \theta \end{vmatrix} \begin{vmatrix} \psi \end{vmatrix} \begin{vmatrix} X \\ Y \\ Z \end{vmatrix}$$

or, in terms of the planar rotation matrices, the intermediate axes are eliminated by

$$\begin{vmatrix} x \\ y \\ z \end{vmatrix} = \begin{vmatrix} 1 & 0 & 0 \\ 0 & \cos\phi & \sin\phi \\ 0 & -\sin\phi & \cos\phi \end{vmatrix} \begin{vmatrix} \cos\theta & 0 & -\sin\theta \\ 0 & 1 & 0 \\ \sin\theta & 0 & \cos\theta \end{vmatrix} \begin{vmatrix} \cos\psi & \sin\psi & 0 \\ -\sin\psi & \cos\psi & 0 \\ 0 & 0 & 1 \end{vmatrix} \begin{vmatrix} X \\ Y \\ Z \end{vmatrix}$$

The direction cosine elements of the transformation matrix are obtained by performing the indicated multiplication. For the yaw-pitch-roll rotational sequence

$$\begin{vmatrix} x \\ y \\ z \end{vmatrix} = \begin{vmatrix} (\cos\theta\cos\psi) & (\cos\theta\sin\psi) & (-\sin\theta) \\ (-\cos\phi\sin\psi + \sin\phi\sin\theta\cos\psi) & (\cos\phi\cos\psi + \sin\phi\sin\theta\sin\psi) & (\sin\phi\cos\theta) \\ (\sin\phi\sin\psi + \cos\phi\sin\theta\cos\psi) & (-\sin\phi\cos\psi + \cos\phi\sin\theta\sin\psi) & (\cos\phi\cos\theta) \end{vmatrix} \begin{vmatrix} X \\ Y \\ Z \end{vmatrix} \qquad (47)$$

(b) Pitch-Yaw-Roll Rotation

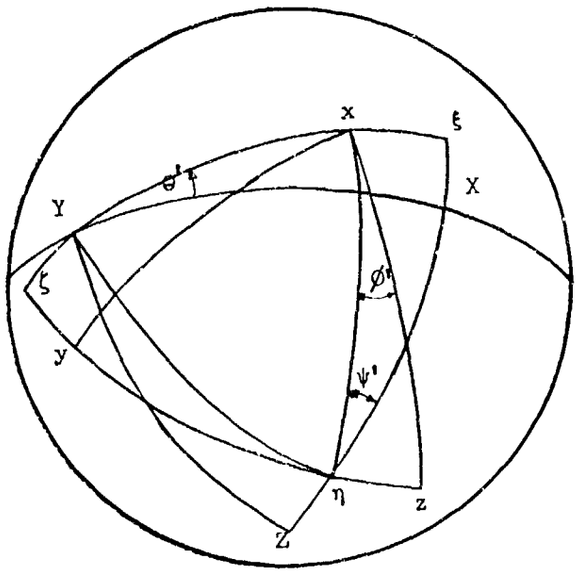

AXIS AND ROTATION			ORDER
X	Y	Z	
	↕ θ'		1.
ξ	Y	η	
		↕ ψ'	2.
x	ζ	η	
↕ φ'			3.
x	y	z	

Figure 8. Unit Sphere for Pitch-Yaw-Roll Sequence of Rotation

FIRST ROTATION

$$\begin{vmatrix} \xi \\ Y \\ \eta \end{vmatrix} = \begin{vmatrix} \cos\theta' & 0 & -\sin\theta' \\ 0 & 1 & 0 \\ \sin\theta' & 0 & \cos\theta' \end{vmatrix} \begin{vmatrix} X \\ Y \\ Z \end{vmatrix}$$

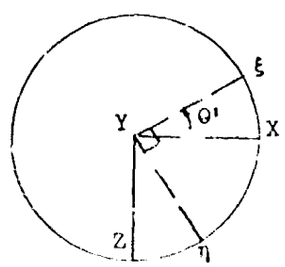

SECOND ROTATION

$$\begin{vmatrix} x \\ \zeta \\ \eta \end{vmatrix} = \begin{vmatrix} \cos\psi' & \sin\psi' & 0 \\ -\sin\psi' & \cos\psi' & 0 \\ 0 & 0 & 1 \end{vmatrix} \begin{vmatrix} \xi \\ Y \\ \eta \end{vmatrix}$$

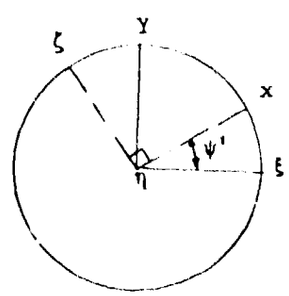

THIRD ROTATION

$$\begin{vmatrix} x \\ y \\ z \end{vmatrix} = \begin{vmatrix} 1 & 0 & 0 \\ 0 & \cos\phi' & \sin\phi' \\ 0 & -\sin\phi' & \cos\phi' \end{vmatrix} \begin{vmatrix} x \\ \zeta \\ \eta \end{vmatrix}$$

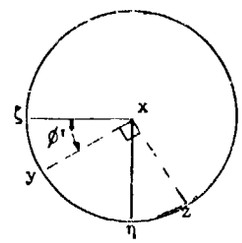

The transformation matrix is given by

$$\begin{vmatrix} x \\ y \\ z \end{vmatrix} = \begin{vmatrix} \phi' \end{vmatrix} \begin{vmatrix} \psi' \end{vmatrix} \begin{vmatrix} \theta' \end{vmatrix} \begin{vmatrix} X \\ Y \\ Z \end{vmatrix}$$

or, in terms of the planar rotation matrices, the intermediate axes are eliminated by

$$\begin{vmatrix} x \\ y \\ z \end{vmatrix} = \begin{vmatrix} 1 & 0 & 0 \\ 0 & \cos\phi' & \sin\phi' \\ 0 & -\sin\phi' & \cos\phi' \end{vmatrix} \begin{vmatrix} \cos\psi' & \sin\psi' & 0 \\ -\sin\psi' & \cos\psi' & 0 \\ 0 & 0 & 1 \end{vmatrix} \begin{vmatrix} \cos\theta' & 0 & -\sin\theta' \\ 0 & 1 & 0 \\ \sin\theta' & 0 & \cos\theta' \end{vmatrix} \begin{vmatrix} X \\ Y \\ Z \end{vmatrix}$$

The direction cosine elements of the transformation matrix are obtained by performing the indicated multiplication. For the pitch-yaw-roll rotational sequence

$$\begin{vmatrix} x \\ y \\ z \end{vmatrix} = \begin{vmatrix} (\cos\psi' \cos\theta') & (\sin\psi') & (-\cos\psi' \sin\theta') \\ (\sin\phi' \sin\theta' - \cos\phi' \sin\psi' \cos\theta') & (\cos\phi' \cos\psi') & (\sin\phi' \cos\theta' + \cos\phi' \sin\theta' \sin\psi') \\ (\cos\phi' \sin\theta' + \cos\theta' \sin\psi' \sin\phi') & (-\sin\phi' \cos\psi') & (\cos\phi' \cos\theta' - \sin\phi' \sin\theta' \sin\psi') \end{vmatrix} \begin{vmatrix} X \\ Y \\ Z \end{vmatrix} \qquad (48)$$

(c) Pitch-Roll-Yaw Rotation

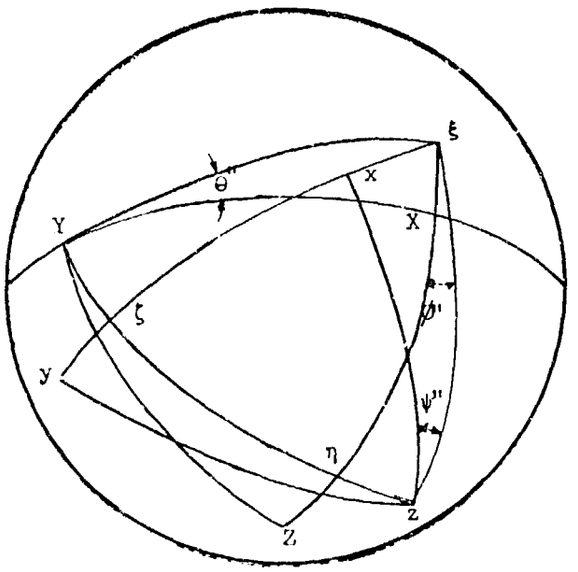

AXIS AND ROTATION			ORDER
X	Y	Z	
	θ"		1.
ξ	Y	η	
ϕ"			2.
ξ	ζ	z	
		ψ"	3.
x	y	z	

Figure 9. Unit Sphere for Pitch-Roll Yaw Sequence of Rotation

FIRST ROTATION

$$\begin{vmatrix} \xi \\ Y \\ \eta \end{vmatrix} = \begin{vmatrix} \cos\theta'' & 0 & -\sin\theta'' \\ 0 & 1 & 0 \\ \sin\theta'' & 0 & \cos\theta'' \end{vmatrix} \begin{vmatrix} X \\ Y \\ Z \end{vmatrix}$$

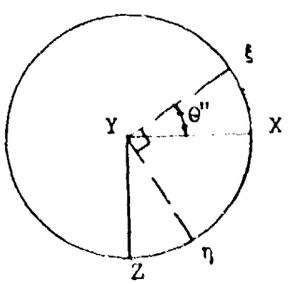

SECOND ROTATION

$$\begin{vmatrix} \xi \\ \zeta \\ Z \end{vmatrix} = \begin{vmatrix} 1 & 0 & 0 \\ 0 & \cos\phi'' & \sin\phi'' \\ 0 & -\sin\phi'' & \cos\phi'' \end{vmatrix} \begin{vmatrix} \xi \\ Y \\ \eta \end{vmatrix}$$

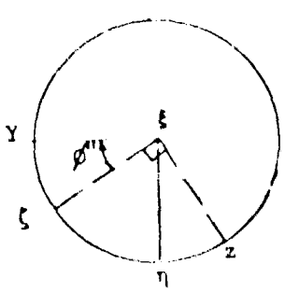

THIRD ROTATION

$$\begin{vmatrix} x \\ y \\ z \end{vmatrix} = \begin{vmatrix} \cos\psi'' & \sin\psi'' & 0 \\ -\sin\psi'' & \cos\psi'' & 0 \\ 0 & 0 & 1 \end{vmatrix} \begin{vmatrix} \xi \\ \zeta \\ z \end{vmatrix}$$

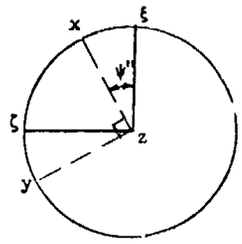

The transformation matrix is given by

$$\begin{vmatrix} x \\ y \\ z \end{vmatrix} = \begin{vmatrix} \psi'' \end{vmatrix} \begin{vmatrix} \phi'' \end{vmatrix} \begin{vmatrix} \theta'' \end{vmatrix} \begin{vmatrix} X \\ Y \\ Z \end{vmatrix}$$

or, in terms of the planar rotation matrices, the intermediate axes are eliminated by

$$\begin{vmatrix} x \\ y \\ z \end{vmatrix} = \begin{vmatrix} \cos\psi'' & \sin\psi'' & 0 \\ -\sin\psi'' & \cos\psi'' & 0 \\ 0 & 0 & 1 \end{vmatrix} \begin{vmatrix} 1 & 0 & 0 \\ 0 & \cos\phi'' & \sin\phi'' \\ 0 & -\sin\phi'' & \cos\phi'' \end{vmatrix} \begin{vmatrix} \cos\theta'' & 0 & -\sin\theta'' \\ 0 & 1 & 0 \\ \sin\theta'' & 0 & \cos\theta'' \end{vmatrix} \begin{vmatrix} X \\ Y \\ Z \end{vmatrix}$$

The direction cosine elements of the transformation matrix are obtained by performing the indicated multiplication. For the pitch-roll-yaw rotational sequence

$$\begin{vmatrix} x \\ y \\ z \end{vmatrix} = \begin{vmatrix} (\cos\psi''\cos\theta'' + \sin\psi''\sin\phi''\sin\theta'') & (\sin\psi''\cos\phi'') & (-\cos\psi''\sin\theta'' + \sin\psi''\sin\phi''\cos\theta'') \\ (-\sin\psi''\cos\theta'' + \cos\psi''\sin\phi''\sin\theta'') & (\cos\psi''\cos\phi'') & (\sin\theta''\sin\psi'' + \cos\psi''\sin\phi''\cos\theta'') \\ (\cos\phi''\sin\theta'') & (-\sin\phi'') & (\cos\phi''\cos\theta'') \end{vmatrix} \begin{vmatrix} X \\ Y \\ Z \end{vmatrix} \quad (49)$$

The directi[illegible]sines relating body and inertial coordinates are assigned the following symbols in the central program (see Equation 22).

$$\begin{vmatrix} x \\ y \\ z \end{vmatrix} = \begin{vmatrix} \ell_1 & \ell_2 & \ell_3 \\ m_1 & m_2 & m_3 \\ n_1 & n_2 & n_3 \end{vmatrix} \begin{vmatrix} X_g \\ Y_g \\ Z_g \end{vmatrix} \tag{50}$$

By comparing identical positions in the matrix of Equation 50 with the matrices in Equations 47, 48, or 49, the direction cosines above are defined in terms of the appropriate sequence of Euler angles.

(4) Platform Angles for a Flat-Planet Problem

For a flat-planet problem, the orientation of the platform coordinate system will be assumed to coincide with the flat-planet coordinates. Therefore, the angles measured on the gimbals of this platform may be determined for the three gimbal arrangements considered. For the yaw-pitch-roll gimbal system, the following direction cosine relationships are obtained by comparing corresponding positions in the matrices used in Equations 47 and 50. Five elements are sufficient to define these angles.

$$\begin{aligned} \ell_3 &= -\text{Sin}\ \Theta \\ \ell_2 &= \text{Cos}\ \Theta\ \ \text{Sin}\ \psi \\ \ell_1 &= \text{Cos}\ \Theta\ \ \text{Cos}\ \psi \\ m_3 &= \text{Sin}\ \phi\ \ \text{Cos}\ \Theta \\ n_3 &= \text{Cos}\ \phi\ \ \text{Cos}\ \Theta \end{aligned} \tag{51}$$

The first equation defines the angle Θ. The angles ψ and ϕ may be defined explicitly by combining the second and third equations and the fourth and fifth equations, thus,

$$\text{Sin}\ \Theta = -\ell_3$$

$$\text{Tan}\ \psi = \ell_2/\ell_1$$

and

$$\text{Tan}\ \phi = m_3/n_3$$

For the flat-planet problem with the platform stabilized to coincide with the X_g-Y_g-Z_g coordinates, these angles represent the angles measured on the gimbals and will be designated with a subscript p.

$$\begin{aligned} \theta_p &= -\mathrm{Sin}^{-1}\, \ell_3 \\ \psi_p &= \mathrm{Tan}^{-1}\, \ell_2/\ell_1 \\ \phi_p &= \mathrm{Tan}^{-1}\, m_3/n_3 \end{aligned} \tag{52}$$

Similarly, the angles measured on a pitch-yaw-roll gimbal arrangement may be computed by comparing identical positions in the matrices used in Equations 48 and 50.

$$\begin{aligned} \ell_2 &= \mathrm{Sin}\, \psi_p' \\ \ell_1 &= \mathrm{Cos}\, \psi_p'\, \mathrm{Cos}\, \theta_p' \\ \ell_3 &= -\mathrm{Cos}\, \psi_p'\, \mathrm{Sin}\, \theta_p' \\ m_2 &= \mathrm{Cos}\, \phi_p'\, \mathrm{Cos}\, \psi_p' \\ n_2 &= -\mathrm{Sin}\, \phi_p'\, \mathrm{Cos}\, \psi_p' \end{aligned} \tag{53}$$

Then

$$\begin{aligned} \mathrm{Sin}\, \psi_p' &= \ell_2 \\ \mathrm{Tan}\, \theta_p' &= -\ell_3/\ell_1 \\ \mathrm{Tan}\, \phi_p' &= -n_2/m_2 \end{aligned}$$

Again for the flat-planet problem, the gimbal angles for this arrangement are:

$$\begin{aligned} \psi_p' &= \mathrm{Sin}^{-1}\, \ell_2 \\ \theta_p' &= \mathrm{Tan}^{-1}\, -\ell_3/\ell_1 \\ \phi_p' &= \mathrm{Tan}^{-1}\, -n_2/m_2 \end{aligned} \tag{54}$$

The appropriate direction cosines for the computation of the angles for a pitch-roll-yaw system are:

$$
\begin{aligned}
n_2 &= -\mathrm{Sin}\ \phi_p'' \\
m_2 &= \mathrm{Cos}\ \psi_p''\ \mathrm{Cos}\ \phi_p'' \\
l_2 &= \mathrm{Sin}\ \psi_p''\ \mathrm{Cos}\ \phi_p'' \\
n_1 &= \mathrm{Cos}\ \phi_p''\ \mathrm{Sin}\ \theta_p'' \\
n_3 &= \mathrm{Cos}\ \phi_p''\ \mathrm{Cos}\ \theta_p''
\end{aligned}
\tag{55}
$$

The platform angles are found from these direction cosines to be:

$$
\begin{aligned}
\phi_p'' &= -\mathrm{Sin}^{-1}\ n_2 \\
\theta_p'' &= \mathrm{Tan}^{-1}\ n_1/n_3 \\
\psi_p'' &= \mathrm{Tan}^{-1}\ l_2/m_2
\end{aligned}
\tag{56}
$$

For the flat-planet problem, the angles derived in Equations 51 through 56 represent the attitudes of the vehicle with respect to the X_g-Y_g-Z_g flat-planet coordinates and also with respect to a platform coordinate system whose respective X_p Y_p-Z_p axes are parallel to $X_g Y_g Z_g$. The computation of these platform relations are summarized, along with the accelerometer indication in Figure 10.

(5) Accelerometer Indications. Let $\bar{A}$ be the vector sum of the platform accelerometer outputs and $\bar{g}$ be the mass attractive acceleration of the planet. The accelerometers are calibrated to read zero when they are unaccelerated and aligned such that the sensitive axis is perpendicular to $\bar{g}$. The vector $\bar{R}$ will represent the displacement of the platform with respect to the inertial axes. It will be shown that $\bar{A} = \ddot{\bar{R}} - \bar{g}$, where $\ddot{\bar{R}}$ is the inertial acceleration of the origin of the platform. Consider the vehicle accelerating vertically at 1g. In inertial components, then

$$\ddot{\bar{R}} = -g\ \bar{i}_{z_g} \tag{57}$$

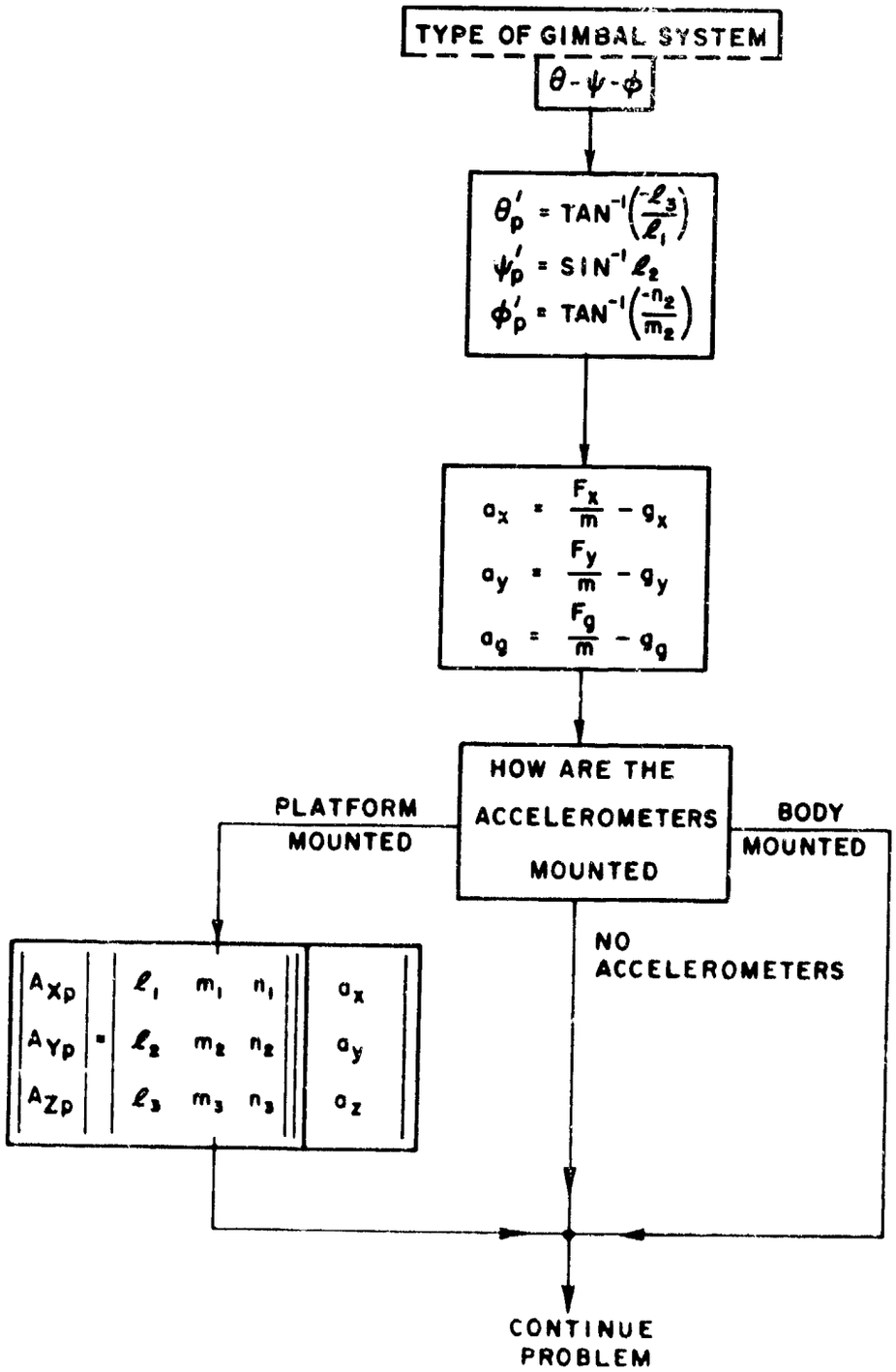

Figure 10. Functional Flow Diagram - Platform Angles for Six-Degree-of-Freedom Flat-Planet Option

In the absence of a gravitational field, the accelerometer should read -1g. Positive motion of the accelerometer mass along the Zg axis represents a negative acceleration in this case, and the vector $\bar{g}$ is equal to g $\bar{1}$Zg. Consideration of the gravitational field will cause an additional displacement of the accelerometer mass in the positive Zg direction, giving a total indication of -2g. The equation

$$\bar{A} = \ddot{\bar{R}} - \bar{g} \tag{58}$$

will be evaluated from the data

$$\ddot{\bar{R}} = -1g\ \bar{1}_{z_g}$$

so that

$$\bar{A} = -2g\ \bar{1}_{z_g} \tag{59}$$

This result is shown schematically in Figure 11.

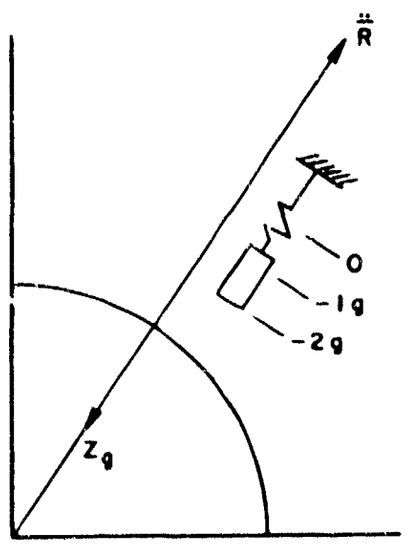

Figure 11. Accelerometer With Sensitive Axis Aligned With Local-Geocentric Vertical

The vector $\bar{A}$ is equal to the vector sum of the accelerations produced by the externally applied forces. The body components of the externally applied forces may be taken from the separate subprogram which gives the summation of forces and moments. F_x, F_y, and F_z are the body components of the external forces plus the weight. The weight must then be substracted to determine the body components of $\bar{A}$:

$$\bar{A} = \ddot{\bar{R}} - \bar{g} = \left(\frac{F_x - m g_x}{m}\right)\bar{i}_x + \left(\frac{F_y - m g_y}{m}\right)\bar{i}_y + \left(\frac{F_z - m g_z}{m}\right)\bar{i}_z = a_x \bar{i}_x + a_y \bar{i}_y + a_z \bar{i}_z \tag{60}$$

3. VEHICLE CHARACTERISTICS

The methods by which the aerodynamic, propulsive, and physical characteristics of a vehicle are introduced into the Takeoff and Landing Analysis computer program are presented in this section. The form and preparation of these input data are discussed together with methods by which stages and staging may be used to increase the effective data storage area allotted to a description of the vehicle's properties.

a. Aerodynamic Coefficients

(1) Form of Data Input

The primary objective of the aerodynamic data input subprogram is to provide for a complete accounting of the various contributions to the aerodynamic forces and moments regardless of the flight conditions or the vehicle. Two powerful techniques are available for use in digital computer programs: (a) an n-dimensional table look-up and interpolation and (b) an m-order polynomial function of n variables prepared by "curve fit" techniques. In the first method, the proper value for each term is obtained by an interpolation in "n" dimensions where the number of dimensions is taken to be the number of parameters to be varied independently plus the dependent variable. This method has the advantage of accurately describing even the most nonlinear variations with a minimum of preparation effort. The amount of storage space which must be allocated to such a method, however, can achieve completely unreasonable proportions and may require

substantial computing time for interpolation as the number of dimensions is increased. The second method has essentially the opposite characteristics; that is, a large amount of data may be represented with a minimum amount of storage space and the computation time is held to reasonable limits but the data variations which may be represented must be regular. A substantial amount of effort is usually required for the preparation of data by a curve-fit technique. Both of these methods are very convenient when the amount of data to be handled is moderate, but tend to become unmanageable when large amounts of data are required. This usually occurs when the program having several degrees of freedom, is committed to one or the other of these two techniques. Therefore, the Takeoff and Landing Analysis computer program will incorporate both of the techniques discussed as a compromise to take advantage of the more desirable features of both. To do this, a general set of data equations will be programmed which define each of the aerodynamic forces or moments. In general, the coefficients for these equations will be obtained from a curve-read interpolation. Several simplifications may be made to the equations, depending on the flight condition and vehicle to be considered.

The effects of the following parameters will be considered:

(a) Angle of attack and its time derivative $(\alpha, \dot{\alpha})$

(b) Angle of sideslip and its time derivative $(\beta, \dot{\beta})$

(c) Roll, pitch, and yaw control deflections $(\delta_p, \delta_q, \delta_r)$

(d) Roll, pitch, and yaw angular rates (p, q, r)

(e) Center-of-gravity position $(X_{C.G.})$

The aerodynamic forces and moments considered with respect to each coordinate axis include the effects of angle of attack and sideslip, primary control deflection with respect to each axis, lag of downwash, and primary damping effects. In addition, the rolling moment due to yaw rate is included. Complete generality in the aerodynamic coupling effects has not been included in the present subprogram options since the descriptive terms required depend upon the particular problem. The storage space provided for the several existing options is considered to be adequate to accommodate other special problem formulations through substitution of terms.

Quite often the particular application will not require some of the terms listed in order to describe completely the flight path and vehicle under consideration. The subprogram will be arranged so that the computer will assign a constant value to any curve for which the data has not been supplied. For most curves, the constant value will be zero. This technique will reduce substantially the time required for the preparation of data. Values intermediate to those introduced in a tabular listing will be obtained by linear interpolation. The method of incorporating data for staged vehicles is discussed in the paragraph entitled Stages and Staging.

(2) Flight Path and Vehicle Types

In most of the cases discussed below, a "curve-fit" technique will be used to obtain all or a portion of the aerodynamic terms. For the purpose of this subprogram, it will be assumed that the curve fit has been selected to represent the variation of the coefficient about the trim conditions. This may have the effect of removing physical significance from some of the individual terms, and only the sum of the terms will represent the data. A typical example is Figure 12.

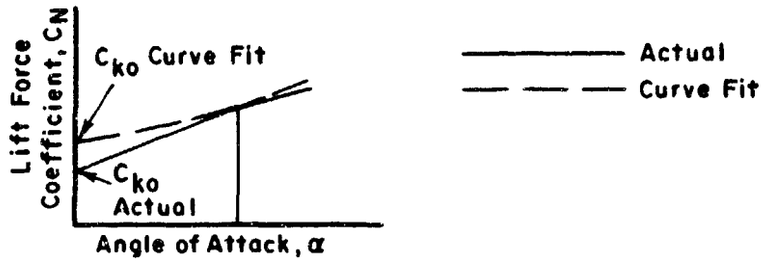

Figure 12. Curve Fit Nonlinear Aerodynamic Characteristics

In this case, the C_{L_0} and C_{L_α} values used in the equation for C are obviously different from the actual values of these parameters.

A functional flow diagram for the solution of the aerodynamic forces and moments is presented in Figure 13. It should be noted that the actual machine programming will not necessarily follow the sequence shown since certain computer operations have been omitted in this description of the problem formulation.

A controlled aircraft represents the most general case that will be considered. In order to account for the many component forces, we made certain restricting assumptions. The assumptions will be made that the aircraft is confined to moderate variations in position angles and control deflections. Center-of-gravity shift along the x-axis is included. The coefficients can then be expressed as shown in Block 3 of Figure 13. The functional computation sequence for this option proceeds from Block 1 to Block 5 in a straightforward manner.

The change in dynamic derivatives due to a change in the center-of-gravity location is programmed as a curve-read in order to avoid the complications of a transfer. The definition of α and β as applied to the TOLA computer program (see Equations 45 and 46) is

$$\alpha = \mathrm{Tan}^{-1}\left(\frac{w - w_w}{u - u_w}\right) \text{ and } \beta = \mathrm{Tan}^{-1}\left(\frac{v - v_w}{u - u_w}\right) \tag{61}$$

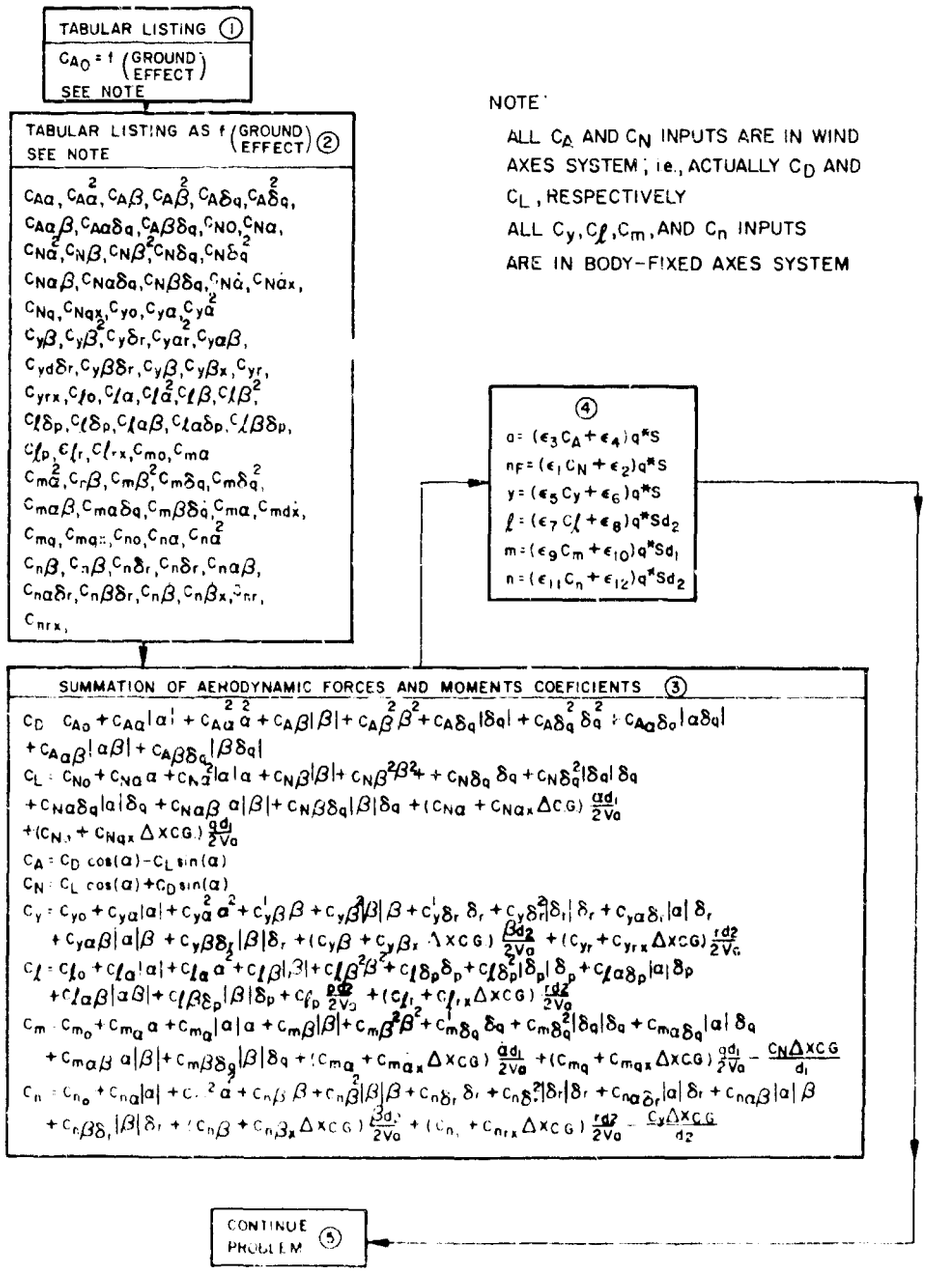

Figure 13. Solution of Aerodynamic Forces and Moments Subprogram

Data supplied must correspond to this definition or an alternate computation of these angles must be formulated to agree with the method of data reduction.

(3) Error Constants

The use of error constants, designated by the symbol e_i, to modify the aerodynamic data characteristics is shown in Figure 13. A detailed explanation of these error constants and their use is given later.

b. Thrust Fuel Flow Data

An airbreathing engine is strongly affected by the environmental conditions under which it is operating. Engines which would be grouped in this classification are turbojets, ramjets, pulsejets, turboprops, and reciprocating machines. The parameters which will be considered of consequence in this program are:

(a) Mach Number (M_N)

(b) Throttle setting (N - units defined by problem).

To accommodate these variables, a three-dimensional tabular listing and interpolation will be used to obtain thrust. The thrust needs no further correction since the effects of all parameters are included in the interpolated value. The functional computation sequence for introducing these data is straightforward, as outlined in Figure 14.

The same thrust table is used for each of i engines, where i = 1, ..., IN. Each throttle may be varied independently by the Throttle Autopilot. All thrust vectors are assumed to act:

$$T_x = \sum_{i=1}^{IN} T_i \, (N_i, M_N) \tag{62}$$

$$T_x = \sum_{i=1}^{IN} T_i \; (N_i, M_N)$$

$$M_T = \sum_{i=1}^{IN} M_{Ti} = \sum_{i=1}^{IN} T_i \, z_{Ni}$$

$$N_T = \sum_{i=1}^{IN} N_{Ti} = \sum_{i=1}^{IN} -T_i \, y_{Ni}$$

CONTINUE PROBLEM

Figure 14. Thrust Forces and Moments Subprogram

where T_x is the x- component of thrust in the vehicle body-axes system. (A positive T produces a positive $\dot{u}$.) This force will introduce moments:

$$M_T = \sum_{i=1}^{IN} M_{Ti} = \sum_{i=1}^{IN} T_i \, z_{Ni}$$
$$N_T = \sum_{i=1}^{IN} N_{Ti} = \sum_{i=1}^{IN} -T_i \, y_{Ni} \tag{63}$$

where M_T and N_T are the thrust moments about the vehicle y and z body axes, respectively, and y_{Ni} and z_{Ni} are the distances to the center of gravity of the ith engine from the reference center of gravity, where i = 1, 2, ..., IN.

c. Physical Characteristics

The methods to be employed for the introduction of vehicle physical characteristics into the Takeoff and Landing Analysis computer program are outlined in this section. A table look-up and interpolation technique is used to determine those parameters which are variable. A provision is made for introducing error constants into several of the parameters.

(1) Categories of Physical Characteristics

Physical characteristics are introduced into the computer program in two groups: (a) characteristics used in the general solution of the equations of motion, and (b) characteristics used only in specific, or auxiliary, subprograms. The following items will be defined in the general vehicle characteristics subprogram:

(a) Initial mass of the vehicle ($\mathcal{M}_0$),

(b) Reference area (S),

(c) Reference lengths (d_1, d_2),

(d) Reference center-of-gravity location ($X_{cg\ Ref}$),

(e) Rotating machinery pitch angle (θ_r),

(f) Rotating machinery angular rate (ω_r),

(g) Rotating machinery moments of inertia (I_{x_r}, I_{y_r}, I_{z_r}),

(h) Vehicle center-of-gravity location (x_{cg}),

(i) Vehicle moments of Inertia (I_{xx}, I_{yy}, I_{zz}, I_{xy}, I_{xz}, I_{yz}), and

(j) Reference jet-damping lengths (l_y, l_z, l_l, l_m, l_n).

Items (a) through (g) will be constant throughout any stage. Items (h) through (j) will be variable during the stage due to the variation in mass caused by fuel consumption. Figure 15 presents a functional flow diagram defining the manner in which these characteristics are introduced into the computer program.

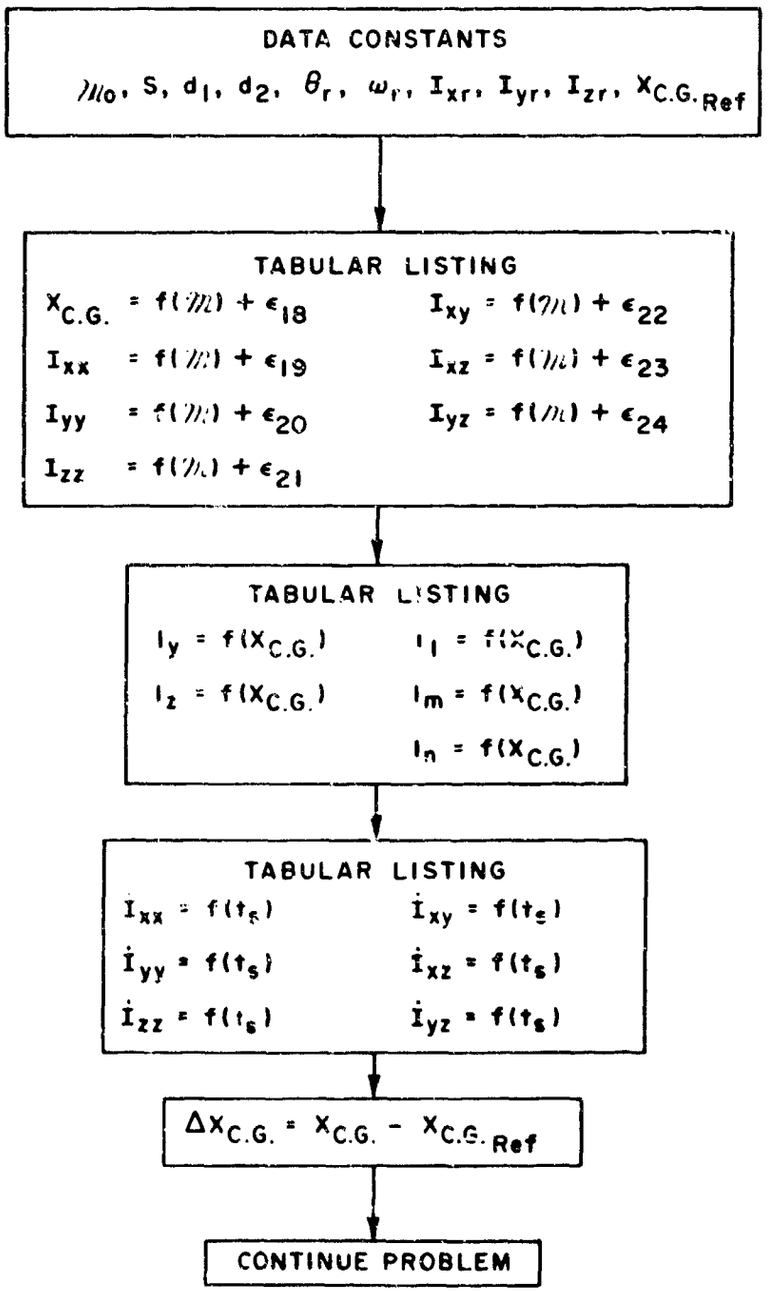

Figure 15. Vehicle Physical Characteristics Subprogram

(2) Reference Weight. The instantaneous mass is used in the computation of the body motion. The reference weight is obtained by:

$$W_T = \mathcal{M}(32.174) \tag{64}$$

(3) Error Constants. The use of error constants, designated by the symbol ϵ_i, to modify the general vehicle physical characteristics is shown in Figure 15. A detailed explanation of these error constants and their use is given later.

d. Stages and Staging

A problem encountered frequently in airplane performance work is that of staging to allow a set of aerodynamic data to be changed. Stage changes at constant weight, such as extending drag brakes or turning on afterburners, may also require revising the aerodynamic or physical characteristics of the vehicle. Another use of the staging technique is possible with the present computer program which does not involve physical changes to the configuration; this technique may be used to revise the aerodynamic descriptors as a function of aerodynamic attitude or Mach number. With this use of the stage concept, accurate descriptions of the forces and moments acting upon a vehicle may be maintained over wide attitude ranges if required. Other applications of this stage technique are possible. Normally it is not practical to stop the computer and manually insert a new set of data. A better approach is to have the computer do this automatically: new data will be loaded automatically on the basis of whether a specified variable has exceeded or become less than a preselected value. For generality, it is possible to test on four values in each direction.

When the new data are read in, the conditions representing the last time step will be read in as initial conditions for the next stage. This avoids the discontinuity that would result from an infinite rate of change of center-of-gravity location. It also will cause the integration routine to be started over, which will reduce the computer-induced transients due to staging.

e. Error Analyses

The Takeoff and Landing Analysis computer program will incorporate a provision for conveniently performing flight-path error and dispersion analyses by trajectory computation. This problem involves the determination of flight-path dispersion due to deviations of input quantities from their predicted nominal values. The usual approach to this type of problem requires that a series of trajectories be computed in which standard deviations, or errors, are systematically introduced for each parameter while the remaining parameters are held at their nominal values. These results are then combined to determine the "probable" dispersion. This approach will be implemented in the Takeoff and Landing Analysis computer program by providing a simple and efficient method of introducing the deviations. The capability of modifying a nominal value by either an error constant multiplier or an additive error constant is provided for many of the parameters as outlined below. The provision of these error constants will reduce substantially the number of tabular data listings that must be changed for an error analysis, thereby reducing the work of the analyst. The determination of the standard deviation of each of the parameters and the method of combining the trajectory variations are left to the analyst in view of the multiplicity of combinations possible.

(1) Aerodynamic Data. The provision to modify the aerodynamic coefficients through the use of error constants, ϵ_i, is outlined in Figure 13. The constants are applied as follows:

$$
\begin{aligned}
h_F &= (\epsilon_1 C_N + \epsilon_2) q^* S \\
q &= (\epsilon_3 C_A + \epsilon_4) q^* S \\
y &= (\epsilon_5 C_y + \epsilon_6) q^* S \\
l &= (\epsilon_7 C_L + \epsilon_8) q^* S d_2 \\
m &= (\epsilon_9 C_m + \epsilon_{10}) q^* S d_1 \\
n &= (\epsilon_{11} C_n + \epsilon_{12}) q^* S d_2
\end{aligned}
$$

These error constants allow the total aerodynamic coefficient to be modified to account for configuration modification, experimental or analytical error, or misalignments.

(2) Vehicle Physical Characterisitcs

The provision to modify some of the vehicle physical characteristics through the use of error constants is outlined in Figure 15. The constants are applied as follows:

$$
\begin{aligned}
x_{CG} &= f(m) + \epsilon_{18} \\
I_{xx} &= f(m) + \epsilon_{19} \\
I_{yy} &= f(m) + \epsilon_{20} \\
I_{zz} &= f(m) + \epsilon_{21} \\
I_{xy} &= f(m) + \epsilon_{22} \\
I_{xz} &= f(m) + \epsilon_{23} \\
I_{yz} &= f(m) \quad \epsilon_{24}
\end{aligned}
$$

In the application of error constants in the above equations caution must be exercised to insure that the units are consistent. Each of the error constants will be assigned a nominal value which will be used when no other value is specified. The constants which are multipliers will have a nominal value of unity, and those that are additive will have a nominal value of zero.

(3) Additional Errors. Not all of the system input constants can be modified for error analysis studies as indicated above. In certain cases, it may be found unrealistic to modify the input data through the use of error constants because the actual deviation would not appear as simply a constant increment or percentage change. An example of such a case would be the change in thrust-time history of a rocket due to temperature changes of the propellant since such a change affects both thrust level and burning time. For an accurate representation of such a case, it would be necessary to modify the entire tabular listing accordingly.

4. VEHICLE ENVIRONMENT

The models for simulating the environment in which a vehicle will operate are presented in this section. This environment includes the atmospheric wind. In the discussions which follow, the descriptions of vehicle environment pertain to the planet Earth. The environmental simulation may be extended to any planet by replacing appropriate constants in the describing equations.

a. Atmospheres

The concept of a model atmosphere was introduced many years ago, and over the years several models have been developed. Reference 16 outlines the historical background of the gradual evolution of the ARDC model. The original (1956) ARDC model has been revised to reflect the density variation with altitude that was obtained from an analysis of artificial satellite orbit data. This revision is the 1959 ARDC Model Atmosphere.

The advantage of a model atmosphere is that it provides a common reference upon which performance calculations can be based. The model is not intended to be the "final word" on the properties of the atmosphere for a particular time and location. It must be realized that the properties of the atmosphere are quite variable and are affected by many parameters other than altitude. At the present time, the "state-of-the-art" is not advanced to the point where these parameters can be accounted for, and it may be several years before the effects of some parameters can be evaluated.

(1) 1959 ARDC Model Atmosphere.

The 1959 ARDC Model Atmosphere is specified in layers assuming either isothermal or linear temperature lapse-rate sections. This construction makes it very convenient to incorporate other atmospheres, either from specifications for design purposes or for

other planets. The relations which mathematically specify the 1959 ARDC Model Atmosphere are as follows (Reference 17):

The 1959 ARDC Model Atmosphere is divided into 11 layers as follows:

Layer	H_b-Lower Altitude (Geopotential) Meters	Upper Altitude (Geopotential) Meters
1	0	11,000
2	11,000	25,000
3	25,000	47,000
4	47,000	53,000
5	53,000	79,000
6	79,000	90,000
7	90,000	105,000
8	105,000	160,000
9	160,000	170,000
10	170,000	200,000
11	200,000	700,000

For layers 1, 3, 5, 7, 8, 9, 10, and 11, a linear molecular-scale temperature lapse-rate is assumed and the following equations are used:

$$H_{gp} = \frac{0.3048h}{1+0.3048/6356766} \quad \text{meters} \tag{65}$$

$$T_M = (T_M)_b\left[1+K_1(H_{gp}-H_b)\right] \quad {}^\circ R \tag{66}$$

$$T = T_M\left[A-B\tan^{-1}\left(\frac{H_{gp}-C}{D}\right)\right] \quad {}^\circ R \tag{67}$$

$$P = P_b\left[1+K_1(H_{gp}-H_b)\right]^{-K_2} \quad lb/ft^2 \tag{68}$$

$$\rho = \rho_b\left[1+K_1(H_{gp}-H_b)\right]^{-(1+K_2)} \quad slugs/ft^3 \tag{69}$$

$$V_s = 49.020576(T_M)^{1/2} \quad ft/sec \tag{70}$$

$$\nu = 0.0226988\times10^{-6}\left[\frac{T^{3/2}}{(T+198.72)\rho}\right] \quad ft^2/sec \tag{71}$$

For the isothermal layers 2, 4, and 6, the following changes are made in the above equations:

$$P = P_b \, e^{-K_3(H_{gp}-H_b)} \tag{72}$$

$$\rho = \rho_b \, e^{-K_3(H_{gp}-H_b)} \tag{73}$$

Values for temperature, pressure, density, and altitude at the base of each altitude layer are listed below, along with the appropriate values of K_1, K_2, and K_3.

Quantity	1	2	3	4	5	6
K_1	$-.225569^{-4}$	0	$.138466^{-4}$	0	$-.159202^{-4}$	0
K_2	-5.25612	-	11.3883	-	-7.59218	-
K_3	-	$.157689^{-3}$	-	$.120869^{-3}$	-	$.206234^{-3}$
T_b	518.688	389.988	389.988	508.788	508.788	298.188
P_b	2116.21695	472.73	51.979	2.5155	1.2181	2.1080^{-2}
ρ_b	2.37692^{-3}	7.0620^{-4}	7.7650^{-5}	2.8304^{-6}	1.39468^{-6}	4.1189^{-8}
H_b	0	11000.	25000.	47000.	53000.	79000.

Quantity	7	8	9	10	11
K_1	$.241458^{-4}$	$.886289^{-4}$	$.754341^{-5}$	$.350715^{-5}$	$.222129^{-5}$
K_2	8.54120	1.70824	3.41648	6.83296	9.76137
K_3	-	-	-	-	-
T_b	298.188	406.188	2386.188	2566.188	2836.188
P_b	2.1809^{-3}	1.5560^{-4}	7.5578^{-6}	5.8954^{-6}	2.9759^{-6}
ρ_b	4.261^{-9}	2.232^{-10}	1.845^{-12}	1.338^{-12}	6.113^{-13}
H_b	90000.	105000.	160000.	170000.	200000.

Values of the appropriate constants to be applied in the temperature equation (Equation 67) are as follows:

H_{gp}(Km)	A	B	C	D
0-90	1.	0.	-	-
90-180	0.759511	0.174164	220	25
180-1200	0.935787	0.273966	180	140

(2) Limitations. The validity of the 1959 ARDC model is limited to altitudes below 700 km, although the program is arranged to extrapolate the relationships to greater altitudes, if desired. Extrapolation to greater altitudes is accomplished by altering the cutoff altitude. At an altitude of 90 km (approximately 300,000 ft.) the subprogram normally ceases to calculate kinematic viscosity and speed of sound and assigns a value of zero to each of these parameters as an indication that the computation has stopped. This is done for the following reasons: (a) the molecular composition of the atmosphere is unknown; (b) the variation of the ratio of specific heats above 90 km, is not known; and (c) the numerical value of the speed of sound has little physical significance. The validity of Sutherland's empirical formula for viscosity is also reduced because of the extremely low pressures which exist.

(3) Accuracy. Due to a lack of knowledge of the rounding-off procedures used to evaluate the constants in Reference 16, it was impossible to obtain exact agreement between the subprogram and the values tabulated there. A comparison of the results over an altitude range of 0 - 1,000,000 ft. revealed that the deviation of the computed from the reference values never exceeded one tenth of one percent and in most cases was less than one half of this value.

b. Winds Aloft

The winds-aloft subprogram provides for three separate methods of introducing the wind vector - as a function of altitude, a function of range, and a function of time. This will facilitate the investigation of winds effects for the conventional performance studies. The wind vector will be approximated by a series of straight-line segments for each of the methods mentioned above. Statistically derived profiles of the type presented in Reference 13 can be represented by this approach and it is presumed that the analyst will resort to sources of this type to obtain the wind input data. The present subprogram will not be particularly concerned with the method used to determine the wind vector, as this is a separate problem outside the scope of the Takeoff and Landing Analysis computer program.

Four options will be used to define the wind vector in the SDF computer program. The three components of the wind vector in the inertial coordinate system will be specified as tabular listings with linear interpolations (curve reads) in the following options.

Wind Option (0). In this option the wind vector is zero throughout the problem. This will allow the analyst the option of evaluating performance without the effects of wind. This option causes the wind-aloft subprogram to be bypassed in the computational sequence.

Wind Option (1). In this option the components of the wind vector will be specified as a function of time for the estimated altitude. Wind speed will be specified in feet per second and time will be specified in seconds.

Wind Option (2). The three components of the wind vector will be introduced as a function of altitude in this option. Wind speed will be specified in feet per second and altitude will be specified in feet.

Wind Option (3). In this option the components of the wind vector will be introduced as a function of range for the estimated altitude. Wind speed will be specified in feet per second and range will be specified in nautical miles. The range used in this computation will be the range from the starting point, Rg.

By staging of the wind option, it will be possible to switch from one method of reading wind data to another during the computer run. Care must be exercised in this operation, however, as the switching will introduce sharp-edged gusts if there are sizeable differences in the wind vector from one option to another at the time of switching. This effect should be avoided except in cases where gust effects are being studied.

Figure 16 presents a functional flow diagram of the wind-aloft subprogram. For Wind Option (3) the range from the starting point must be defined. Therefore

$$R_g = \sqrt{(X_g - X_{g_0})^2 + (Y_g - Y_{g_0})^2} \tag{74}$$

5. SDF-2 CHANGES

Nearly all of the autopilot logic requires additions to SDF-2 and not changes in the basic SDF-2 concepts. Because it is desired to simulate ground effect, multiple engines, and a drag chute, some direct changes in SDF-2 must be made.

a. Aerodynamics (SACS) Changes

The aerodynamics subroutine in SDF-2 (called SACS) will not simulate a smooth transition into ground effect and has several options that take up needed computer storage and are not needed in a landing analysis. Aerodynamic dependence on Mach number is also no longer needed (see Assumptions in Section II of Appendix III). Special requirements of the autopilot (i.e. aerodynamic force coefficients C_L and C_D are needed in a pseudo-wind axes system, and the side force

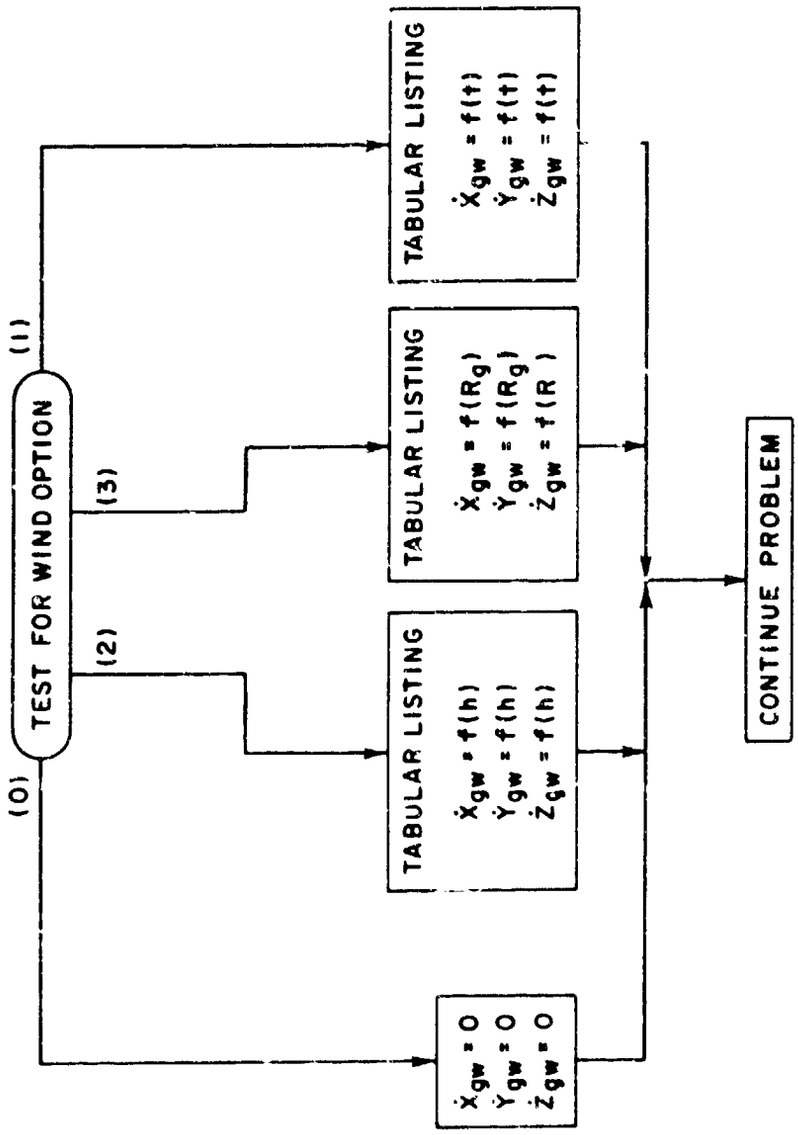

Figure 16. Functional Flow Diagram - Winds-Aloft Subprogram

coefficient, C_y, and the aerodynamic moment coefficients are needed in the body axes system) can also be met at the outset by a rewrite of SACS.

Ground effect data, if available at all, is usually given by giving the aerodynamic coefficients for no ground effect (i.e., aircraft is sufficiently away from the ground) and by giving the aerodynamic coefficients in ground effect (i.e., aircraft is essentially on the ground). References 7 and 19 indicate that the aerodynamic coefficients affected begin to change when the aircraft reaches one wing span above the ground, and the transition into full ground effect appears to be exponential. For this reason, the following equation was adopted to simulate the ground effect transition:

$$A_{hG} = A_o + (A_{GF} - A_o)e^{-4.6\left(\frac{h_G - \epsilon(x_{R2}) - h_{CG}}{b \cdot h_{CG}}\right)} \tag{75}$$

where

$\epsilon(x_{R2})$ = runway perturbation at the displacement of gear number two from the runway origin (can represent an aircraft carrier deck for takeoff)

A_{hG} = aerodynamic coefficient at altitude h_G

A_o = aerodynamic coefficient for no ground effect

A_{GF} = aerodynamic coefficient for full ground effect

h_G = altitude aircraft mass center is above the ground

h_{CG} = sec "glide slope"

b = wing span

Note that for $h_G \geq b$, the value of A_{hG} is essentially A_o. As h_G approaches h_{cg}, the value of A_{hG} is essentially A_{GF}. In this manner the ground effect transition is simulated.

The details of the rewrite of SACS will not be given here. Suffice it to say that the modified SACS subroutine will include the following:

(1) Same equations and aerodynamics coefficients used in Option I (page 45)

(2) Eliminate all other SACS Options and the aerothermoelastic calculation.

(3) Aerodynamic coefficients will not be a function of Mach number and two data points are needed for each coefficient: one for no ground effect and one for full ground effect.

(4) Force coefficients C_L and C_D must be input in the pseudo wind axes.

(5) Side force coefficient, C_y, and the moment coefficients must be input in body axes.

b. Multiple Engine Changes

As originally designed, SDF-2 only allowed for the simulation of one airbreathing engine. The thrust table look-up routine, TFFS, included the effects of altitude on thrust and determined the fuel rate, both of which are no longer needed (see Assumption in Section II of Appendix III). Some provision must also be made to determine thrust for engine reversing, thrust for engine failure, and the net thrust forces and moments acting on the multiple engine aircraft. We begin by discussing the thrust table lookup.

The thrust table is now a function of throttle setting and Mach number alone. Because of the throttle autopilot logic, the ranges for the throttle setting, N, must be as follows:

N = -2 means full reverse
N = -1 means idle reverse

$N = 0$ means engine failure

$N = +1$ means idle forward

$N = +2$ means full forward

Negative values of thrust are stored for the negative throttle settings. In this manner reverse thrust is simulated. The zero value of N is used for the data simulating engine failure (note that failure thrust may be zero or some negative value, depending on Mach number). The actual reversing is achieved in the throttle autopilot by requesting a negative value of desired throttle setting, N_{di}. The change of sign on N_{di} is sensed in the control response (see Figure 29 of Appendix III) and this changes the sign of the actual N_i used in the thrust table.

Every time thrust is needed by the main program, the thrust table is entered IN times - once for each engine - and the actual thrust array T(IN) is obtained depending on the values in the actual throttle setting array N (IN). The engine thrust vector is assumed parallel to the longitudinal body axis (this is also assumed in the autopilot equations) and therefore causes no roll moments. The engine position arrays, 3_N (IN) and Y_3 (IN), along with the actual thrust array T (IN) determine the engine pitch moment array M_T(IN) and the engine yaw moment array N_T(IN). These arrays are then used to obtain the net longitudinal thrust, T_x, (note T_y and T_3 are zero by assumption) the net engine pitch moment, M_T, and the net engine yaw moment, N_T. The net values T_x, M_T, and N_T are then used in SDF-2 and the calculation proceeds as normal.

c. Drag Chute Changes

A drag chute simulation is included for analysis of those aircraft using chutes for deceleration on landing roll. The chute drag vector force, $\bar{F}_{DC}$, is assumed opposite the relative airspeed vector $\bar{V}_a$ and is written as follows:

$$\bar{F}_{DC} = -F_{DC} \frac{\bar{V}_a}{V_a} \tag{76}$$

where

$$F_{DC} = C_{DCH} S_{SH} \; q^* \tag{77}$$

and

F_{DC} = magnitude of chute drag force

C_{DCH} = chute drag coefficient (assumed a constant)

S_{SH} = chute reference area

q^* = dynamic pressure (see SDF-2)

In terms of SDF-2 variables, the relative airspeed vector in body axes $\bar{i}_x$, $\bar{i}_y$, $\bar{i}_z$ is

$$\bar{V}_a = (u - u_w)\,\bar{i}_x + (v - v_w)\,\bar{i}_y + (w - w_w)\,\bar{i}_z \tag{78}$$

Equation 76 can therefore be written

$$\bar{F}_{DC} = \frac{-F_{DC}}{V_a}\left[(u-u_w)\,\bar{i}_x + (v-v_w)\,\bar{i}_y + (w-w_w)\,\bar{i}_z\right] \tag{79}$$

The vector, R_{CH}, from the aircraft mass center to the chute attachment point is written in body axes as

$$\bar{R}_{CH} = X_{CH}\,\bar{i}_x + Y_{CH}\,\bar{i}_y + Z_{CH}\,\bar{i}_z \tag{80}$$

The vector moment, $\bar{M}_{CH}$, of $\bar{F}_{DC}$ about the aircraft mass center is

$$\bar{M}_{CH} = \bar{R}_{CH} \times \bar{F}_{DC} \tag{81}$$

If $\bar{F}_{DC}$ is written

$$\bar{F}_{DC} = F_{cx}\,\bar{i}_x + F_{cy}\,\bar{i}_y + F_{cz}\,\bar{i}_z \tag{82}$$

and $\bar{M}_{CH}$ is written as,

$$\bar{M}_{CH} = M_{Dx}\,\bar{i}_x + M_{Dy}\,\bar{i}_y + M_{Dz}\,\bar{i}_z \tag{83}$$

then the scalar components F_{cx}, F_{cy}, F_{c3}, M_{DX}, M_{DY} and M_{D3} are as follows:

$$F_{cx} = -F_{DC}(u-u_w)/V_a \tag{84}$$

$$F_{cy} = -F_{DC}(v-v_w)/V_a \tag{85}$$

$$F_{cz} = -F_{DC}(w-w_w)/V_a \tag{86}$$

$$M_{Dx} = Y_{CH}\,F_{cz} - Z_{CH}\,F_{cy} \tag{87}$$

$$M_{Dy} = Z_{CH}\,F_{cx} - X_{CH}\,F_{cz} \tag{88}$$

$$M_{Dz} = X_{CH}\,F_{cy} - Y_{CH}\,F_{cx} \tag{89}$$

Figure 17 is a flow chart of the drag chute equations. The ICS indicator is normally input at a value other than one. As such, the chute body forces and moments (i.e., Equations 84-89) are all zero. The drag chute is deployed some time during the landing rollout (see Figure 11 of Apendix III), at which time the ICS indicator is made one, which indicates to the program that the drag chute is deployed. The chute body forces and moments are finally used in the SDF-2 total summation of body forces and moments (i.e., F_x, F_y, F_z, L, M, N) acting on the aircraft.

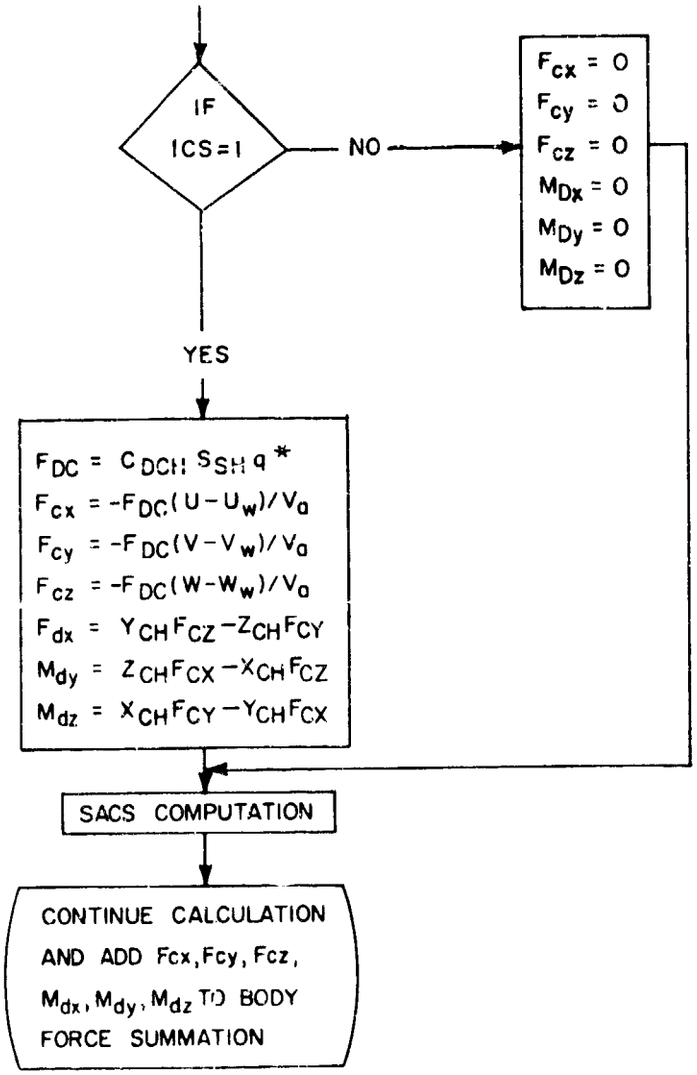

Figure 17. Drag Chute Forces and Moments

APPENDIX II

LANDING GEAR EQUATIONS TO SDF-2

SECTION I

INTRODUCTION

This appendix shows how the present equations of motion in SDF-2 must be modified to include the landing gear dynamics and ground reactions. In this formulation the main aircraft frame is assumed a rigid body; however, the gears are allowed to move, and the dynamics of this motion is included in the formulation. The formulation is generalized to a vehicle with any number of oleo struts (single or double chamber) with balloon tires. Though specific application is first intended for the C-5A aircraft, a modification of SDF-2 will allow takeoff and landing analysis of many aircraft.

For a detailed understanding of the formulation, we reference the reader to two reports: Reference 1, which is the original documentation of SDF-2; and Reference 6, which is a derivation of the equations of motion for a series of nonrigid bodies.

SECTION II

MODIFIED EQUATIONS

1. SDF-2

The equations of motion in Option 2 of the SDF are written in a body-fixed-axes system, $\bar{i}_{xo}$, $\bar{i}_{yo}$, $\bar{i}_{zo}$, which is located at the vehicle mass center. The mass center is located relative to an earth-fixed-axes system, $\bar{i}_{xg}$, $\bar{i}_{yg}$, $\bar{i}_{zg}$, ($\bar{i}_{zg}$ points in the direction of gravity, i.e., down) by a vector $\bar{R}$ which has coordinates X_g, Y_g, Z_g along the $\bar{i}_{xg}$, $\bar{i}_{yg}$, $\bar{i}_{zg}$ axes, respectively. The body-fixed-axes $\bar{i}_{xo}$, $\bar{i}_{yo}$, $\bar{i}_{zo}$ are oriented with respect to earth axes $\bar{i}_{xg}$, $\bar{i}_{yg}$, $\bar{i}_{zg}$ through the $\left[l_{m_n}\right]$ matrix of direction cosines. This is illustrated in Figure 18.

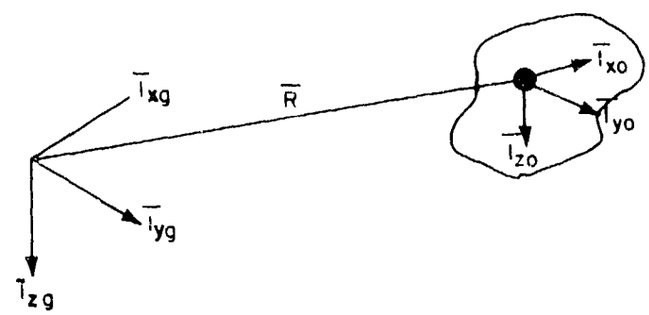

Figure 18. SDF-2 Coordinate Systems

As such, the displacement vector $\bar{R}$ can be written

$$\bar{R} = X_g \bar{i}_{xg} + Y_g \bar{i}_{yg} + Z_g i_{zg} \tag{90}$$

and the transformation matrix from the $\bar{i}_g$ axes system to the $\bar{i}_o$ axes system is

$$\begin{bmatrix} \bar{i}_{xo} \\ \bar{i}_{yo} \\ \bar{i}_{zo} \end{bmatrix} = \begin{bmatrix} \ell_1 & \ell_2 & \ell_3 \\ m_1 & m_2 & m_3 \\ n_1 & n_2 & n_3 \end{bmatrix} \begin{bmatrix} \bar{i}_{xg} \\ \bar{i}_{yg} \\ \bar{i}_{zg} \end{bmatrix} \tag{91}$$

Before proceeding with deriving the modified equations of motion, it is instructive to examine the landing gear to be simulated.

2. LANDING GEAR

Reference 26 describes the C-5A landing gear. The basic gear configuration is shown in Figure 19.

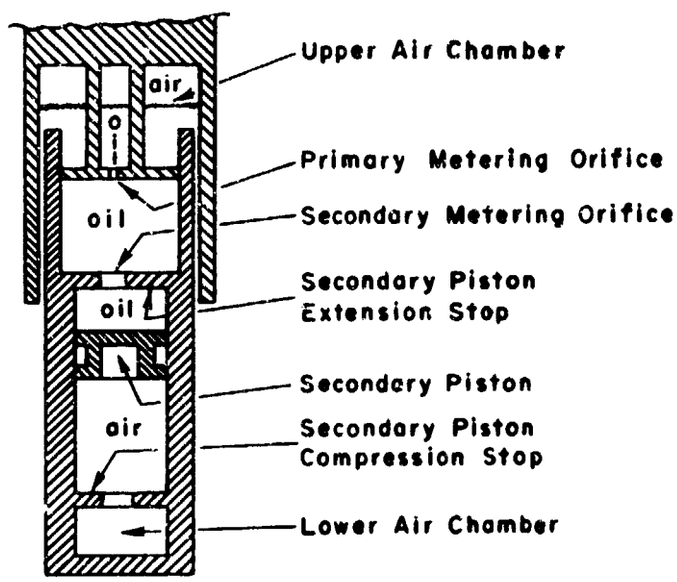

Figure 19. Strut Configuration

The strut configuration is unique in that it has a secondary piston and associated air chamber. Both the upper and lower air chambers are preloaded, with the lower chamber having the higher preload pressure. The secondary piston remains forced against its extension stop until the strut has deflected to the state where the upper chamber forces exceed the preload pressure force of the lower air chamber. Once this occurs, the secondary piston begins to move downward to seek an equilibrium position. With this design, the secondary piston allows continued strut movement without severely increasing the air compression load on the strut. Since most gear struts have only one air chamber, the final formulation will have an input indicator which will allow the secondary piston and lower air chamber to be removed from the problem.

3. MODIFIED EQUATIONS OF MOTION

a. Present SDF-2 Equations of Motion

The present SDF-2 equations of motion (see Reference 1, pgs 5-7) are written with the mass center of the entire vehicle as the reference point and in a body-fixed-axes system. As such, the vector application of Newton's Law takes the form

$$\bar{F} = \frac{m\,d\bar{v}}{dt} = m(\dot{\bar{v}} + \bar{\omega} \times \bar{v}) \tag{92}$$

$$\bar{M} = \frac{d\bar{H}}{dt} = \frac{d}{dt}(\bar{\bar{I}} \cdot \bar{\omega}) = \bar{\bar{I}} \cdot \dot{\bar{\omega}} + \bar{\omega} \times (\bar{\bar{I}} \cdot \bar{\omega}) \tag{93}$$

where

$\bar{F}$ = total applied vector force

m = **total** mass

$\bar{V}$ = inertial velocity vector of mass center in body-fixed-axes system

$\dot{\bar{V}}$ = velocity vector rate as seen from the body-fixed-axes system

$\bar{\omega}$ = inertial rotation rate vector of body axes

$\bar{H}$ = rigid body angular momentum about mass center

$\bar{\bar{I}}$ = moment of inertia matrix about mass center

$\dot{\bar{\omega}}$ = rate of change of $\bar{\omega}$ vector

Equation 92 is the same as Equation 14 of Appendix I, and Equation 93 is the same as Equation 17 of Appendix I.

b. Modified Equations of Motion

(1) Identification of Problem

Although the problem definition of TOLA does not include body flexure as part of the problem, it does include the rigid body movement of the struts. Thus one has a problem where rigid bodies are in contact with and moving relative to one another. In the strict sense of the word, this is no longer a rigid body problem.

The equations of motion for such a system have been derived in Reference 6. The general equations of motion (see Equations 48 and 50 of Reference 6) are therefore:

$$\bar{F}_T = \sum_{k=0}^{K} \bar{F}_k = m_T \ddot{\bar{R}} + \sum_{k=0}^{K} m_k \Big\{ (\ddot{\bar{R}}_k)_0 + 2\bar{\omega}_0 \times (\dot{\bar{R}}_k)_0 + \dot{\bar{\omega}}_0 \times (\bar{R}_k)_0 + \bar{\omega}_0 \times \left[\bar{\omega}_0 \times (\bar{R}_k)_0 \right] + (\ddot{\bar{r}}_{kc})_k + 2\bar{\omega}_k \times (\dot{\bar{r}}_{kc})_k + \dot{\bar{\omega}}_k \times \bar{r}_{kc} + \bar{\omega}_k \times (\bar{\omega}_k \times \bar{r}_{kc}) \Big\} \tag{94}$$

$$\bar{M}_0 = \sum_{k=0}^{K} \bar{m}_{k0} = m_T \bar{r}_c \times \ddot{\bar{R}} + \sum_{k=0}^{K} m_k \left[(\bar{R}_k)_0 + \bar{r}_{kc} \right] \times \Big\{ (\ddot{\bar{R}}_k)_0 + 2\bar{\omega}_0 \times (\dot{\bar{R}}_k)_0 + \dot{\bar{\omega}}_0 \times (\bar{R}_k)_0 + \bar{\omega}_0 \times \left[\bar{\omega}_0 \times (\bar{R}_k)_0 \right] + (\ddot{\bar{r}}_{kc})_k + 2\bar{\omega}_k \times (\dot{\bar{r}}_{kc})_k + \dot{\bar{\omega}}_k \times \bar{r}_{kc} + \bar{\omega}_k \times (\bar{\omega}_k \times \bar{r}_{kc}) \Big\} + \sum_{k=0}^{K} \dot{\bar{H}}_k \tag{95}$$

The derivation of Equations 94 and 95 is quite long and details may be found in Reference 6. The definition of each term in Equations 94 and 95 is, however, given here as a point of departure, and is illustrated in Figure 20.

$\bar{F}_T$ = the total applied vector force to the system of K + 1 bodies

$\bar{F}_k$ = total applied vector force on the kth body

k = a given body: k = 0 is the first body, and k = K is the last body.

m_T = total mass of K + 1 bodies

$\bar{R}$ = vector to reference point on 0th body

m_k = total mass of kth body

$\bar{\omega}_o$ = inertial rotation rate vector of 0th body

$(\bar{R}_k)_o$ = vector position of kth body reference point from 0th body reference point

$\bar{r}_{kc}$ = vector position of kth body mass center from k^{th} body reference point

$(\ )_k$ = a symbol meaning "as seen by the kth coordinate system"

$\bar{\omega}_k$ = inertial rotation rate vector of kth body axes

$\bar{M}_o$ = total vector moment of all applied forces to the K + 1 bodies about the oth body reference point

$\bar{m}_{ko}$ = total vector moment of applied forces to k^{th} body about o^{th} body reference point

$\bar{r}_c$ = vector position of mass center of the K + 1 bodies from o^{th} body reference point

$\bar{H}_{ko}$ = vector moment of linear momentum of kth body about k^{th} body mass center

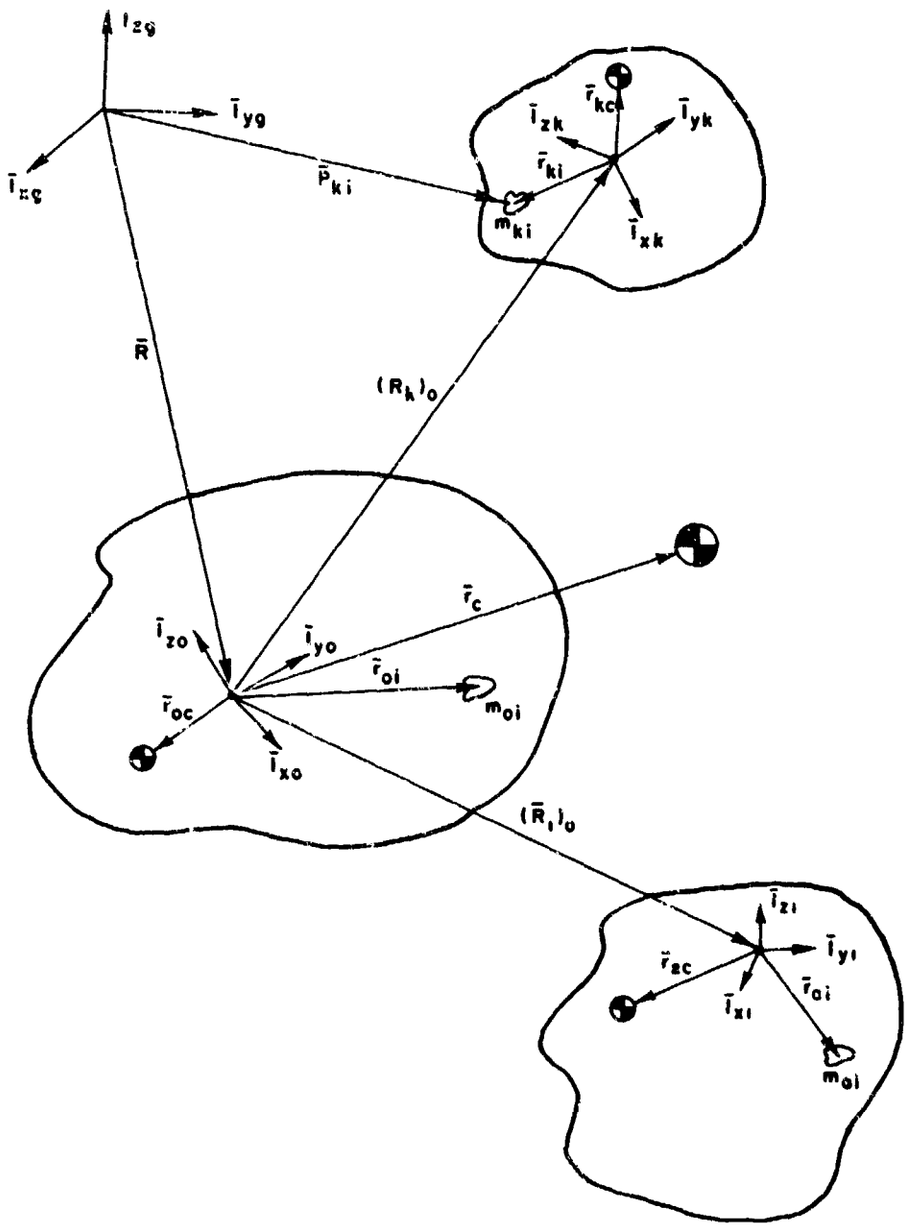

Figure 20. Coordinate Systems

Equations 94 and 95 are very general and therefore very complicated, but have the added feature of being very complete and rigorous as regards their dynamics formulation. At present, Equations 94 and 95 bear very little resemblance to the SDF-2 equations of motion (i.e., Equations 92 and 93), and, at first examination, the necessary modification to Equations 92 and 93 may appear extremely large. Specific application of Equations 94 and 95 will show this not to be true. We begin by giving physical meaning to the coordinate system in Figure 20.

The $\bar{1}_{xg}$, $\bar{1}_{yg}$, $\bar{1}_{zg}$ axes system in Figure 20 is the same as the SDF-2 axes system in Figure 18 (i.e., the inertial axes system). The oth body is presently chosen to the vehicle structure less the moving gear struts. The other K bodies represent the moving gear struts. In reality, there are two moving masses per strut, i.e., the main strut and secondary piston; the secondary piston mass, however, is so small in comparison to the main strut mass (approximately 1/50), its inertial effects on the overall motion of the vehicle are neglected.

Each strut mass has assigned to it a coordinate system $\bar{1}_{xk}$, $\bar{1}_{y}{}^{k}$, $\bar{1}_{zk}$ fixed to the oth body (note that makes $\bar{\omega}_k$ equal $\bar{\omega}_o$, and conveniently oriented with respect to the oth body coordinate system $\bar{1}_{xo}$, $\bar{1}_{yo}$, $\bar{1}_{zo}$ as shown in Figure 21.

The strut coordinate system $\bar{1}_{xk}$, $\bar{1}_{yk}$, $\bar{1}_{zk}$ is located by the vector $(\bar{R}_k)$ (note since the oth body is assumed rigid, this vector does not vary) and is rotated about the positive $\bar{1}_{yk}$ axis by the angle θ_k. The angle θ_k is chosen so that the direction of gear movement is along the unit vector $\bar{1}_{zk}$.

With these physical meanings given to the coordinate systems, let us now examine Equation 95.

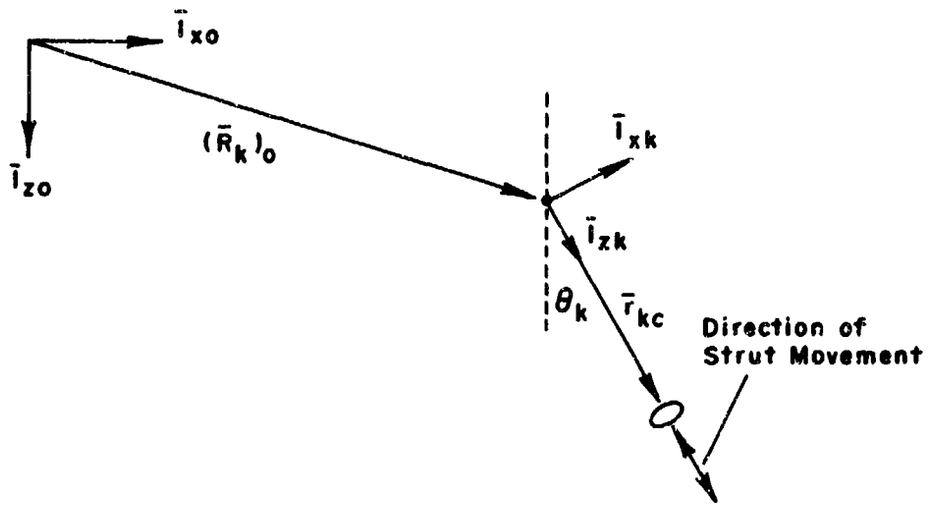

Figure 21. Strut Coordinate System

(2) Application of Equation 95

The terms of Equation 95 can be divided into two groups: terms which depend on position and terms which depend on rate of change of position. Equation 95 is first rearranged into this division.

$$\bar{M}_o = \sum_{k=o}^{K} \Big[m_k \big[(\bar{R}_k)_o + \bar{r}_{kc} \big] \times \Big\{ \dot{\bar{\omega}}_o \times (\bar{R}_k)_o + \bar{\omega}_o \times \big[\bar{\omega}_o \times (\bar{R}_k)_o \big] + \dot{\bar{\omega}}_k \times \bar{r}_{kc} + \bar{\omega}_k \times (\bar{\omega}_k \times \bar{r}_{kc}) \Big\} + \bar{\bar{I}}_k \cdot \dot{\bar{\omega}}_k + \bar{\omega}_k \times (\bar{\bar{I}}_k \cdot \omega_k) \Big] + \sum_{k=o}^{K} \Big[\ddot{\bar{I}}_k + \dot{\bar{\bar{I}}}_k \cdot \omega_k + m_k \big[(\bar{R}_k)_o + \bar{r}_{kc} \big] \times \Big\{ (\ddot{\bar{R}}_k)_o + 2\,\bar{\omega}_o \times (\dot{\bar{R}}_k)_o + (\ddot{\bar{r}}_{kc})_k + 2\,\bar{\omega}_k \times (\dot{\bar{r}}_{kc})_k \Big\} \Big] + m_T\, \bar{r}_c \times \ddot{\bar{R}} \tag{96}$$

The first summation in Equation 96 includes the terms that depend on position, i.e., the rigid body contribution to rate of change of angular momentum about the oth body reference point. The second summation is that which depends on the time derivatives of position, i.e., the nonrigid body contribution to rate of change of angular momentum about the oth body reference point. Note that $\dot{\bar{H}}_{ko}$ has been replaced with its equivalent expression (Equation 37 Reference 6), i.e.,

$$\dot{\bar{H}}_{k\bullet} = \ddot{\bar{\bar{I}}}_k + \dot{\bar{\bar{I}}}_k \cdot \bar{\omega}_k + \bar{\bar{I}}_k \cdot \dot{\bar{\omega}}_k + \bar{\omega}_k \times (\bar{\bar{I}}_k \cdot \bar{\omega}_k) \tag{97}$$

The entire first summation in Equation 96 can be replaced with $\bar{\bar{I}}_o \cdot \dot{\bar{\omega}}_o + \bar{\omega}_o \times (\bar{\bar{I}}_o \cdot \bar{\omega}_o$ where $\bar{\bar{I}}_o$ is the familiar rigid body inertia tensor for the entire K + 1 bodies about the oth body reference point. Note that $\bar{\bar{I}}_o$ will vary in time ever so slightly because $\bar{r}_{kc}$ is changing for each gear. The variation of $\bar{r}_{kc}$ is normally on the order of 10-12 inches, as compared to vehicle dimensions on the order of hundreds of feet. The variation of $\bar{\bar{I}}_o$ due to gear strut movement will therefore be extremely small and justifiably neglected.

We next choose to let the reference point of the oth body be the nominal mass center of the entire vehicle (i.e., the mass center for the gears in their average deflected position). As such, $\bar{r}_c$ will be very small at any given time and can be considered approximately zero.

Reference 6 shows that $\ddot{\bar{\bar{I}}}_k$ and $\dot{\bar{\bar{I}}}_k \cdot \bar{\omega}_k$ are identically zero since each mass is a rigid body within itself. The vectors $(\ddot{\bar{R}}_k)_o$ and $(\dot{\bar{R}}_k)_o$ are also identically zero since the oth body is considered rigid.

The foregoing specific application of Equation 96 has presently reduced Equation 96 to

$$\begin{aligned} \dot{\bar{H}}_o &= \bar{\bar{I}}_o \cdot \dot{\bar{\omega}}_o + \bar{\omega}_o \times (\bar{\bar{I}}_o \cdot \bar{\omega}_o) \\ &+ \sum_{k=o}^{K} m_k \left[(\bar{R}_k)_o + \bar{r}_{kc} \right] \times \left\{ (\ddot{\bar{r}}_{kc})_k + 2\bar{\omega}_k \times (\dot{\bar{r}}_{kc})_k \right\} \end{aligned} \tag{98}$$

Separating the gear struts from the main vehicle structure in the summation yields

$$\bar{M}_o = \bar{\bar{I}}_o \cdot \dot{\bar{\omega}}_o + \bar{\omega}_o \times (\bar{\bar{I}}_o \cdot \bar{\omega}_o) + m_o \left[(\bar{R}_o)_o + \bar{r}_{oc} \right] \times$$

$$\left[(\ddot{\bar{r}}_{oc})_o + 2\bar{\omega}_o \times (\dot{\bar{r}}_{oc})_o \right] + \sum_{k=1}^{K} m_k \left[(\bar{R}_k)_o + \bar{r}_{kc} \right] \times \left[(\ddot{\bar{r}}_{kc})_k \right. \tag{99}$$

$$\left. + 2\bar{\omega}_k \times (\dot{\bar{r}}_{kc})_k \right]$$

The middle term in Equation 99 is identically zero since the oth body is rigid, i.e., $(\ddot{\bar{r}}_{oc})_o = (\dot{\bar{r}}_{oc})_o = 0$. Equation 99 therefore becomes

$$\bar{M}_o = \bar{\bar{I}}_o \cdot \dot{\bar{\omega}}_o + \bar{\omega}_o \times (\bar{\bar{I}}_o \cdot \bar{\omega}_o)$$

$$+ \sum_{k=1}^{K} m_k \left[(\bar{R}_k)_o + \bar{r}_{kc} \right] \times \left[(\ddot{\bar{r}}_{kc})_k + 2\bar{\omega}_k \times (\dot{\bar{r}}_{kc})_k \right] \tag{100}$$

Realizing that the coriolis acceleration of the strut, $2\bar{\omega}_k \times (\dot{\bar{r}}_{kc})_k$, will be very small (mainly because the rotational velocity of the vehicle, ω_k, at landing is very small) in comparison to the strut acceleration $(\ddot{\bar{r}}_{kc})_k$, reduces Equation 100 to its final form

$$\bar{M}_o = \bar{\bar{I}}_o \cdot \dot{\bar{\omega}}_o + \bar{\omega}_o \times (\bar{\bar{I}}_o \cdot \bar{\omega}_o)$$

$$+ \sum_{k=1}^{K} m_k \left[(\bar{R}_k)_o + \bar{r}_{kc} \right] \times (\ddot{\bar{r}}_{kc})_k \tag{101}$$

Note that Equation 101 is the same as the SDF-2 equation (Equation 93) except for the summation involving the struts.

(3) Application of Equation 94

We next examine Equation 94. Let us first realize that $(\ddot{\bar{R}}_k)_o$ and $(\dot{\bar{R}}_k)_o$ are zero because the oth body is rigid. Next we

realize that $(\ddot{\bar{r}}_{oc})_o$ and $(\dot{\bar{r}}_{oc})_o$ are zero for the same reason. $(\bar{R}_o)_o$ is zero by definition (i.e., the displacement of the oth body reference point with respect to itself is zero). Next we realize that $\bar{\omega}_k = \bar{\omega}_o$ since all coordinate systems are attached to the oth body. This reduces Equation 94

$$\bar{F}_T = m_T \ddot{\bar{R}} + \sum_{k=o}^{K} m_k \left\{ \dot{\bar{\omega}}_o \times \left[(\bar{R}_k)_o + \bar{r}_{kc} \right] + \bar{\omega}_o \times \left(\bar{\omega}_o \times \left[(\bar{R}_k)_o + \bar{r}_{kc} \right] \right) \right\} + \sum_{k=1}^{K} m_k \left[(\ddot{\bar{r}}_{kc})_k + 2\bar{\omega}_o \times (\dot{\bar{r}}_{kc})_k \right] \tag{102}$$

Equation 102 may be rearranged

$$\bar{F}_T = m_T \ddot{\bar{R}} + \dot{\bar{\omega}} \times \sum_{k=o}^{K} m_k \left[(\bar{R}_k)_o + \bar{r}_{kc} \right] + \bar{\omega}_o \times \left(\bar{\omega}_o \times \sum_{k=o}^{K} m_k \left[(\bar{R}_k)_o + \bar{r}_{kc} \right] \right) + \sum_{k=1}^{K} m_k \left[(\ddot{\bar{r}}_{kc})_k + 2\bar{\omega}_o \times (\dot{\bar{r}}_{kc})_k \right] \tag{103}$$

Since Equation 47 of Reference 6 is the definition

$$m_T \bar{r}_c = \sum_{k=o}^{K} m_k \left[(\bar{R}_k)_o + \bar{r}_{kc} \right] \tag{104}$$

and since $\bar{r}_c$ can be considered approximately zero, then Equation 103 reduces to

$$\bar{F}_T = m_T \ddot{\bar{R}} + \sum_{k=1}^{K} m_k \left[(\ddot{\bar{r}}_{kc})_k + 2\bar{\omega}_o \times (\dot{\bar{r}}_{kc})_k \right] \tag{105}$$

Neglecting the small coriolis term, as was done in Equation 100 yields the final form of Equation 94.

$$\bar{F}_T = m_T \ddot{\bar{R}} + \sum_{k=1}^{K} m_k (\ddot{\bar{r}}_{kc})_k \tag{106}$$

Note that Equation 106 is the same as the SDF-2 equation (see Equation 92 and realize that $\ddot{\bar{R}}$ is $\frac{dv}{dt}$) except for the summation involving the struts.

Equations 101 and 106 are therefore the modified equations of motion for a vehicle with moving struts. Note that if the struts are not accelerating, i.e. $(\ddot{\bar{r}}_{kc})_k = 0$, the modified equations of motion reduce to the original SDF equations of motion for a rigid body.

(4) Discussion of Modified Equations of Motion

The vector $\bar{F}_T$ in Equation 106 represents the total applied vector force on the vehicle. Because the gears have been added to the problem, $\bar{F}_T$ is composed partly of the ground reaction forces, and partly of the forces making up $\bar{F}_T$, which are gravity, aerodynamics, and thrust. The summation $\sum_{k=1}^{K} m_k (\ddot{\bar{r}}_{kc})_k$ can be looked upon as the inertial force of the accelerated gear struts.

The vector $\bar{M}_o$ in Equation 101 represents the total moment of all the vehicle applied forces about the oth body reference position (which was chosen as the nominal vehicle mass center). $\bar{M}_o$ includes the moments of the ground reaction, aerodynamic, and thrust forces. The summation $\sum_{k=1}^{K} m_k \left[(\bar{R}_k)_o + \bar{r}_{kc} \right] \times (\ddot{\bar{r}}_{kc})_k$ can be looked upon as the moment about the oth body reference position of the gear strut inertia forces.

Considerable effort was expended in reducing the general Equations 94 and 95 to a reference point, which was defined as the "nominal mass center." This extra ejfort was not without cause, for it simplifies the equations of motion and allows the present moment of inertia definition in SDF-2 (which was defined about the vehicle mass center) to be applicable.

Vector Equations 101 and 106 yield six scalar equations for the second derivatives of the six rigid-body degrees of freedom for the vehicle. Before these equations can be numerically integrated, the ground reactions and the strut accelerations must be defined from known quantities.

c. Auxiliary Equations

(1) Coordinate Systems

Figure 21 shows the relationship between the strut coordinate system $\bar{i}_{xk}$, $\bar{i}_{yk}$, $\bar{i}_{zk}$ and the body fixed coordinate system $\bar{i}_{xo}$, $\bar{i}_{yo}$, $\bar{i}_{zo}$. The coordinate transformation is

$$\begin{aligned} \bar{i}_{xk} &= \cos\theta_k \bar{i}_{xo} - \sin\theta_k \bar{i}_{zo} \\ \bar{i}_{yk} &= \bar{i}_{yo} \\ \bar{i}_{zk} &= \sin\theta_k \bar{i}_{xo} + \cos\theta_k \bar{i}_{zo} \end{aligned} \tag{107}$$

Equation 107 can be conveniently written in matrix form as

$$\begin{bmatrix} \bar{i}_{xk} \\ \bar{i}_{yk} \\ \bar{i}_{zk} \end{bmatrix} = \begin{bmatrix} \alpha_{k11} & 0 & \alpha_{k13} \\ 0 & 1 & 0 \\ \alpha_{k31} & 0 & \alpha_{k33} \end{bmatrix} \begin{bmatrix} \bar{i}_{xo} \\ \bar{i}_{yo} \\ \bar{i}_{zo} \end{bmatrix} \tag{108}$$

where

$$\begin{aligned} \alpha_{k11} &= \cos\theta_k \\ \alpha_{k13} &= -\sin\theta_k \\ \alpha_{k31} &= \sin\theta_k \\ \alpha_{k33} &= \cos\theta_k \end{aligned} \tag{109}$$

The landing runway and its coordinate system is shown in Figure 22.

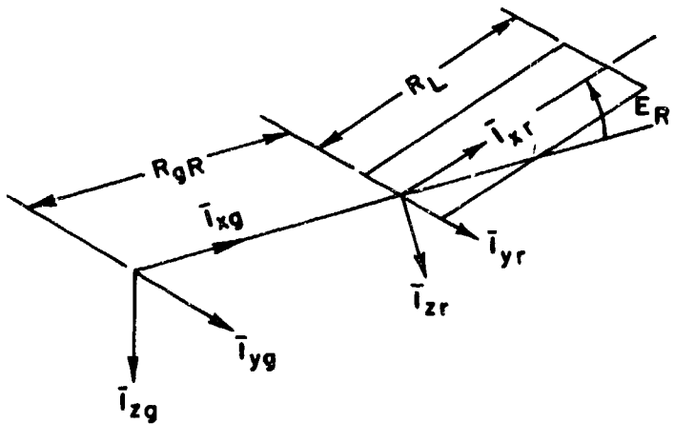

Figure 22. Runway Coordinate System

The runway coordinate system $\bar{i}_{xr}$, $\bar{i}_{yr}$, $\bar{i}_{zr}$ is located down the $\bar{i}_{xg}$ axis a distance R_{gr}. The runway also has an elevation angle, E_R, with respect to the $\bar{i}_{kg}$ axis (E_R allows the calculation to examine landing on elevated runways if desired). The runway length is R_L. The coordinate transformation between the $\bar{i}_r$ axes system and the $\bar{i}_g$ axes system is

$$\begin{aligned} \bar{i}_{xr} &= \cos E_R \bar{i}_{xg} - \sin E_R \bar{i}_{zg} \\ \bar{i}_{yr} &= \bar{i}_{yg} \\ \bar{i}_{zr} &= \sin E_R \bar{i}_{xg} + \cos E_R \bar{i}_{zg} \end{aligned} \qquad (110)$$

Equation 110 in matrix form is

$$\begin{bmatrix} \bar{i}_{xr} \\ \bar{i}_{yr} \\ \bar{i}_{zr} \end{bmatrix} = \begin{bmatrix} R_{G11} & 0 & R_{G13} \\ 0 & 1 & 0 \\ R_{G31} & 0 & R_{G33} \end{bmatrix} \begin{bmatrix} \bar{i}_{xg} \\ \bar{i}_{yg} \\ \bar{i}_{zg} \end{bmatrix} \qquad (111)$$

where

$$R_{G11} = \cos E_R$$
$$R_{G13} = -\sin E_R$$
$$R_{G31} = \sin E_R \qquad (112)$$
$$R_{G33} = \cos E_R$$

The position of the runway origin, $\bar{R}_{gr}$, can be written

$$\bar{R}_{gr} = R_{gr}\,\bar{i}_{xg} \qquad (113)$$

The position of each strut coordinate system $(\bar{R}_k)_o$ can be written

$$(\bar{R}_k)_o = R_{kx}\bar{i}_{xo} + R_{ky}\bar{i}_{yo} + R_{kz}\bar{i}_{zo} \qquad (114)$$

Figure 23 shows the strut coordinate system and associated strut displacements.

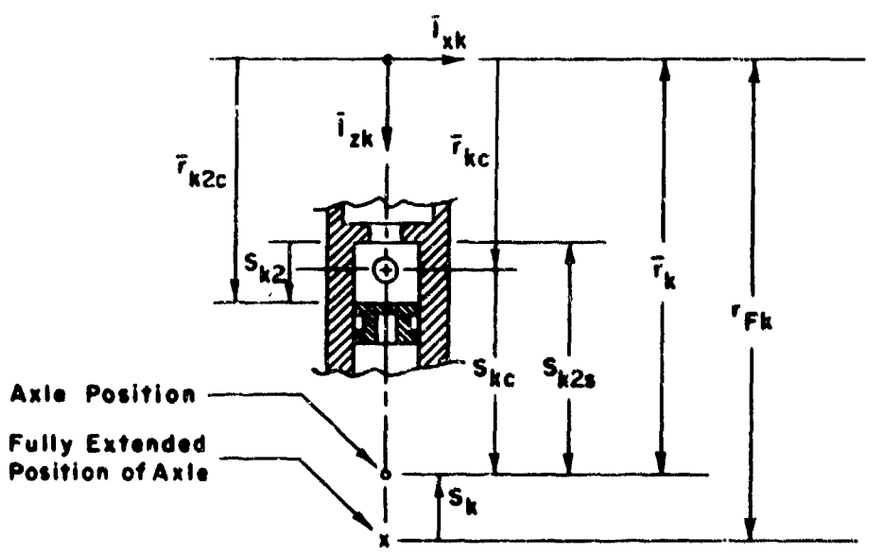

Figure 23. Strut Displacements

The definition of each strut displacement is:

$\bar{r}_{kc}$ = displacement of kth moving strut mass center

or

$$\bar{r}_{kc} = (r_{Fk} - S_{kc} - S_k)\,\bar{i}_{3k} \tag{115}$$

where

r_{Fk} = fully extended position of axle

S_k = main strut displacement

S_{kc} = distance between strut axle and strut mass center

$\bar{r}_{k2c}$ = displacement of secondary piston

or

$$\bar{r}_{k2c} = (r_{Fk} - S_{k2s} + S_{k2} - S_k)\,\bar{i}_{zk} \tag{116}$$

where

S_{k2S} = displacement between axle and secondary piston extension stop

$S_{\bar{k}2}$ = displacement of secondary piston from its extension stop

(2) Strut Equations of Motion

The modified equations of motion, Equations 101 and 106, require the variable $(\ddot{\bar{r}}_{kc})_k$. Note that $(\ddot{\bar{r}}_{kc})_k$ is the acceleration of the kth strut mass center as viewed from the kth coordinate system (i.e., the vehicle). Again we apply Newtor's Law (note in an inertial frame).

The total displacement of the kth strut mass center, $\bar{R}_{kc}$, can be expressed as

$$\bar{R}_{kc} = \bar{R} + (R_k)_o + (\bar{r}_{kc})_k \tag{117}$$

Newton's Law states that

$$\sum \bar{F}_k = m_k \ddot{\bar{R}}_{kc} \tag{118}$$

where

$\bar{F}_k$ = one of many vector forces applied to the kth strut

$\ddot{\bar{R}}_{kc}$ = inertial vector acceleration of kth strut mass center

The first derivative of Equation 117 is:

$$\dot{\bar{R}}_{kc} = \dot{\bar{R}} + \bar{\omega}_o \times (\bar{R}_k)_o + (\dot{\bar{r}}_{kc})_k + \bar{\omega}_o \times (\bar{r}_{kc})_k \tag{119}$$

where $(\dot{\bar{R}}_k)_o = 0$ because the oth body is rigid.

The second derivative of Equation 117 is

$$\begin{aligned}\ddot{\bar{R}}_{kc} = \ddot{\bar{R}} + \dot{\bar{\omega}} \times (\bar{R}_k)_o + \bar{\omega}_o \times \left[\bar{\omega}_o \times (\bar{R}_k)_o\right] + (\ddot{\bar{r}}_{kc})_k \\ + \dot{\bar{\omega}}_o \times (\bar{r}_{kc})_k + 2\bar{\omega}_o \times (\dot{\bar{r}}_{kc})_k + \bar{\omega}_o \times \left[\bar{\omega}_o \times (\bar{r}_{kc})_k\right]\end{aligned} \tag{120}$$

Since $\bar{\omega}_o$ and $\dot{\bar{\omega}}_o$ will be very small at landing and $(\bar{R}_k)_o >> (\bar{r}_{kc})_k$, the last three terms of Equation 120 are neglected which yields

$$\ddot{\bar{R}}_{kc} \simeq \ddot{\bar{R}} + \dot{\bar{\omega}} \times (\bar{R}_k)_o + \bar{\omega}_o \times \left[\bar{\omega}_o \times (\bar{R}_k)_o\right] + (\ddot{\bar{r}}_{kc})_k \tag{121}$$

Note that the term $\ddot{\bar{R}} + \dot{\bar{\omega}}_o \times (\bar{R}_k)_o + \bar{\omega}_o \times \left[\bar{\omega}_o \times (\bar{R}_k)_o\right]$

is the acceleration of the strut coordinate system origin and the term

$(\ddot{\bar{r}}_{kc})_k$ is the acceleration of the strut mass center as viewed from the strut coordinate system (i.e., the term required in the modified equations of motion).

Substituting Equation 121 into Equation 118 yields

$$\sum \bar{F}_k = m_k \left\{ \ddot{\bar{R}} + \dot{\bar{\omega}}_o \times (\bar{R}_k)_o + \bar{\omega}_o \times \left[\bar{\omega}_o \times (\bar{R}_k)_o \right] + (\ddot{\bar{r}}_{kc})_k \right\} \tag{122}$$

Since the strut is physically constrained to move in only one direction, $\bar{1}_{zk}$, we obtain that scalar equation of motion by the dot product of Equation 122 and the unit vector $\bar{1}_{zk}$.

$$\begin{aligned} \sum \bar{F}_k \cdot \bar{1}_{zk} = {} & m_k \left\{ \ddot{\bar{R}} + \dot{\bar{\omega}}_o \times (\bar{R}_k)_o + \bar{\omega}_o \times \left[\bar{\omega}_o \times (\bar{R}_k)_o \right] \right\} \cdot \bar{1}_{zk} \\ & + m_k (\ddot{\bar{r}}_{kc})_k \cdot \bar{1}_{zk} \end{aligned} \tag{123}$$

The term $\bar{F}_k \cdot \bar{1}_{zk}$ represents the forces applied to the strut along the unit vector $\bar{1}_{zk}$ and will be replaced by F_{kz}. Note also that $(\ddot{\bar{r}}_{kc})_k$ can be obtained from Equation 115 and is

$$(\ddot{\bar{r}}_{kc})_k = -\ddot{S}_k \bar{1}_{zk} \tag{124}$$

Equation 123 therefore becomes

$$\begin{aligned} \sum F_{kz} = {} & m_k \left\{ \ddot{\bar{R}} + \dot{\bar{\omega}}_o \times (\bar{R}_k)_o + \bar{\omega}_o \times \left[\bar{\omega}_o (\bar{R}_k)_o \right] \right\} \cdot 1_{zk} \\ & - m_k \ddot{S}_k \end{aligned} \tag{125}$$

Solving for the strut displacement acceleration $\ddot{S}_k$, yields

$$\ddot{S}_k = \left\{\ddot{\bar{R}} + \dot{\bar{\omega}}_0 K(\bar{R}_k)_0 + \bar{\omega}_0 K\left[\bar{\omega}_0 K(\bar{R}_k)_0\right]\right\}\cdot \bar{i}_{zk} - \sum F_{kz}/m_k \tag{126}$$

The only term not defined from known quantities in Equation 126 is $\sum F_{k3}$. F_{k3} is composed of several kinds of forces: air compression forces, orifice drag forces, friction forces, tire forces (i.e., the ground reaction), secondary piston force, and gravity forces. Let us examine each in turn.

(a) Air Compression Force

Figure 19 shows the C-5A strut configuration. There are two air chambers. The pressure, P_k, in the upper air chamber is transmitted through the oil to the upper surface of the secondary piston extension stop and the upper surface of the secondary piston. The pressure, P_{k2}, in the lower air chamber is transmitted to the lower surface of the secondary piston and the bottom of the main strut. Let A_k be the area of the main piston and A_{k2} be the area of the secondary piston. The air compression force, P_{Ak}, acting directly on the main strut is therefore $P_{Ak} = P_k \ (A_k - A_{k2}) + P_{k2} A_{k2}$ (127)

The pressures in the upper and lower air chambers depend upon the main strut displacement, S_k, the secondary piston displacement S_{k2}, and initial conditions. When the strut is fully extended and the secondary piston is against its extension stop, the initial conditions are:

P_{ok} = preload pressure of upper chamber

V_{ok} = preload volume of upper chamber

P_{ok2} = preload pressure of lower chamber

V_{ok2} = preload volume of lower chamber

The relationship between P and V in general is PV^k = constant where k depends on the kind of compression process. Since there is little time for heat transfer, one might think that $k = \frac{cp}{cv}$ (i.e., adiabatic process) would be a good representation. Many references indicate, though, that vaporization of the oil in the orifices makes the process approach isothermal (i.e., k = 1). Experiments show that k = 1.06 is a very good representation. For all practical purposes, then, isothermal compression will suffice. The equations for P_k and P_{k2} for any combination of S_k and S_{k2} are therefore

$$P_k = \frac{P_{ok} V_{ok}}{V_{ok} - A_k S_k + A_{k2} S_{k2}} \tag{128}$$

$$P_{k2} = \frac{P_{ok2} V_{ok2}}{V_{ok2} - A_{k2} S_{k2}} \tag{129}$$

Note that the air compression force always acts along the positive $\bar{1}_{zk}$ direction.

(b) Orifice Drag Forces

Figure 24 shows a typical orifice configuration. The force, F_v, required to move the piston at a velocity V generally takes the form $F_v = CV^2$

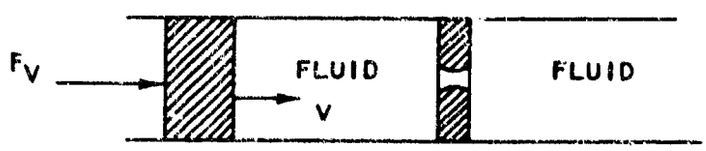

Figure 24. Orifice Drag

where the value of C depends on the fluid and orifice design (i.e., shape, roughness, etc). Depending on the orifice design, C can depend on the direction which the fluid is moving through the orifice. Note that V is the velocity of the fluid upstream of the orifice.

The secondary piston (see Figure 19) is the surface which pushes the oil through the orifices, and it is this surface which feels the major resistance to the oil flow. The only resistance to oil flow that the main strut feels directly is that associated with oil flow through the secondary orifice. This resistance can be formulated $C_{k2}\,\dot{S}_{k2}\left|\dot{S}_{k2}\right|$ where C_{k2} is the secondary orifice coefficient of the kth strut. Note that for positive $\dot{S}_{k2}$, the orifice drag on the main strut is in the positive $\bar{1}_{zk}$ direction.

(c) Friction Forces

There are two obvious friction forces associated with the strut: friction between secondary piston and walls of main strut, and friction between main strut and wing gear root.

The friction force exerted on the main strut by the movement of the secondary piston can be expressed as $C_{k21}\,\dot{S}_{k2}$, where C_{k21} is the linear drag coefficient associated with the kth strut secondary piston movement. Note that is $\dot{S}_{k2}$ is positive, this force is in the positive direction of $\bar{1}_{zk}$.

The friction force exerted by the outer sleeve of the strut due to movement of the main strut, F_{fk}, for the kth strut can be written

$$F_{fk} = \mu_{sk} N_{fk} \tag{130}$$

where

μ_{sk} = coefficient of friction at wing gear support

N_{fk} = normal force at wing gear support

The normal force, N_{fk}, can be caused by many forces such as fit forces, inertia forces, or binding loads caused by ground reactions. Many references neglect the F_{fk} friction force because the contribution of fit normal forces and inertia normal forces to F_{fk} are small in comparison to other forces acting on the strut. The references, however, indicate that for struts which are not perpendicular to the runway, the friction force resulting from ground reaction binding loads at the gear support can be considerable. For this reason, the normal force, N_{fk}, resulting from ground reactions will be simulated. N_{fk} will be formulated once the ground reactions are determined. Since F_{fk} will oppose the strut movement $\dot{S}_k$, Equation 130 becomes

$$F_{fk} \frac{\dot{S}_k}{|\dot{S}_k|} = \mu_{sk} N_{fk} \frac{\dot{S}_k}{|\dot{S}_k|} \tag{131}$$

Note that when $\dot{S}_k$ is positive, $F_{fk} \frac{\dot{S}_k}{|\dot{S}_k|}$ is in the positive direction of $\bar{1}_{zk}$.

(d) Ground Reaction Forces

The force of the ground pushing up on the kth strut along the strut will be given the symbol F_{tk}. Its formulation will depend on the formulation of the ground reaction. Note that F_{tk} is positive in the negative direction of $\bar{1}_{zk}$.

(e) Gravity Forces

The gravity force, $\bar{F}_{kg}$, acting on the kth strut can be written

$$\bar{F}_{kg} = m_k \bar{g} \tag{132}$$

where $\bar{g}$ is the gravity vector. SDF-2 already calculates the gravity vector in the oth body axes system as

$$\bar{g} = g_x \bar{1}_{xo} + g_y \bar{1}_{yo} + g_z \bar{1}_{zo} \tag{133}$$

However, it is the component of $\bar{g}$ along the strut direction of movement, $\bar{1}_{zk}$ that is needed. The gravity force, F_{kgz}, along the direction $\bar{1}_{zk}$ can therefore be written (see Equation 108)

$$F_{kgz} = m_k \, g_{zk} \tag{134}$$

where

$$g_{zk} = g_x a_{kzl} + g_z a_{kzz} \tag{135}$$

(f) Stop Contact Forces

Whenever the secondary piston is against either of its stops, it can transmit a force to the main strut. This contact force is given the symbol F_{ck2} and is assumed to act positive on the main strut in the negative $\bar{1}_{zk}$ direction.

Having looked at the major forces acting on the strut, we now return to the main strut equation of motion, Equation 126, and substitute the major forces in the summation $\sum F_{kz}$. Since F_{kz} was defined positive along the direction $\bar{1}_{zk}$ and s_k was defined negative along the direction $\bar{1}_{zk}$ the result is

$$\begin{aligned} \ddot{s}_k = & \left\{ \ddot{\bar{R}} + \dot{\bar{\omega}}_o \times (\bar{R}_k)_o + \bar{\omega}_o \times \left[\bar{\omega}_o \times (\bar{R}_k)_o \right] \right\} \cdot \bar{1}_{zk} \\ & - \frac{1}{m_k} \left\{ P_{Ak} - F_{ck2} + C_{k2} \dot{s}_{k2} \left| \dot{s}_{k2} \right| + C_{k2L} \dot{s}_{k2} \right. \\ & \left. + F_{fk} \frac{\dot{s}_k}{|\dot{s}_k|} - F_{Tk} + m_k g_{zk} \right\} \end{aligned} \tag{136}$$

Equation 136 is rewritten

$$\ddot{S}_k = \left\{\ddot{\bar{R}} + \dot{\bar{\omega}}_o \times (\bar{R}_k)_o + \bar{\omega}_o \times \left[\bar{\omega}_o \times (\bar{R}_k)_o\right]\right\} \cdot l_{zk} + a_k - g_{zk} \qquad (137)$$

where

$$a_k = \left[F_{Tk} - P_{Ak} + F_{ck2} - C_{k2}\,\dot{S}_{k2}\,|\dot{S}_{k2}| - C_{k2L}\,\dot{S}_{k2} - F_{fk}\left|\frac{\dot{S}_k}{\dot{S}_k}\right|\right] / m_k \qquad (138)$$

From Equation 138, the sum of the forces resisting the kth strut movement may be obtained as

$$S_{Fk} = m_k a_k - F_{Tk} = -P_{Ak} + F_{ck2} - C_{k2}\dot{S}_{k2}|\dot{S}_{k2}| - C_{k2L}\dot{S}_{k2} - F_{fk}\left|\frac{\dot{S}_k}{\dot{S}_k}\right| \qquad (139)$$

In developing the general equations of motion (Equations 101 and 106), the inertia effects of the secondary piston were neglected (valid assumption) because its mass was very small in comparison to that of the main strut. In developing the equation for $\ddot{S}_k$, however, we find that the position and velocity and a contact force of the secondary piston are needed to determine the major forces acting on the main strut. Therefore, we must develop an equation for $\ddot{S}_{k2}$ (which can be numerically integrated to obtain $\dot{S}_{k2}$ and S_{k2}) in a manner similar to what was done for $\ddot{S}_k$. The derivation of $\ddot{S}_{k2}$ follows.

The inertial vector acceleration, $\ddot{\bar{R}}_{k2g}$, of the secondary piston is the same as Equation 121 except $\ddot{\bar{R}}_{kc}$ is replaced with $\ddot{\bar{R}}_{k2g}$ and $(\ddot{\bar{r}}_{kc})_k$ is replaced with $(\ddot{\bar{r}}_{k2g})_k$ yielding

$$\ddot{\bar{R}}_{k2c} = \ddot{\bar{R}} + \dot{\bar{\omega}}_o \times (\bar{R}_k)_o + \bar{\omega}_o \times \left[\bar{\omega}_o \times (\bar{R}_k)_o\right] + (\ddot{\bar{r}}_{k2c})_k \qquad (140)$$

Application of Newton's Law yields

$$\sum \bar{F}_{k2} = m_{k2} \ddot{\bar{R}}_{k2c} \tag{141}$$

where

$\bar{F}_{k2}$ = applied vector force on secondary piston in k^{th} strut

m_{k2} = secondary piston mass in k^{th} strut

Since the secondary piston is also constrained to move along the $\bar{1}_{zk}$ direction, the equation of motion in that direction becomes

$$\sum \bar{F}_{k2} \cdot \bar{1}_{zk} = m_{k2} \ddot{\bar{R}}_{k2c} \cdot \bar{1}_{zk} \tag{142}$$

Equation 142 therefore becomes

$$\sum F_{k2z} = m_{k2} \left\{ \left[\ddot{\bar{R}} + \dot{\bar{\omega}}_o \times (\bar{R}_k)_o + \bar{\omega}_o \times \left[\bar{\omega}_o \times (\bar{R}_k)_o \right] \right] \cdot \bar{1}_{zk} + (\ddot{\bar{r}}_{k2c})_k \cdot \bar{1}_{zk} \right. \tag{143}$$

where F_{k2z} is the component of $\bar{F}_{k2}$ in the positive $\bar{1}_{zk}$ direction. The vector $(\ddot{\bar{r}}_{k2c})_k$ is obtained from Equation 116 to be

$$(\ddot{\bar{r}}_{k2c})_k = (\ddot{S}_{k2} - \ddot{S}_k) \bar{1}_{zk} \tag{144}$$

Substituting Equation 144 into Equation 143 and solving for $\ddot{S}_{k2}$ yields

$$\ddot{S}_{k2} = \frac{\sum F_{k2z}}{m_{k2}} - \left[\ddot{\bar{R}} + \dot{\bar{\omega}}_o \times (\bar{R}_k)_o + \bar{\omega}_o \times \left[\bar{\omega}_o \times (\bar{R}_k)_o \right] \right] \cdot 1_{zk} + \ddot{S}_k \tag{145}$$

Note that the acceleration of the secondary piston displacement from its extension stop, $\ddot{S}_{k2}$, is coupled with the acceleration of the main strut, $\ddot{S}_k$, which is determined by Equation 137. The only unknowns in Equation 145 are the applied forces, F_{k2z} which are composed of air compression force, orifice drag forces, friction force, gravity force, and contact forces at the stops.

(g) Air Compression Force

The net air compression force (see Figure 19) acting on the secondary piston is simply $(P_k - P_{k2})\, A_{k2}$. Note that it acts in the positive $\bar{1}_{zk}$ direction.

(h) Orifice Drag Forces

As was mentioned previously, the secondary piston is the surface which pushes the oil through the orifices. If the velocity of the secondary piston is zero (i.e., $\dot{S}_{k2} = 0$), the force required of the secondary piston to push the oil through the primary orifice is simply $C_k\, \dot{S}_k \left|\dot{S}_k\right|$ where $\dot{S}_k$ is the velocity of approach of the oil. When the secondary piston is moving, however, the equivalent velocity of approach is $\dot{S}_k - \frac{A_{k2}}{A_k}\, \dot{S}_{k2}$ (use continuity of flow). The general equation then for the force required of the secondary piston to push the oil through the primary orifice is therefore

$$C_k\left(\dot{S}_k - \frac{A_{k2}}{A_k}\,\dot{S}_{k2}\right)\left|\dot{S}_k - \frac{A_{k2}}{A_k}\,\dot{S}_{k2}\right| .$$

Note that is $\dot{S}_k$ and $\dot{S}_{k2}$ are positive, the force on the secondary piston is in the positive direction of $\bar{1}_{zk}$.

The secondary orifice also requires a force of the secondary piston to push the oil through this orifice. Since the velocity of approach is $\dot{S}_{k2}$ this force is $C_{k2}\, \dot{S}_{k2}\left|\dot{S}_{k2}\right|$. For positive $\dot{S}_{k2}$, this force acts in the negative $\bar{1}_{zk}$ direction.

(i) Friction Force

The friction force between the secondary piston and main strut walls is simply $C_{k21}\,\dot{S}_{k2}$. This force acts in the negative $\bar{i}_{zk}$ direction for positive $\dot{S}_{k2}$.

(j) Gravity Force

The gravity force is simply $m_{k2}\,g_{zk}$ is given by Equation 135.

(k) Stop Contact Forces

The stop contact force F_{ck2} exists only when the secondary piston is against either of its stop. Its value is that which is necessary to put the secondary piston in equilibrium as seen by the strut (i.e., $\ddot{S}_{k2} = 0$). Since its equal and opposite reaction on the main strut was assumed positive in the negative $\bar{i}_{zk}$ direction, the force of the stop on the secondary piston must be positive in the positive $\bar{i}_{zk}$ direction.

The summation of forces on the secondary piston is therefore

$$\sum F_{k2z} = (P_k - P_{k2})A_{k2} + C_k\left(\dot{S}_k - \frac{A_{k2}}{A_k}\dot{S}_{k2}\right)\left|\dot{S}_k - \frac{A_{k2}}{A_k}\dot{S}_{k2}\right| - C_{k2}\,\dot{S}_{k2}\left|\dot{S}_{k2}\right| - C_{k2L}\,\dot{S}_{k2} + m_{k2}\,g_{zk} + F_{ck2} \tag{146}$$

Substituting Equation 146 into Equation 145 yields

$$\ddot{S}_{k2} = \left[(P_k - P_{k2})A_{k2} + C_k\left(\dot{S}_k - \frac{A_{k2}}{A_k}\dot{S}_{k2}\right)\left|\dot{S}_k - \frac{A_{k2}}{A_k}\dot{S}_{k2}\right| - C_{k2}\,\dot{S}_{k2}\left|\dot{S}_{k2}\right| C_{k2L}\,\dot{S}_{k2} + F_{ck2}\right] \Big/ m_{k2} + g_{zk} - \left[\ddot{\bar{R}} + \dot{\bar{\omega}}_o \times (\bar{R}_k)_o + \bar{\omega}_o \times \left[\bar{\omega}_o \times (\bar{R}_k)_o\right]\right]\cdot \bar{i}_{zk} + \ddot{S}_k \tag{147}$$

Whenever the secondary piston is at a stop, the value of F_{ck2} is that which is necessary to make $\ddot{S}_{k2}$ equal to zero. Therefore F_{ck2} is

$$F_{ck2} = \Big\{\Big[\ddot{\bar{R}} + \dot{\bar{\omega}}_o \times (\bar{R}_k)_o + \bar{\omega}_o \times \big[\bar{\omega}_o \times (\bar{R}_k)_o\big]\Big] \cdot i_{zk}$$

$$- g_{zk} - \ddot{S}_k \Big\} m_{k2} - \Big[(P_k - P_{k2}) A_{k2}$$

$$+ C_k \Big(\dot{S}_k - \frac{A_{k2}}{A_k} \dot{S}_{k2}\Big) \Big| \dot{S}_k - \frac{A_{k2}}{A_k} \dot{S}_{k2} \Big| - C_{k2} \dot{S}_{k2} \big| \dot{S}_{k2} \big|$$

$$- C_{k2L} \dot{S}_{k2} \Big]$$

or

$$F_{ck2} = m_{k2} (-S_{k2\,STOP})$$

where $\ddot{S}_{k2STOP}$ = the value of Equation 147 with F_{ck2} removed.

One could substitute Equation 137 for $\ddot{S}_k$ into Equation 147 and obtain a much simpler equation. There are some physical constraints in the problem, however, that make the simpler equation for $\ddot{S}_{k2}$ more difficult to use. Therefore, Equation 147 will be left in its present form. Note that when all secondary piston terms are deleted, F_{ck2} reduces to $F_{ck2} = -C_k \dot{S}_k \left| \dot{S}_k \right|$.

(3) Physical Constraints

Equation 137 and 147 will be numerically integrated to obtain the velocity and displacements of the main strut and secondary piston. The range over which S_k and S_{k2} are allowed to vary, however, are constrained. The constraints are as follows:

$$\begin{aligned} 0 \le S_k &\le S_{kb} \\ 0 \le S_{k2} &\le S_{k2T} \end{aligned} \qquad (148)$$

where S_{kb} is the maximum allowable displacement of the kth main strut (i.e., strut bottoming) and S_{k2T} is the maximum displacement of secondary piston (i.e., resting against the secondary piston compression stop). As the numerical integration of $\ddot{S}_k$ and $\ddot{S}_{k2}$ approaches these constraints, the values of $\ddot{S}_k$, $\dot{S}_k$, $\ddot{S}_{k2}$, and $\dot{S}_{k2}$ must be appropriately constrained to ensure that the integrated values of S_k and S_{k2} meet the constraints of Equation 148. The constraints on $\ddot{S}_{k2}$, $\dot{S}_{k2}$m $\ddot{S}_k$, and $\dot{S}_k$ are therefore as follows:

(a) If $|S_k| \leq E_{Sk}$, then $\dot{S}_k \geq 0$ and $\ddot{S}_k \geq 0$

(b) If $(S_{kb} - E_{sk}) \leq S_k \leq (S_{kb} + E_{sk})$ then $\dot{S}_k \leq 0$ and $\ddot{S}_k \leq 0$ to exist

(c) If $|S_{k2}| \leq E_{sk2}$, then $\dot{S}_{k2} \geq 0$ and $\ddot{S}_{k2} \geq 0$ to exist.

(d) If $(S_{k2T} - E_{sk2}) \leq S_{k2} \leq (S_{k2T} + E_{sk2})$ then $\dot{S}_{k2} \leq 0$ and $\ddot{S}_{k2} \leq 0$ to exist.

where

E_{sk} = error allowed in integrating S_k around the positions zero and S_{kb}.

E_{sk2} = error allowed in integrating S_{k2} around the positions zero and S_{k2T}.

If the values of S_k do not fall into constraints "a" or "b", then the numerical integration of $\ddot{S}_k$ proceeds normally. If the values of S_{k2} do not fall into constraints "c" or "d", then the numerical integration of $\ddot{S}_{k2}$ proceeds normally. In this way the constraints of Equations 148 are met and the "real system" is simulated.

(4) Ground Reactions

The ground reactions interface the landing simulation in two main areas: strut applied forces (i.e., N_{fk} and F_{tk}); ground reaction contributions to $\bar{M}_0$ in Equation 101; and ground reaction contributions to $\bar{F}_T$ in Equation 106. We begin by examining the ground reactions in general.

(a) Ground Reaction Discussion

The ground reactions, obviously, do not exist until any or all wheels touch the runway. Examine Figure 25.

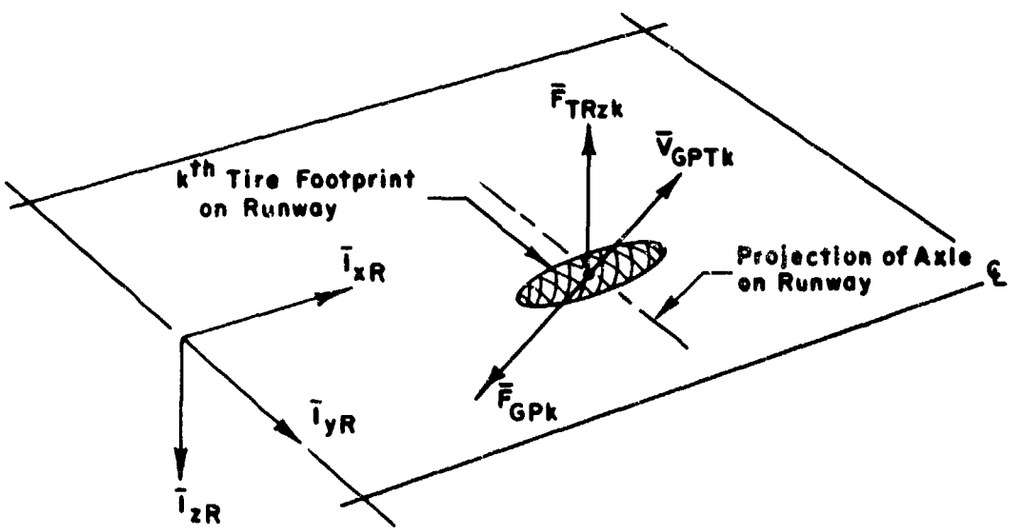

Figure 25. Ground Reaction Forces

As the aircraft settles onto the runway, the tires are depressed and a certain portion of the tire surface (i.e., the tire footprint) interfaces the runway. The foot print is allowed to skid on the runway with a vector velocity $\bar{V}_{gPTk}$ (note $\bar{V}_{gPTk}$ is in the runway plane). The vector $\bar{V}_{gPTk}$ depends on the wheel axle velocity and the rotation rate of the tire.

The ground reaction normal to the runway, $\bar{F}_{Trzk}$, depends on the tire deflection, δ_k, and can be written

$$\bar{F}_{TRzk} = F_{TRzk}\,\bar{i}_{zR} \tag{149}$$

where

$$F_{TRzk} = -n_k f_k(S_k) \tag{150}$$

and

n_k = number of tires on k^{th} strut

$f_k(\delta_k)$ = force deflection curve for a single tire on k^{th} strut

The ground reaction force, $\bar{F}_{Gpk}$, in the runway plane is assumed to have a direction opposite the footprint velocity, $\bar{V}_{Gpt_k}$, and can be written

$$\bar{F}_{GPk} = -F_{GPk}\,\bar{i}_{VGPk} \tag{151}$$

where

$$F_{GPk} = -\mu_k F_{TRzk} \tag{152}$$

and

$$\bar{i}_{VGPk} = \frac{\bar{V}_{GPTk}}{|\bar{V}_{GPTk}|} \tag{153}$$

Substituting Equation 152 and 153 into Equation 151 yields

$$\bar{F}_{GPk} = \mu_k F_{TRzk} \frac{\bar{V}_{GPTk}}{|\bar{V}_{GPTk}|} \tag{154}$$

The variable μ_k is the coefficient of friction between the tire and runway and, in general, is not a constant. The predominant dependence of μ_k is on $|\bar{V}_{gpTk}|$ and the footprint pressure, P_{pk}. In general, μ_k is found to decrease with increasing $|\bar{V}_{gpTk}|$ and decrease with increasing P_{pk}. The nominal footprint pressure, P_{pk}, can be written as

$$P_{Pk} = \frac{|F_{TRzk}|}{\mu_k A_{pk}} \tag{155}$$

where A_{pk} = the footprint area for one tire.

A_{pk} is mainly a function of the tire geometry and the tire deflection, δ_k. Page 62 of Reference 20 gives the empirical formula for A_{pk} as

$$A_{pk} = 2.25(\delta_k - .03W_k)\sqrt{2r_{ok}W_k} \tag{156}$$

where

w_k = tire width

r_{ok} = tire outer radius

Note that $A_{pk} < 0$ for $\delta_k < .03\ W_k$, which has no apparent physical meaning. Knowledgeable people at WPAFB (ASNFL) indicated that P_{pk} was essentially the airpressure of the tire, which remains approximately constant during landing. The whole point of this is that it may not be necessary to include the variable effects of P_{pk} on μ_k during landing. Therefore, μ_k will be assumed as a function of $|\bar{V}_{GPTk}|$ only.

The total ground reaction force, $\bar{F}_{TRk}$, can therefore be written

$$\bar{F}_{TRk} = \bar{F}_{GPk} + \bar{F}_{TRzk} \tag{157}$$

If $\bar{F}_{GPk}$ is written

$$\bar{F}_{GPk} = F_{TRXk}\bar{i}_{XR} + F_{TRyk}\bar{i}_{yR} \tag{158}$$

then substituting Equations 149 and 158 into Equation 157 yields $\bar{F}_{TRk}$ in the runway coordinate system as

$$\bar{F}_{TRk} = F_{TRXk}\bar{i}_{XR} + F_{TRyk}\bar{i}_{yR} + F_{TRzk}\bar{i}_{zR} \tag{159}$$

Furthermore, if the tire footprint velocity $\bar{V}_{GPTk}$ is written

$$\bar{V}_{GPTk} = V_{TXk}\bar{i}_{XR} + V_{Tyk}\bar{i}_{yR} \tag{160}$$

then Equation 154 becomes

$$\bar{F}_{GPk} = \mu_k F_{TRzk} \frac{V_{TXk}}{|\bar{V}_{GPTk}|}\bar{i}_{XR} + \mu_k F_{TRzk} \frac{V_{Tyk}}{|\bar{V}_{GPTk}|}\bar{i}_{yR} \tag{161}$$

Comparing Equation 158 and 161 yields

$$F_{TRXk} = \mu_k F_{TRzk} \frac{V_{TXk}}{|\bar{V}_{GPTk}|} \tag{162}$$

$$F_{TRyk} = \mu_k F_{TRzk} \frac{V_{Tyk}}{|\bar{V}_{GPTk}|} \tag{163}$$

Note that $\left|\bar{V}_{GPTk}\right|$ is

$$|\bar{V}_{GPTk}| = V_{GPTk} = \sqrt{V_{TXk}^2 + V_{Tyk}^2} \tag{164}$$

Equations 150, 162, and 163, therefore, define the total ground reaction $\bar{F}_{TRk}$ (see Equation 159) as seen by the runway coordinate system.

(b) Formulation of F_{Tk}

F_{Tk} is the ground reaction component along the negative $\bar{1}_{zk}$ direction in the gear coordinate system. Since the strut is not necessarily perpendicular to the runway, the formulation of F_{Tk} in terms of F_{TRXk}, F_{TRYk}, F_{TRZk}, is not intuitively obvious. The matrices defining the transformation have already been defined in Equations 91, 108, and 111. In particular, the transformation from the runway coordinate axes 1_R to the strut coordinate axes $\bar{1}_k$ is

$$\begin{bmatrix} 1_{xk} \\ 1_{yk} \\ 1_{zk} \end{bmatrix} = \begin{bmatrix} \alpha_{k11} & 0 & \alpha_{k13} \\ 0 & 1 & 0 \\ \alpha_{k31} & 0 & \alpha_{k33} \end{bmatrix} \begin{bmatrix} \ell_1 & \ell_2 & \ell_3 \\ m_1 & m_2 & m_3 \\ n_1 & n_2 & n_3 \end{bmatrix} \begin{bmatrix} R_{G11} & 0 & R_{G31} \\ 0 & 1 & 0 \\ R_{G13} & 0 & R_{G33} \end{bmatrix} \begin{bmatrix} 1_{xR} \\ 1_{yR} \\ 1_{zR} \end{bmatrix} \quad (165)$$

The product of the two matrices to the right make Equation 165

$$\begin{bmatrix} \bar{1}_{xk} \\ \bar{1}_{yk} \\ \bar{1}_{zk} \end{bmatrix} = \begin{bmatrix} \alpha_{k11} & 0 & \alpha_{k13} \\ 0 & 1 & 0 \\ \alpha_{k31} & 0 & \alpha_{k33} \end{bmatrix} \begin{bmatrix} R_{L11} & R_{L12} & R_{L13} \\ R_{L21} & R_{L22} & R_{L23} \\ R_{L31} & R_{L32} & R_{L33} \end{bmatrix} \begin{bmatrix} \bar{1}_{xR} \\ \bar{1}_{yR} \\ \bar{1}_{zR} \end{bmatrix} \quad (166)$$

where

$$\begin{aligned}
R_{L11} &= \ell_1 R_{G11} + \ell_3 R_{G13} \\
R_{L12} &= \ell_2 \\
R_{L13} &= \ell_1 R_{G31} + \ell_3 R_{G33} \\
R_{L21} &= m_1 R_{G11} + m_3 R_{G13} \\
R_{L22} &= m_2 \\
R_{L23} &= m_1 R_{G31} + m_3 R_{G33} \\
R_{L31} &= n_1 R_{G11} + n_3 R_{G13} \\
R_{L32} &= n_2 \\
R_{L33} &= n_1 R_{G31} + n_3 R_{G33}
\end{aligned} \quad (167)$$

The final expansion of Equation 166 is

$$\begin{bmatrix} \bar{l}_{xk} \\ \bar{l}_{yk} \\ \bar{l}_{zk} \end{bmatrix} = \begin{bmatrix} R_{I11k} & R_{I12k} & R_{I13k} \\ R_{I21k} & R_{I22k} & R_{I23k} \\ R_{I31k} & R_{I32k} & R_{I33k} \end{bmatrix} \begin{bmatrix} \bar{l}_{xR} \\ \bar{l}_{yR} \\ \bar{l}_{zR} \end{bmatrix} \tag{168}$$

where

$$\begin{aligned}
R_{I11k} &= \alpha_{k11} R_{L11} + \alpha_{k13} R_{L31} \\
R_{I12k} &= \alpha_{k11} R_{L12} + \alpha_{k13} R_{L32} \\
R_{I13k} &= \alpha_{k11} R_{L13} + \alpha_{k13} R_{L33} \\
R_{I21k} &= R_{L21} \\
R_{I22k} &= R_{L22} \\
R_{I23k} &= R_{L23} \\
R_{I31k} &= \alpha_{k31} R_{L11} + \alpha_{k33} R_{L31} \\
R_{I32k} &= \alpha_{k31} R_{L12} + \alpha_{k33} R_{L32} \\
R_{I33k} &= \alpha_{k31} R_{L13} + \alpha_{k33} R_{L33}
\end{aligned} \tag{169}$$

By definition of F_{Tk}, it can be formulated as follows

$$F_{Tk} = F_{TRk} \cdot (-l_{zk}) \tag{170}$$

From matrix 168, l_{zk} can be written

$$\bar{l}_{zk} = R_{I31k} \bar{l}_{XR} + R_{I32k} \bar{l}_{yR} + R_{I33k} \bar{l}_{zR} \tag{171}$$

Substituting Equations 159 and 171 into Equation 170 yields the formula for F_{Tk}.

$$F_{Tk} = -(F_{TRXk} R_{I31k} + F_{TRyk} R_{I32k} + F_{TRzk} R_{I33k}) \tag{172}$$

Equation 172 is used to determine F_{Tk}, which is needed in Equation 138 to finally determine $\ddot{S}_k$.

(c) Formulation of N_{fk}

N_{fk} is the ground reaction component normal to the direction of strut movement (i.e., normal to $\bar{1}_{zk}$) at the axle. If $\bar{F}_{TRk}$ (see Equation 159) is written in the strut coordinate system as

$$\bar{F}_{TRk} = F_{dxk}\bar{1}_{xk} + F_{dyk}\bar{1}_{yk} + F_{dzk}\bar{1}_{zk} \tag{173}$$

then N_{fk} is

$$N_{fk} = \sqrt{F_{dxk}^2 + F_{dyk}^2} \tag{174}$$

The forces F_{dxk} and F_{dyk} are determined from F_{TRXk}, F_{TRYk}, F_{TRZk} and Matrix 168 to be

$$F_{dxk} = F_{TRXk} R_{111k} + F_{TRyk} R_{112k} + F_{TRzk} R_{113k} \tag{175}$$

$$F_{dyk} = F_{TRXk} R_{121k} + F_{TRyk} R_{122k} + F_{TRzk} R_{123k} \tag{176}$$

Equation 174 is then used to define N_{fk} in Equation 130, which defines the friction force F_{fk} used in Equation 138, which is ultimately used to help define $\ddot{S}_k$ in Equation 137.

(d) Ground Reaction Contribution to $\bar{F}_T$

The vector $\bar{F}_T$ in Equation 106 is the total applied vector force on the vehicle. The thrust, aerodynamic, and gravity force contributions to $\bar{F}_T$ have already been formulated in SDF-2. To the SDF-2 force formulation must be added the contributions of the ground reactions of each gear. Since SDF-2 ultimately needs the forces expressed in the body fixed axes system ($\bar{1}_{xo}$, $\bar{1}_{yo}$, $\bar{1}_{zo}$), the total ground reaction must finally be written in this system.

The total ground reaction vector, $\bar{F}_{TR}$, may be written in the runway coordinate system as

$$\bar{F}_{TR} = \sum_k \bar{F}_{TRk} = F_{TRX}\bar{i}_{XR} + F_{TRy}\bar{i}_{yR} + F_{TRz}\bar{i}_{zR} \tag{177}$$

where

$$\begin{aligned} F_{TRX} &= \sum_k F_{TRX_k} \\ F_{TRy} &= \sum_k F_{TRyk} \\ F_{TRz} &= \sum_k F_{TRzk} \end{aligned} \tag{178}$$

and $\sum_k$ implies a summation over all of the gears on the vehicle. Equation 177 is then transformed to the body axes through the matrix

$$\begin{bmatrix} \bar{i}_{xo} \\ \bar{i}_{yo} \\ \bar{i}_{zo} \end{bmatrix} = \begin{bmatrix} R_{L11} & R_{L12} & R_{L13} \\ R_{L21} & R_{L22} & R_{L23} \\ R_{L31} & R_{L32} & R_{L33} \end{bmatrix} \begin{bmatrix} \bar{i}_{xR} \\ \bar{i}_{yR} \\ \bar{i}_{zR} \end{bmatrix} \tag{179}$$

which has already been defined by Equation 167. If $\bar{F}_{TR}$ is written in the body axes system as

$$\bar{F}_{TR} = F_{TRA}\bar{i}_{xo} + F_{TRB}\bar{i}_{yo} + F_{TRC}\bar{i}_{zo} \tag{180}$$

then F_{TRA}, F_{TRB}, and F_{TRC} become

$$\begin{aligned} F_{TRA} &= R_{L11}F_{TRX} + R_{L12}F_{TRy} + R_{L13}F_{TRz} \\ F_{TRB} &= R_{L21}F_{TRX} + R_{L22}F_{TRy} + R_{L23}F_{TRz} \\ F_{TRC} &= R_{L31}F_{TRX} + R_{L32}F_{TRy} + R_{L33}F_{TRz} \end{aligned} \tag{181}$$

F_{TRA}, F_{TRB}, and F_{TRC} are the components of the total ground reaction, $\bar{F}_{TR}$, for all the gears written in the body axes system.

(e) Ground Reaction Contribution to $\bar{M}_0$

The vector $\bar{M}_0$ in Equation 101 is the total moment about the nominal mass center of all the forces applied to the vehicle. The thrust and aerodynamic contributions to $\bar{M}_0$ have already been formulated in in SDF-2. To the SDF-2 moment formulation must be added the contributions of the ground reactions of each gear. The position vector, $\bar{R}_{pk}$, to the point of application (i.e., the footprint) of the kth gear ground reaction force, $\bar{F}_{TRk}$, can be written (see Figure 23 and Equation 114) as

$$\bar{R}_{Pk} = (\bar{R}_k)_0 + \bar{r}_k + (r_{ok} - \delta_k)\bar{i}_{zR} \tag{182}$$

where

r_{ok} = outside radius of the tire on the kth strut

The moment vector, $\bar{M}_{TRk}$, of the kth gear ground reaction, $\bar{F}_{TRk}$, is, therefore

$$\bar{M}_{TRk} = \bar{R}_{Pk} \times \bar{F}_{TRk} \tag{183}$$

In order to evaluate the cross product in Equation 183, $\bar{R}_{Pk}$ and $\bar{F}_{TRk}$ must be written in the same coordinate system. Since $\bar{F}_{TRk}$ is already expressed in the runway coordinate system, $\bar{R}_{Pk}$ will be transformed to this system.

The vector $\bar{r}_k$ (see Figure 23) can be written

$$\bar{r}_k = (r_{Fk} - S_k)\bar{i}_{zk} \tag{184}$$

Transforming $\bar{r}_k$ to the body axes system through matrix 108 yields

$$\bar{r}_k = (r_{Fk} - S_k)(a_{k31}\bar{i}_{xo} + a_{k33}\bar{i}_{zo}) \tag{185}$$

Adding Equation 185 to Equation 114 yields

$$(\bar{R}_k)_o + \bar{r}_k = \left[R_{kx} + \alpha_{k31}(r_{Fk} - S_k)\right]\bar{i}_{xo} + \left[R_{ky}\right]\bar{i}_{yo} + \left[R_{kz} + \alpha_{k33}(r_{Fk} - S_k)\right]\bar{i}_{zo} \tag{186}$$

Equation 186 is then written in the inertial axes system $\bar{i}_{xg}$, $\bar{i}_{yg}$, $\bar{i}_{zg}$, as

$$(\bar{R}_k)_o + \bar{r}_k = R_{AXk}\bar{i}_{xg} + R_{Ayk}\bar{i}_{yg} + R_{Azk}\bar{i}_{zg} \tag{187}$$

where (see matrix 91)

$$\begin{bmatrix} R_{AXk} \\ R_{AYk} \\ R_{AZk} \end{bmatrix} = \begin{bmatrix} \ell_1 & m_1 & n_1 \\ \ell_2 & m_2 & n_2 \\ \ell_3 & m_3 & n_3 \end{bmatrix} \begin{bmatrix} \left[R_{kx} + Q_{k31}(r_{Pk} - S_k)\right] \\ \left[R_{ky}\right] \\ \left[R_{kz} + Q_{k33}(r_{Fk} - S_k)\right] \end{bmatrix} \tag{188}$$

Finally, Equation 187 is transformed by matrix 111 to the runway coordinate system, $\bar{i}_R$, and added to $(r_{ok} - S_k)\ \bar{i}_{zR}$ to yield $\bar{R}_{pk}$ expressed in the runway coordinate system as

$$\bar{R}_{pk} = D_{xk}\,\bar{i}_{xR} + D_{yk}\,\bar{i}_{yR} + D_{Zk}\,\bar{i}_{ZR} \tag{189}$$

where

$$\begin{aligned} D_{Xk} &= R_{G11}R_{Axk} + R_{G13}R_{Azk} \\ D_{Yk} &= R_{Ayk} \\ D_{Zk} &= R_{G31}R_{Axk} + R_{G33}R_{Azk} + r_{ok} - \delta_k \end{aligned} \tag{190}$$

Now that $\bar{R}_{pk}$ (Equation 189) is written in the same coordinate system as $\bar{F}_{TRk}$, Equation 183 can be written in determinant form as

$$M_{TRk} = \begin{bmatrix} i_{xR} & i_{yR} & i_{zR} \\ D_{xk} & D_{yk} & D_{zk} \\ F_{TRxk} & F_{TRyk} & F_{TRzk} \end{bmatrix} \tag{191}$$

Expansion of Equation 191 yields

$$\bar{M}_{TRk} = M_{TRxk}\,\bar{i}_{xR} + M_{TRyk}\,\bar{i}_{yR} + M_{TRzk}\,\bar{i}_{zR} \tag{192}$$

where

$$\begin{aligned} M_{TRxk} &= D_{yk}\,F_{TRzk} - D_{zk}\,F_{TRyk} \\ M_{TRyk} &= D_{zk}\,F_{TRxk} - D_{xk}\,F_{TRzk} \\ M_{TRzk} &= D_{xk}\,F_{TRyk} - D_{yk}\,F_{TRxk} \end{aligned} \tag{193}$$

The total moment, $\bar{M}_{TR}$, of all the gear ground reactions can therefore be written

$$\bar{M}_{TR} = \sum_k \bar{M}_{TRk} = M_{TRx}\,\bar{i}_{xR} + M_{TRy}\,\bar{i}_{yR} + M_{TRz}\,\bar{i}_{zR} \tag{194}$$

where

$$\begin{aligned} M_{TRx} &= \sum_k M_{TRxk} \\ M_{TRy} &= \sum_k M_{TRyk} \\ M_{TRz} &= \sum_k M_{TRzk} \end{aligned} \tag{195}$$

If Equation 194 is written in the body axes system as

$$\bar{M}_{TR} = M_{Tx}\,\bar{i}_{xo} + M_{Ty}\,\bar{i}_{yo} + M_{Tz}\,\bar{i}_{zo} \tag{196}$$

then by Equation 167 M_{TX}, M_{TY} and M_{TZ} become

$$\begin{bmatrix} M_{Tx} \\ M_{Ty} \\ M_{Tz} \end{bmatrix} = \begin{bmatrix} R_{L11} & R_{L12} & R_{L13} \\ R_{L21} & R_{L22} & R_{L23} \\ R_{L31} & R_{L32} & R_{L33} \end{bmatrix} \begin{bmatrix} M_{TRx} \\ M_{TRy} \\ M_{TRz} \end{bmatrix} \tag{197}$$

M_{TX}, M_{TY} and M_{TZ} are the total ground reaction moments (written in body axes) that make a contribution to $\overline{M}_o$ in Equation 101.

(f) Tire Deflection, δ_k

In developing Equation 159 for the ground reactions, two new variables, δ_k and $\overline{V}_{GPTk}$, were introduced. The formulation of the kth strut tire deflection δ_k, follows:

The tire deflection arises because of a physical constraint between the position of the wheel axle and the runway, i.e., if the height of the wheel axle above the runway, Z_{ok}, is less than the unloaded outside radius, r_{ok}, of the tire, the difference must be the tire deflection.

$$\delta_k = r_{ok} + z_{ok} \tag{198}$$

The value of Z_{ok} is added in Equation 198 since Z_{ok} will be negative when the axle is above the runway. Note that Equation 198 assumes that the tire shape is a sphere--which is good, provided the wheel axle is not far from being parallel to the runway plane (i.e., wings parallel to runway).

Equation 198 is modified by letting the runway have an arbitrary profile $\epsilon(X_{Rk})$ where ϵ is a function of the position, X_{Rk}, of the kth strut down the runway. The $\epsilon(X_{Rk})$ allows the calculation to compute the effects of

$$\delta_k = r_{ok} + z_{ok} + \epsilon(x_{Rk}) \tag{199}$$

step inputs (or other runway profiles) on gear dynamics. Note the following: $\delta_k < 0$ means the kth tire surface is above the runway; $\delta_k = 0$ means the kth tire surface is just touching the runway; $\delta_k > 0$ means the kth tire is on the runway and is deflected. The formulation of Z_{ok} and X_{Rk} follows.

Let the vector $\bar{R}_{Rk}$ represent the displacement of the kth gear axle as seen by the runway coordinate system origin. The vector $\bar{R}_{Rk}$ can therefore be written (see Figure 18, 21, 22, and 23)

$$\bar{R}_{Rk} = \bar{R} - R_{gR} + (\bar{R}_k)_o + \bar{r}_k \tag{200}$$

where from Equation 90

$$\bar{R} = X_g \bar{i}_{xg} + Y_g \bar{i}_{yg} + Z_g \bar{i}_{zg} \tag{201}$$

and from Equation 113

$$\bar{R}_{gR} = R_{gR} \bar{i}_{xg} \tag{202}$$

and from Equation 114

$$(\bar{R}_k)_o = R_{kx} \bar{i}_{xo} + R_{ky} \bar{i}_{yo} + R_{kz} \bar{i}_{zo} \tag{203}$$

and from Equation 184

$$\bar{r}_k = (r_{Fk} - s_k) \bar{i}_{zk} \tag{204}$$

Now $\bar{R}_{Rk}$ may also be written in the runway coordinate system as

$$\bar{R}_{Rk} = x_{Rk} \bar{i}_{xR} + y_{Rk} \bar{i}_{yR} + z_{ok} \bar{i}_{zR} \tag{205}$$

The formulation of X_{Rk}, Y_{Rk} and Z_{ok} from known quantities involves several coordinate transformations which follow.

The vector $(\bar{R}_k)_o + \bar{r}_k$ has already been formulated in the inertial coordinate system $\bar{i}_{xg}$, $\bar{i}_{yg}$, $\bar{i}_{zg}$ (see Equation 187) as follows:

$$(\bar{R}_k)_o + \bar{r}_k = R_{Axk} \bar{i}_{xg} + R_{Ayk} \bar{i}_{yg} + R_{Azk} \bar{i}_{zg} \tag{206}$$

Substituting Equations 206, 202 and 201 into Equation 200 yields

$$\bar{R}_{Rk} = (X_g - R_{gR} + R_{Axk})\,\bar{i}_{xg} + (Y_g + R_{Ayk})\,\bar{i}_{yg} + (Z_g + R_{Azk})\,\bar{i}_{zg} \tag{207}$$

Equation 207 can be transformed to the $\bar{i}_R$ axes system (i.e., Equation 205) through matrix 111 as follows

$$\begin{bmatrix} x_{Rk} \\ y_{Rk} \\ z_{ok} \end{bmatrix} = \begin{bmatrix} R_{G11} & 0 & R_{G13} \\ 0 & 1 & 0 \\ R_{G31} & 0 & R_{G33} \end{bmatrix} \begin{bmatrix} (X_g - R_{gR} + R_{Axk}) \\ (Y_g + R_{Ayk}) \\ (Z_g + R_{Azk}) \end{bmatrix} \tag{208}$$

The value of X_{Rk} is used to determine $\epsilon(X_{Rk})$. The values of Z_{ok} and r_{ok} (a constant) then completely determine the tire deflection, δ_k, for the kth strut.

(g) Tire Ground Plane Velocity, $\bar{V}_{GPTk}$

The total velocity $\dot{\bar{R}}_{Tk}$ of the bottom surface of the kth strut tires as seen by the runway can be written

$$\dot{\bar{R}}_{Tk} = \bar{V}_{GPT_k} + V_{Tzk}\,\bar{i}_{zR} \tag{209}$$

Substituting Equation 160 for $\bar{V}_{GPTk}$ yields

$$\dot{\bar{R}}_{Tk} = V_{Txk}\,\bar{i}_{xR} + V_{Tyk}\,\bar{i}_{yR} + V_{Tzk}\,\bar{i}_{zR} \tag{210}$$

The formulation of V_{TXk}, V_{TYk} and V_{TZk} from known variables follows:

Let the vector $\bar{R}_{Tk}$ be the position of the kth strut bottom tire surface as seen by the runway coordinate system origin. $\bar{R}_{Tk}$ can therefore be expressed as

$$\bar{R}_{Tk} = \bar{R} - \bar{R}_{gR} + (\bar{R}_k)_o + \bar{r}_k + (r_{ok} - \delta_k)\,\bar{i}_{zR} \tag{211}$$

where $(r_{ok} - \delta_k)\ \bar{i}_{ZR}$ is the vector from the wheel axle to the bottom surface of the tire. The first derivative of Equation 211 yields

$$\dot{\bar{R}}_{Tk} = \dot{\bar{R}} - \dot{\bar{R}}_{gR} + (\dot{\bar{R}}_k)_o + \dot{\bar{r}}_k + \frac{d}{dt}\left[(r_{ok} - \delta_k)\,\bar{i}_{zR}\right] \tag{212}$$

where from Equation 90

$$\dot{\bar{R}} = \dot{X}_g\,\bar{i}_{xg} + \dot{Y}_g\,\bar{i}_{yg} + \dot{Z}_g\,\bar{i}_{zg} \tag{213}$$

and from Equation 113

$$\dot{\bar{R}}_{gR} = 0 \tag{214}$$

and from Equation 114

$$(\dot{\bar{R}}_k)_o = \bar{\omega}_o \times (\bar{R}_k)_o = \bar{\omega}_o \times (R_{kx}\,\bar{i}_{xo} + R_{ky}\,\bar{i}_{yo} + R_{kz}\,\bar{i}_{zo}) \tag{215}$$

and from Equation 184

$$\dot{\bar{r}}_k = -\dot{s}_k\,\bar{i}_{zk} + \bar{\omega}_o \times (r_{Fk} - s_k)\,\bar{i}_{zk} \tag{216}$$

and

$$\frac{d}{dt}\left[(r_{ok} - \delta_k)\,\bar{i}_{zR}\right] = -\dot{\delta}_k\,\bar{i}_{zR} + (\bar{\omega}_o + \bar{\omega}_{Tk}) \times (r_{ok} - \delta_k)\,\bar{i}_{zR} \tag{217}$$

where $\bar{\omega}_{Tk}$ is the rotational vector velocity of the tires on the kth strut as viewed by the vehicle body axes. Equations 213-217 each must be written in the runway coordinate system. We begin with Equation 217.

First $\dot{\delta}_k$ is assumed negligible and $\bar{\omega}_{Tk} >> \bar{\omega}_o$. Therefore Equation 217 becomes

$$\frac{d}{dt}\left[(r_{ok} - \delta_k)\bar{i}_{zR}\right] \simeq \bar{\omega}_{Tk} \times (r_{ok} - \delta_k)\bar{i}_{zR} \tag{218}$$

Since the wheel is constrained to spin about its axle, $\bar{\omega}_{Tk}$ can be written

$$\bar{\omega}_{Tk} = \omega_{Tk}\,\bar{i}_{yk} \tag{219}$$

Since the vector $\bar{i}_{yk}$ can be written (see matrix 168)

$$\bar{i}_{yk} = R_{I21k}\,\bar{i}_{xR} + R_{I22k}\,\bar{i}_{yR} + R_{I23k}\,\bar{i}_{zR} \tag{220}$$

then Equation 218 can be written in determinant form as

$$\frac{d}{dt}\left[(r_{ok} - \delta_k)\bar{i}_{zR}\right] = \omega_{Tk}\begin{vmatrix} \bar{i}_{xR} & \bar{i}_{yR} & \bar{i}_{zR} \\ R_{I21k} & R_{I22k} & R_{I23k} \\ 0 & 0 & (r_{ok} - \delta_k) \end{vmatrix} \tag{221}$$

Expansion of Equation 221 yields

$$\begin{aligned} \frac{d}{dt}\left[(r_{ok} - \delta_k)\bar{i}_{zR}\right] &= \omega_{Tk}(r_{ok} - \delta_k)\,R_{I22k}\,\bar{i}_{xR} \\ &\quad - \omega_{Tk}(r_{ok} - \delta_k)\,R_{I21k}\,\bar{i}_{yR} \end{aligned} \tag{222}$$

Equation 215 and 216 will be expanded together. First the vector $\bar{i}_{zk}$ in Equation 216 is written (see matrix 108)

$$\bar{i}_{zk} = a_{k31}\,\bar{i}_{xo} + a_{k33}\,\bar{i}_{zo} \tag{223}$$

Therefore Equation 216 becomes

$$\dot{\bar{r}}_k = -\dot{s}_k(a_{k31}\bar{i}_{xo} + a_{k33}\bar{i}_{zo})$$

$$+(r_{Fk} - s_k)\begin{vmatrix} \bar{i}_{xo} & \bar{i}_{yo} & \bar{i}_{zo} \\ p & q & r \\ a_{k31} & o & a_{k33} \end{vmatrix} \tag{224}$$

where

$$\dot{\bar{i}}_o = p\,\bar{i}_{xo} + q\,\bar{i}_{yo} + r\,\bar{i}_{zo} \tag{225}$$

On expanding, Equation 224 becomes

$$\begin{aligned} \dot{\bar{r}}_k = & \left[-\dot{s}_k a_{k31} + q\,a_{k33}(r_{Fk} - s_k)\right]\bar{i}_{xo} \\ & + \left[(r_{Fk} - s_k)(r\,a_{k31} - p\,a_{k33})\right]\bar{i}_{yo} \\ & + \left[-\dot{s}_k a_{k33} - q\,a_{k31}(r_{Fk} - s_k)\right]\bar{i}_{zo} \end{aligned} \tag{226}$$

Equation 215 on expanding becomes

$$\begin{aligned} (\dot{\bar{R}}_k)_o = & \begin{vmatrix} \bar{i}_{xo} & \bar{i}_{yo} & \bar{i}_{zo} \\ p & q & r \\ R_{kx} & R_{ky} & R_{kz} \end{vmatrix} \\ = & (q R_{kz} - r R_{ky})\bar{i}_{xo} \\ & + (r R_{kx} - p R_{kz})\bar{i}_{yo} \\ & + (p R_{ky} - q R_{kx})\bar{i}_{zo} \end{aligned} \tag{227}$$

The vector summation $(\dot{\bar{R}}_k)_o + \dot{\bar{r}}_k$ can therefore be written

$$(\dot{\bar{R}}_k)_o + \dot{\bar{r}}_k = R_{Dxk}\,\bar{i}_{xo} + R_{Dyk}\,\bar{i}_{yo} + R_{Dzk}\,\bar{i}_{zo} \tag{228}$$

where

$$\begin{aligned}
R_{Dxk} &= -\dot{s}_k a_{k31} + q a_{k33}(r_{Fk} - s_k) \\
&\quad + (qR_{kz} - rR_{ky}) \\
R_{Dyk} &= (r_{Fk} - s_k)(r a_{k31} - p a_{k33}) \\
&\quad + (rR_{kx} - pR_{kz}) \\
R_{Dzk} &= -\dot{s}_k a_{k33} - q a_{k31}(r_{Fk} - s_k) \\
&\quad + (pR_{ky} - qR_{kx})
\end{aligned} \tag{229}$$

Equation 228 is now transformed to the inertial axes $\bar{i}_g$ by Matrix 91 as

$$(\dot{\bar{R}}_k)_o + \dot{\bar{r}}_k = \begin{bmatrix} \ell_1 & m_1 & n_1 \\ \ell_2 & m_2 & n_2 \\ \ell_3 & m_3 & n_3 \end{bmatrix} \begin{bmatrix} R_{Dxk} \\ R_{Dyk} \\ R_{Dzk} \end{bmatrix} \tag{230}$$

and added with $\dot{\bar{R}} - \dot{\bar{R}}_{gr}$ to yield

$$\dot{\bar{R}} - \dot{\bar{R}}_{gR} + (\dot{\bar{R}}_k)_o + \dot{\bar{r}}_k = R_{DXGk}\,\bar{i}_{xg} + R_{DYGk}\,\bar{i}_{yg} + R_{DZGk}\,\bar{i}_{zg} \tag{231}$$

where the inertial axis system components of the velocity of the axle as seen by the runway origin are

$$
\begin{aligned}
{}^{R}D_{XGk} &= \dot{X}_g + \ell_1 \, {}^{R}D_{xk} + m_1 \, {}^{R}D_{yk} + n_1 \, {}^{R}D_{zk} \\
{}^{R}D_{YGk} &= \dot{Y}_g + \ell_2 \, {}^{R}D_{xk} + m_2 \, {}^{R}D_{yk} + n_2 \, {}^{R}D_{zk} \qquad (232) \\
{}^{R}D_{ZGk} &= \dot{Z}_g + \ell_3 \, {}^{R}D_{xk} + m_3 \, {}^{R}D_{yk} + n_3 \, {}^{R}D_{zk}
\end{aligned}
$$

Equation 231 is now transformed to the runway coordinate system through Matrix 111 and is added with Equation 222 to yield R_{Tk} (see Equation 212) expressed in the runway coordinate system. The result is

$$
\begin{aligned}
\dot{\bar{R}}_{Tk} &= \dot{\bar{R}} - \dot{\bar{R}}_{GR} + (\dot{\bar{R}}_k)_o + \dot{\bar{r}}_k + \frac{d}{dt}\left[(r_{ok} - \delta_k)\bar{i}_{zR}\right] = \\
&\left[{}^{R}G_{11} \, {}^{R}D_{XGk} + {}^{R}G_{13} \, {}^{R}D_{ZGk} + \omega_{Tk}(r_{ok} - \delta_k) \, {}^{R}I_{22k}\right]\bar{i}_{xR} \qquad (233) \\
&+ \left[{}^{R}D_{YGk} - \omega_{Tk}(r_{ok} - \delta_k) \, {}^{R}I_{21k}\right]\bar{i}_{yR} \\
&+ \left[{}^{R}G_{31} \, {}^{R}D_{XGk} + {}^{R}G_{33} \, {}^{R}D_{ZGk}\right]\bar{i}_{zR}
\end{aligned}
$$

Comparing Equations 233 and 210 yields

$$
\begin{aligned}
V_{Txk} &= {}^{R}G_{11} \, {}^{R}D_{XGk} + {}^{R}G_{13} \, {}^{R}D_{ZGk} + \omega_{Tk}(r_{ok} - \delta_k) \, {}^{R}I_{22k} \\
V_{Tyk} &= {}^{R}D_{YGk} - \omega_{Tk}(r_{ok} - \delta_k) \, {}^{R}I_{21k} \qquad (234) \\
V_{Tzk} &= {}^{R}G_{31} \, {}^{R}D_{XGk} + {}^{R}G_{33} \, {}^{R}D_{ZGk}
\end{aligned}
$$

Equations 234 for V_{TXk} and V_{TYk} are then used to calculate the ground plane forces F_{TRXk} and F_{TRYk} (see Equations 162 and 163). Note that Equation 234 for V_{TZk} is not used but is useful when one realizes it is the vertical velocity (i.e., sink rate) of the kth gear axle as seen by the runway.

(h) Wheel Equations of Motion

In deriving an expression for the ground plane velocity, $\bar{V}_{GPTk}$, of the kth tire footprint, the rotational velocity, ω_{Tk}, was introduced. Since ω_{Tk} changes during landing, another equation of motion is needed. Applying Newton's Law about the wheel axle yields

$$\sum M_k = n_k I_k \dot{\omega}_{Tk} \tag{235}$$

where

M_k = applied moment about k^{th} axle

I_k = moment of inertia of a tire, wheel, and anything else constrained to rotate with that wheel about the axle.

The applied moments are predominantly the moments of the ground reaction forces and braking moments (if applied). Let M_{Ak} be the moment of the ground reaction forces about the axle and let M_{Bk} be a braking moment which will be determined by the Brake Autopilot as shown in Appendix III. Equation 235, therefore, becomes

$$M_{Ak} - M_{Bk} \frac{\omega_{Tk}}{|\omega_{Tk}|} = n_k I_k \dot{\omega}_{Tk} \tag{236}$$

Note that the braking moment always opposes the motion, ω_{Tk}. Solving Equation 236 for $\dot{\omega}_{Tk}$ yields

$$\dot{\omega}_{Tk} = \left(M_{Ak} - M_{Bk} \frac{\omega_{Tk}}{\omega_{Tk}} \right) / I_k n_k \tag{237}$$

Equation 237 is then solved numerically to obtain ω_{Tk}. The variable M_{Ak} must be defined however, in terms of known quantities before the integration can proceed.

The vector from the axle to the footprint of the tire is $(r_{ok} - \delta_k)\,\bar{i}_{ZR}$. The vector moment $\bar{M}_{Ak}$ of the ground reaction $\bar{F}_{TRk}$ (see Equation 159) about the axle is

$$\bar{M}_{Ak} = (r_{ok} - \delta_k)\,\bar{i}_{ZR} \times \bar{F}_{TR_k} \tag{238}$$

Substituting Equation 159 for $\bar{F}_{TRk}$ and writing Equation 238 in determinant form yields

$$\bar{M}_{Ak} = \begin{bmatrix} \bar{i}_{XR} & \bar{i}_{YR} & \bar{i}_{ZR} \\ 0 & 0 & (r_{ok} - \delta_k) \\ F_{TRxk} & F_{TRyk} & F_{TRzk} \end{bmatrix} \tag{239}$$

Expanding Equation 239 yields

$$\bar{M}_{Ak} = -F_{TRyk}(r_{ok} - \delta_k)\,\bar{i}_{xR} + F_{TRxk}(r_{ok} - \delta_k)\,\bar{i}_{yR} \tag{240}$$

Since M_{Ak} (see Equation 236) is the component of $\bar{M}_{Ak}$ along the axle direction $\bar{i}_{yk}$, Matrix 168 performs the desired transformation of Equation 240 and shows to be

$$M_{Ak} = -F_{TRyk}(r_{ok} - \delta_k)\,R_{121k} + F_{TRxk}(r_{ok} - \delta_k)\,R_{122k} \tag{241}$$

This completes the derivation of all quantities needed for all the equations of motion (see Equation 101, 106, 137, 147 and 237).

d. Expanded Equations of Motion

Five kinds of equations of motion were needed to describe the landing vehicle with gears. Each equation is repeated here for convenience.

$$\bar{M}_o = \bar{\bar{I}}_o \cdot \dot{\bar{\omega}}_o + \bar{\omega}_o \times (\bar{\bar{I}}_o \cdot \bar{\omega}_o) + \sum_{k=1}^{K} m_k \left[(\bar{R}_k)_o + \bar{r}_{kc} \right] \times (\ddot{\bar{r}}_{kc})_k \tag{101}$$

$$\bar{F}_T = m_T \ddot{\bar{R}} + \sum_{k=1}^{K} m_k (\ddot{\bar{r}}_{kc})_k \tag{106}$$

$$\ddot{S}_k = \left\{ \ddot{\bar{R}} + \dot{\bar{\omega}}_o \times (\bar{R}_k)_o + \bar{\omega}_o \times \left[\bar{\omega}_o \times (\bar{R}_k)_o \right] \right\} \cdot \bar{I}_{zk} + \alpha_k - g_{zk} \tag{137}$$

$$\begin{aligned} \ddot{S}_{kz} = & \left[(P_k - P_{k2}) A_{k2} + C_k (\dot{S}_k - \frac{A_{k2}}{A_k} \dot{S}_{k2}) \left| \dot{S}_k - \frac{A_{k2}}{A_k} \dot{S}_{k2} \right| \right. \\ & \left. - C_{k2} \dot{S}_{k2} \left[\dot{S}_{k2} \right] - C_{k2L} \dot{S}_{k2} + F_{ck2} \right] / m_{k2} + g_{zk} \\ & - \left[\ddot{\bar{R}} + \dot{\bar{\omega}}_o \times (\bar{R}_k)_o + \bar{\omega}_o \times \left[\bar{\omega}_o \times (\bar{R}_k)_o \right] \right] \cdot \bar{I}_{zk} + \ddot{S}_k \end{aligned} \tag{147}$$

$$\dot{\omega}_{Tk} = (M_{Ak} - M_{Bk} \frac{\omega_{Tk}}{|\omega_{Tk}|}) / I_k n_k \tag{237}$$

Equations 101, 106, 137, and 147 contain vector operations (though completely defined) that are yet to be expanded before numerical integration can proceed. We begin with Equation 101.

Since the counterpart to Equation 101 in SDF-2 is written in body fixed axes, the vector operations in Equation 101 must finally be expressed in body fixed axes. The vector $(\bar{R}_k)_o$ (see Equation 114) is first transformed to the $\bar{I}_k$ axes system through Matrix 108 and then added $(r_{Fk} - S_{kc})\bar{I}_{zk}$ (see Equation 115) to yield

$$(\bar{R}_k)_o + (r_{Fk} - S_{kc}) \bar{I}_{zk} = R_{RICGX} \bar{I}_{xk} + R_{RICGX} \bar{I}_{yk} + R_{RICGZ} \bar{I}_{zk} \tag{242}$$

where

$$R_{RICGX} = \alpha_{k11} R_{kx} + \alpha_{k13} R_{kz}$$

$$R_{RICGY} = R_{ky} \tag{243}$$

$$R_{RICGZ} = \alpha_{k31} R_{kx} + \alpha_{k33} R_{kz} + r_{Fk} - S_{kc}$$

Note that Equations 243 are constants. The vector $(\bar{R}_k)_o + \bar{r}_{kc}$ can therefore be written

$$(\bar{R}_k)_o + \bar{r}_{kc} = R_{RICGX} \bar{i}_{xk} + R_{RICGY} \bar{i}_{yk} + (R_{RICGZ} - s_k) \bar{i}_{zk} \tag{244}$$

Since $(\ddot{\bar{r}}_{kc})_k$ can be written (see Equation 115),

$$(\ddot{\bar{r}}_{kc})_k = -\ddot{S}_k \bar{i}_{zk} \tag{245}$$

Then the vector cross product in Equation 101 can be expressed as

$$\left[(\bar{R}_k)_o + \bar{r}_{kc}\right] \times (\ddot{\bar{r}}_{kc})_k = \begin{vmatrix} \bar{i}_{xk} & \bar{i}_{yk} & \bar{i}_{zk} \\ R_{RICGX} & R_{RICGY} & (R_{RICGZ} - S_k) \\ 0 & 0 & -\ddot{S}_k \end{vmatrix} = \tag{246}$$

$$-\ddot{S}_k R_{RICGY} \bar{i}_{xk} + \ddot{S}_k R_{RICGX} \bar{i}_{yk}$$

Transforming Equation 246 back to body axes (see Matrix 108) yields

$$\left[(\bar{R}_k)_o + \bar{r}_{kc}\right] \times (\ddot{\bar{r}}_{kc})_k = -\alpha_{k11} \ddot{S}_k R_{RICGY} \bar{i}_{xo} + \tag{247}$$

$$-\ddot{S}_k R_{RICGX} \bar{i}_{yo} - \alpha_{k13} \ddot{S}_k R_{RICGY} \bar{i}_{zo}$$

Substituting Equation 247 into Equation 101 yields

$$\bar{M}_o = \bar{\bar{I}}_o \cdot \dot{\bar{\omega}}_o + \bar{\omega}_o \times (\bar{\bar{I}}_o \cdot \bar{\omega}_o) + \sum_{k=1}^{K} m_k \ddot{S}_k (-\alpha_{k11} R_{RICGY} \bar{i}_{xo} + R_{RICGX} \bar{i}_{yo} - \alpha_{k13} R_{RICGY} \bar{i}_{zo}) \tag{248}$$

Equation 248 (i.e., also Equation 101) is now expressed in body axes.

Equation 106 is written in body axes by substituting Equation 245 for $(\ddot{\bar{r}}_{kc})_k$ and realizing that $\bar{i}_{zk} = \alpha_{k31} \bar{i}_{xo} + \alpha_{k33} \bar{i}_{zo}$ (see Matrix 108). The result is

$$\bar{F}_T = m_T \ddot{\bar{R}} - \sum_{k=1}^{K} m_k \ddot{S}_k (\alpha_{k31} \bar{i}_{xo} + \alpha_{k33} \bar{i}_{zo}) \tag{249}$$

Equations 137 and 147 contain the vector expression

$$\left\{ \ddot{\bar{R}} + \dot{\bar{\omega}}_o \times (\bar{R}_k)_o + \bar{\omega}_o \times \left[\bar{\omega}_o \times (\bar{R}_k)_o \right] \right\} \cdot \bar{i}_{zk}$$

Each expression is taken in turn.

(1) $\ddot{\bar{R}} \cdot \bar{i}_{zk}$

The vector $\ddot{\bar{R}}$ is obtained directly from SDF-2 as

$$\ddot{\bar{R}} = \frac{F_x}{m_T} \bar{i}_{xo} + \frac{F_y}{m_T} \bar{i}_{yo} + \frac{F_z}{m_T} \bar{i}_{zo} \tag{250}$$

Since by Matrix 108 $\bar{i}_{zk} = a_{k31} \bar{i}_{xo} + a_{k33} \bar{i}_{zo}$

then the scalar $\ddot{\bar{R}} \cdot \bar{i}_{zk}$ is

$$\ddot{\bar{R}} \cdot i_{zk} = \frac{F_x}{M_T} \alpha_{k31} + \frac{F_z}{M_T} \alpha_{k33} \tag{251}$$

(2) $\left[\dot{\bar{\omega}} \times (\bar{R}_k)_o \right] \cdot \bar{i}_{zk}$

The vector $\dot{\bar{\omega}}_o$ is obtained directly from SDF-2 as

$$\dot{\bar{\omega}}_o = \dot{p}\bar{i}_{xo} + \dot{q}\bar{i}_{yo} + \dot{r}\bar{i}_{zo} \tag{252}$$

The vector $(\bar{R}_k)_o$ is Equation 114. The vector cross product $\dot{\bar{\omega}}_o \times (\bar{R}_k)_o$ is therefore

$$\dot{\omega}_o \times (R_k)_o = \begin{vmatrix} \bar{i}_{xo} & \bar{i}_{yo} & \bar{i}_{zo} \\ \dot{p} & \dot{q} & \dot{r} \\ R_{kx} & R_{ky} & R_{kz} \end{vmatrix} = (\dot{q}R_{kz} - \dot{r}R_{ky})\, i_{xo} + \tag{253}$$

$$(\dot{r}R_{kx} - \dot{p}R_{kz})\bar{i}_{yo} + (\dot{p}R_{ky} - \dot{q}R_{kx})\bar{i}_{zo}$$

Using the expression previously used for $\bar{i}_{zk}$ yields the scalar expression

$$\left[\dot{\bar{\omega}}_o \times (\bar{R}_k)_o\right] \cdot \bar{i}_{zk} \text{ to be}$$

$$\left[\dot{\bar{\omega}}_o \times (\bar{R}_k)_o\right] \cdot \bar{i}_{zk} = \alpha_{k31}(\dot{q}R_k - \dot{r}R_{ky}) + \alpha_{k33}(\dot{p}R_{ky} - \dot{q}R_{kx}) \tag{254}$$

(3) $\bar{\omega}_o \times \left[\bar{\omega}_o \times (\bar{R}_k)_o\right] \cdot \bar{i}_{zk}$

The vector $\bar{\omega}_0 \times \left[\bar{\omega}_0 \times (\bar{R}_k)_0\right]$ is

$$\bar{\omega}_0 \times \left[\bar{\omega}_0 \times (\bar{R}_k)_0\right] = \begin{vmatrix} \bar{i}_{xo} & \bar{i}_{yo} & \bar{i}_{zo} \\ p & q & r \\ (qR_{kz}-rR_{ky}) & (rR_{kx}-pR_{kz}) & (pR_{ky}-qR_{kx}) \end{vmatrix} =$$

$$\left[q(pR_{ky}-qR_{kx})-r(rR_{kx}-pR_{kz})\right]\bar{i}_{xo}$$

$$+\left[r(qR_{kz}-rR_{ky})-p(pR_{ky}-qR_{kx})\right]\bar{i}_{yo} \tag{255}$$

$$+\left[p(rR_{kx}-pR_{kz})-q(qR_{kz}-rR_{ky})\right]\bar{i}_{zo}$$

Once again using the expression for $\bar{i}_{zk}$ yields the scalar $\bar{\omega}_0 \times \left[\bar{\omega}_0 \times (\bar{R}_k)_0\right] \cdot \bar{i}_{zk}$ to be

$$\bar{\omega}_0 \times \left[\bar{\omega}_0 \times (\bar{R}_k)_0\right] \cdot \bar{i}_{zk} = \alpha_{k31}\left[q(pR_{ky}-qR_{kx})\right.$$

$$\left.-r(rR_{kx}-pR_{kz})\right] + \alpha_{k33}\left[p(rR_{kx}-pR_{kz})-q(qR_{kz}-rR_{ky})\right] \tag{256}$$

Summing the results of paragraphs (1), (2) and (3) and letting the result be S_{Rk} which is the $\bar{i}_{zk}$ component of the inertial acceleration of the kth strut axes system, yields

$$S_{Rk} = \left\{\ddot{\bar{R}} + \dot{\bar{\omega}}_0 \times (\bar{R}_k)_0 + \bar{\omega}_0 \times \left[\bar{\omega}_0 \times (\bar{R}_k)_0\right]\right\} \cdot \bar{i}_{zk} =$$

$$\frac{F_x}{m_T}\alpha_{k31} + \frac{F_z}{m_T}\alpha_{k33} + \alpha_{k31}(\dot{q}R_{kz} - \dot{r}R_{ky})$$

$$+\alpha_{k33}(\dot{p}R_{ky} - \dot{q}R_{kx}) + \alpha_{k31}\left[q(pR_{ky}-qR_{kx})\right. \tag{257}$$

$$\left.-r(rR_{kx}-pR_{kz})\right] + \alpha_{k33}\left[p(rR_{kx}-pR_{kz})-q(qR_{kz}-rR_{ky})\right]$$

Equations 137 and 147 therefore become

$$\ddot{S}_k = S_{Rk} + \alpha_k - g_{zk} \tag{258}$$

$$\begin{aligned}\ddot{S}_{k2} = \Big[& (P_k - P_{k2}) A_{k2} + C_k \left(\dot{S}_k - \frac{A_{k2}}{A_k} \dot{S}_{k2}\right) \left| \dot{S}_k - \frac{A_{k2}}{A_k} \dot{S}_{k2} \right| \\ & - C_{k2} \dot{S}_{k2} \left| \dot{S}_{k2} \right| - C_{k2L} \dot{S}_{k2} + F_{ck2} \Big] / m_{k2} \\ & + g_{zk} - S_{Rk} + \ddot{S}_k\end{aligned} \tag{259}$$

Equations 237, 248, 249, 258, and 259 are the five equations of motion written in the proper coordinate systems and are in a form convenient for numerical integration.

SECTION III

DISCUSSION

The SDF-2 equations of motion are written with the total applied force $\bar{F}_T$ and total applied moment $\bar{M}_o$ written in body axes as

$$\bar{F}_T = F_x \bar{i}_{xo} + F_y \bar{i}_{yo} + F_z \bar{i}_{zo} \tag{260}$$

$$\bar{M}_o = L \bar{i}_{xo} + M \bar{i}_{yo} + N \bar{i}_{zo} \tag{261}$$

By rewriting the modified equations of motion (i.e., Equations 248 and 249) with the added terms as applied forces and moments (i.e., on the left sides of the equations), the added terms can be looked upon as changes in the SDF-2 applied forces and moments brought on by adding the landing gears and ground reactions to the simulation. If the new $\bar{F}_T$ and $\bar{M}_o$ are written as

$$\begin{aligned} \bar{F}_T &= (F_x + F_{xm})\bar{i}_{xo} + (F_y + F_{ym})\bar{i}_{yo} \\ &\quad + (F_z + F_{zm})\bar{i}_{zo} \\ \bar{M}_o &= (L + L_m)\bar{i}_{xo} + (M + M_m)\bar{i}_{yo} \\ &\quad + (N + N_m)\bar{i}_{zo} \end{aligned} \tag{262}$$

where F_{xm}, F_{ym}, F_{zm}, L_m, M_m, and N_m are the changes in F_x, F_y, F_z, L, M, N, respectively, which are presently in the SDF-2 formulation, then the changes are

$$
\begin{aligned}
F_{xm} &= F_{TRA} + \sum_k m_k \ddot{s}_k a_{k31} \\
F_{ym} &= F_{TRB} \\
F_{zm} &= F_{TRC} + \sum_k m_k \ddot{s}_k a_{k33} \\
L_m &= M_{Tx} + \sum_k m_k \ddot{s}_k a_{k11} R_{ky} \\
M_m &= M_{Ty} - \sum_k m_k \ddot{s}_k R_{RICGx} \\
N_m &= M_{Tz} + \sum_k m_k \ddot{s}_k a_{k13} R_{ky}
\end{aligned}
\tag{263}
$$

This concludes the formulation of the equations defining the SDF-2 modification to include landing gear dynamics and ground reactions.

SECTION IV

LANDING GEAR FLOW CHARTS

The following flow charts show the previous equations in their required order of calculation. The corresponding equation numbers are given on the right side of the equation to serve as a handy reference in finding a desired derivation.

CALCULATIONS DONE ONCE

$$a_{k11} = \cos\theta_k$$
$$a_{k13} = -\sin\theta_k$$
$$a_{k31} = \sin\theta_k$$
$$a_{k33} = \cos\theta_k$$

(109)

$$R_{G11} = \cos E_R$$
$$R_{G13} = -\sin E_R$$
$$R_{G31} = \sin E_R$$
$$R_{G33} = \cos E_R$$

(112)

$$R_{RkcGX} = a_{k11} R_{kx} + a_{k13} R_{kz}$$

(243)

[RL] MATRIX ELEMENTS

$$R_{L11} = \ell_1 R_{G11} + \ell_3 R_{G13}$$
$$R_{L12} = \ell_2$$
$$R_{L13} = \ell_1 R_{G31} + \ell_3 R_{G33}$$
$$R_{L21} = m_1 R_{G11} + m_3 R_{G13}$$
$$R_{L22} = m_2$$
$$R_{L23} = m_1 R_{G31} + m_3 R_{G33}$$
$$R_{L31} = n_1 R_{G11} + n_3 R_{G13}$$
$$R_{L32} = n_2$$
$$R_{L33} = n_1 R_{G31} + n_3 R_{G33}$$

(167)

→ A

(A)

$[RI]$ MATRIX ELEMENTS

$$
\begin{aligned}
R_{I11k} &= a_{k11} R_{L11} + a_{k13} R_{L31} \\
R_{I12k} &= a_{k11} R_{L12} + a_{k13} R_{L32} \\
R_{I13k} &= a_{k11} R_{L13} + a_{k13} R_{L33} \\
R_{I21k} &= R_{L21} \\
R_{I22k} &= R_{L22} \\
R_{I23k} &= R_{L23} \\
R_{I31k} &= a_{k31} R_{L11} + a_{k33} R_{L31} \\
R_{I32k} &= a_{k31} R_{L12} + a_{k33} R_{L32} \\
R_{I33k} &= a_{k31} R_{L13} + a_{k33} R_{L33}
\end{aligned}
\tag{169}
$$

$$
\begin{bmatrix} R_{AXk} \\ R_{AYk} \\ R_{AZk} \end{bmatrix} = \begin{bmatrix} \ell_1 & m_1 & n_1 \\ \ell_2 & m_2 & n_2 \\ \ell_3 & m_3 & n_3 \end{bmatrix} \begin{bmatrix} R_{kx} + a_{k31}(r_{Fk} - S_k) \\ R_{ky} \\ R_{kz} + a_{k33}(r_{Fk} - S_k) \end{bmatrix}
\tag{188}
$$

(B)

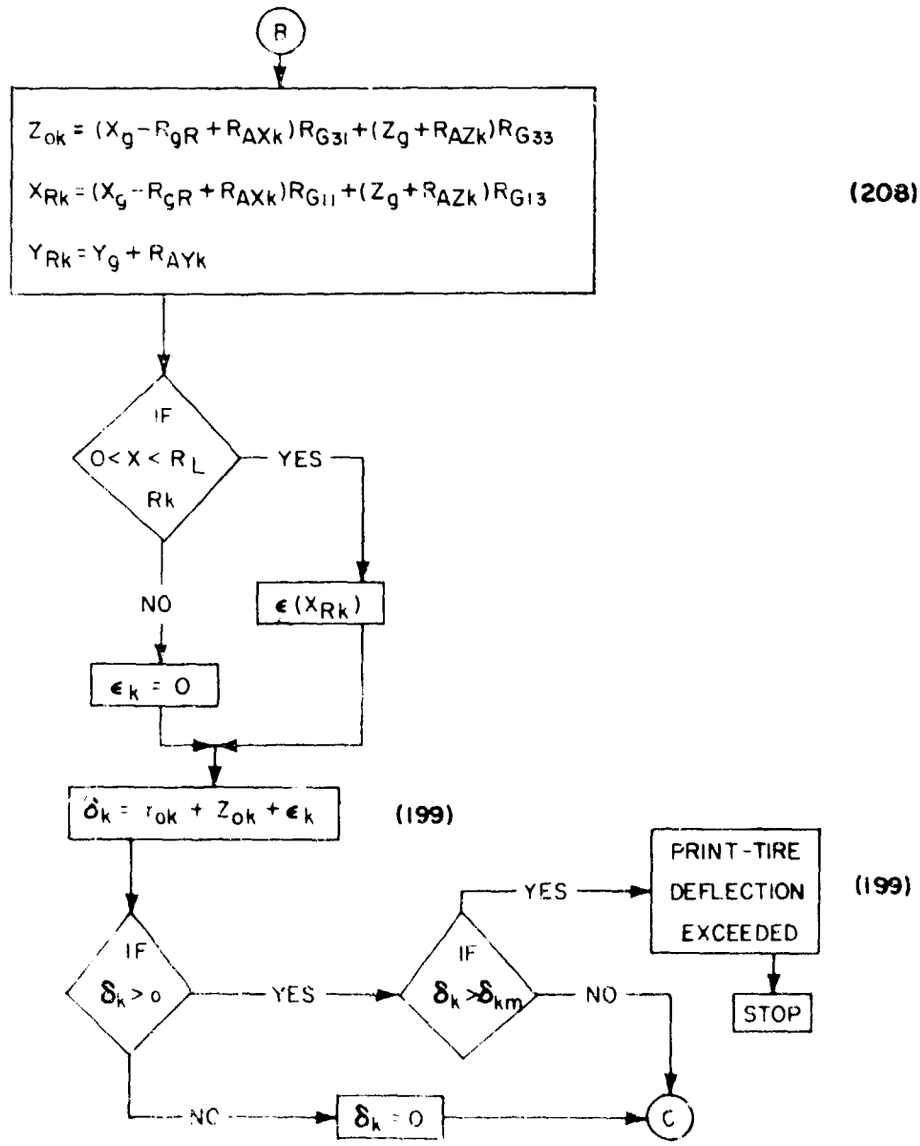
R
$Z_{ok} = (X_g - R_{gR} + R_{AXk})R_{G31} + (Z_g + R_{AZk})R_{G33}$
$X_{Rk} = (X_g - R_{gR} + R_{AXk})R_{G11} + (Z_g + R_{AZk})R_{G13}$
$Y_{Rk} = Y_g + R_{AYk}$
(208)
IF $0 < X < R_L$ Rk
YES
NO
$\epsilon(X_{Rk})$
$\epsilon_k = 0$
$\delta_k = r_{ok} + Z_{ok} + \epsilon_k$
(199)
IF $\delta_k > o$
YES
IF $\delta_k > \delta_{km}$
YES
PRINT-TIRE DEFLECTION EXCEEDED
(199)
STOP
NO
NO
$\delta_k = 0$
C

C

$$P_k = \frac{P_{ok} V_{ok}}{V_{ok} - A_k S_k + A_{k2} S_{k2}} \tag{128}$$

$$P_{k2} = \frac{P_{ok2} V_{ok2}}{V_{ok2} - A_{k2} S_{k2}} \tag{129}$$

$$f_k(\delta_k)$$

$$F_{TRZk} = -n_k f_k(\delta_k) \tag{150}$$

$$\begin{aligned} R_{DXk} &= -S_k a_{k31} + (r_{Fk} - S_k) q a_{k33} + q R_{kz} - r R_{ky} \\ R_{DYk} &= (r_{Fk} - S_k)(r a_{k31} - p a_{k33}) + r R_{kx} - p R_{kz} \\ R_{DZk} &= -\dot{S}_k a_{k33} - (r_{Fk} - S_k) q a_{k31} + p R_{ky} - q R_{kx} \end{aligned} \tag{229}$$

$$\begin{bmatrix} R_{DXGk} \\ R_{DYGk} \\ R_{DZGk} \end{bmatrix} = \begin{bmatrix} \dot{X}_g \\ \dot{Y}_g \\ \dot{Z}_g \end{bmatrix} + \begin{bmatrix} \ell_1 & m_1 & n_1 \\ \ell_2 & m_2 & n_2 \\ \ell_3 & m_3 & n_3 \end{bmatrix} \begin{bmatrix} R_{DXk} \\ R_{DYk} \\ R_{DZk} \end{bmatrix} \tag{232}$$

D

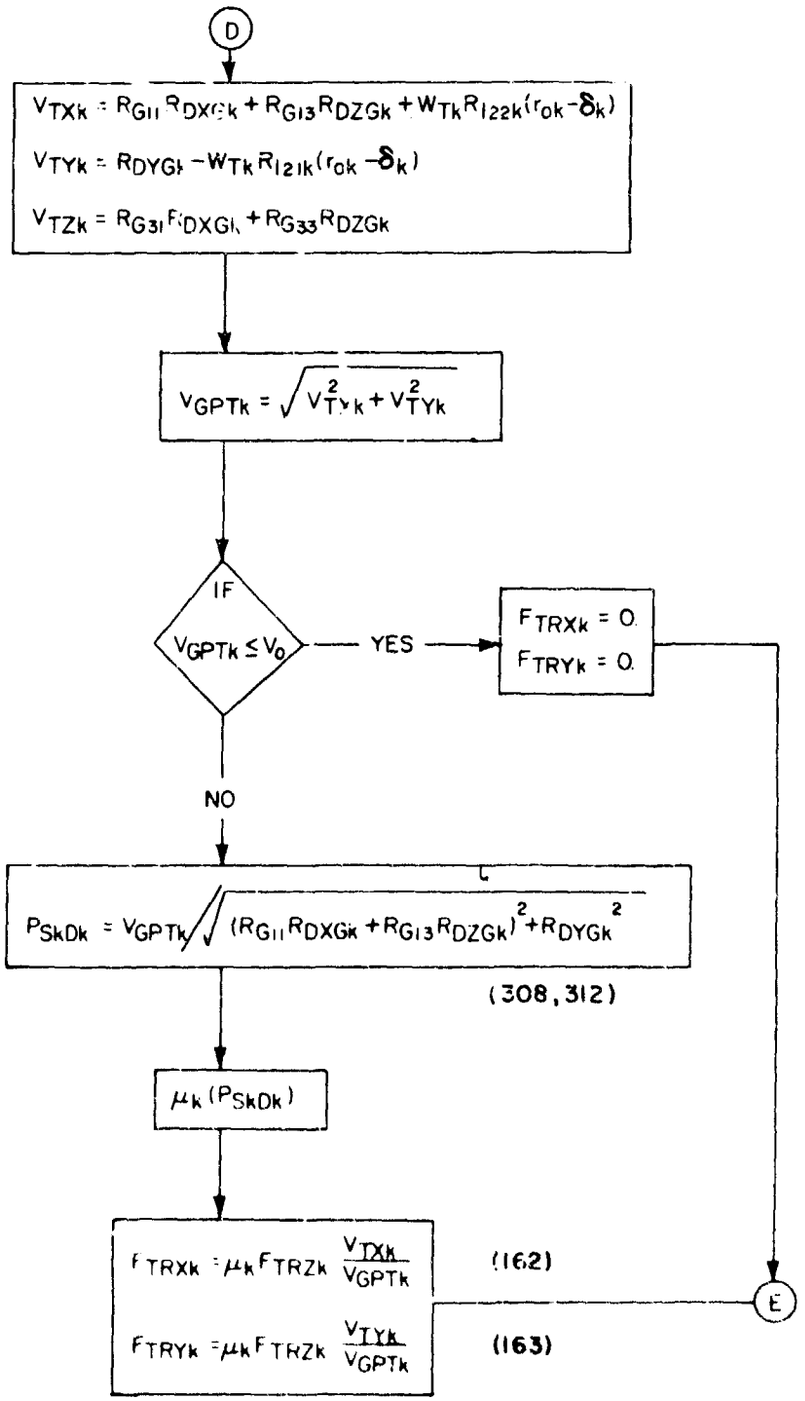
D
$V_{TXk} = R_{G11}R_{DXGk} + R_{G13}R_{DZGk} + W_{Tk}R_{122k}(r_{ok} - \delta_k)$
$V_{TYk} = R_{DYGk} - W_{Tk}R_{121k}(r_{ok} - \delta_k)$
$V_{TZk} = R_{G31}R_{DXGk} + R_{G33}R_{DZGk}$
(234)
$V_{GPTk} = \sqrt{V_{TXk}^2 + V_{TYk}^2}$
(164)
IF
$V_{GPTk} \leq V_0$
YES
$F_{TRXk} = 0.$
$F_{TRYk} = 0.$
NO
$P_{SkDk} = V_{GPTk} / \sqrt{(R_{G11}R_{DXGk} + R_{G13}R_{DZGk})^2 + R_{DYGk}^2}$
(308, 312)
$\mu_k(P_{SkDk})$
$F_{TRXk} = \mu_k F_{TRZk} \frac{V_{TXk}}{V_{GPTk}}$
(162)
$F_{TRYk} = \mu_k F_{TRZk} \frac{V_{TYk}}{V_{GPTk}}$
(163)
E

E

$$D_{Xk} = R_{G11} R_{AXk} + R_{G13} R_{AZk}$$

$$D_{Yk} = R_{AYk} \qquad (190)$$

$$D_{Zk} = R_{G31} R_{AXk} + R_{G33} R_{AZk} + r_{ok} - \delta_k$$

$$M_{TRXk} = D_{Yk} F_{TRZk} - D_{Zk} F_{TRYk}$$

$$M_{TRYk} = D_{Zk} F_{TRXk} - D_{Xk} F_{TRZk} \qquad (193)$$

$$M_{TRZk} = D_{Xk} F_{TRYk} - D_{Yk} F_{TRXk}$$

$$F_{Tk} = -F_{TRXk} R_{131k} - F_{TRYk} R_{132k} - F_{TRZk} R_{133k} \qquad (172)$$

$$F_{dxk} = R_{111k} F_{TRXk} + R_{112k} F_{TRYk} + R_{113k} F_{TRZk} \qquad (175)$$

$$F_{dyk} = R_{121k} F_{TRXk} + R_{122k} F_{TRYk} + R_{123k} F_{TRZk} \qquad (176)$$

$$F_{fk} = \mu_{sk} \sqrt{F_{dxk}^2 + F_{dyk}^2} \qquad (130, 174)$$

$$g_{Zk} = a_{k31} g_x + a_{k33} g_z \qquad (135)$$

F

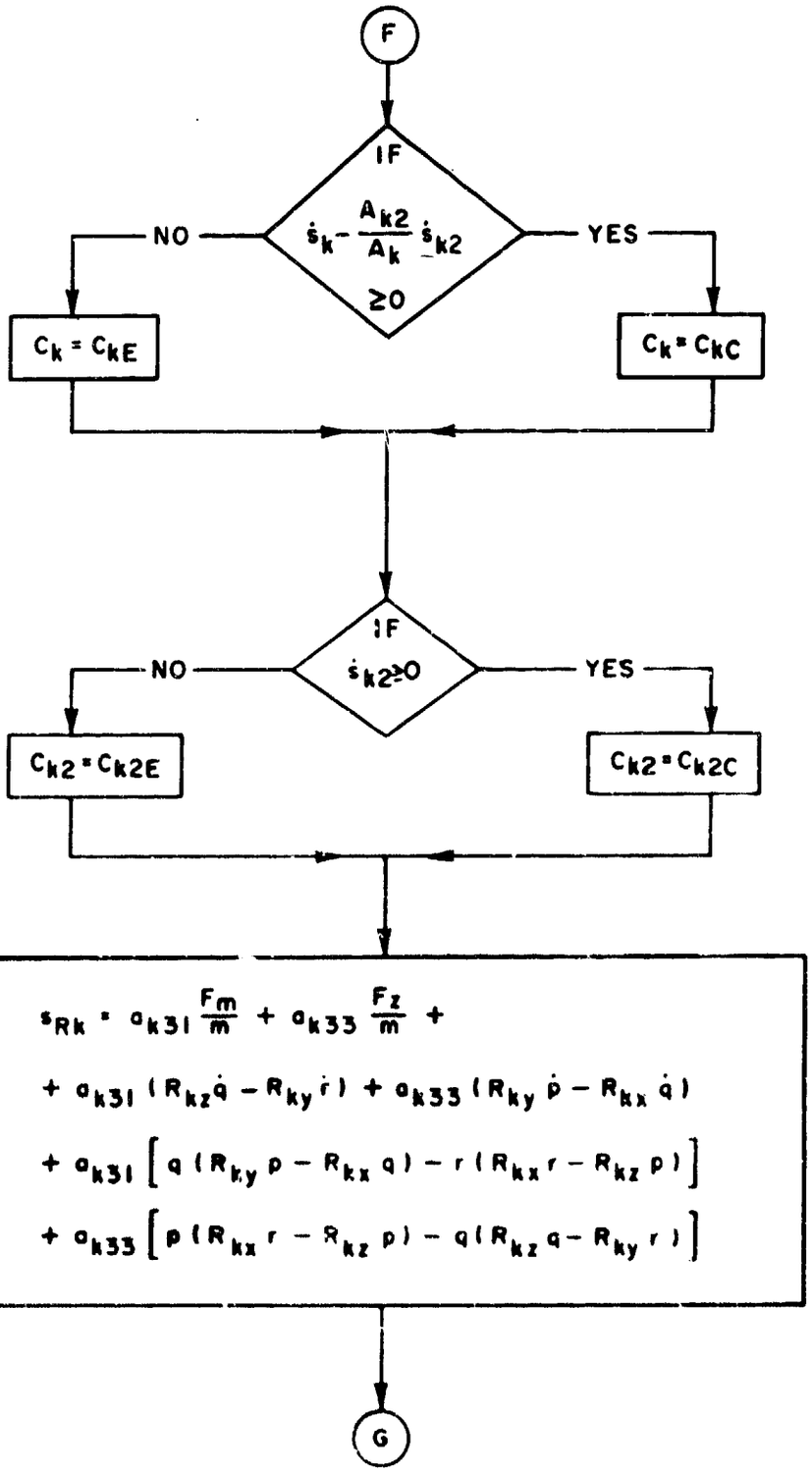
F
IF
$\dot{s}_k - \frac{A_{k2}}{A_k}\dot{s}_{k2} \geq 0$
NO
YES
$C_k = C_{kE}$
$C_k = C_{kC}$
IF
$\dot{s}_{k2} \geq 0$
NO
YES
$C_{k2} = C_{k2E}$
$C_{k2} = C_{k2C}$
$s_{Rk} = a_{k31}\frac{F_m}{m} + a_{k33}\frac{F_z}{m} +$
$+ a_{k31}(R_{kz}\dot{q} - R_{ky}\dot{r}) + a_{k33}(R_{ky}\dot{p} - R_{kx}\dot{q})$
$+ a_{k31}\left[q(R_{ky}p - R_{kx}q) - r(R_{kx}r - R_{kz}p)\right]$
$+ a_{k33}\left[p(R_{kx}r - R_{kz}p) - q(R_{kz}q - R_{ky}r)\right]$
G

(257)

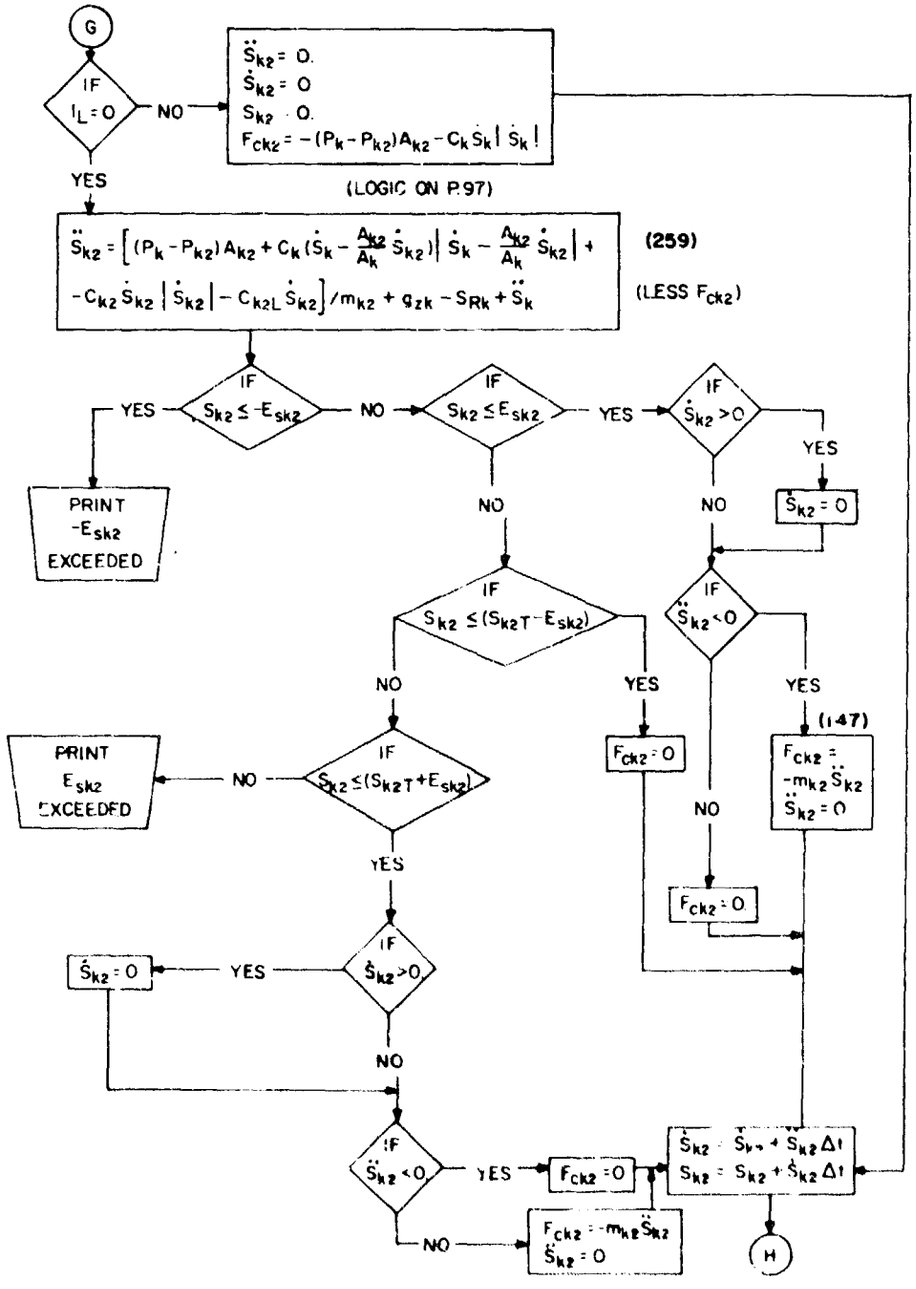
G
IF $I_L = 0$
NO
YES
$\ddot{S}_{k2} = 0.$
$\dot{S}_{k2} = 0$
$S_{k2} = 0.$
$F_{ck2} = -(P_k - P_{k2})A_{k2} - C_k \dot{S}_k |\dot{S}_k|$
(LOGIC ON P.97)
$\ddot{S}_{k2} = \left[(P_k - P_{k2})A_{k2} + C_k(\dot{S}_k - \frac{A_{k2}}{A_k}\dot{S}_{k2})\left|\dot{S}_k - \frac{A_{k2}}{A_k}\dot{S}_{k2}\right| + -C_{k2}\dot{S}_{k2}|\dot{S}_{k2}| - C_{k2L}\dot{S}_{k2}\right]/m_{k2} + g_{zk} - S_{Rk} + \ddot{S}_k$
(259)
(LESS F_{ck2})
IF $S_{k2} \le -E_{sk2}$
YES
PRINT $-E_{sk2}$ EXCEEDED
NO
IF $S_{k2} \le E_{sk2}$
YES
IF $\dot{S}_{k2} > 0$
YES
$\dot{S}_{k2} = 0$
NO
NO
IF $S_{k2} \le (S_{k2T} - E_{sk2})$
NO
YES
IF $\ddot{S}_{k2} < 0$
YES
(147)
$F_{ck2} = -m_{k2}\ddot{S}_{k2}$
$\ddot{S}_{k2} = 0$
$F_{ck2} = 0$
NO
$F_{ck2} = 0$
PRINT E_{sk2} EXCEEDED
NO
IF $S_{k2} \le (S_{k2T} + E_{sk2})$
YES
IF $\dot{S}_{k2} > 0$
YES
$\dot{S}_{k2} = 0$
NO
IF $\ddot{S}_{k2} < 0$
YES
$F_{ck2} = 0$
$\dot{S}_{k2} = \dot{S}_{k2} + \ddot{S}_{k2}\Delta t$
$S_{k2} = S_{k2} + \dot{S}_{k2}\Delta t$
NO
$F_{ck2} = -m_{k2}\ddot{S}_{k2}$
$\ddot{S}_{k2} = 0$
H

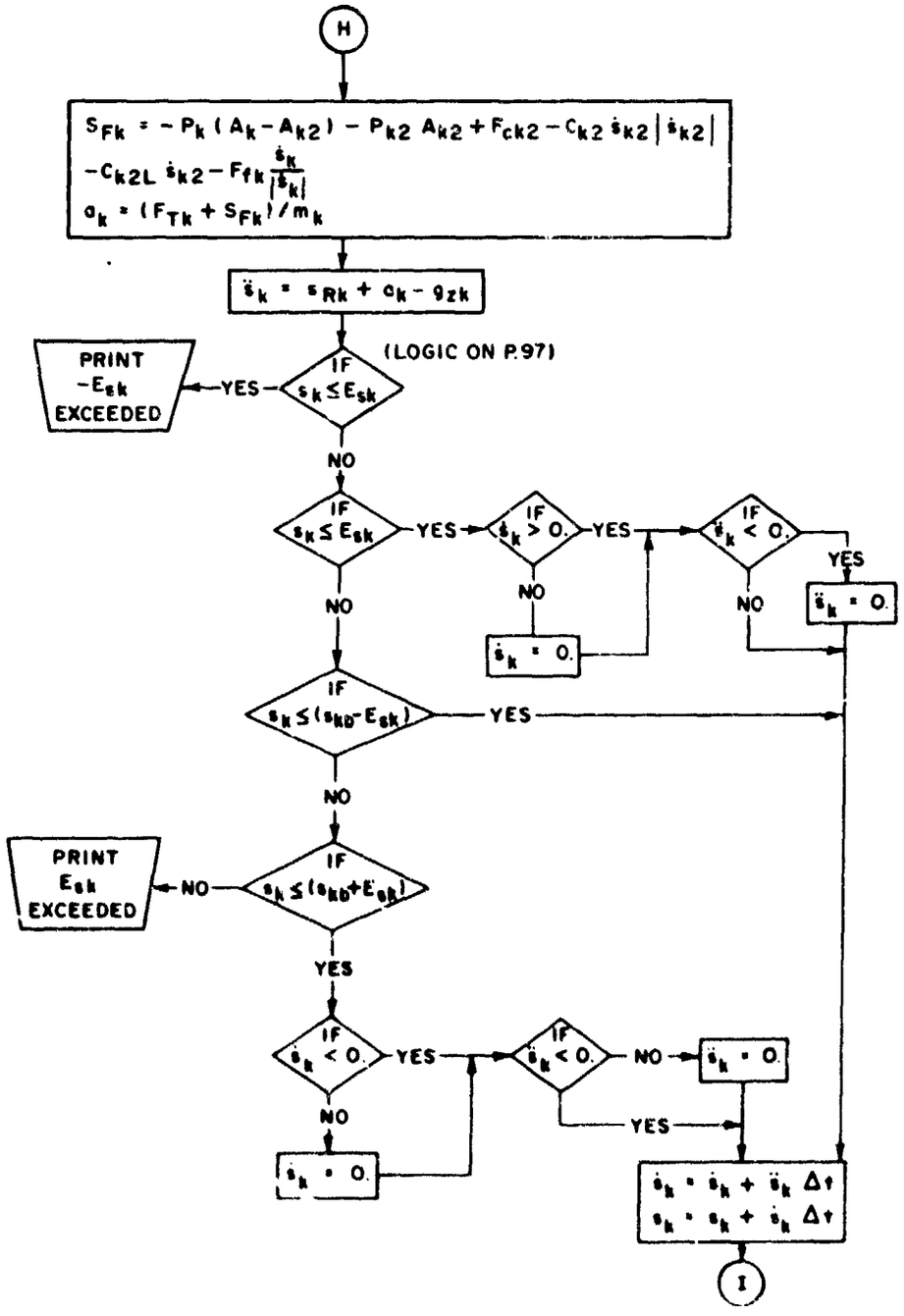
H
$S_{Fk} = -P_k(A_k - A_{k2}) - P_{k2}A_{k2} + F_{ck2} - C_{k2}\dot{s}_{k2}|\dot{s}_{k2}|$ (127)
$-C_{k2L}\dot{s}_{k2} - F_{fk}\frac{\dot{s}_k}{|\dot{s}_k|}$ (138)
$a_k = (F_{Tk} + S_{Fk})/m_k$ (139)
$\ddot{s}_k = s_{Rk} + a_k - g_{zk}$ (258)
(LOGIC ON P.97)
IF $s_k \le E_{sk}$
YES
PRINT $-E_{sk}$ EXCEEDED
NO
IF $s_k \le E_{sk}$
YES
IF $\dot{s}_k > 0.$
YES
IF $\ddot{s}_k < 0.$
YES
$\ddot{s}_k = 0.$
NO
$\dot{s}_k = 0.$
NO
IF $s_k \le (s_{kD} - E_{sk})$
YES
NO
IF $s_k \le (s_{kD} + E_{sk})$
NO
PRINT E_{sk} EXCEEDED
YES
IF $\dot{s}_k < 0.$
YES
IF $\ddot{s}_k < 0.$
NO
$\ddot{s}_k = 0.$
YES
NO
$\dot{s}_k = 0.$
$\dot{s}_k = \dot{s}_k + \ddot{s}_k \Delta t$
$s_k = s_k + \dot{s}_k \Delta t$
I

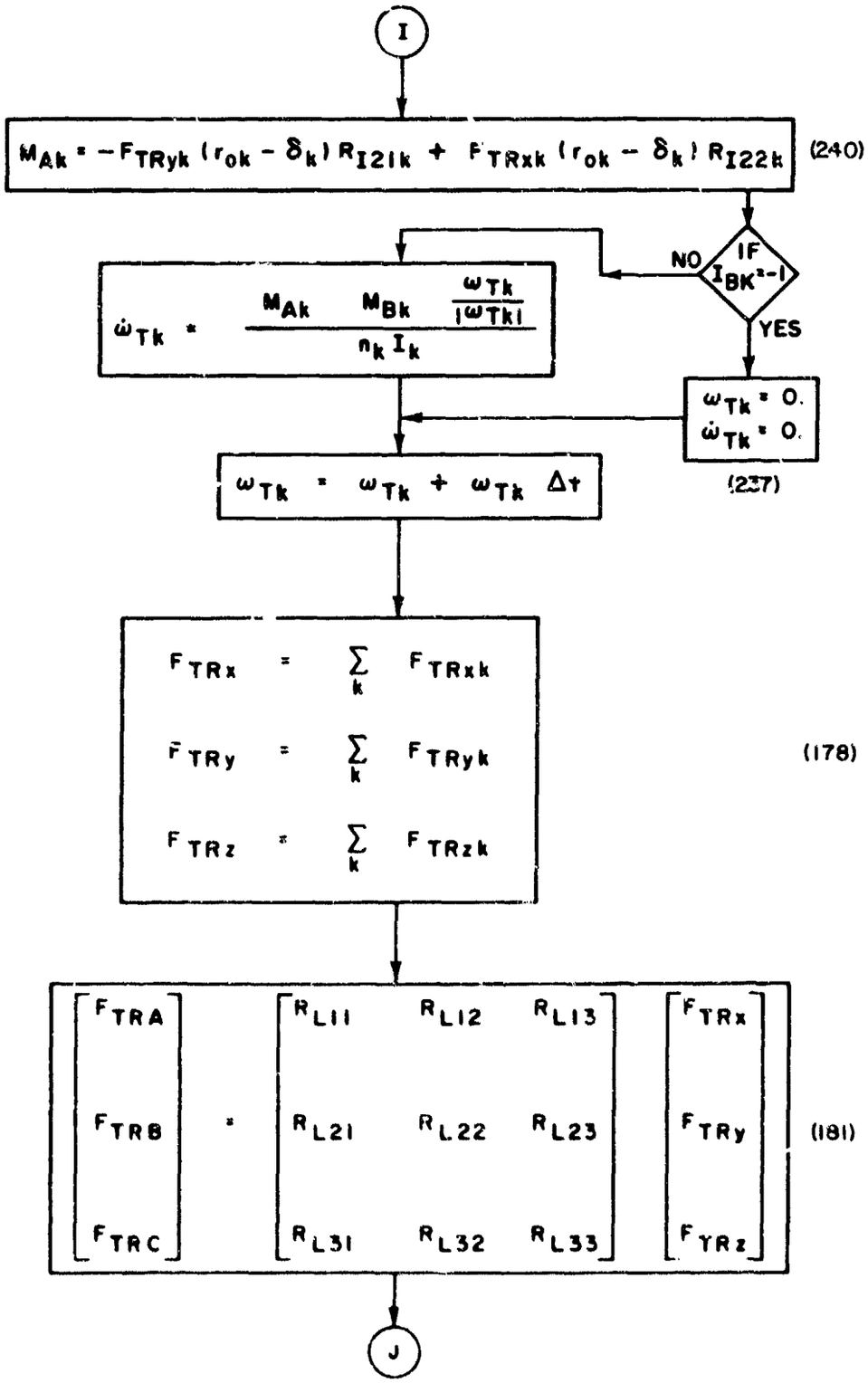
I
$M_{Ak} = -F_{TRyk}(r_{ok} - \delta_k) R_{I21k} + F_{TRxk}(r_{ok} - \delta_k) R_{I22k}$
(240)
IF $I_{BK} = -1$
NO
YES
$\dot{\omega}_{Tk} = \frac{M_{Ak} \quad M_{Bk} \quad \frac{\omega_{Tk}}{|\omega_{Tk}|}}{n_k I_k}$
$\omega_{Tk} = 0.$
$\dot{\omega}_{Tk} = 0.$
(237)
$\omega_{Tk} = \omega_{Tk} + \omega_{Tk} \Delta t$
$F_{TRx} = \sum_k F_{TRxk}$
$F_{TRy} = \sum_k F_{TRyk}$
$F_{TRz} = \sum_k F_{TRzk}$
(178)
$\begin{bmatrix} F_{TRA} \\ F_{TRB} \\ F_{TRC} \end{bmatrix} = \begin{bmatrix} R_{L11} & R_{L12} & R_{L13} \\ R_{L21} & R_{L22} & R_{L23} \\ R_{L31} & R_{L32} & R_{L33} \end{bmatrix} \begin{bmatrix} F_{TRx} \\ F_{TRy} \\ F_{TRz} \end{bmatrix}$
(181)
J

J

$$M_{TRx} = \sum_k M_{TRxk}$$
$$M_{TRy} = \sum_k M_{TRyk} \qquad (195)$$
$$M_{TRz} = \sum M_{TRzk}$$

$$\begin{bmatrix} M_{Tx} \\ M_{Ty} \\ M_{Tz} \end{bmatrix} = \begin{bmatrix} R_{L11} & R_{L12} & R_{L13} \\ R_{L21} & R_{L22} & R_{L23} \\ R_{L31} & R_{L32} & R_{L33} \end{bmatrix} \begin{bmatrix} M_{TRx} \\ M_{TRy} \\ M_{TRz} \end{bmatrix} \qquad (197)$$

$$F_{xM} = F_{TRA} + \sum_k m_k \ddot{s}_k a_{k31}$$
$$F_{yM} = F_{TRB}$$
$$F_{zM} = F_{TRC} + \sum_k m_k \ddot{s}_k a_{k33} \qquad (263)$$
$$L_M = M_{Tx} + \sum_k m_k \ddot{s}_k a_{k11} R_{ky}$$
$$M_M = M_{Ty} - \sum_k m_k \ddot{s}_k R_{RkCGx}$$
$$N_M = M_{Tz} + \sum_k m_k \ddot{s}_k a_{k13} R_{ky}$$

K

(K)

ADD $F_{xM}, F_{yM}, F_{zM}, L_M, M_M, N_M$ TO SDF-2
CALCULATIONS OF F_x, F_y, F_z, L, M, N AS FOLLOWS:

$$
\begin{aligned}
F_x &= T_x - a + m g_x + \Delta F_x + F_{xM} \\
F_y &= T_y + y + m g_y + \Delta F_y + F_{yM} \\
F_z &= T_z - n_F + m g_z + \Delta F_z + F_{zM} \\
L &= L_T + \Delta L_T + \ell + L_M \\
M &= M_T + \Delta M_T + m + M_M \\
N &= N_T + \Delta N_T + n + N_M
\end{aligned}
\tag{262}
$$

CONTINUE SDF-2
CALCULATIONS

APPENDIX III

CONTROL MANAGEMENT EQUATIONS

SECTION I

AUTOPILOT PROBLEM DEFINITION

1. PROBLEM DISCUSSION

The aerodynamics subroutine in SDF-2 (called SACS - see pgs 41-45 of Appendix I) can simulate the aerodynamic effects of a single control surface in each of the axes pitch, yaw and roll. The input aerodynamic data can also be "staged" (i.e. changed during the running of the program) to simulate the deployment of flaps, slats, spoilers, etc. The thrust subroutine in SDF-2 (called TFFS see pgs 46-47 of Appendix I) can simulate the thrust and fuel flow of a single airbreathing engine as a function of altitude, Mach number, angle of attack, and throttle setting. Therefore, SDF-2 as originally formulated has sufficient control variables, with limited modification, to control the aircraft in six degrees of freedom. The question which remains unanswered, however, is that concerning the magnitude of the control variables at any time. This is the function of the autopilot which can be stated in question form as follows: Given the state of the aircraft, what values should the control variables be? This Appendix concerns itself with the answer to this question. Figure 26 shows this basic interface between SDF-2 and the autopilot.

In finally arriving at the control variable values, the autopilot must necessarily answer the following questions:

a. What is the desired state of the aircraft?

b. Given the present state of the aircraft, does an error in state exist and if so what maneuver will be done to correct the state error?

c. What control variable values (i.e., elevator, rudder, and aileron deflections and throttle settings) will result in the desired maneuvers?

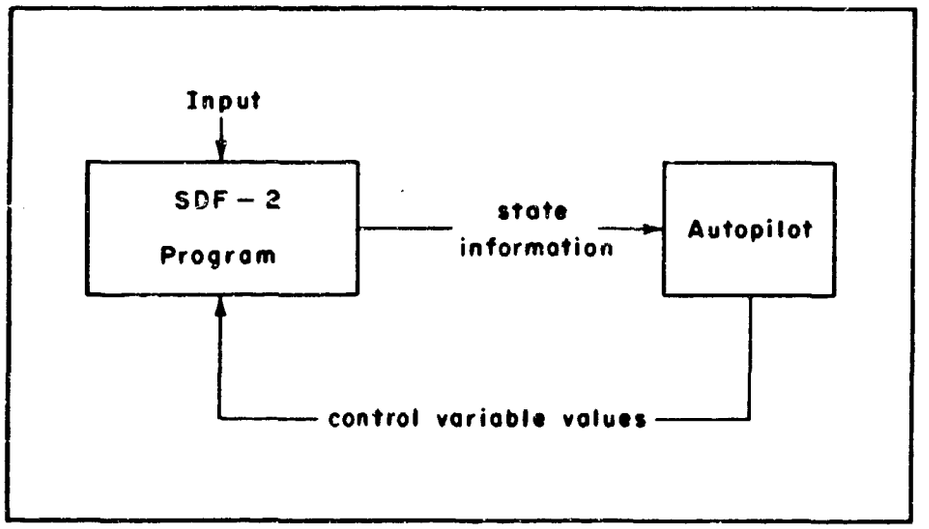

Figure 26. Autopilot - SDF-2 Interface

2. DESIRED CAPABILITIES

The following is a list of the major capabilities required of the autopilot:

a. Control the aircraft in six degrees of freedom during the glide slope, flare, landing roll, and takeoff roll within the capability of a given aircraft.

b. Perform aircraft control with changing winds.

c. Be capable of analyzing multiple engine aircraft with engine failures and engine reverse.

d. Simulate control as aircraft transitions into ground effect.

e. Examine first order effects of control surface and engine lags.

f. Examine braking capability and selected braking failures.

g. Include a drag chute simulation.

h. Be able to start at any point in the landing or takeoff sequence and terminate calculation at selected points.

3. ASSUMPTIONS

The basic assumption is that initially the aircraft is on or near the desired spatial position and is trimmed in all three axes and power such that if no further perturbations occur, (such as wind changes, engine failures, changing aerodynamics due to ground effect, etc.) the aircraft will remain on the nominal glide slope position and inertial velocity. It is further assumed that the approach speeds are low enough (such as 1.2 - 1.3 V_{stall}) so that the aerodynamic coefficients are predominantly a function of aircraft control surface configuration and altitude (i.e., ground effect) and not Mach number. It is also assumed that the aircraft is low enough so that runway level thrust properties are valid. This eliminates engine performance dependence on altitude changes. Variation of aircraft weight during landing and takeoff is also considered negligible.

SECTION II

MANEUVER LOGIC

The maneuver logic concerns itself with the answer to questions 1 and 2 in Section I. As shall be seen, the maneuver logic determines the desired values of angle of attack, angle of sideslip, roll angle, and thrust (along with other commands) which define a maneuver to correct a state error. The organization of this logic is divided into four areas: glide slope, flare, landing roll, and takeoff roll.

1. GLIDE SLOPE

The basic requirements of the aircraft while in the glide slope phase are two: to be vectorially near the glide slope within an allowed error; and to maintain the inertial speed down the glide slope a constant. We begin by defining the position error.

a. Postion Error

Examine Figure 27, part of which is extracted from Figure 22.

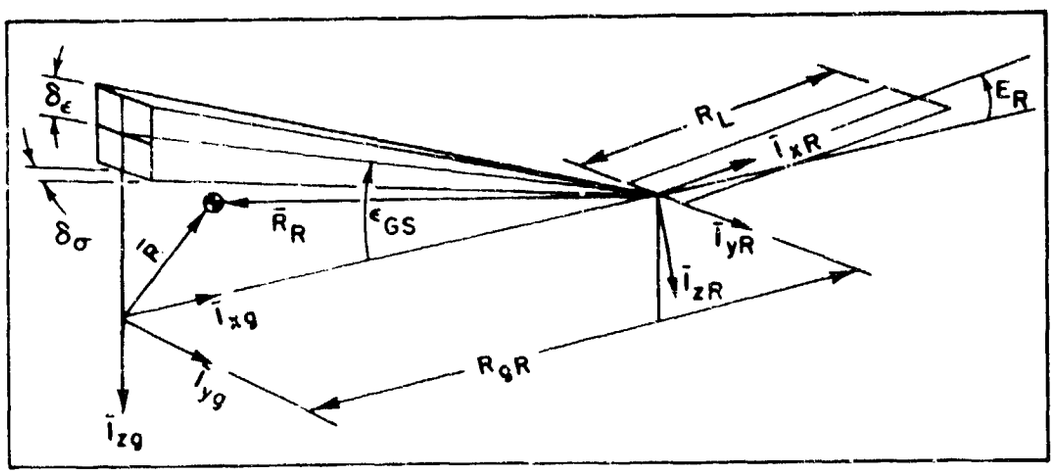

Figure 27. Glide Slope Geometry

The nominal glide slope position is defined in the vertical plane (i.e., plane containing the unit vector $\bar{i}_{zg}$ and $\bar{i}_{xg}$) and has the glide slope angle, ϵ_{GS}, measured up from the horizontal plane. The glide slope origin begins at a distance, h_{CG}, above (not indicated in Figure 27) the runway origin. The variable, h_{CG}, is the fixed distance between the aircraft mass center and a line parallel to the longitudinal body axis which is tangent to the bottom tire surface of the main landing gear. As such, if the aircraft were on the glide slope at the runway origin, the tires would just touch the runway. Figure 28 shows this geometry for the vertical plane. The allowed glide slope position error in the vertical plane, h_{ea} (see Figure 28), is defined by the fixed angular perturbation, δ_ϵ, and the position vector $\bar{R}_R$. The allowed glide slope position error in the horizontal plane, h_{pa}, (see Figure 29) is defined by a similar fixed angular

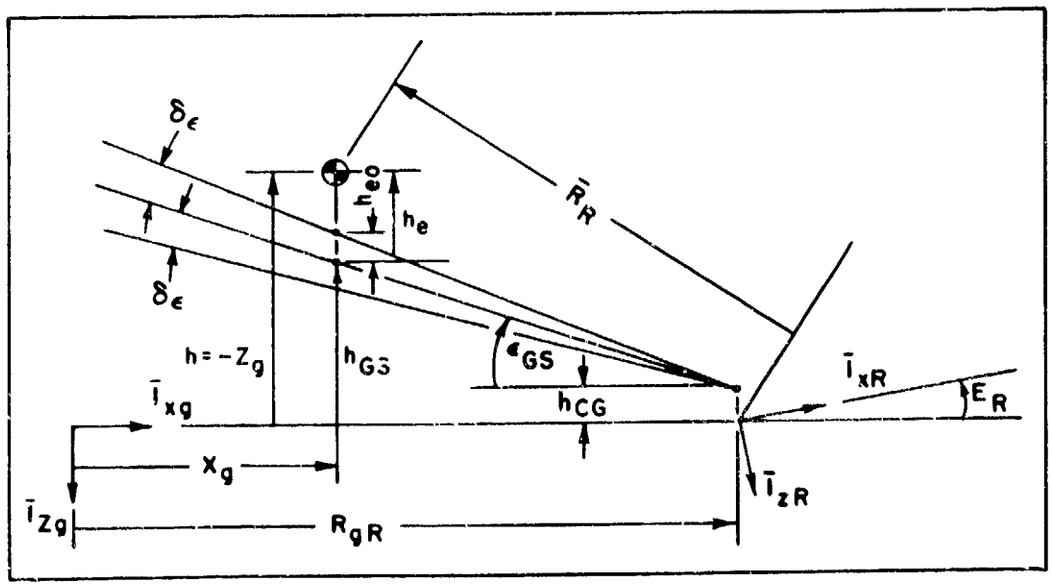

Figure 28. Vertical Plane Glide Slope

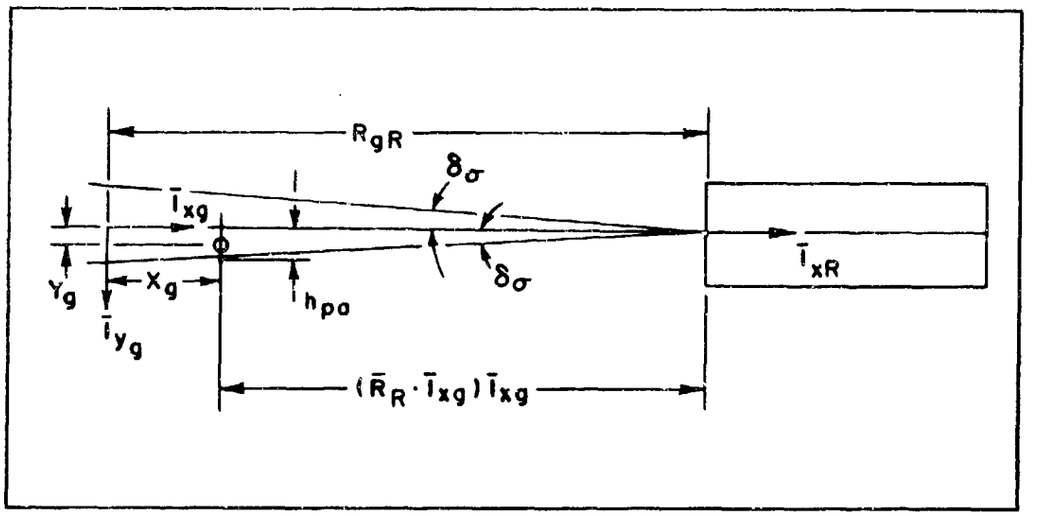

Figure 29. Horizontal Plane Glide Slope

perturbation, δ_σ, and the position vector $\bar{R}_R$. Note that as the aircraft gets closer to the runway origin, the allowed position errors h_{ea} and h_{pa} reduce gradually to a very small value. The equations for h_{ea} and h_{pa} will be approximated (i.e., realizing that ϵ_{GS} is small and $|\bar{R}_R| >> h_{CG}$) as follows:

$$h_{ea} = |\bar{R}_R| \, \delta_\epsilon \tag{264}$$

$$h_{pa} = |\bar{R}_R| \, \delta_\sigma \tag{265}$$

where

$$|\bar{R}_R| = \sqrt{(X_g - R_{gR})^2 + Z_g^2} \tag{266}$$

and δ_ϵ and δ_σ are in radian units. The variables X_g and Z_g are available from the existing SDF-2 formulation and the distance R_{gR} is available from the landing gear modification (see pg 81). The nominal glide slope altitude, h_{GS}, (see Figure 28) is dependent on the position coordinate X_g as follows:

$$h_{GS} = \left| X_g - R_{gR} \right| \tan \epsilon_{GS} + h_{CG} \tag{267}$$

The vertical glide slope position error, h_e, (see Figure 28) is therefore

$$h_e = h - h_{GS} \tag{268}$$

Note that h_e is positive when the aircraft is above the nominal glide slope and is negative when the aircraft is below the nominal glide slope.

The nominal glide slope position in the horizontal plane (see Figure 29) is identically zero (i.e., the aircraft ideally should remain in the vertical glide slope plane). The horizontal glide slope position error is therefore the position coordinate, Y_g, which is also defined in the existing SDF-2 formulation. Note that Y_g is positive to the right of the vertical plane and negative to the left.

In controlling the aircraft to remain within the allowed spatial error (see Figure 27 for a pictorial view), it is helpful to know the rate at which the glide slope position error is changing (i.e., rate feedback). The rate of the vertical glide slope position error, $\dot{h}_e$, can be expressed as follows:

$$\dot{h}_e = -\dot{Z}_g + \dot{X}_g \tan \epsilon_{GS} \tag{269}$$

Note that $\dot{h}_e$ is coupled with the horizontal velocity X_g and h_e is zero only when the aircraft sink rate, $\dot{Z}_g$, is equal to the apparent rate at which the glide slope is falling. The rate of the horizontal glide slope position error is simply $\dot{Y}_g$. The variables $\dot{X}_g$, $\dot{Y}_g$, and $\dot{Z}_g$, are all available from the existing SDF-2 formulation.

The total vertical glide slope position error, h_{eT}, and the total horizontal glide slope position error, h_{PT}, are written as the sum of a position error and a rate error as follows:

$$h_{eT} = h_e + RF_h \dot{h}_e \tag{270}$$

$$h_{PT} = Y_g + RF_y \dot{Y}_g \tag{271}$$

The RF_h and RF_y are input constants and determine the amount of rate feedback in the vertical and horizontal planes respectively. This completes the formulation of the glide slope position error.

b. Velocity Error

If the aircraft is controlled such that h_{eT}, and h_{PT} fall within the allowed errors h_{ea} and h_{pa}, respectively, this only guarantees that the aircraft is vectorially near the nominal glide slope position and does not control the inertial velocity with which the aircraft comes down the glide slope. The inertial velocity error, V_e, must therefore be sensed and is formulated as follows:

$$V_e = V_g - V_d \tag{272}$$

V_g is the inertial velocity magnitude (as formulated in the existing SDF-2) and V_d is the desired inertial velocity down the glide slope which is input as a constant.

c. Glide Slope Dynamic

The two basic requirements for the glide slope (see Pg 147) define a steady-state descent maneuver at constant ground speed. The nominal values of angle of attack, angle of sideslip, roll angle, and thrust to perform this maneuver can be obtained by a steady-state summation of forces acting on the aircraft. We begin by examining forces in the aircraft pitch plane. Examine Figure 30 and the following definitions.

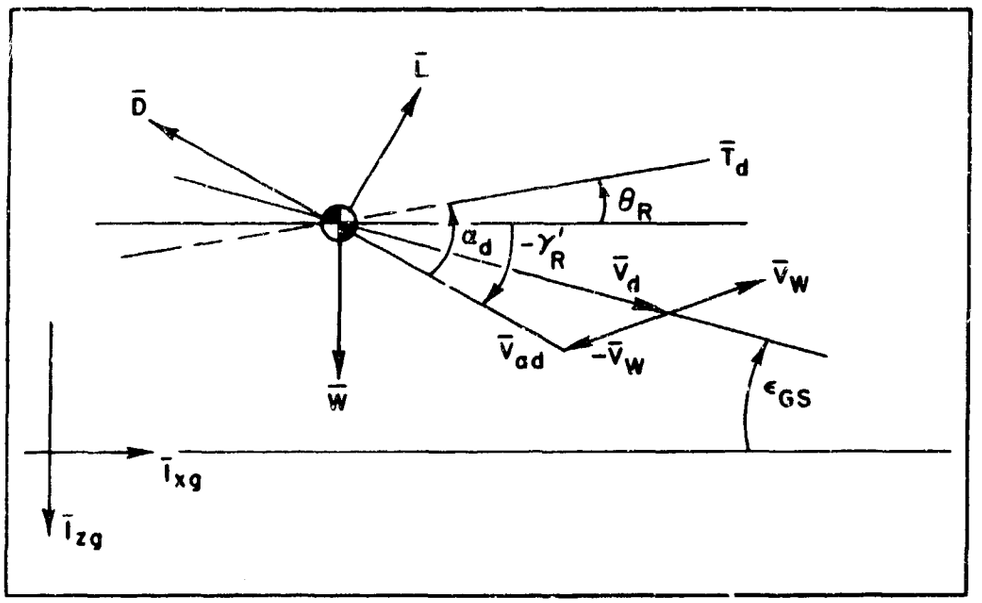

Figure 30. Nominal Forces in Glide Slope

$\bar{V}_d$ = desired inertial vector velocity down the glide slope

$\bar{V}_w$ = wind vector

$\bar{V}_{ad}$ = desired airspeed vector

θ_R = pitch angle of aircraft from horizon

α_d = desired angle of attack

γ'_R = desired flight path angle of V_{ad}

$\bar{T}_d$ = desired thrust vector

$\bar{L}$ = lift vector

$\bar{D}$ = drag vector

$\bar{W}$ - weight vector

ρ = atmospheric density

S = aircraft reference area

C_{LR} = required lift coefficient

Summing forces in the vertical direction (assume aircraft wings approximately level) yields:

$$L\cos(-\gamma_R') + T_d \sin\theta_R + D\sin(-\gamma_R') - W = 0 \tag{273}$$

This may be solved for the required trim value of lift coefficient for the desired static equilibrium gliding condition as:

$$C_{LR} = \frac{\left[M_{gREF} + D_R \sin(\gamma_R') - T_d \sin(\theta_R)\right]}{Q_R S \cos(\gamma_R')} \tag{274}$$

Summing forces in the horizontal direction yields:

$$T_d \cos\theta_R + W\sin(-\gamma_R') - D\cos(-\gamma_R') = 0 \tag{275}$$

solving for T_d yields:

$$T_d = \frac{W\sin\gamma_R' + D\cos\gamma_R'}{\cos\theta_R} \tag{276}$$

Equation 274 can also be written as

$$C_{LR} = \frac{W}{\frac{1}{2}\rho\left|\bar{V}_{ad}\right|^2 S} = \frac{\mathcal{M}_{gREF}}{Q_R S} \tag{277}$$

where T_d and γ_R' are both set to zero as a first approximation. The value of C_{LR} in Equation 277 is used to find an estimate of trim α_d and δ_{q_N}, as will be shown subsequently. T_d is then calculated using Equation 276, followed by a more accurate estimate of C_{LR} through Equation 274, and of T_d through Equation 276.

C_{LR} is dependent on $\left|\bar{V}_{ad}\right|$, which is also dependent on the wind vector $\bar{V}_w$ through the following relationship (see Figure 30):

$$\left|\bar{V}_{ad}\right| = \sqrt{(V_d \cos \epsilon_{GS} - \dot{X}_{gw})^2 + \dot{Y}_{gw}^2 + (V_d \sin \epsilon_{GS} - \dot{Z}_{gw})^2} \qquad (278)$$

The variables $\dot{X}_{gw}$, $\dot{Y}_{gw}$ and $\dot{Z}_{gw}$ are components of the wind vector, $\bar{V}_w$ on the $\bar{1}_{xg}$, $\bar{1}_{yg}$, $\bar{1}_{zg}$, axes, respectively, and are available from the existing SDF-2 formulation.

The coefficient of lift, C_L, is primarily a function of angle of attack, α, and secondarily a function of elevator deflection, δq, through the following relationship:

$$C_L = C_{Lo} + C_{L\alpha}\alpha + C_{L\alpha^2}\left|\alpha\right|\alpha + C_{L\delta_g}\delta_g + C_{L\delta_g^2}\left|\delta_g\right|\delta_g \qquad (279)$$

where C_{Lo}, $C_{L\alpha}$, $C_{L\alpha 2}$, and $C_{L\delta q2}$ are the predominant aerodynamic coefficients contributing to lift. Therefore, for a given elevator deflection, Equation 279 ultimately defines the desired angle of attack α_d, to meet the requirements of Equation 274 for the glide slope. The nominal elevator deflection for use in Equation 279 is obtained using Equation 302 which will be discussed under Pitch Autopilot.

Equation 276 defines the required thrust magnitude, T_d, to maintain the glide slope as a function of W, γ_R', D, and θ_R. The drag force, D, is evaluated at α_d and $\left|\bar{V}_{ad}\right|$ through the following equations:

$$D = C_D \frac{1}{2}\rho \left|V_{ad}\right|^2 S \qquad (280)$$

where

$$C_D = C_{D_o} + C_{D_\alpha}\alpha_d + C_{D_{\alpha^2}}\alpha_d^2 \qquad (281)$$

and C_{Do}, $C_{D\alpha}$, and $C_{D\alpha 2}$ are the predominant aerodynamic coefficients contributing to drag.

The equations defining γ_R' and θ_R can be obtained by referring to Figure 30.

$$\gamma_R' = \tan^{-1} - \left[\frac{V_d \sin \epsilon_{GS} - \dot{Z}_{gw}}{V_d \cos \epsilon_{GS} - \dot{X}_{gw}} \right] \tag{282}$$

$$\theta_R = \gamma_R' + \alpha_d \tag{283}$$

The α_d resulting from Equations 277, 302, and 279 and the T_d resulting from evaluating Equation 276, as indicated, are the nominal airplane requirements in the pitch plane to satisfy the requirements of the glide slope in the vertical plane. Summing forces in the horizontal plane yields the basic requirements for the aircraft to remain in the glide slope vertical plane and not drift horizontally. The nominal requirements are: wings level (i.e., no aircraft roll), and sideslip angle of attack zero (i.e., crab aircraft into wind).

The preceding analysis allows the autopilot to determine the nominal trim requirements for a steady descent at constant ground speed for an arbitrary wind vector. Unfortunately, changing winds, engine failures, changing aerodynamic coefficients due to ground effect, etc., require the aircraft to transition between nominal trim requirements which can put all six degrees of freedom into undesired oscillations. Of primary concern in the glide slope are the long-period oscillations of the mass center position about the nominal glide slope position. Though these long-period oscillations present no real control problem to the pilot in real life, they must be sensed in the autopilot simulation and appropriately controlled. A means of sensing these oscillations has already been provided through the variables h_{eT} and h_{PT} in Equations 270 and 271.

The vertical oscillations will be indicated by h_{eT} and will be controlled by modifying the desired angle of attack, α_d, as follows:

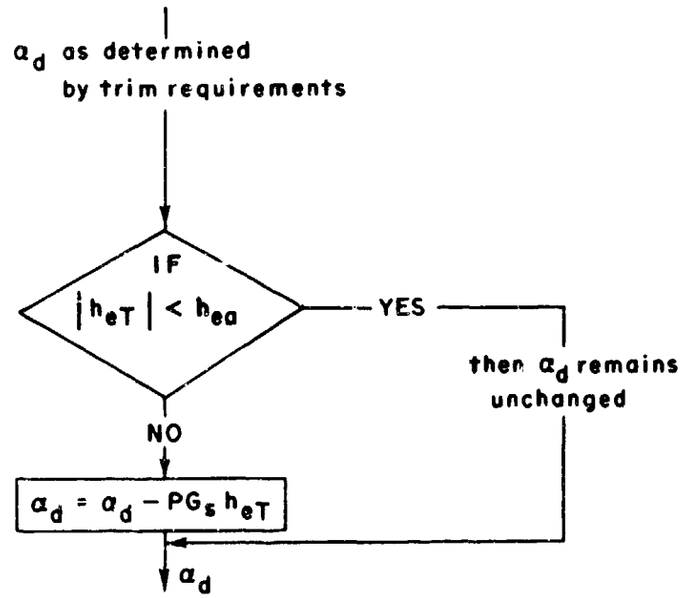

The logic for the modification of α_d comes from an understanding of the nature of the longitudinal long-period mode, but can be briefly stated as follows: when the aircraft is rising above the allowed vertical glide slope error, lower the α_d; when the aircraft is falling below the allowed vertical glide slope error, increase the α_d. The magnitude of the modification to α_d is determined by the input constant PG_s and will depend on the particular aircraft simulated.

The horizontal oscillations will be indicated by h_{PT} and will be controlled by modifying the desired roll angle, ϕ_d, about the zero position (i.e., wings level position) as follows:

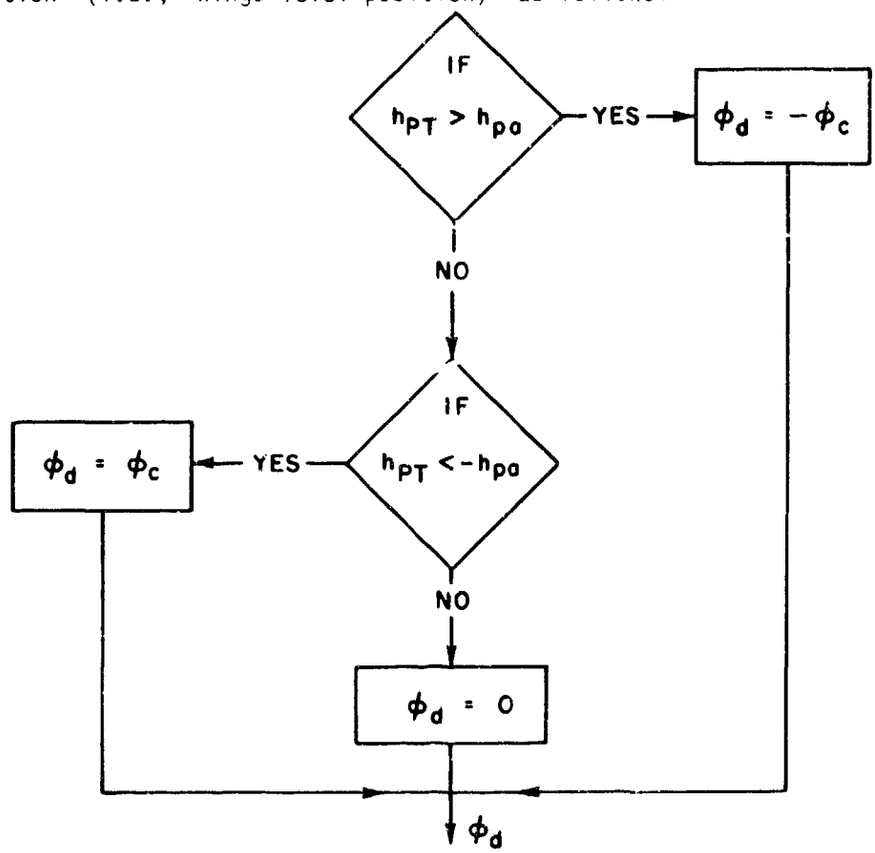

Briefly stated, the horizontal logic is as follows: When the aircraft drift to the right of the glide slope vertical plane exceeds the allowed value h_{Pa}, roll the aircraft - ϕ_c (left); when the aircraft drift to the left of the glide slope vertical plane exceeds the allowed value $-h_{Pa}$, roll the aircraft ϕ_c (right). Since the ϕ_c command will cause a component of the large lift vector to project on the horizontal plane, ϕ_c can be small (3°, etc.) and still control the horizontal oscillations.

This concludes the equations defining the maneuver logic for the glide slope phase of the problem. Figure 31 presents a summary of the equations and logic.

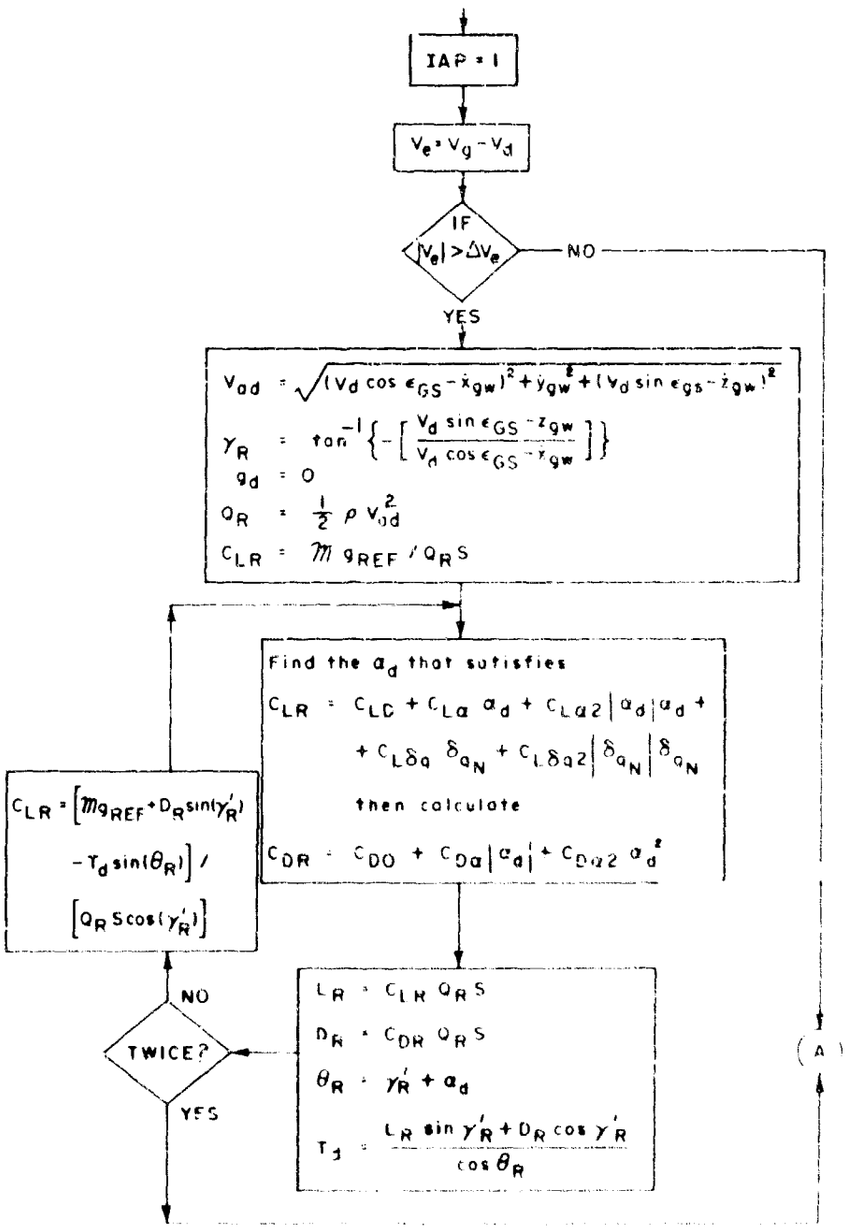

Figure 81. Glide Tow Loop

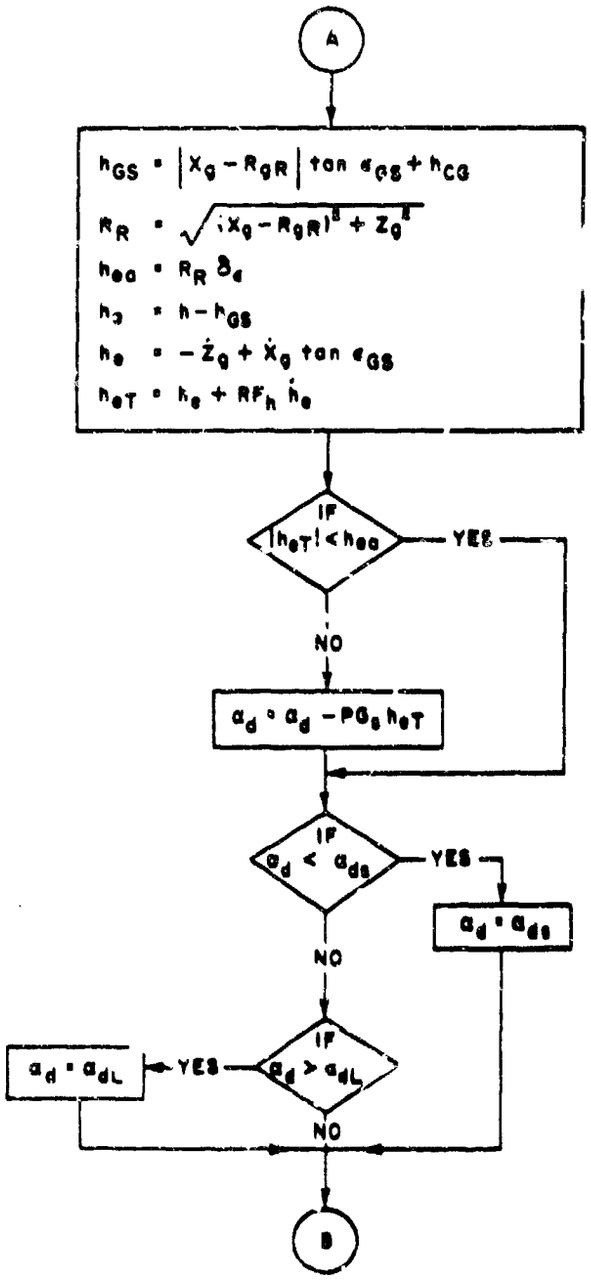

Figure 31. Glide Slope Logic (Contd)

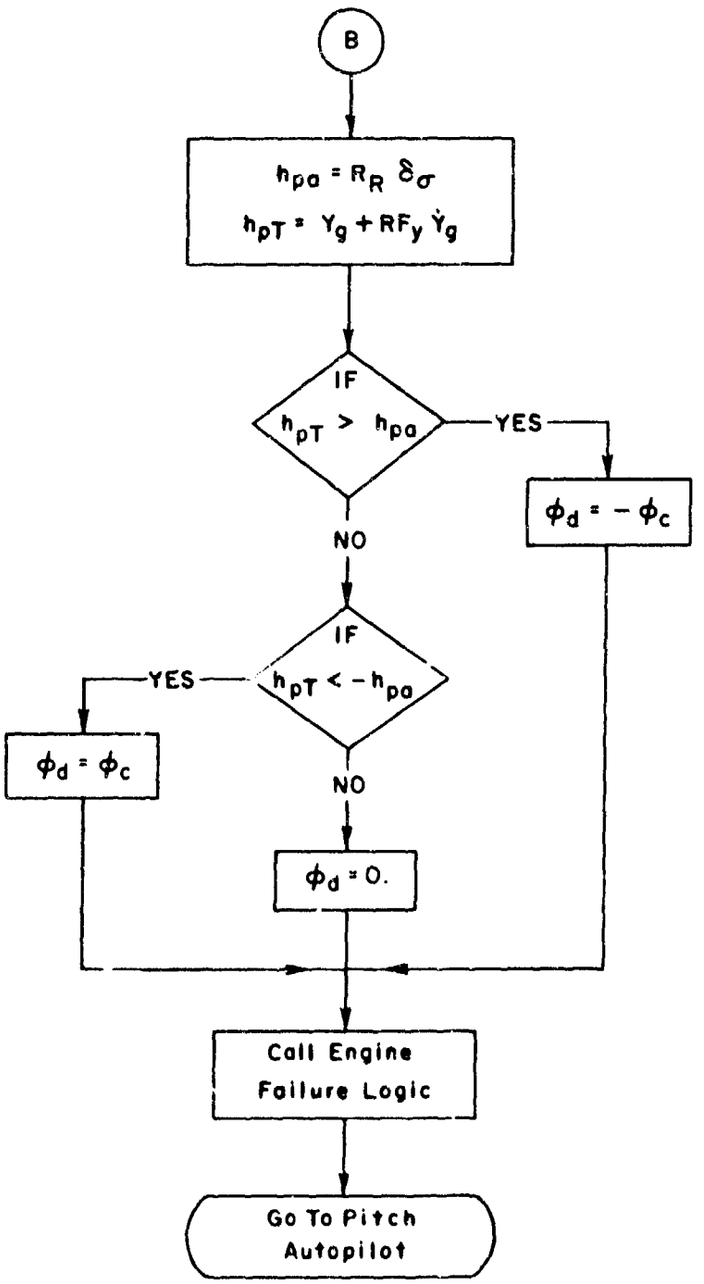

Figure 31. Glide Slope Logic (Concluded)

2. FLARE

The basic requirement of the flare maneuver is to transition the aircraft from an arbitrary vector position and vector velocity in the glide slope, to a desired touchdown vector position and touchdown vector velocity, simultaneously, on the runway. For a realistic landing, the touchdown vector position is limited by runway length and landing distance required to stop the aircraft. The touchdown vector velocity is also limited by acceptable landing speeds and aircraft sink rates. Since there always exists the possible effects of engine failures, wind changes, and limited aircraft flare capability for a given situation, some basic logic is necessary to sacrifice the desired touchdown constraints logically and still make an acceptable landing. The problem is typically a guidance problem subject to constraints. The development of basic guidance laws to perform this function follows:

a. Guidance Laws

The flare guidance laws will be based on a constant acceleration maneuver. Flare initiation will be staged on a particular altitude, h_F, above the ground (see Figure 32). At the time of flare initiation, it is assumed that the glide slope cross range control has the aircraft sufficiently close to the vertical plane so that the wings may be leveled (note aircraft will still remain crabbed into the wind). As such, the flare maneuver is essentially a planar problem and occurs near the vertical plane.

Since the runway can have an elevation angle, E_R, the guidance laws will be developed in the runway coordinate system X_R, h_R where

x_R = aircraft scalar distance down runway

h_R = aircraft altitude above runway

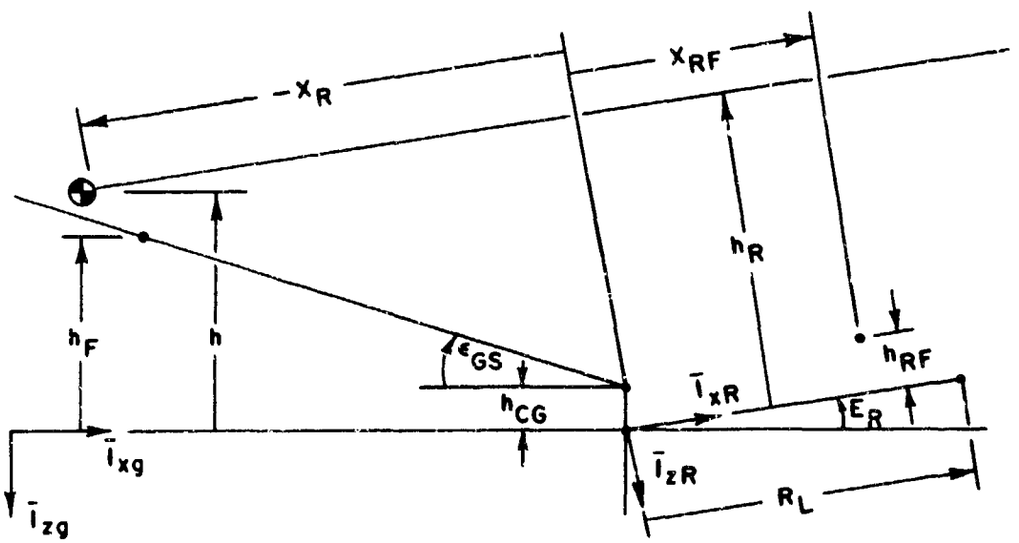

Figure 32. Flare Coordinate System

The desired touchdown conditions are as follows:

x_{RF} = distance down runway for touchdown

h_{RF} = mass center altitude normal to runway for touchdown

$\dot{x}_{RF}$ = landing speed parallel to runway for touchdown

$\dot{h}_{RF}$ = altitude rate normal to runway for touchdown

Consider the following general derivation for any scalar variable, S, with constant acceleration, $\ddot{S}$:

$$\dot{S}_f = \ddot{S}t_s + \dot{S}_i \tag{284}$$

where

t_s = elapsed time

$\dot{S}_i$ = initial $\dot{S}$

$\dot{S}_f$ = final $\dot{S}$

Integrating Equation 284 again yields

$$S_f = \ddot{S}\frac{t_s^2}{2} + \dot{S}_i t_s + S_i \tag{285}$$

where

S_i = initial S

S_f = final S

Solving for t_s in Equation 284 yields:

$$t_s = \frac{\dot{S}_f - \dot{S}_i}{\ddot{S}} \tag{286}$$

Substituting Equation 286 into Equation 285 and expanding yields:

$$\begin{aligned} S_f - S_i &= \frac{\ddot{S}}{2}\left(\frac{\dot{S}_f - \dot{S}_i}{\ddot{S}}\right) + \dot{S}_i\left(\frac{\dot{S}_f - \dot{S}_i}{\ddot{S}}\right) = \\ &= \frac{\dot{S}_f^2 - \dot{S}_i^2}{2\ddot{S}} = \frac{(\dot{S}_f - \dot{S}_i)(\dot{S}_f + \dot{S}_i)}{2\ddot{S}} \end{aligned} \tag{287}$$

Solving Equation 287 for $\ddot{S}$ yields

$$\ddot{S} = (\dot{S}_f - \dot{S}_i)\frac{(\dot{S}_f + \dot{S}_i)}{2(S_f - S_i)} \tag{288}$$

Substituting Equation 288 into Equation 286 yields

$$t_s = \frac{2(S_f - S_i)}{\dot{S}_f + \dot{S}_i} \tag{289}$$

Equation 288 expresses the constant acceleration, $\ddot{S}$, required to transition from the initial state S_i, $\dot{S}_i$, to the final state S_f, $\dot{S}_f$, in terms of the initial present conditions and desired final conditions. Equation 289 expresses the time required, based on constant accelerations,

to make the transition in state. Comparable equations for the scalar variables x_R and h_R are therefore:

$$A_{xR} = (\dot{x}_{RF} - \dot{x}_R)\frac{(\dot{x}_{RF} + \dot{x}_R)}{2(x_{RF} - x_R)} \tag{290}$$

$$t_x = \frac{2(x_{RF} - x_R)}{(\dot{x}_{RF} + \dot{x}_R)} \tag{291}$$

$$A_{hR} = (\dot{h}_{RF} - \dot{h}_R)\frac{(\dot{h}_{RF} + \dot{h}_R)}{2(h_{RF} - h_R)} \tag{292}$$

$$t_h = \frac{2(h_{RF} - h_R)}{(\dot{h}_{RF} + \dot{h}_R)} \tag{293}$$

where

A_{xR} = required acceleration of x_R

t_x = time to perform the x_R state change

A_{hR} = required acceleration of h_R

t_h = time to perform the h_R state change

If Equations 290 and 292 can be satisfied at all times during the flare, they guarantee that the x_{RF}, $\dot{x}_{RF}$ touchdown constraints will occur simultaneously and that the h_{RF}, $\dot{h}_{RF}$, touchdown constraints will occur simultaneously. However, this does not guarantee that the two individual sets of scalar constraints will occur simultaneously. This latter constraint can be met by requiring t_x to equal t_h. This is achieved by the following logic.

Calculate t_x and t_h from present conditions (i.e., x_R, $\dot{x}_R$, h_R, $\dot{h}_R$) and the desired touchdown condition (i.e., x_{RF}, $\dot{x}_{RF}$, h_{RF}, $\dot{h}_{RF}$). Compare the values of t_x and t_h. If t_h is greater than t_x, Equations 291 and 293 suggest four possible sacrifices of the desired touchdown constraints to make t_h and t_x equal:

(1) Increase x_{RF} (i.e., land further down the runway).

(2) Reduce the landing speed, $\dot{x}_{RF}$.

(3) Increase h_{RF} (note $h_R \geq h_{RF}$).

(4) Increase $\dot{h}_{RF}$ in the negative direction.

Sacrifice 3 is eliminated since this would require the aircraft to flare out above the runway. Sacrifice 2 is eliminated since the desired landing speed will already be close to the stall speed. Sacrifice 1 is possible provided there is sufficient runway length left after touchdown to stop the aircraft. Sacrifice means an increase in sink rate at touchdown; this is undesirable, but can be tried once the possibilities of Sacrifice 1 have been exhausted. This logic is formulated as follows: Let

$$x_{RF} = x_{TD} + D_m \tag{294}$$

where

x_{TD} = distance down the runway before which the aircraft must not touchdown. (This is normally zero but can have a positive value which in effect places the closest allowable touchdown point ahead of the effective runway beginning.)

D_m = distance down runway from x_{TD} to desired touchdown point. Apply Sacrifice 1 by equating t_x and t_h in Equations 291 and 293, substitute Equation 294 for x_{RF} in Equation 291, and solve for the required D_m.

$$D_m = (\dot{x}_{RF} + \dot{x}_R)\frac{(h_{RF} - h_R)}{(\dot{h}_{RF} + \dot{h}_R)} + x_R - x_{TD} \tag{295}$$

Equation 295 expresses the D_m that will allow t_x to increase to the value of t_h. This value of D_m, however, may be too large i.e., D_m must be constrained as follows:

$$L_D + D_m \leq R_L \tag{296}$$

where

R_L = runway length

L_D = required landing distance to stop aircraft

If D_m is too large to meet the constraint of Equation 296, the maximum value of D_m is $R_L - L_D$. If this occurs, t_h will still be greater than t_x, then Sacrifice 4 is applied as a last resort. Sacrifice 4 is applied by equating t_x and t_h in Equations 291 and 293, by substituting

$$x_{RF} = x_{TD} + R_L - L_D$$

as the limiting value for x_{RF} in Equation 291, and solving for the increased $\dot{h}_{RF}$.

$$\dot{h}_{RF} = \frac{(\dot{x}_R + \dot{x}_{RF})}{(x_{RF} - x_R)}(h_{RF} - h_R) - \dot{h}_R \tag{297}$$

If a landing situation is such that Sacrifice 4 is necessary, the sacrifice is one of deciding to land the aircraft harder versus landing further down the runway and risk running off the runway end.

The preceding sacrifices are for the case in which t_h is greater than t_x. For the case in which t_x is greater than t_h, Equations 291 and 293 also suggest four possible sacrifices of the desired touchdown constraints to make $t_h = t_x$:

(1) Decrease x_{RF}, that is, touchdown shorter

(2) Increase the landing speed, $\dot{x}_{RF}$

(3) Decrease h_{RF}

(4) Make $\dot{h}_{RF}$ less negative

Sacrifice 3 here is eliminated for the same reason as previously. Sacrifices 1 and 4 are applied in the same order as before except with different constraints. The constraint on D_m is that it cannot be negative i.e., one does not want to touchdown prior to the effective runway beginning. In the event the required D_m is negative, then Sacrifice 4 is applied and $\dot{h}_{RF}$ is made less negative; however, $\dot{h}_{RF}$ cannot be positive. The equations for D_m and $\dot{h}_{RF}$ are the same as Equations 295 and 297, respectively. In the event $\dot{h}_{RF}$ is reduced to zero, Sacrifice 2 (though undesirable) can be applied as a last resort. The equation for $\dot{x}_{RF}$ is obtained by equating t_x to t_h, substituting $x_{RF} = x_{TD}$ and $\dot{h}_{RF} = 0$, and solving for the required $\dot{x}_{RF}$ as follows:

$$\dot{x}_{RF} = \dot{h}_R \frac{(x_{RF}-x_R)}{(h_{RF}-h_R)} - \dot{x}_R \tag{298}$$

At this point, the desired touchdown conditions have been logically manipulated so as to occur at the same time within specific constraints of the runway and aircraft. These updated values of x_{RF}, $\dot{x}_{RF}$, $\dot{h}_{RF}$, and h_{RF} (not changed) are then used with the present conditions x_R, $\dot{x}_R$, h_R, $\dot{h}_R$ in Equations 290 and 292 to calculate the required accelerations A_{xR} and A_{hR} to make the transition.

b. Flare Dynamics

The preceding paragraph merely defines the required accelerations A_{xR} and A_{hR} to perform the flare maneuver. The values of angle of attack, angle of sideslip, roll angle, and thrust to achieve the particular A_{xR} and A_{hR} are yet to be found. As indicated in the preceding paragraph, the flare maneuver will be done with wings level (desired roll angle = 0) and the aircraft crabbed (desired angle of sideslip = 0) into the relative wind. Assuming the aircraft yaw is small, A_{xR} and A_{hR} are [illegible] fo[illegible] [illegible]lly in the aircraft pitch plane and are predominantly determined by angle of attack and thrust.

The relationship between the scalar accelerations A_{xR} and A_{hR} and the independent variables α and T is as follows. Examine Figure 33,

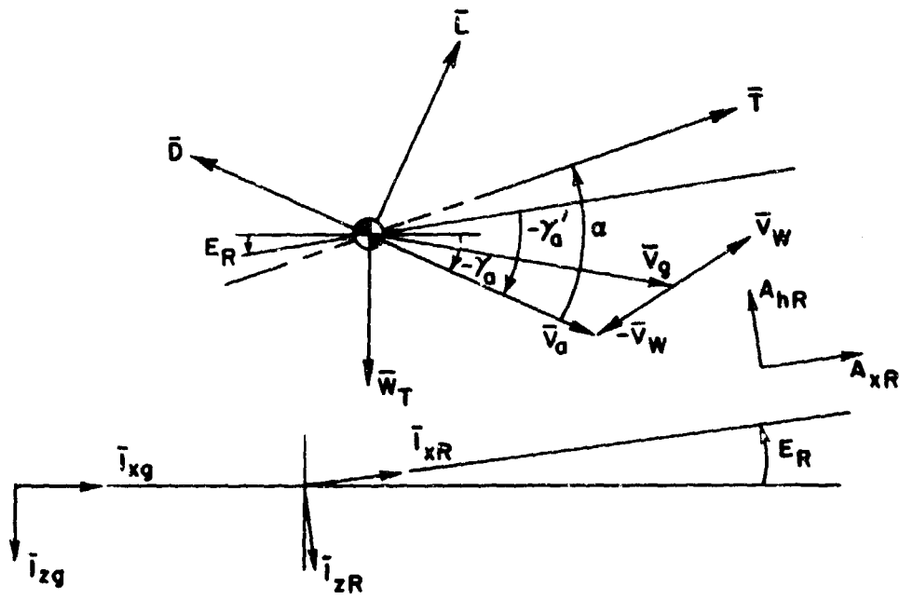

Figure 33. Flare Forces

where

$\bar{V}_g$ = velocity vector

$\bar{V}_w$ = wind vector

$\bar{V}_a$ = airspeed vector

α = angle of attack

γ_a' = elevation angle of $\bar{V}_a$ relative to runway

γ_a = elevation angle of $\bar{V}_a$ relative to earth

E_R = runway elevation angle

$\bar{T}$ = thrust vector

$\bar{W}_T$ = weight vector

$\bar{L}$ = lift vector

D = drag vector

Since A_{xR} and A_{hR} are defined relative to the runway, they are:

$$A_{xR} = \left[T\cos(\alpha + \gamma_a') + L\sin(-\gamma_a') - D\cos(-\gamma_a') - W_T \sin E_R \right] / m \tag{299}$$

$$A_{hR} = \left[T\sin(\alpha + \gamma_a') + L\cos(-\gamma_a') + D\sin(-\gamma_a') - W_T \cos E_R \right] / m \tag{300}$$

For a given airspeed vector, L and D are predominantly quadratic polynomials in α (see Equations 279 and 281). Equations 299 and 300 are therefore nonlinear functions of α and T whose solution is not immediately obvious. The observation that Equation 300 is predominantly a function of L and W_T and is not appreciably affected by T and D indicates that A_{hR} is primarily dependent on α. This also indicates that the final value of A_{xR} in Equation 299 is achieved through T. Both of these observations are helpful in constructing a numerical solution. Suffice it to say, that Equations 299 and 300 can be solved for the desired angle of attack, α_d, and desired thrust, T_d, to achieve the required accelerations A_{xR} and A_{hR}. It should be noted that both α_d and T_d have upper and lower bounds so that a situation can arise in which the requested accelerations are outside the capability of the aircraft. In such cases, the α_d and T_d will be those that give the least vector error in the requested acceleration. A flow chart of the equations and logic which determine α_d and T_d for the flare maneuver is presented in Figure 34. A pitch rate calculation is made based on the desired angle of attack rate and the nominal rotation rate of the velocity vector. This pitch rate is called q_d, the desired pitch rate in the flare.

c. Hold - Decrab Maneuver

As the aircraft approaches touchdown, it must be "decrabbed" (i.e., aligned with the runway center line) to allow the tires to roll and not skid. This is accomplished in the yaw autopilot (see yaw

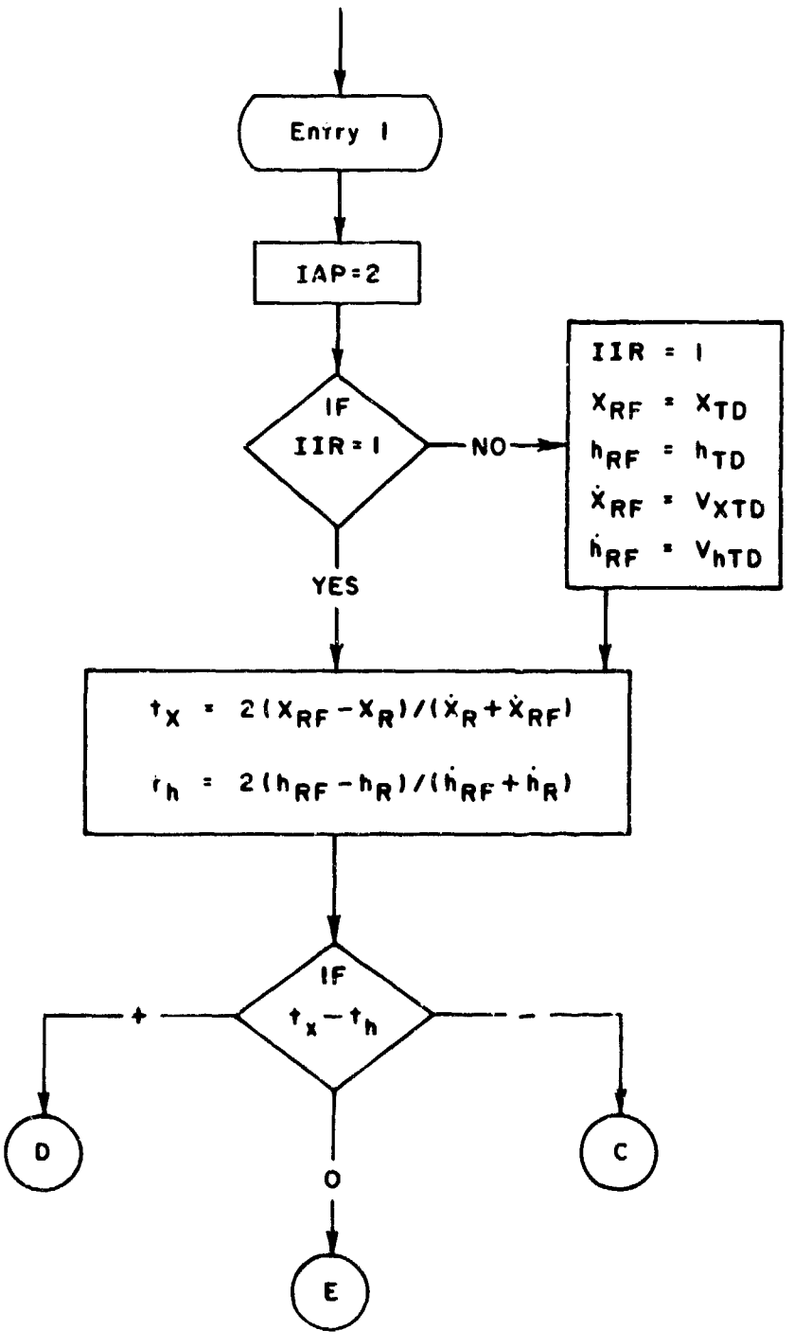

Figure 34. Flare Logic

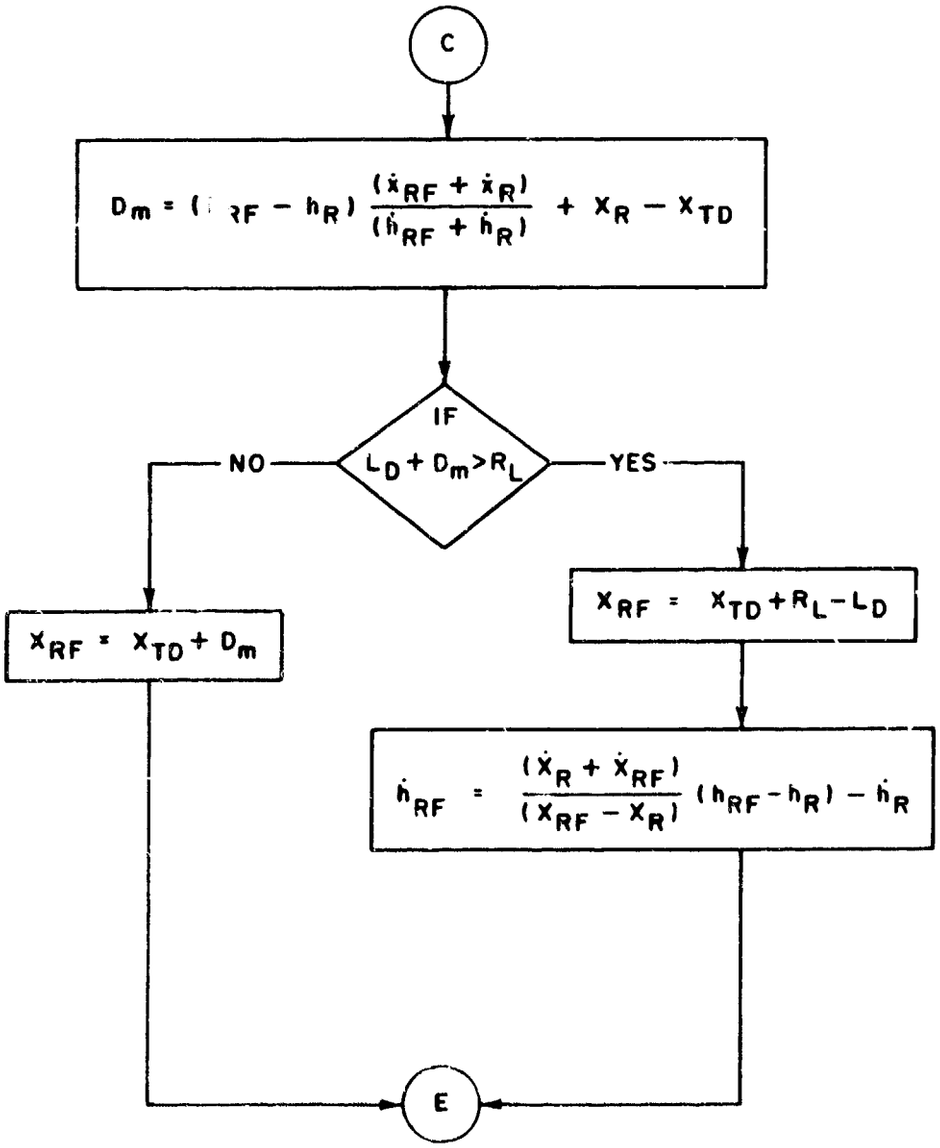

Figure 34. Flare Logic (Contd)

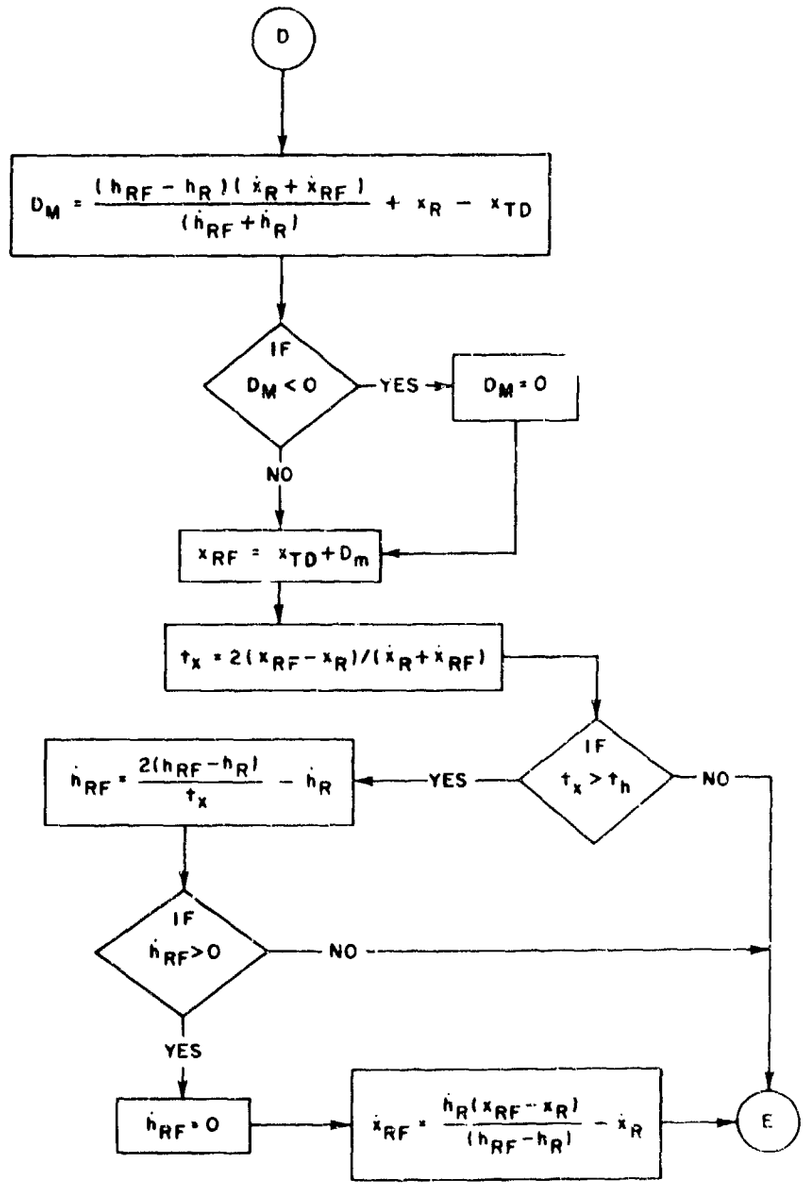

Figure 34. Flare Logic (Contd)

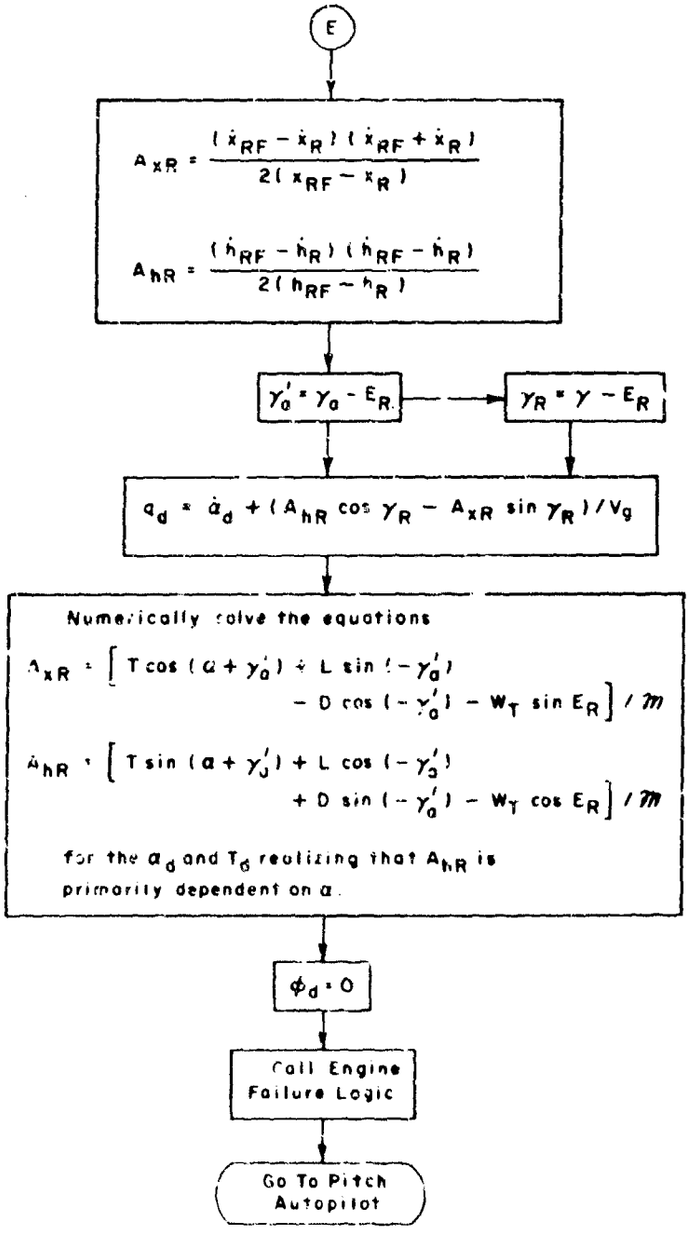

Figure 34. Flare Logic (Concluded)

autopilot development) by commanding the Euler yaw angle, ψ_p, (see Appendix I) to be zero. The Euler roll angle, ϕ_p, is also commanded zero for a "wings level" impact. More aircraft also have a "tail down" constraint which limits the maximum allowable angle of attack near the ground.

The "hold-decrab" maneuver is staged on the mass center altitude above the runway. When this occurs, the desired angle of attack, α_d, is held constant at the last value requested in the flare unless it must be limited by the tail-down constraint. The desired thrust, T_d, is also held constant at the last value requested in the flare unless the "kill-power" option (see throttle autopilot development) is exercised. Most of the logic for the "hold-decrab" maneuver is directly in the autopilots. That logic which is necessary prior to autopilot entry is summarized in Figure 35.

3. LANDING ROLLOUT

The landing rollout begins at the instant any one of the tires touches the runway. The following maneuver will automatically occur in the landing rollout: control the aircraft yaw, ψ_p, to be zero (i.e., keep the aircraft aligned with the runway); reduce roll control surface deflections to neutral position. The following events can be sequenced (on time after impact, t_r) if so desired:

(1) Actuate ground spoilers ($t_r \geq t_{sp}$)

(2) Kill power and reverse engines ($t_r \geq t_{rv}$)

(3) Actuate drag chute ($t_r \geq t_{ch}$)

(4) Actuate tire braking ($t_r \geq t_{bk}$)

(5) Change elevator deflection from value at impact to a desired final value (in Pitch Autopilot, if $t_r > t_{st}$).

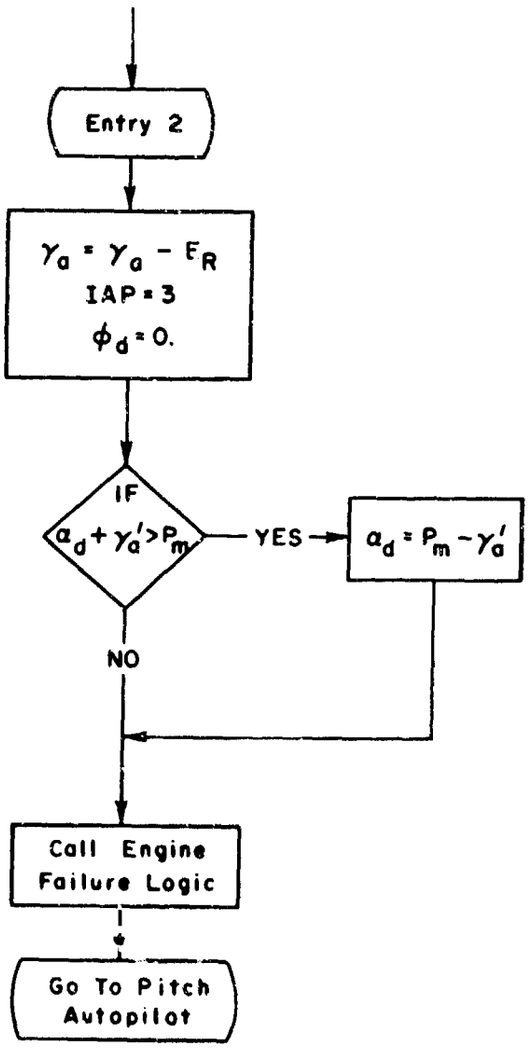

Figure 35. Hold-Decrab Logic

Most of the logic for the landing rollout maneuver is contained directly in the autopilots. That logic necessary prior to autopilot entry is shown in Figure 36.

4. TAKEOFF ROLL

The takeoff roll maneuver is simply one of rotating the aircraft in pitch to the desired takeoff angle of attack once the takeoff airspeed has been reached. Throttle setting is held constant through the roll at the takeoff value. The aircraft yaw angle, ψ_p, is commanded zero in the yaw autopilot to keep the aircraft aligned with the runway, and the roll control surface deflections are kept in the neutral position. Elevator deflection is kept at a fixed value until the command to rotate the aircraft to the takeoff angle of attack is given. The takeoff roll maneuver is terminated on a particular mass center altitude, h_s, above the runway. Most of the logic for the takeoff roll maneuver is contained directly in the autopilots. That logic which is necessary prior to autopilot entry is shown in Figure 37.

5. PROBLEM PHASE LOGIC

Given appropriate input, the phase logic determines which maneuver logic (i.e. glide slope, flare, hold-decrab, landing roll, takeoff roll) to use. The phase logic also determines where the problem is to terminate. Figure 38 shows the phase logic.

The indicator ITO determines whether the problem is a takeoff or landing problem. If the altitude of the aircraft is above h_F, the aircraft is in the glide slope phase. When the altitude h_F is reached, an option is provided to stop the program (see NF indicator) or go to the flare phase. The hold-decrab phase begins when the mass center altitude above the runway, h_R, is less than or equal to $h_{RF} + \delta_h$ or if the distance down the runway X_R has exceeded the desired value x_{RF}. The input value of h_{RF} is normally h_{CG}, so that δ_h represents the vertical distance between the runway and tire bottom surface at which the hold-decrab phase begins. The KP indicator is used to start the

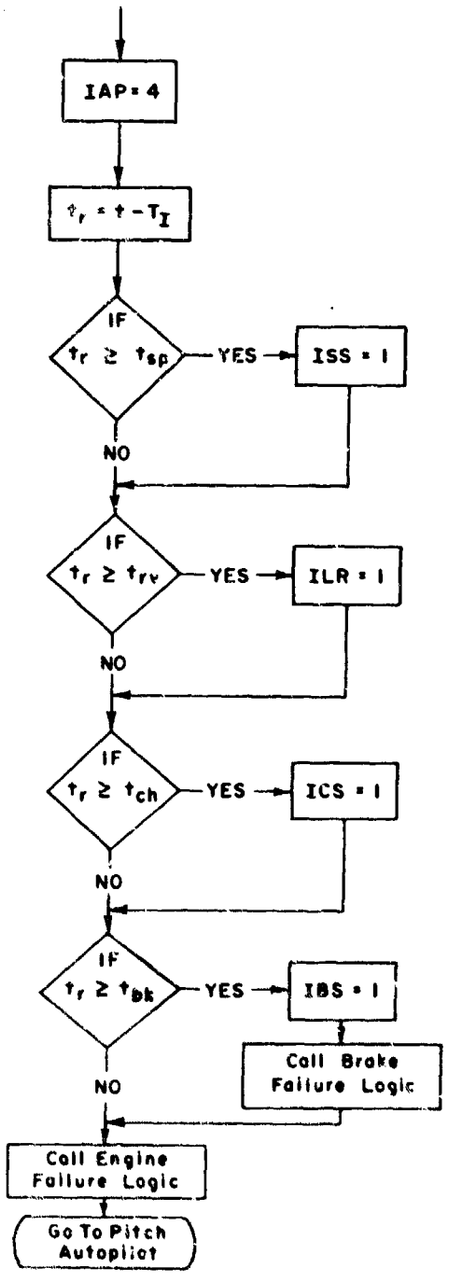

Figure 36. Landing Roll Logic

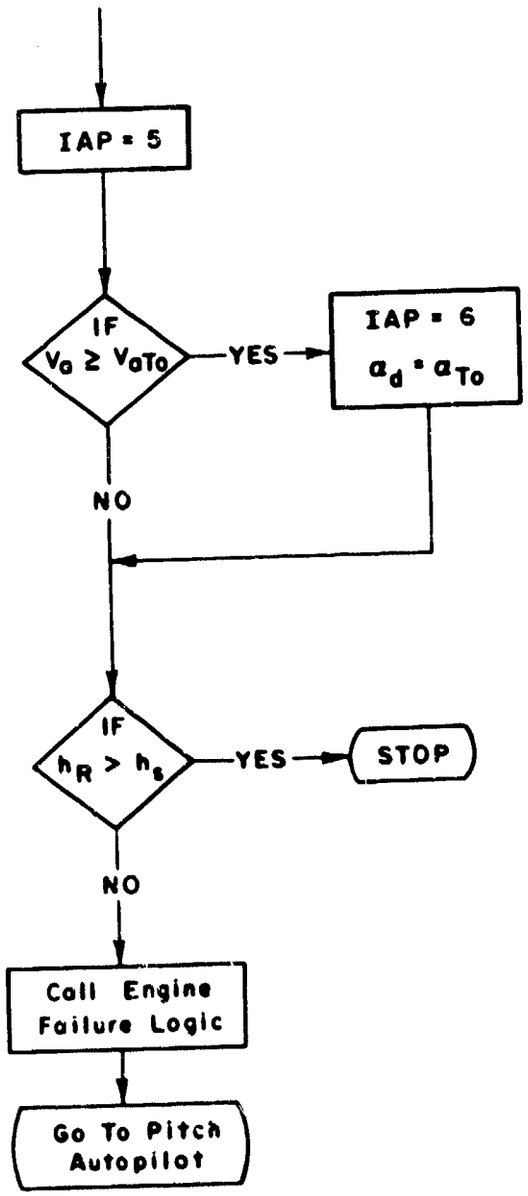

Figure 37. Takeoff Roll Logic

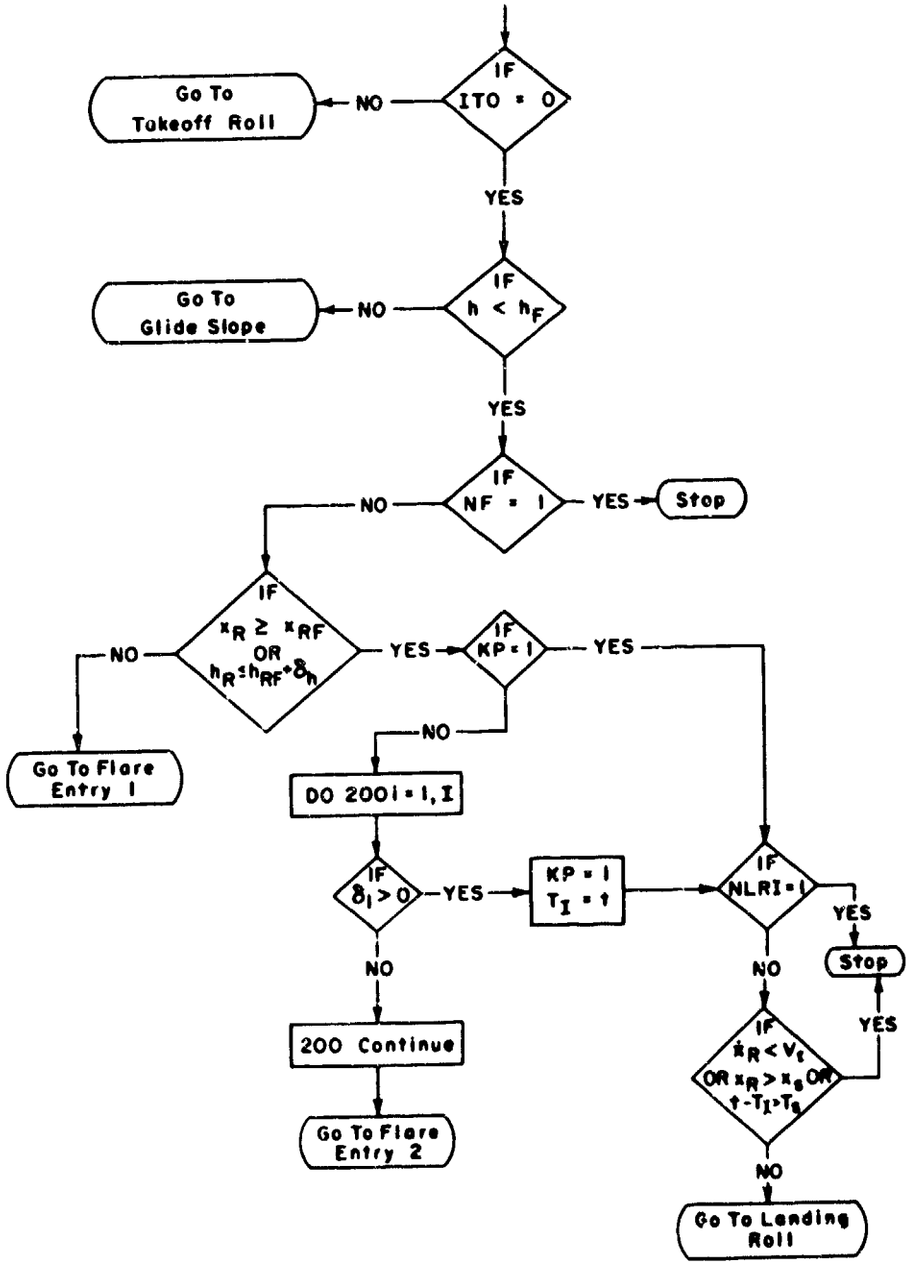

Figure 38. Problem Phase Logic

program in the landing roll phase. If KP = 1, the time of impact, T_I, must be provided by initial data input. If KP ≠ 1 the problem remains in the hold-decrab phase until any one of the tires receives a deflection, δ_i. As soon as a tire deflection is received, the time of impact is stored in T_I and is never changed (even if the aircraft bounces on the runway). Immediately on impact, the NLRI indicator allows the program to be stopped or to continue with the landing roll phase. The landing roll phase can be terminated on a velocity, position, or time constraint, whichever occurs first.

6. FAILURE LOGICS

Prior to going to the autopilots, each maneuver logic checks for possible engine failures. In the event the aircraft is in the landing roll phase, a check is also made on possible brake failures.

a. Engine Failure Logic

Figure 39 is a flow diagram of the engine failure logic. The indicator array IC determines the failure (IC = 0) of up to four independent engines. While in the glide slope phase (i.e., IAP = 1), engine failures can be sequenced on two different altitudes h_1 and h_2. While in the flare or hold-decrab phases (i.e., IAP = 2,3), engine failures can be sequenced on two different runway altitudes h_{R1} and h_{R2}. While in the landing roll phase (i.e., IAP = 4) engine failures can be sequenced on two different times after impact t_{r1} and t_{r2}. While in the takeoff phase (i.e., IAP = 5, 6) engine failures can be sequenced on two different positions down the runway x_{RF1} and x_{RF2}. The IC array is used in the throttle autopilot.

b. Brake Failure Logic

Figure 40 shows the brake failure logic. The indicator array I_B determines the conditions of each gear brake. The I_B array can be changed from its initial array on two different times after impact t_{bk1} and $t_{bk}2$. The I_B array is used in the brake autopilot.

This concludes the maneuver logic.

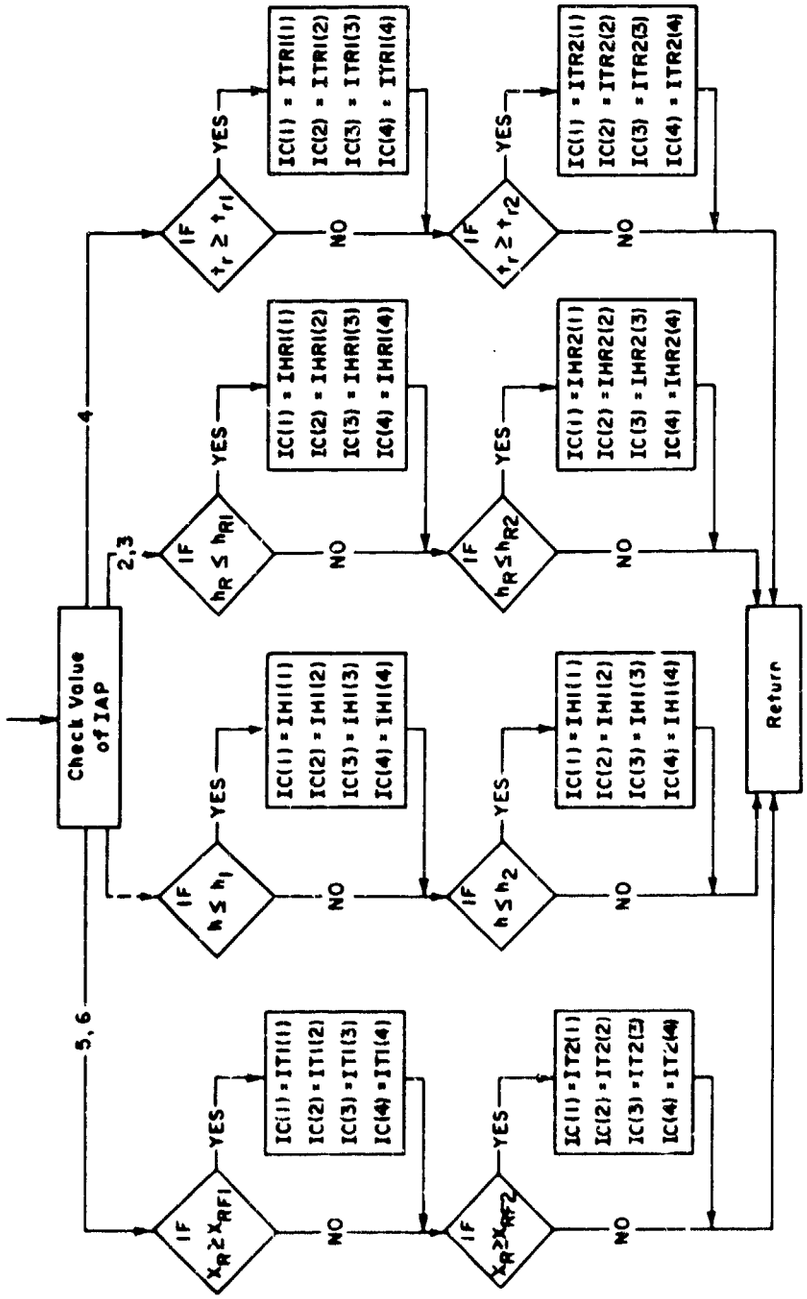

Figure 39. Engine Failure Logic

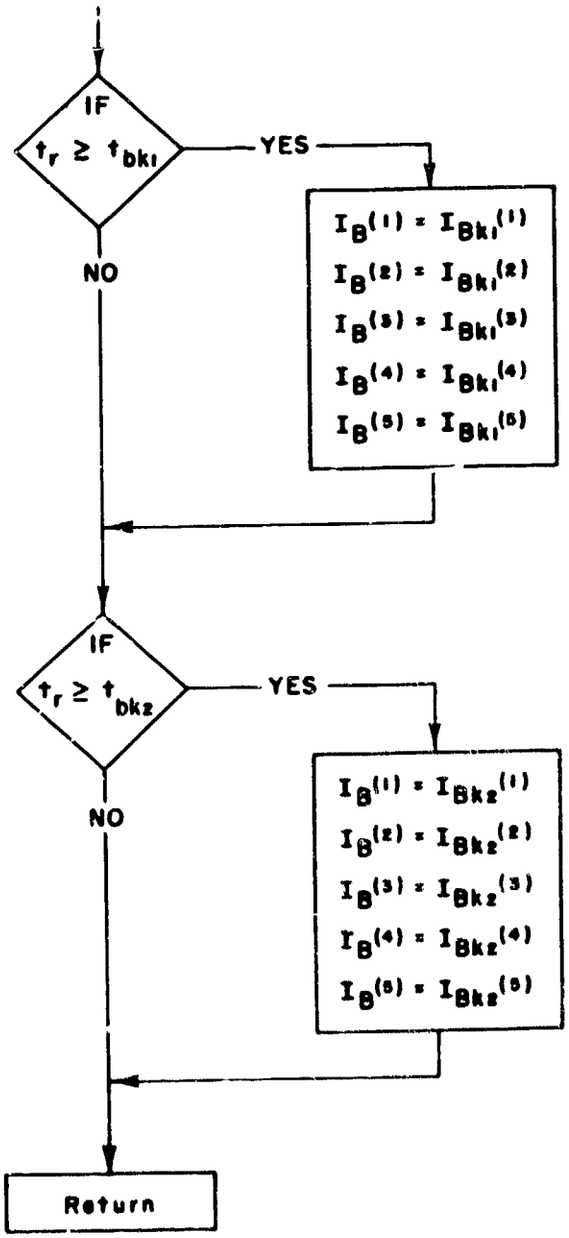

Figure 40. Brake Failure Logic

SECTION III

AUTOPILOTS

The maneuver logic of Section II defined control of the aircraft by specifying desired values of angle of attack, angle of sideslip or yaw angle, roll angle, thrust, and status of the engines and brakes. It then becomes the function of the pitch, yaw, roll, throttle, and brake autopilots to achieve, within the capability of the aircraft, the desired values requested. Each autopilot development is discussed in turn.

1. PITCH AUTOPILOT

The basic function of the pitch autopilot is to control the aircraft angle of attack to the desired value requested by the maneuver logic. The aerodynamic surface for this control is the elevator on the horizontal stabilizer. Equation 38 expresses the major static moments acting about the body mass center pitch axis (excluding landing gear pitching moment, M_m).

$$\left[C_{m_o} + C_{m_\alpha}\alpha + C_{m_\alpha 2}|\alpha|\alpha - C_N\frac{\Delta X}{d_l} + C_{m_{\delta q}}\delta q + C_{m_{\delta q}^2}|\delta q|\delta q + C_{m_q} q_a\left(\frac{d_l}{2V_a}\right)\right] q^* S d_l + M_T + M_M \tag{301}$$

where

C_{mo} = pitching moment coefficient about the aerodynamic reference station at zero angle of attack and zero elevator deflection

α = angle of attack

$C_{m\alpha}$, $C_{m\alpha\,2}$ = pitching moment coefficients for angle of attack dependence about aerodynamic reference station

M_m = ground reaction moments in pitch (net moment)

C_N = normal force coefficient

ΔX = distance from aerodynamic reference station to mass center

$C_{m\delta q}$, $C_{m\delta q^2}$ = elevator pitching moment coefficients

δ_q = elevator deflection

d_1 = pitch reference length (usually mean aerodynamic chord)

S = reference area

q^* = dynamic pressure

M_T = engine thrust moments in pitch (net moment)

C_{m_q} = dynamic damping derivative in pitch

q_d = pitch rate based on $\dot{\alpha}_d$ and flare accelerations

V_a = airspeed

The nominal pitch trim requirements (i.e., the control surface deflection required to attain a particular desired angle of attack under equilibrium conditions) are obtained by requiring Equation 301 to zero. As mentioned in Section I, the aircraft is initially trimmed for the desired glide slope conditions. If this initial pitch trim is done by some surface other than the elevator, as with a moveable trim tab or flap, this is done through appropriate data input of C_{mo}. All pitch trim changes from the initial are assumed to be done by the elevator. The nominal elevator deflection, δ_{qN}, for a particular desired angle of attack, α_d, is therefore obtained by solving Equation 301 set to zero.

$$\left[C_{mo} + C_{m\alpha}\alpha_d + C_{m\alpha 2}|\alpha_d|\alpha_d - C_N\frac{\Delta x}{d_1}\right.$$
$$\left. + C_{m\delta q}\delta_{qN} + C_{m\delta q^2}|\delta_{qN}|\delta_{qN} + C_{mq}q_d\left(\frac{d_1}{2V_a}\right)\right]q^* S d_1 + M_T + M_m = 0 \qquad (302)$$

Note that the equation is quadratic in δ_{qN} and is also dependent on engine conditions.

Because there may be insufficient natural damping and because the α_d command may constantly change (as in the flare), the δ_{qN} command to the elevator must be augmented to obtain good aircraft response and the desired angle of attack control. The pitch autopilot flow diagram is given in Figure 41.

Three distinct routes are provided in the pitch autopilot, depending on the value of the indicator, IAP. When IAP = 5, this indicates a takeoff roll problem in which the takeoff airspeed has not been reached. For this case the desired elevator deflection, δ_{qd}, remains fixed at the input, δ_{qTO}. When IAP = 4, this indicates a landing roll problem in which one may choose to change the impact value of δ_{qd} (i.e., δ_{qI}) to some final value δ_{qF}, at a rate $\dot{\delta}_F$, and begin the change at time, t_{st}, after impact. This impact maneuver can be used to change the horizontal stabilizer loads during the landing roll. The final route, IAP = 1, 2, 3, 6, indicates a maneuver in which a particular angle of attack, α_d, is required. Here the pitch autopilot computes the angle of attack error α_e, the rate of change of error α_{Re}, and includes rate feedback $R_{F\alpha}$, into the total angle of attack error signal, α_{eT}. The allowed error in α_{eT} is a fixed input, $\Delta\alpha_a$. If α_{eT} is within the allowed $\Delta\alpha_a$, δ_{qd} is set to the trim value δ_{qN}. If α_{eT} exceeds the allowed error $\Delta\alpha_a$, δ_{qd} is set to the trim value δ_{qN} plus some overcontrol, which is determined by the product of α_{eT}, and an input constant PS_H. The desired elevator deflection, δ_{qd}, is finally limited by the aircraft constraints δ_{qL} (lower limit) and δ_{qu} (upper limit). The rate of feedback constant, $R_{F\alpha}$, and the overcontrol constant PS_H, allow the pitch autopilot to be adjusted to a particular aircraft configuration.

ALPDL prevents discontinuities in α_d from entering the pitch autopilot thru $\dot{\alpha}_d$. δ_{qc} adds a "bang-bang" control capability to the pitch autopilot.

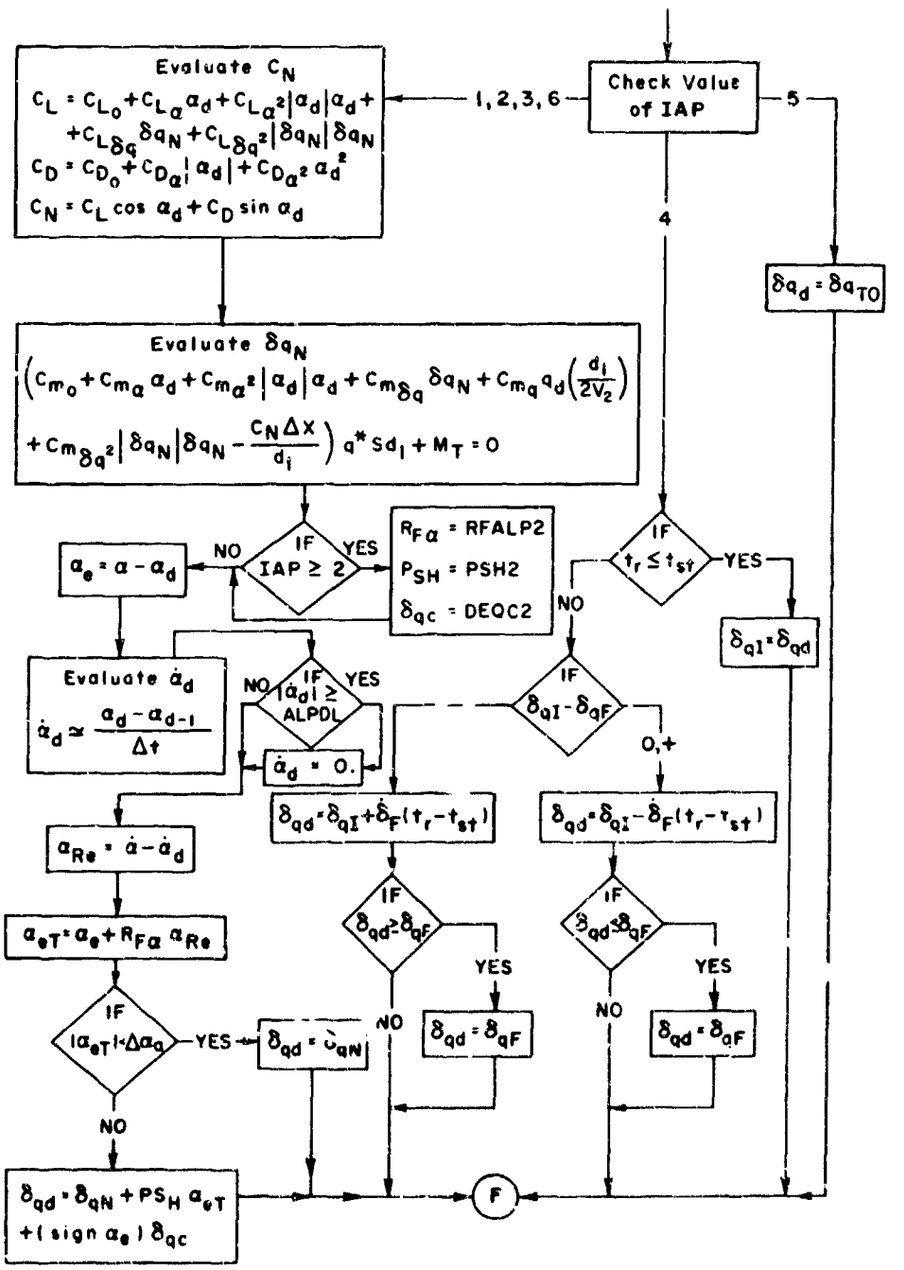

Figure 41. Pitch Autopilot Logic

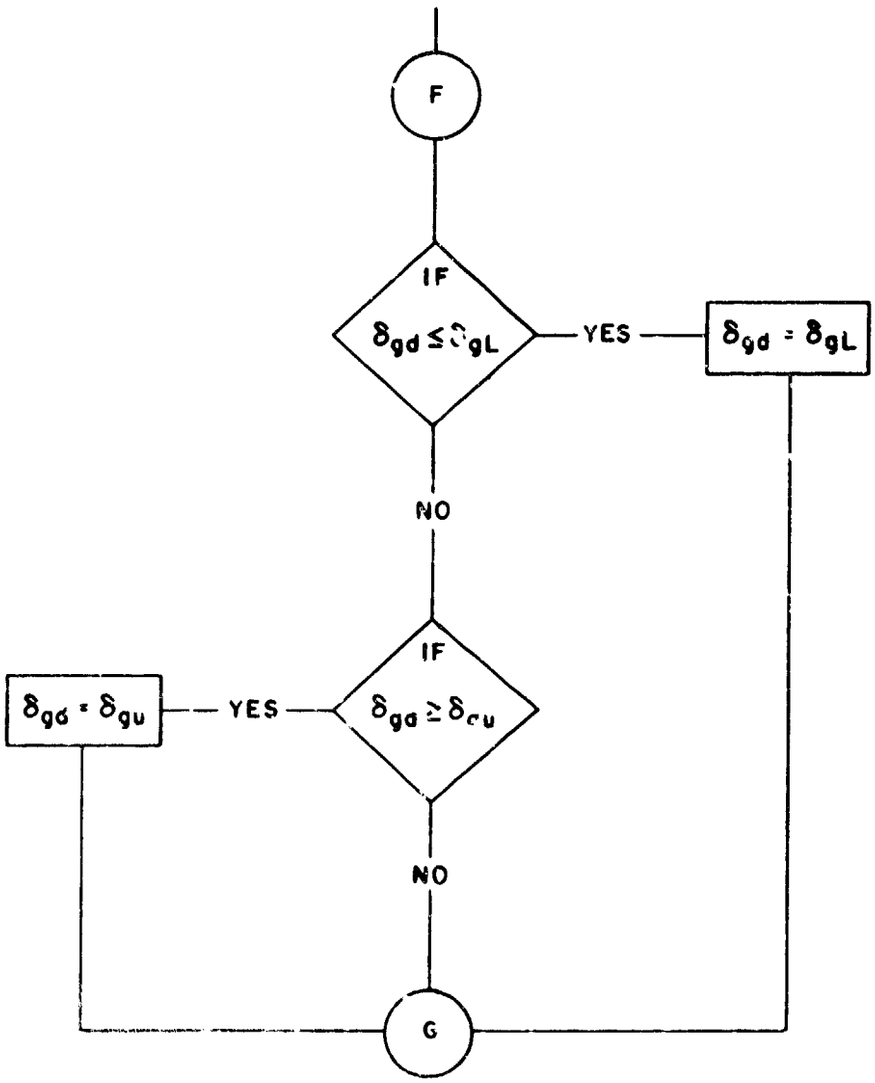

Figure 41. Pitch Autopilot Logic (Concluded)

2. YAW AUTOPILOT

The function of the yaw autopilot is to control either the sideslip angle of attack or the Euler yaw angle. In both cases the desired value of the angle is zero. The aerodynamic surface for this control is the rudder on the vertical stabilizer. Equation 303 expresses the major static moments acting about the body yaw axis.

$$\left[C_{n\beta}\beta + C_{n\beta^2}|\beta|\beta - C_y\frac{\Delta X}{d_2} + C_{n\delta r}\delta r + C_{n\delta r^2}|\delta r|\delta r\right]q^* S d_2 + N_T \tag{303}$$

where

β	= sideslip angle of attack
$C_{n\beta}$, $C_{n\beta}{}^2$	= yaw moment coefficients for β dependence about aerodynamic reference station
C_y	= body side force coefficient
d_2	= yaw reference length (usually wing span)
$C_{n\delta r}$, $C_{n\delta r}{}^2$	= rudder yaw moment coefficients
δr	= rudder deflection
N_T	= engine thrust yaw moment

The body side force coefficient is also predominantly expressed by

$$C_y \simeq C_{y\beta}\beta + C_{y\beta^2}|\beta|\beta \tag{304}$$

where $C_{y\beta}$ and $C_{y\beta}{}^2$ are the side force coefficients for β. Substituting Equation 304 into Equation 303 yields

$$\left[\left(C_{n\beta} - C_{y\beta}\frac{\Delta X}{d_2}\right)\beta + \left(C_{n\beta^2} - C_{y\beta^2}\frac{\Delta X}{d_2}\right)|\beta|\beta + C_{n\delta r}\delta r + C_{n\delta r^2}|\delta r|\delta r\right]q^* S d_2 + N_T \tag{305}$$

When Equation 305 is set to zero, it can be used to solve for the nominal rudder deflection, δ_{rN}, to trim the aircraft at a particular desired sideslip angle of attack, β_d. Note that Equation 305 is quadratic in δ_r and is dependent on engine conditions. Examine Figure 42, which is the flow chart for the yaw autopilot.

Two distinct routes exist in the yaw autopilot, depending on the value of the indicator, IAP. If IAP = 1, 2 (i.e., glide slope or flare) the desired value of β is zero. The solution to Equation 305 for the nominal rudder deflection, δ_{rN}, will also be zero, except in the case where the engine thrust yaw moment is nonzero. Rate feedback, R_{FB}, and overcontrol, PS_R, are provided for the same reasons discussed in the pitch autopilot. If IAP = 3, 4, 5, 6, the aircraft may have to operate at a non-zero steady sideslip (only for a cross wind situation) to make the Euler yaw angle, ψ_p, zero. The nominal rudder deflection, δ_{rN}, for this case is obtained from Equation 305 by substituting Equation 306 for β Equation 306 expresses approximately

$$B_d = \sin^{-1} - \frac{\dot{y}_{g\omega}}{V_o} \qquad \textbf{(306)}$$

the steady sideslip β at which the aircraft must operate in order to align with the runway). Rate feedback, $R_{F\psi}$, and overcontrol, PS_ψ, are also provided in this route of the yaw autopilot. The desired rudder deflection, δ_{rd}, is finally limited by the aircraft constraints δ_{rL} (lower limit) and δ_{ru} (upper limit). As with the pitch autopilot, the yaw autopilot can also be adapted to a particular aircraft configuration through the rate feedback constants, R_{FB} and $R_{F\psi}$, and the overcontrol constants, PS_R and PS_ψ

3. ROLL AUTOPILOT

The function of the roll autopilot is to control the Euler roll angle to the desired value requested by the maneuver logic. The aerodynamic surface for this control is the aileron. The roll autopilot differs from the pitch and yaw autopilots in that it assumes there is no major static moment developed about the roll axes for the maneuvers

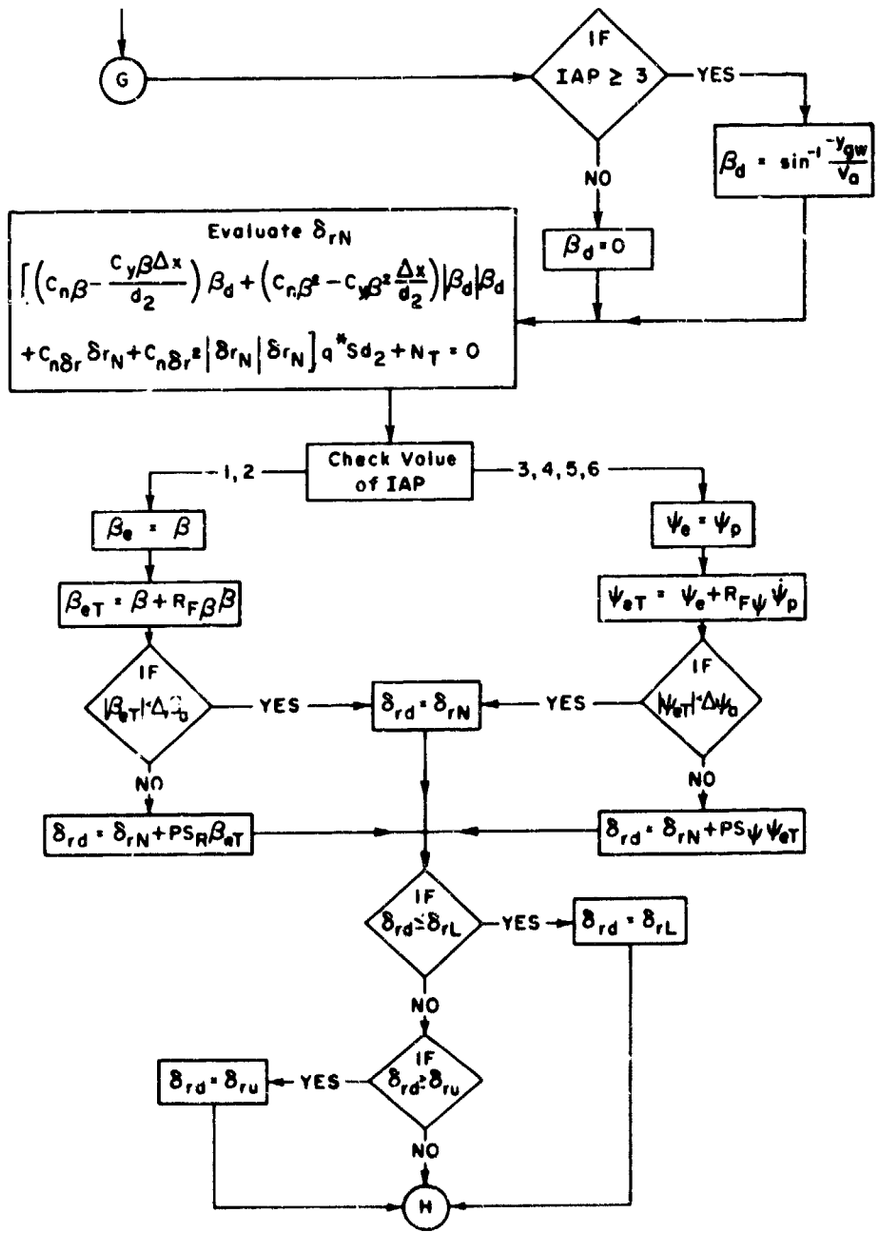

Figure 42. Yaw Autopilot Logic

requested. As such, the nominal aileron deflection, δ_{PN}, to trim the aircraft about the roll axis is always zero. Other than this trim requirement, the roll autopilot is similar in concept to the pitch and yaw autopilot. The roll autopilot flow diagram is given in Figure 43.

Two distinct routes exists in the roll autopilot, depending on the values of the indicator, IAP. If IAP = 4, 5, 6, the aircraft is on or has just left the runway and the roll attitude is determined primarily by the landing gear runway interface. As such, the desired value of aileron deflection, δ_{Pd}, is zero. If IAP - 1, 2, 3, the aircraft is in flight and a particular desired roll angle, ϕ_d, is commanded by the maneuver logic. Rate feedback, $R_{F\phi}$, and over control, PS_A, are provided, as was done in the pitch and yaw autopilots. The final desired aileron deflection, δ_{Pd}, is limited by the aircraft constraints δ_{PL} (lower limit) and δ_{PU} (upper limit). As with the pitch and yaw autopilots, the roll autopilot can be adapted to a particular aircraft configuration by appropriate selection of the constants $R_{F\phi}$ and PS_A.

4. THROTTLE AUTOPILOT

The basic function of the throttle autopilot is to achieve the desired thrust, T_d, requested by the maneuver logic. It performs this function by commanding desired values of the throttle settings. The throttle settings must be arrived at under any combination of the following conditions: 1, 2, 3, or 4 engine aircraft, all engine failure combinations practicable, engine reverse under selected throttle constraints, capability to let some engines carry more load than others.

The throttle autopilot is divided into four logics = one for each of the engine-aircraft combinations (see Figure 44). Each of these logics is built up from two other basic engine logics called, "common engine logic" and "common two-engine logic."

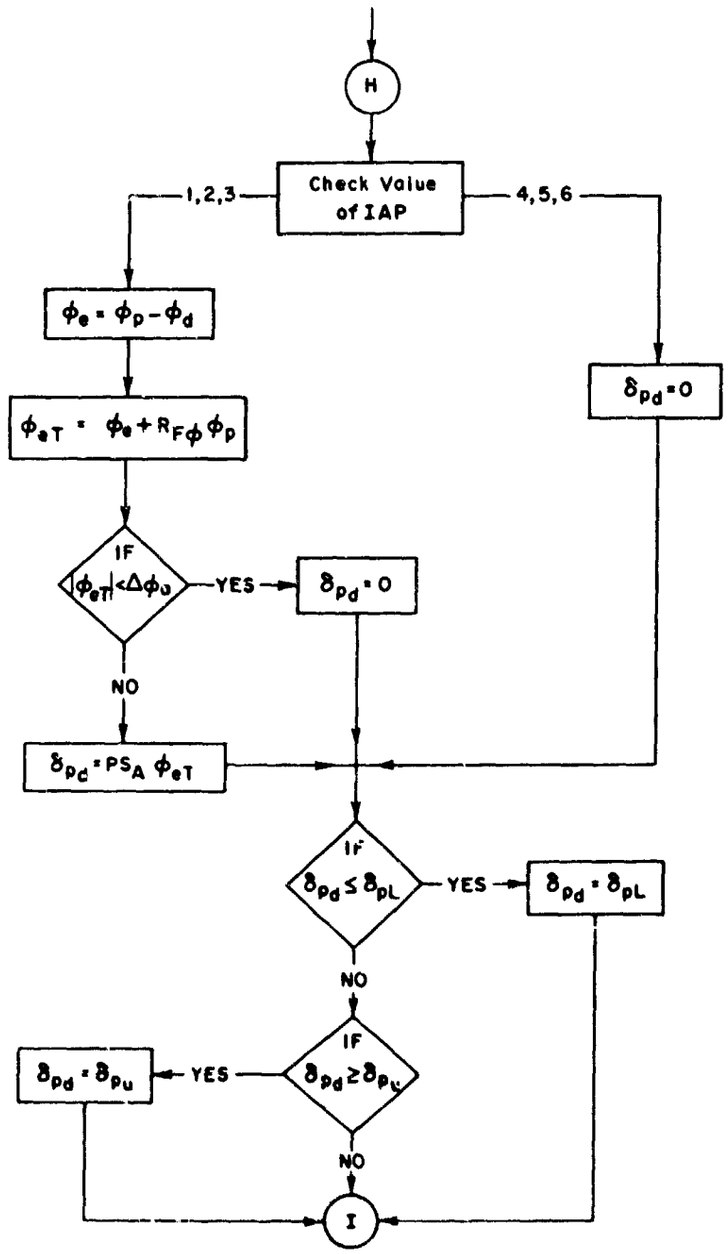

Figure 43. Roll Autopilot Logic

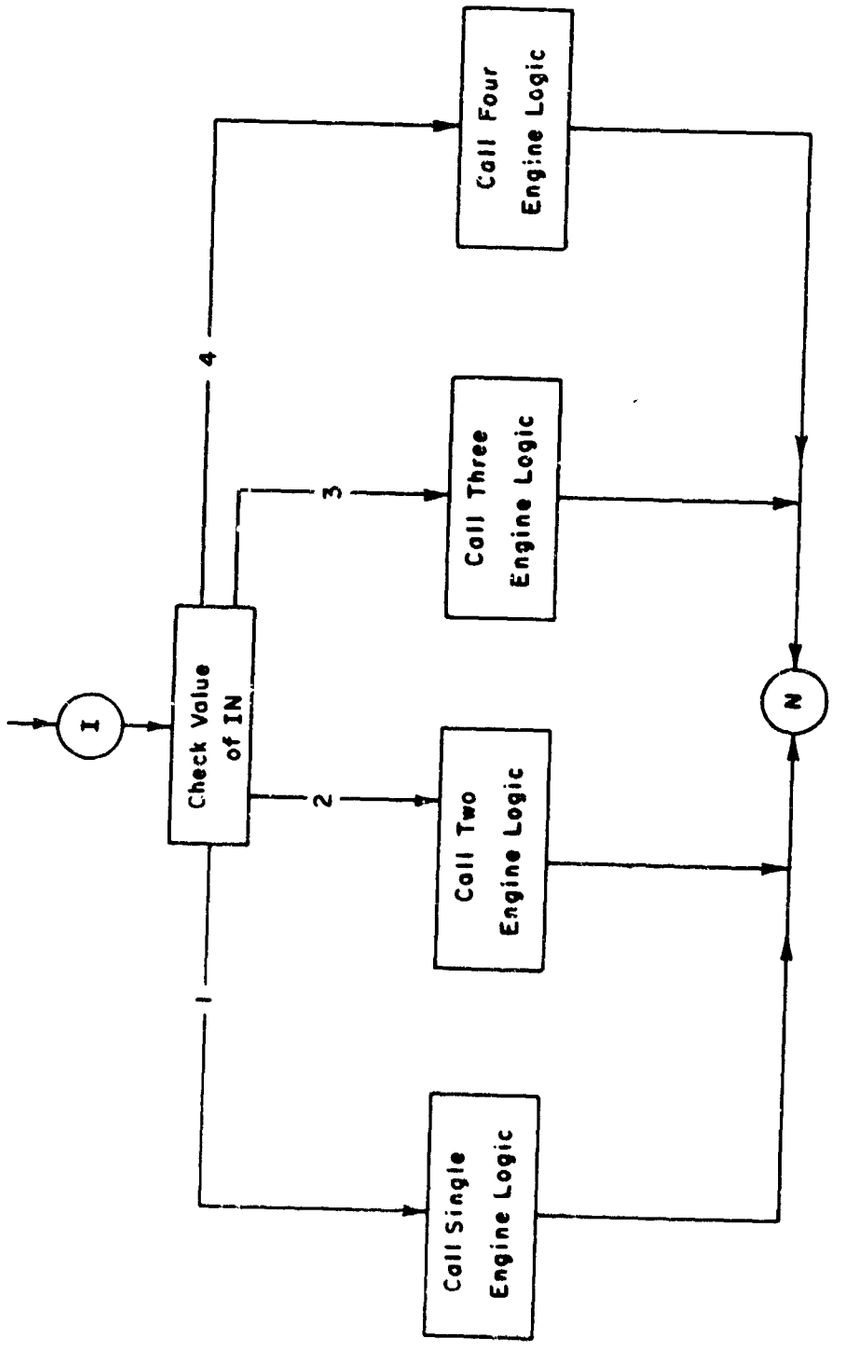

Figure 44. Number of Engines Logic

a. Single-Engine Logic (SEL)

The single-engine logic determines the desired throttle setting, N_d (1), for a single-engine aircraft. A "fixed throttle" mode and a failure mode is provided. Figure 45 is a flow diagram of the SEL. In this logic, a check is first made to see if the engine is in the "fixed throttle" mode. This is done by examining the value of the first element in the fixed throttle indicator array, TF(I) - the TF(I) array is read on initial data input. If TF(1) = 1, this indicates a fixed throttle mode for which $N_d(1)$ is given the value $N_{dF}(1)$ (the N_{dF} array is read in on input). A landing reverse check is then made to determine if this is desired. This is followed by a failure check (i.e. IC(1) = 0, as shown in Figure 39). If the engine has failed, $N_d(1)$ is set to zero; otherwise $N_d(1)$ remains unchanged. If the engine is not in a fixed throttle mode (i.e., TF(1) = 1), a failure check is again made. If there is no failure, the data set up (use first element of input arrays) for the CEL is done. Entry into the CEL is made and the desired throttle setting, $N_d(1)$ is determined. Note that the SEL is predominantly the CEL except that the fixed and failure modes are determined outside the CEL.

b. Common Engine Logic (CEL)

The CEL is applicable to any "variable throttle" engine on the aircraft. Given a set of variables, the CEL assumes the engine has not failed and finds a desired throttle setting. The set of variables required by the CEL is:

IAP = problem phase indicator; available from maneuver logic

N_c = actual throttle setting; available from calling program.

T_c = desired thrust; available from calling program.

ILR = reverse engine signal; available from maneuver logic

IRC = indicator for engine reverse capability; available from calling program

N_{BC} = throttle setting above which reverse should not be calling program actuated; available from calling program.

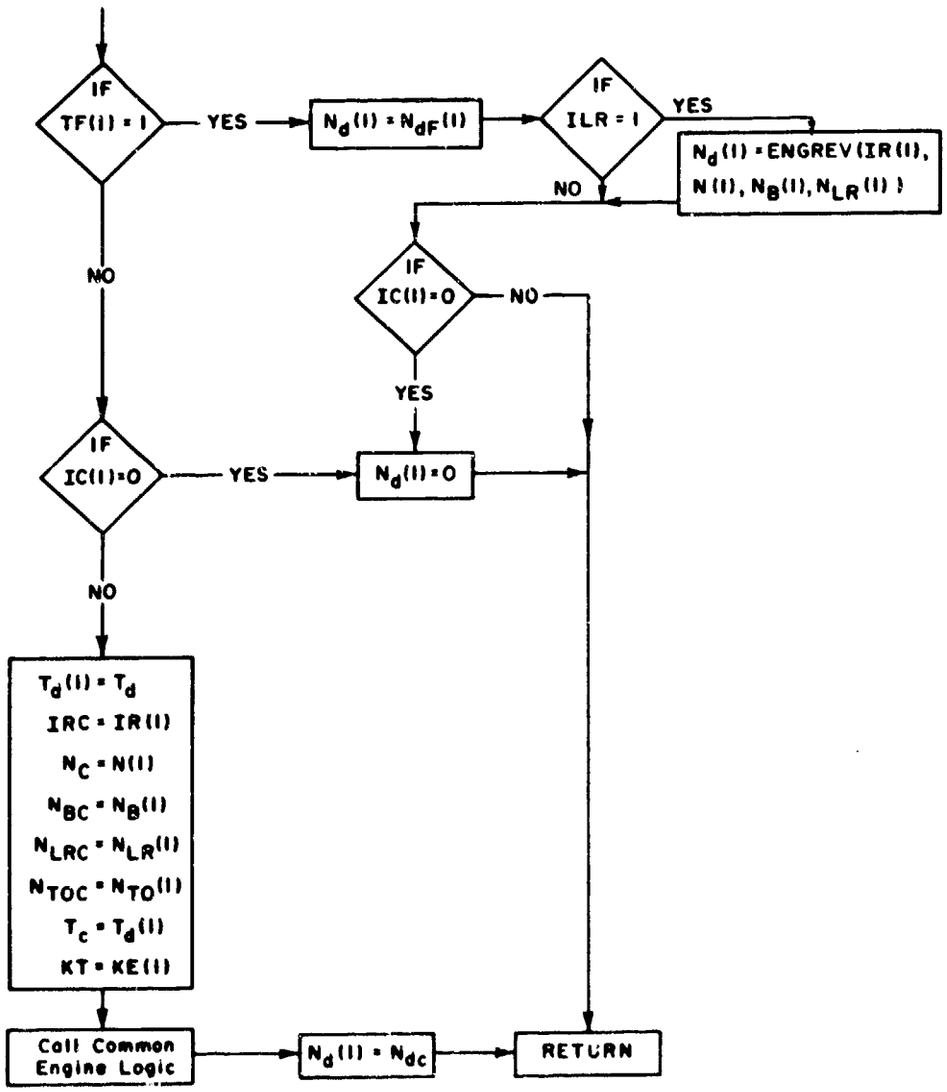

Figure 45. Single-Engine Logic

N_{LRC} = throttle setting for landing reverse; available from calling program.

N_{TOC} = throttle setting for takeoff; available from calling program.

KT = kill engine indicator; available from calling program.

Figure 46 is a flow diagram of the CEL.

The ILR indicator is initially input to the program as a value other than 1. The landing reverse engine signal (i.e., ILR = 1) is given in the landing rollout phase of the maneuver logic (see Figure 36). If ILR = 1, a check is made on IRC (a value of 1 indicates that the engine has a reverse capability). If IRC ≠ 1, the desired throttle setting, N_{dC}, is set at 1.0 (this value of throttle setting is assigned to forward idle - see Section VI) which is the lowest possible forward throttle setting. If IRC = 1, a check is made to see if the actual throttle setting, N_C, is below the value required, N_{BC}, to engage the reverse. If the check is not true, the desired throttle setting, N_{dC}, is made 1 so that N_C will reduce below N_{BC}. When $N_C \leq N_{BC}$, the reverse is engaged by requesting N_{dC} to equal the throttle setting for landing reverse, N_{LRC}.

If the landing reverse signal has not been given (i.e., ILR ≠ 1), the CEL has three routes depending on the value of the indicator, IAP. If IAP = 5, 6, this indicates a takeoff problem and N_{dC} is set to the takeoff throttle setting, N_{TOC}. If IAP = 3, 4 (i.e., hold-decrab or landing roll maneuver) an option is provided to kill power. This is done during data input by making the kill engine indicator KE(I) = 1. If KT ≠ 1, the problem goes to the IAP = 1, 2 route where thrust will be maintained during the hold-decrab maneuver and will be maintained during the landing rollout maneuver until the landing reverse signal is given. If IAP = 1, 2 (glide slope or flare), a route is desired to find the throttle setting for a particular thrust, T_c. Here an interpolation is done in the thrust tables from N = -2.0 (full reverse)

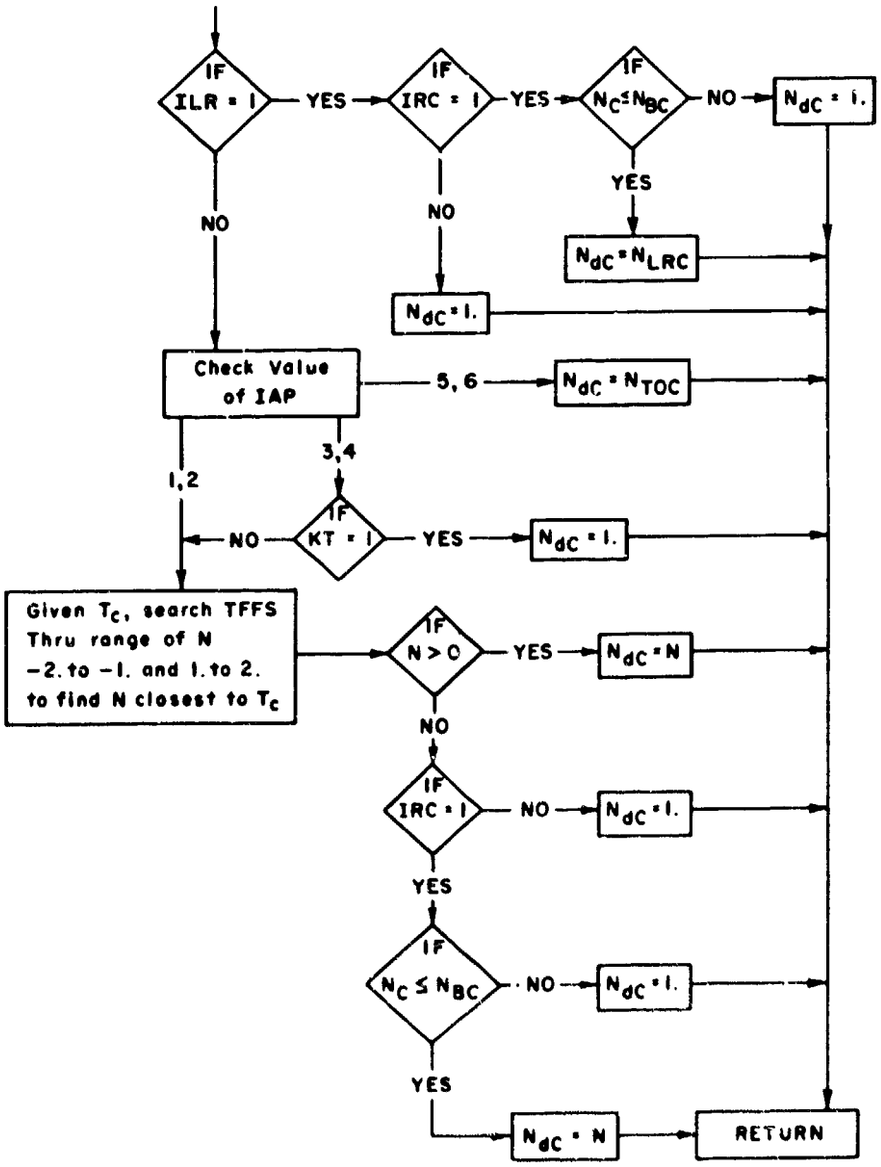

Figure 46. Common-Engine Logic

to N = -1.0 (idle reverse) and from N = +1.0 (idle forward) to N = +2.0 (max forward) to find the throttle setting, N, that gives T_c or comes closest to T_c. If the final interpolated value of N is negative (reverse thrust requested), the same throttle constraint is applied as was done for the landing reverse. It should be noted that the throttle constraint on reverse thrust applies only when engaging reverse and does not limit disengagement (N_{dC} can always have a positive value).

c. Function ENGREV

As originally designed, any engine in a "fixed throttle" mode could not reverse when the reverse signal (ILR = 1) was given. A function called ENGREV was added, which allows a "fixed throttle" engine to change to reverse landing provided ILR has a value of one, the engine has a reverse capability (if not, forward idle is commanded), and the throttle constraint for reverse is met. This addition was necessary since the "fixed throttle" engines do not go through the "common engine logic" (CEL). The function performs essentially the same flow as that portion of CEL which occurs if ILR = 1, as shown in Figure 47.

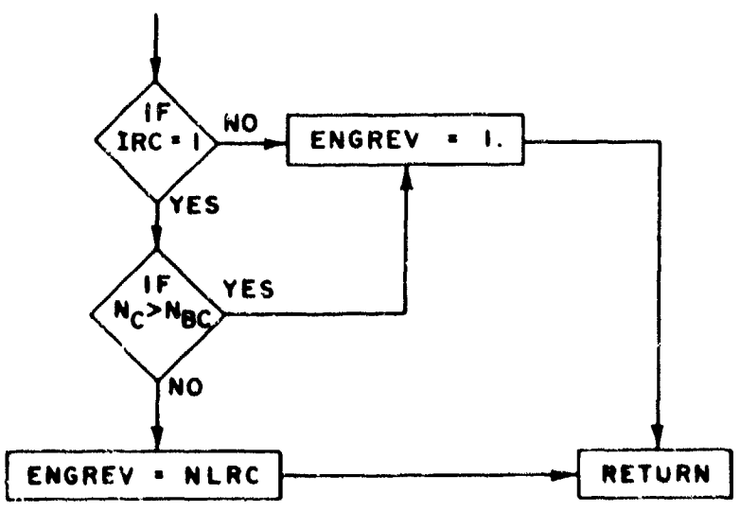

Figure 47. Function ENGREV

d. Two-Engine Logic (2EL)

The two-engine logic determines the desired throttle settings $N_d(1)$ and $N_d(2)$ for a two-engine aircraft. One fixed throttle mode and all possible failure modes are provided. Figure 48 is a flow diagram of the 2EL.

First a check is made on the one fixed throttle mode allowed (i.e., if one engine is fixed the other is assumed fixed also). If the fixed throttle mode is indicated, a failure check follows and $N_d(1)$ and $N_d(2)$ are determined in a manner similar to that done in the SEL. If the fixed throttle mode is not indicated, the data set up for entry into the CTEL is done. Here the T_{dx} of the two engines is the desired thrust, T_d, which comes from the maneuver logic. The data set up for engine A is the appropriate data from the arrays for engine 1. The data set up for engine B is the appropriate data from the arrays for engine 2. The thrust fractions K_A and K_B are determined by the constant $k_{(2)121}$ (see list of symbols for meaning of numerical subscripts). Note that the sum of K_A and K_B is numerically 1. The output of the CTEL is the desired throttle settings N_{dA} and N_{dB}. Note that except for the fixed throttle mode, the 2EL is predominantly the CTEL.

e. Common Two-Engine Logic (CTEL)

The CTEL determines the desired throttle settings N_{dA} and N_{dB} for two "variable throttle" engines, A and B, which can have any possible failure mode (i.e., A and B failed, only A failed, only B failed, no failures). The set of variables required for the CTEL is much the same as that required for the CEL except that engine A is distinguished from B by a suffix in the variable name. The variables required for the CTEL are:

T_{dx}	=	total thrust required of the two engines
ICA, ICB	=	failure indicators for engines A and B
K_A, K_B	=	fractions of T_{dx} for each engines A and B
IRA, IRB	=	reverse capability indicators for engines A and B

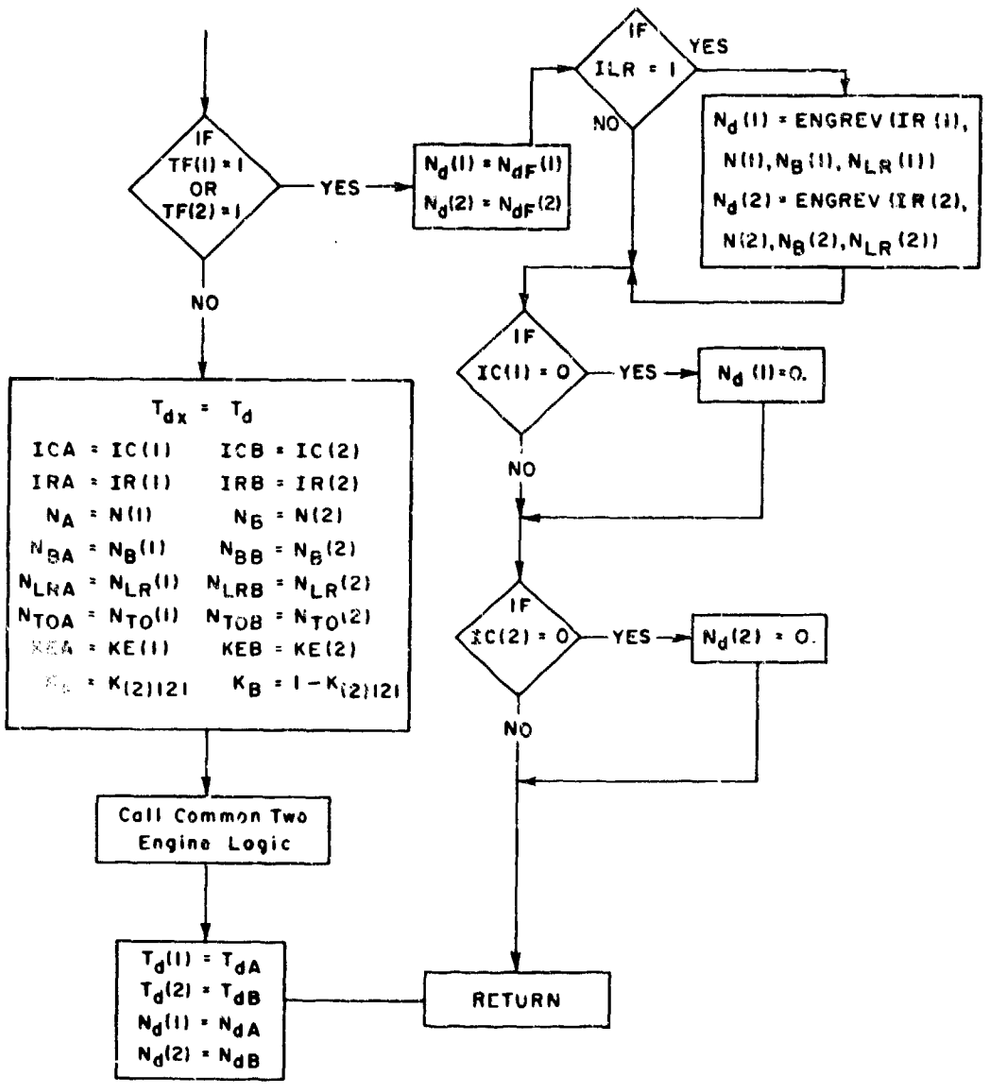

Figure 48. Two-Engine Logic

N_A, N_B = actual throttle setting for engines A and B

N_{BA}, N_{BB} = throttle settings above which reverse should not be actuated for engines A and B.

N_{LRA}, N_{LRB} = throttle settings for landing reverse of engines A and B

N_{TOA}, N_{TOB} = takeoff throttle settings for engines A and B

KEA, KEB = kill engine indicator for engines A and B

Figure 49 is a flow diagram of the CTEL.

First a check is made to see if both engines have failed (i.e., ICA = 0 and ICB = 0). If both have failed, both N_{dA} and N_{dB} are set to zero (this is used for engine failure in the thrust table look-up which is stored under the N = 0. data - see Section VI). If both engines have not failed, a failure check of engine A is done. If engine A has failed, N_{dA} is set to zero and the thrust table lookup is entered at N = 0 to determine the desired thrust, T_{dA}, of engine A (in this case T_{dA} is actually the failure thrust). The required thrust of engine B, T_{dB}, is found by subtracting T_{dA} from T_{dx} (engine B carries the full thrust load). The input variables for the CEL (IRC, N_c . . . etc.) are set up using the data for engine B after, which the CEL is entered. The output throttle setting of the CEL, N_{dC}, becomes the desired throttle setting, N_{dB}, of engine B. If engine A has not failed, a failure check on engine B is done. If engine B has failed, engine A is assumed to carry the full thrust load. The determination of N_{dA} when engine B has failed is similar to the previous case where N_{dB} was determined when engine A failed. If engine B has not failed, this indicates that both engines are working. In this case, the thrust fraction K_A and K_B determine what portion of T_{dx} each engine carries. The CEL, with appropriate engine input data, is used to determine the desired throttle settings N_{dA} and N_{dB} of each engine.

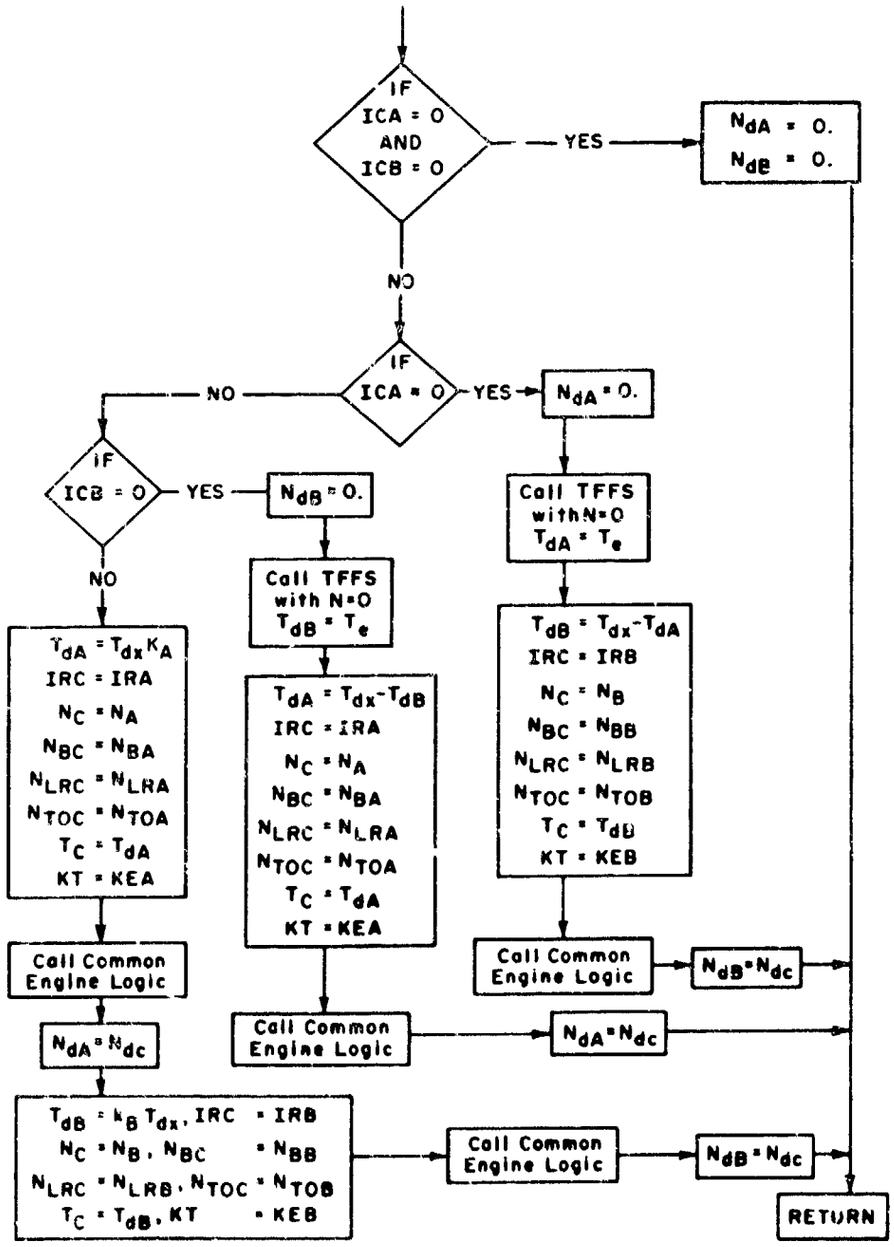

Figure 49. Common Two-Engine Logic

f. Three-Engine Logic (3EL)

The three-engine logic determines the desired throttle settings $N_d(1)$, $N_d(2)$ and $N_d(3)$ for a three-engine aircraft. Three-throttle fix modes and all possible failure modes are provided. Figure 50 is a flow diagram of the fixed-throttle mode section of the 3EL.

The first fixed-throttle mode allowed, that is checked, is the mode where all engines are fixed TF(1) = 1 and TF(2) = 1 and TF(3) = 1. Here the desired throttle settings are arrived at in a fashion similar to that done in the SEL and the 2EL. If this fixed-throttle mode is not indicated (note all this takes is for one of the three TF indicators not to be equal to 1), the next allowed fixed-throttle mode is checked. This mode is one where the outboard engines (engines 1 and 3) are assumed fixed, and the center engine (engine 2) is assumed variable. Both of the two fixed engines are allowed to fail. The thrust table look-up is then called to evaluate the desired thrusts of engines 1 and 3, be they failed or not. Failure of the variable engine (engine 2) is also allowed. If engine 2 is not failed, it is assumed to take the remaining thrust load required to meet the T_d requirement of the maneuver logic. Data set up for the CEL is made using array data for engine 2. Entry is made to the CEL and $N_d(2)$ is determined. The final fixed throttle mode allowed is where the center engine (engine 2) is fixed and the two outboard engines (1 and 3) are assumed variable. Again, engine 2 is allowed to fail and the thrust table look-up is called to get the desired thrust of engine 2, $T_d(2)$, be the engine failed or not. Data set up is then made to enter the CTEL, where $T_{dx} = T_d - T_d(2)$. Engine 1 data is assigned to engine A and engine 3 data is assigned to engine B. The thrust fractions k_A and k_B are determined by the constant $k_{(3)131}$. Note again that K_A plus K_B is numerically 1. The CTEL is entered and the desired throttle settings $N_d(1)$ and $N_d(3)$ are determined. If none of the three fixed throttle modes is indicated, all engines are assumed variable throttle. For this section of the 3EL, the flow diagram is given in Figure 51.

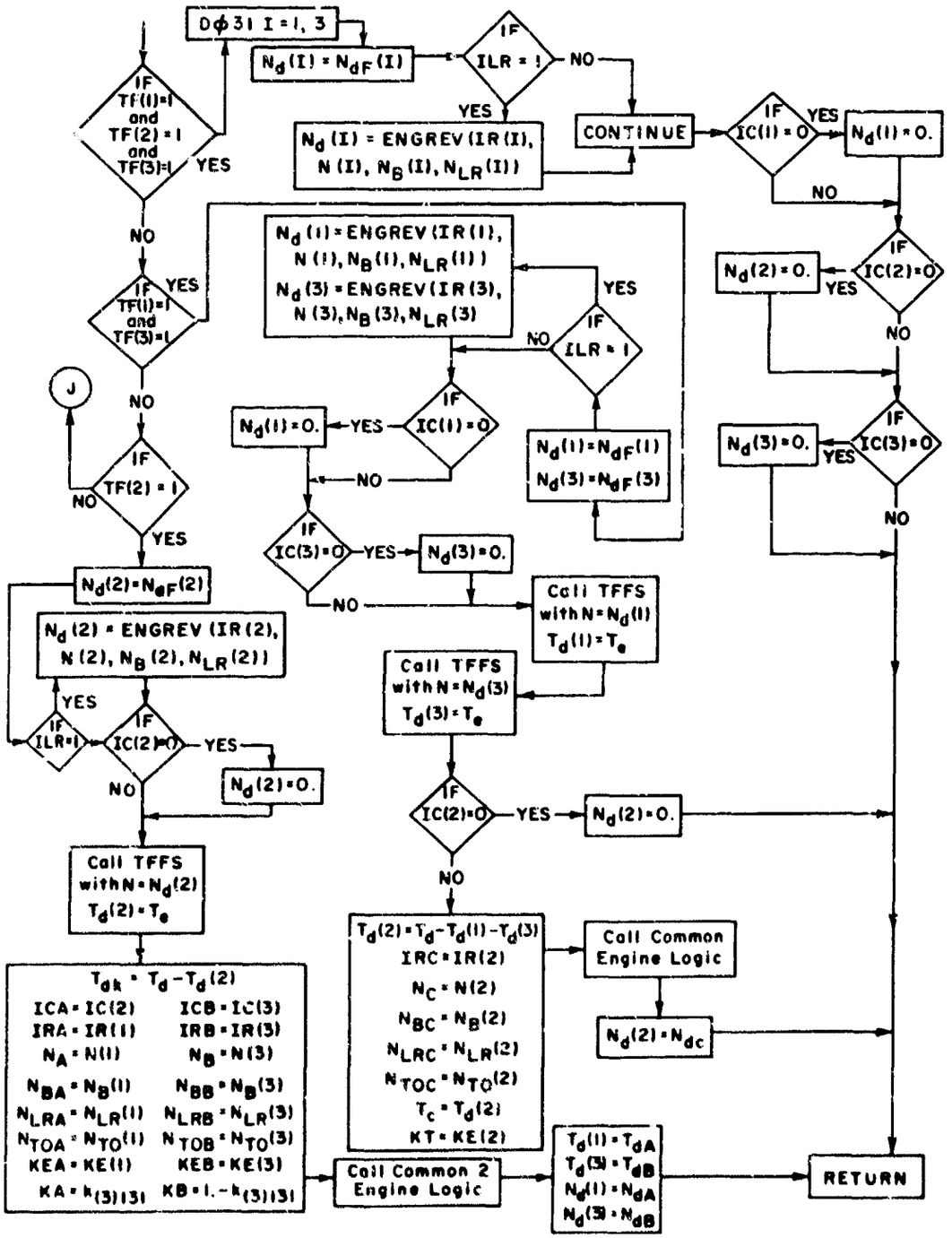

Figure 50. Fixed Three-Engine Logic

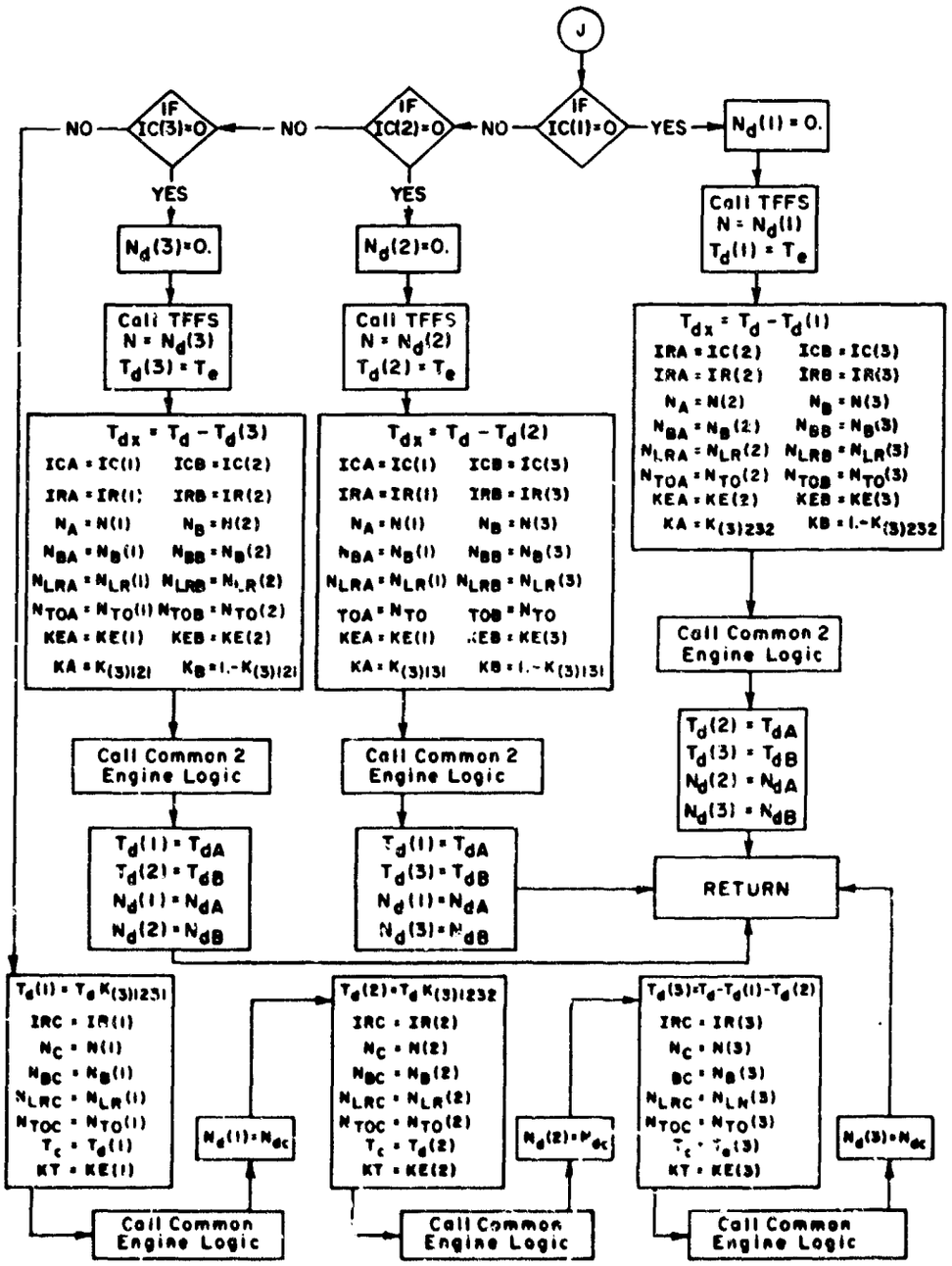

Figure 51. Three-Engine Logic

This section of the 3EL allows for all possible failure combinations of the three engines. The logic is as follows: if engine 1 has failed, call the CTEL for engines 2 and 3; if engine 2 has failed, call the CTEL for engines 1 and 3; if engine 3 has failed, call the CTEL for engines 1 and 2. CTEL, in turn, checks for failure in the remaining two engines. Note that in any engine failure combination, the required thrust load is carried by the remaining working engines. If no engines have failed, the CEL is called for each of the three engines separately.

g. Four-Engine Logic (4EL)

The four-engine logic determines the desired throttle settings $N_d(1)$, $N_d(2)$, $N_d(3)$ and $N_d(4)$ for a four-engine aircraft. Three throttle fix modes and all possible symmetric failure modes are provided (failure of engines 1 and 2 is similar to failure of engines 3 and 4, etc., and therefore only one mode is simulated). Figure 52 is a flow diagram of the fixed-throttle mode section of the 4EL.

The first fixed throttle mode is for all four engines fixed. The logic here is much the same as was done in the 2EL and the 3EL. The second fixed-throttle mode is for the two inboard engines (i.e, engines 2 and 3) fixed and the outboard engines (1 and 4) variable. The desired throttle settings, $N_d(1)$ and $N_d(4)$, for the two variable engines are obtained by calling the CTEL for engines 1 and 4. The third and last fixed-throttle mode is for the two outboard engines fixed and the two inboard engines variable. The logic is similar to the previous case. If none of the three fixed-throttle modes is indicated, all four engines are assumed variable. Figure 53 is a flow diagram of this section of the 4EL.

The symmetric failure modes allowed are as follows: four-engine-failure, 1-2-3-4; three-engine-failure, 1-2-3 and 1-2-4; two-engine failure 1-2, 1-3, 1-4, and 2-3; and single-engine failure 1 and 2.

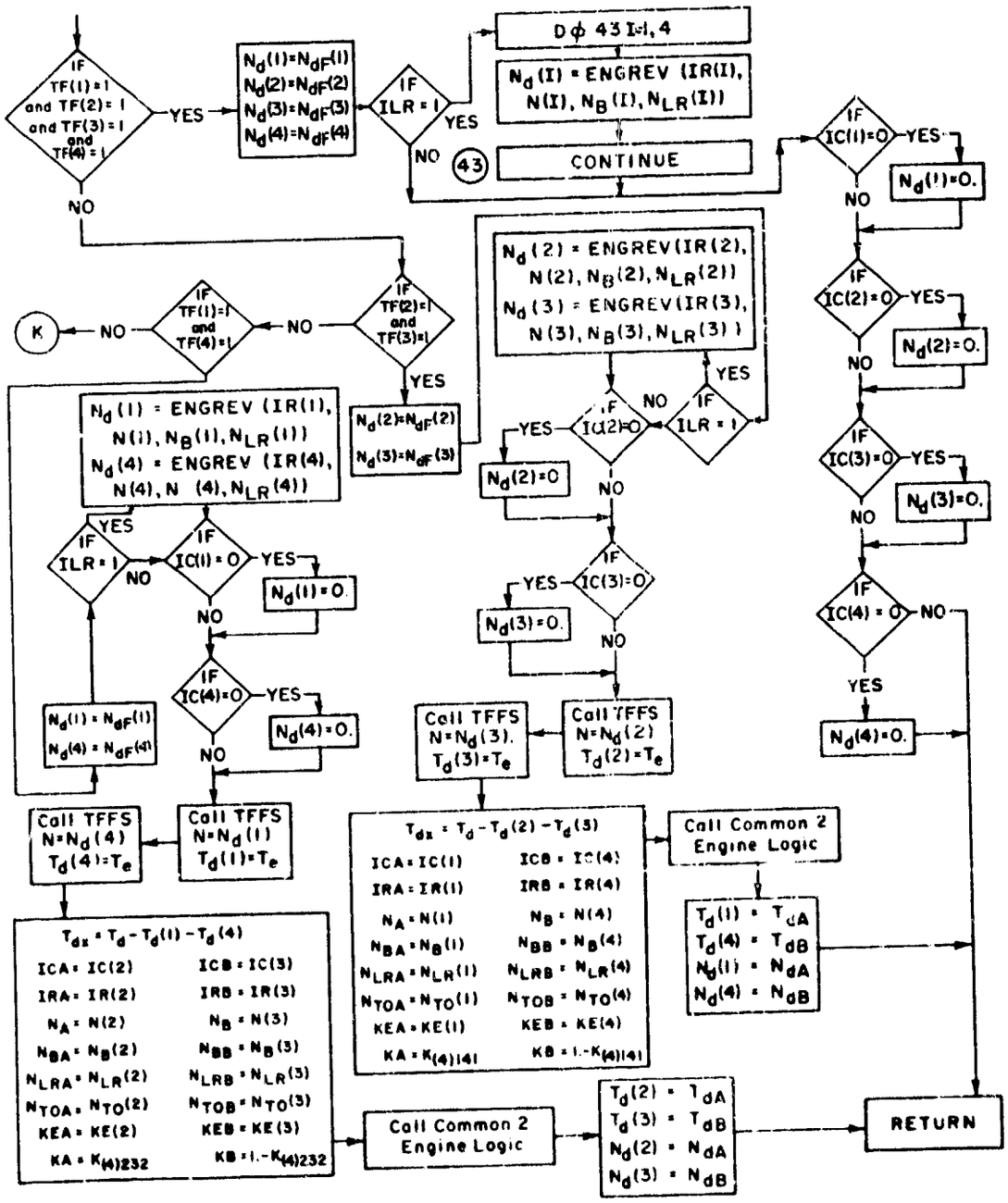

Figure 52. Fixed Four-Engine Logic

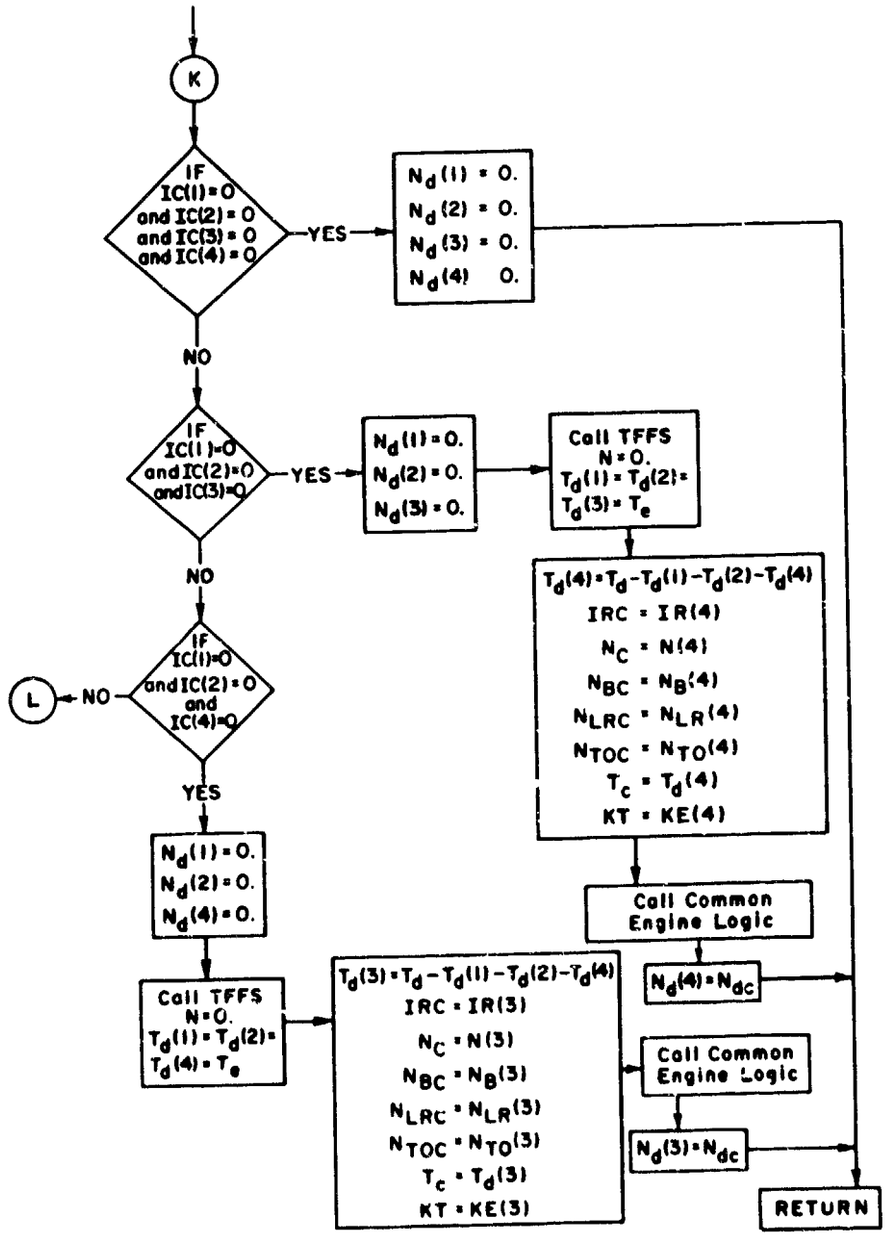

Figure 53. Four-Engine Logic

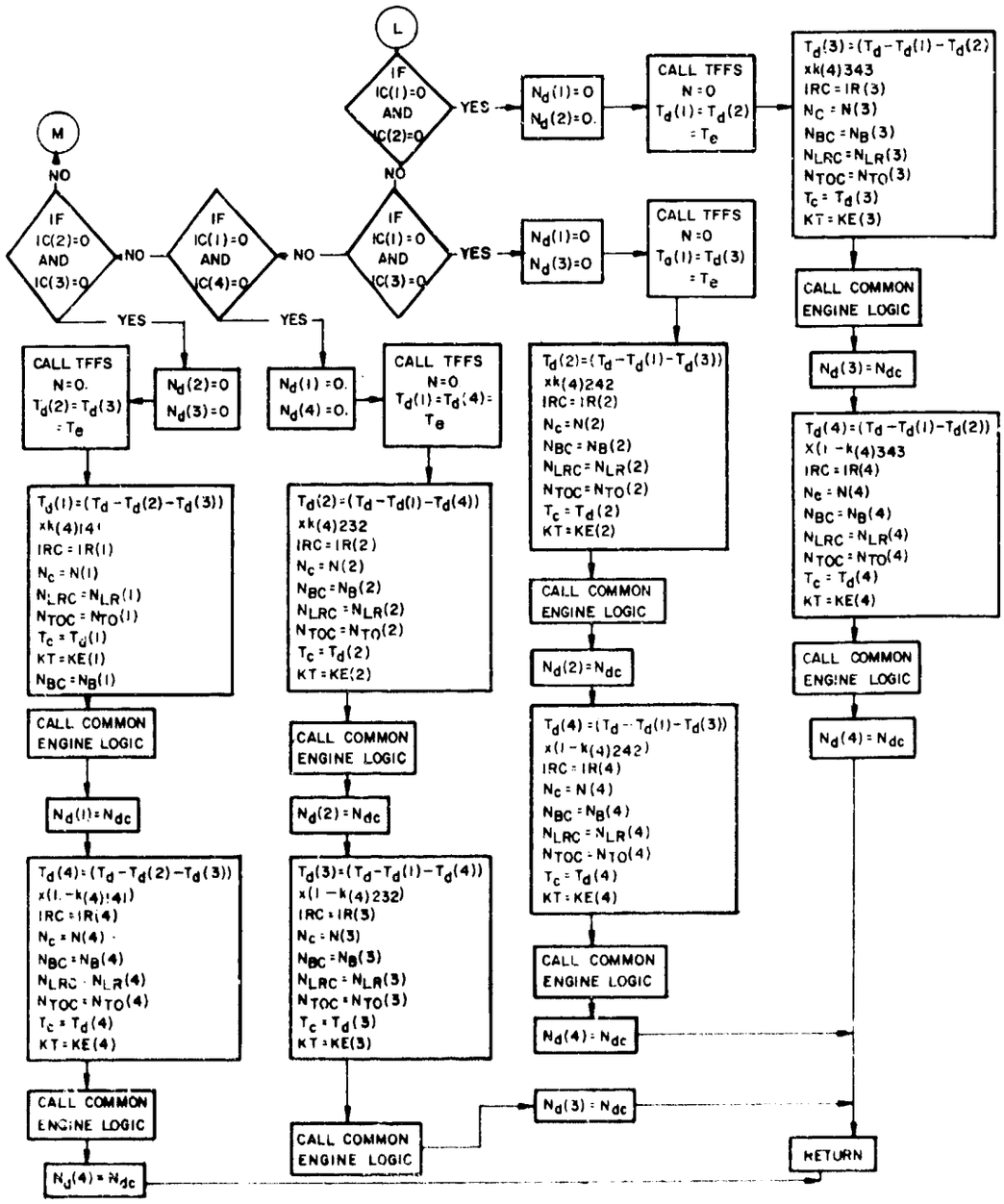

Figure 53. Four Engine Logic (Cont)

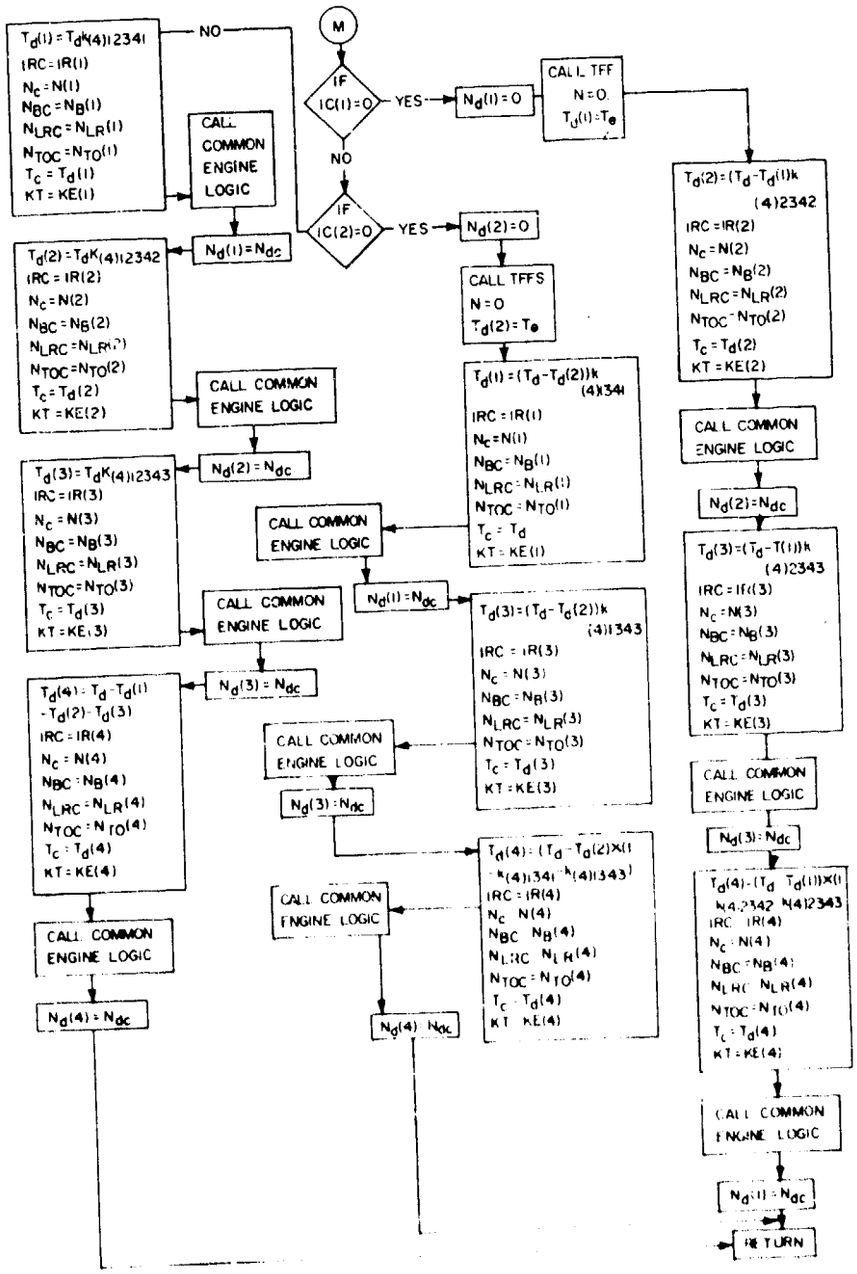

Figure 53. Four Engine Logic (Concluded)

The four-engine failure mode is checked first. This is followed by a check on the three-engine failure mode 1-2-3. In this mode engine 4 is assumed to carry the thrust load. If the three-engine failure mode 1-2-3 is not indicated, a check is made on the last three engine failure mode 1-2-4, where engine 3 is assumed to carry the thrust load. If failure mode 1-2-4 is not indicated, the two-engine failure mode 1-2 is checked, where engines 3 and 4 carry the thrust load. This is followed by successive checks of the remaining two-engine failure modes 1-3, 1-4, and 2-3. In each case, the remaining engines carry the required thrust load. If none of the two-engine failure modes are indicated, the two single-engine failure modes (engine 1 and/or engine 2) are checked. If a single-engine failure mode is indicated, the remaining three engines carry the thrust load. If no single-engine failures are indicated, all engines are working, and the desired throttle setting of each engine is obtained by calling the CEL for each of the four engines. This completes the 4EL and the throttle autopilot discussion.

5. BRAKING AUTOPILOT

The function of the braking autopilot is to control the braking moments applied to each landing gear on the aircraft. The braking autopilot provides the following four options for each landing gear:

(1) No braking (i.e., braking moment zero)

(2) Constant braking moment (comparable to constant braking pressure)

(3) Locked wheel (i.e., wheel angular velocity zero)

(4) Controlled braking

The wheel equation of motion is documented in Appendix II. This equation, Equation 23C is repeated here for convenience.

$$M_{Ai} - M_{Bi} \frac{\omega_{Ti}}{|\omega_{Ti}|} = n_i \Sigma_i \dot{\omega}_{Ti} \qquad (307)$$

where

M_{Ai} = ground reaction moment along axle of ith gear

M_{Bi} = braking moment applied along axle of ith gear (only + values allowed)

W_{Ti} = wheel rotational velocity on i^{th} gear

n_i = number of tires on i^{th} gear axle

I_i = moment of inertia of a tire wheel, and anything else constrained to rotate with that tire about the ith gear axle.

$\dot{W}_{Ti}$ = wheel angular acceleration on i^{th} gear axle

The function of the braking autopilot, therefore, becomes one of specifying the value of M_{Bi} in Equation 307. Figure 54 is a flow diagram of the braking autopilot logic.

The braking autopilot logic is contained in a "do loop," which is repeated I times. The indicator, I, is the number of gears on the aircraft. When the "do loop" is finished, the M_{Bi} array contains the braking moment for each gear. The first check inside the do loop is on the value of the brake actuate indicator, IBS. IBS is normally input at some other value that 1 so that M_{Bi} remains at the initial values read into the program (the initial values of M_{Bi} are usually zero). The braking signal (IBS = 1) is given in the landing rollout phase of the maneuver logic (see Figure 36). When the brake signal is given, the brake condition indicator, I_{Bi} (see Figure 40) is examined to determine which of the four brake options is to be applied. If the value of I_{Bi} is 0, brake option 1 is exercised and M_{Bi} is set to 0. If I_{Bi} has the value 2, brake option 2 is exercised and M_{Bi} is set to the constant value M_{BCi}, which is read in on input. If the value of I_{Bi} is -1, brake option 3 is exercised and W_{Ti} is made 0 to simulate brake locking. If the value of I_{Bi} is 1, controlled braking option 4 is exercised.

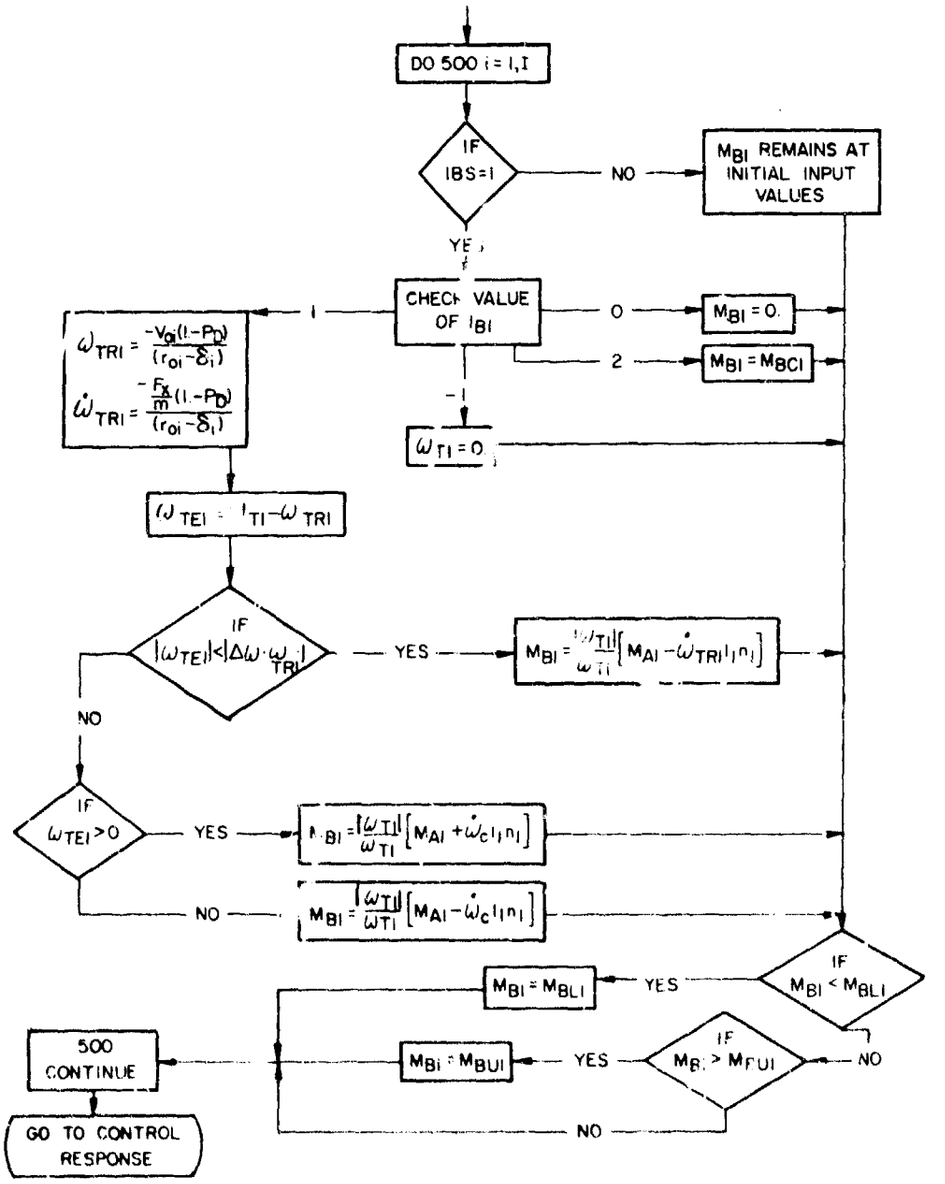

Figure 54. Brake Autopilot

Controlled braking option 4 controls the wheel angular speed, ω_{Ti}, to that value which results in a particular desired value of "percent skid," P_p. Since the coefficient of friction between the tire and runway is predominantly a function of "percent skid," controlling "percent skid" actually controls the braking forces applied to the aircraft. "Percent skid" is defined as follows:

$$P_{si} = \left|\frac{V_{Ti}}{V_{ai}}\right| \tag{308}$$

where

P_{si} = percent skid of ith wheel

V_{Ti} = tire footprint velocity of ith wheel

V_{ai} = axle velocity of ith wheel

The tire footprint velocity can be written as:

$$V_{Ti} = V_{ai} + \omega_{Ti}(r_{oi} - \delta_i) \tag{309}$$

where

r_{oi} = undeflected radius of tire

δ_i = tire deflection

Equation 308 can therefore be written as

$$P_{si} = \frac{\left|V_{ai} + \omega_{Ti}(r_{oi} - \delta_i)\right|}{\left|V_{ai}\right|} \tag{310}$$

Note that when ω_{Ti} is 0 (full skid), the value of P_{si} is 1; and when the tire is fully rolling ($V_{Ti} = 0$), the value of P_{si} is zero.

Let ω_{TRi} be the required value of ω_{Ti} that results in the desired percent skid P_D. Since V_{ai} is always positive, Equation 310 yields

$$\omega_{TRi} = -V_{ai} \frac{(1-P_D)}{(r_{oi} - \delta_i)} \tag{311}$$

where

$$V_{ai} = \sqrt{(R_{G11} R_{DXGk} + R_{G13} R_{DZGk})^2 + R_{DYGk}^2} \tag{312}$$

Assuming the tire deflection reaches a nominal value, the value of ω_{TRi} reduces because the axle speed V_{ai} reduces during the landing roll. The rate at which ω_{TRi} should reduce to maintain P_D is therefore

$$\dot{\omega}_{TRi} = -\dot{u} \frac{(1-P_D)}{(r_{oi} - \delta_i)} \tag{313}$$

The variable $\dot{u}$ is the body longitudinal acceleration and is approximately Fx/m (see Appendix I) where

F_x = sum of forces acting in x direction

m = aircraft mass

(Note that F_x includes not only ground forces, but also forces of drag, reverse thrust, drag chutes, etc. Equation 313, therefore, becomes

$$\dot{\omega}_{TRi} = -\frac{F_x}{m} \frac{(1-P_D)}{(r_{oi} - \delta_i)} \tag{314}$$

(See Figure 54 and the option 4 branch).

First the desired value of wheel angular speed, ω_{TRi}, is calculated using Equation 311. The required rate of change of ω_{TRi}, $\dot{\omega}_{TRi}$, is also calculated using Equation 314. This is followed by a calculation of the error, ω_{TEi}, in wheel angular speed. If the error, ω_{TEi}, is less than a certain fraction ($\Delta\omega$ is the allowed fractional error in ω_{TRi}) of ω_{TRi}, then the braking moment, M_{Bi}, should be such that the wheel angular acceleration $\dot{\omega}_{TRi}$ is maintained (this helps to avoid further error development). The required value of M_{Bi} is obtained by rearranging Equation 307 and substituting $\dot{\omega}_{TRi}$ for $\dot{\omega}_{Ti}$.

$$M_{Bi} = \frac{|\omega_{Ti}|}{\omega_{Ti}}\left[M_{Ai} - \dot{\omega}_{TRi} I_i n_i\right] \tag{315}$$

If the allowed error is exceeded and the error is positive, this means the value of ω_{Ti} needs to be more negative (i.e., more rolling and less braking). This requires a negative $\dot{\omega}_{Ti}$. The absolute magnitude of this control acceleration is picked a constant value $\dot{\omega}_c$ (chosen at data input). The required braking moment in this case is found by substituting $-\dot{\omega}_c$ into Equation 307 for $\dot{\omega}_{Ti}$ and solving for the required braking moment. Note in this case

$$M_{Bi} = \frac{|\omega_{Ti}|}{\omega_{Ti}}\left[M_{Ai} + \dot{\omega}_c I_i n_i\right] \tag{316}$$

M_{Bi} will be less than $|M_{Ai}|$. If the allowed error is exceeded and the error is negative, this means the value of ω_{Ti} needs to be less negative (i.e., more braking). This requires a positive $\dot{\omega}_{Ti}$ and, as previously, will have a control magnitude of $\dot{\omega}_c$. Substituting $+\dot{\omega}_c$ into Equation 307 for $\dot{\omega}_{Ti}$ yields the required braking moment.

$$M_{Bi} = \frac{|\omega_{Ti}|}{\omega_{Ti}}\left[M_{Ai} - \dot{\omega}_c I_i n_i\right] \tag{317}$$

Note in this case M_{Bi} will exceed $|M_{Ai}|$. Finally, the requested value of M_{Bi} is checked against the braking moment limits M_{BLi} (lower limit - not less than zero) and M_{BUi} (upper limit). This completes the braking autopilot discussion.

SECTION IV

CONTROL VARIABLE RESPONSE

The main aircraft control variables (i.e., elevator deflection, rudder deflection, aileron deflection, and engine throttle) do not in reality respond instantaneously to the desired values requested by the autopilots. To get a first order approximation of the effects of control surface and engine lags on landing performance, a "constant rate" control variable response is built into the autopilot simulation. Figure 55 is a flow chart of the control variable response logic. This logic allows the control variables to move at a fixed rate (rate depends on initial data input) toward the desired values requested by the autopilots. No overshoot is allowed; that is, as the actual value of the control variable approaches the desired value, the response logic locks the actual value to the desired value until a situation arises where the rate of change of the desired value exceeds the rate at which the control variable can respond. In this way, the first order effects of control variable lags are simulated. Note that a system with essentially instantaneous response can be built by input of large numbers for the control variable rates.

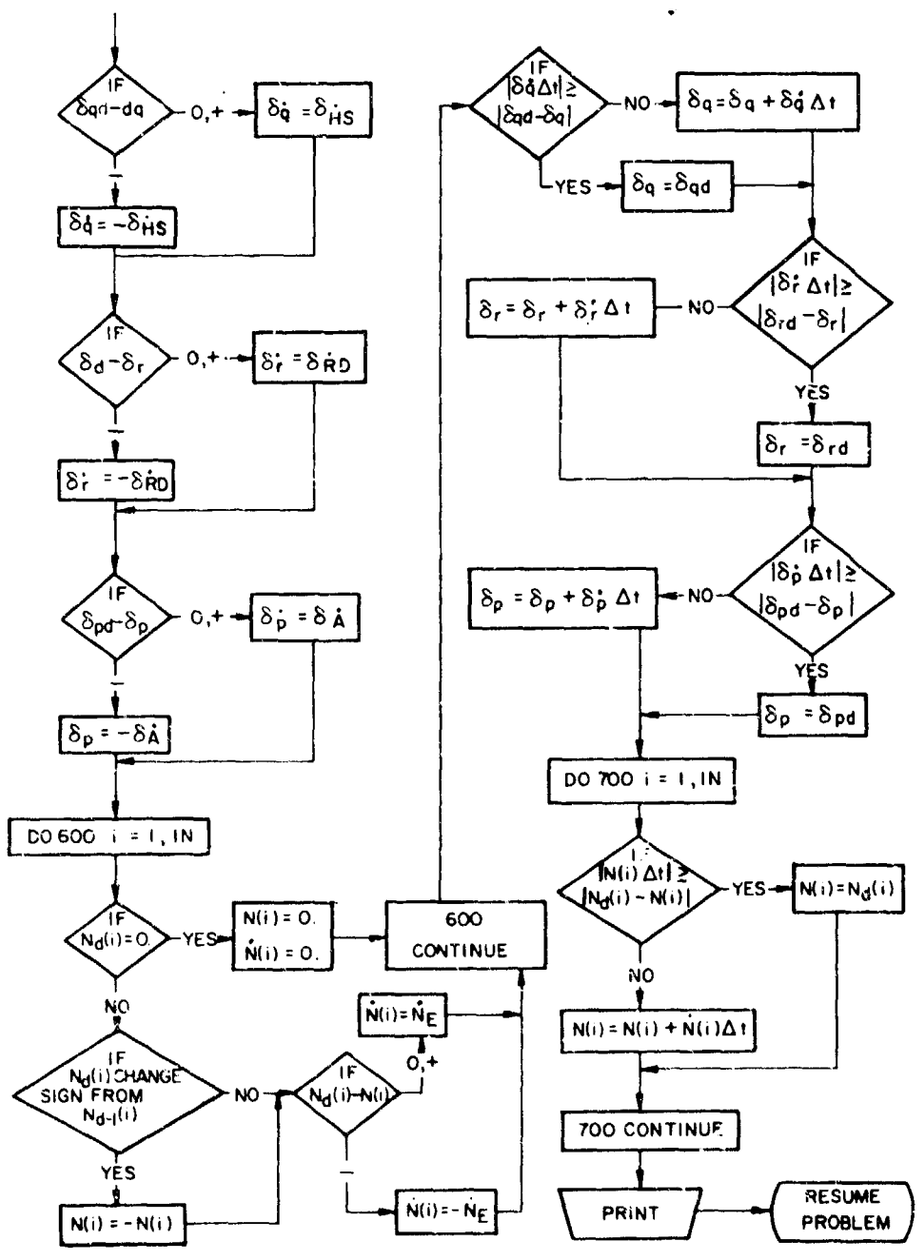

Figure 55. Control Response

SECTION V

SDF-2 CHANGES

1. MULTIPLE ENGINE CHANGES

This section was written in Appendix I. It is repeated here for emphasis.

As originally designed, SDF-2 only allowed for the simulation of one airbreathing engine. The thrust table look-up routine, TFFS, also included the effects of altitude on thrust and determined the fuel rate, both of which are no longer needed (see Assumption in Section I). Some provision must also be made to determine thrust for engine reversing, thrust for engine failure, and the net thrust forces and moments acting on the multiple engine aircraft. We begin by discussing the thrust table lookup.

The thrust table is now a function of throttle setting and Mach number alone. Because of the throttle autopilot logic, the ranges for the throttle setting, N, must be as follows:

N = -2. means full reverse

N = -1. means idle reverse

N = 0. means engine failure

N = +1. means idle forward

N = +2. means full forward

Negative values of thrust are stored for the negative throttle settings. In this manner reverse thrust is simulated. The zero value of N is used for the data simulating engine failure (note that failure thrust may be zero or some negative value, depending on Mach number). The actual reversing is achieved in the throttle autopilot by requesting a negative

value of desired throttle setting, N_{di}. The change of sign on N_{di} is sensed in the control response (see Figure 55) and this changes the sign of the actual N_i used in the thrust table.

Every time thrust is needed by the main program, the thrust table is entered IN times - once for each engine - and the actual thrust array T(IN) is obtained depending on the values in the actual throttle setting array N (IN). The engine thrust vector is assumed parallel to the longitudinal body axis (this is also assumed in the autopilot equations) and therefore causes no roll moments. The engine position arrays, z_N (IN) and y_N (IN), along with the actual thrust array T (IN) determine the engine pitch moment array M_T(IN) and the engine yaw moment array N_T(IN). These arrays are then used to obtain the net longitudinal thrust, T_x, (note T_y and T_z are zero by assumption) the net engine pitch moment, M_T, and the net engine yaw moment, N_T. The net value T_x, M_T, and N_T are then used in SDF-2 and the calculation proceeds as normal.

2. AUXILIARY COMPUTATION

Several state variables used by the autopilot must be defined in terms of the state variables existing in SDF-2. The variables that need to be defined are as follows: x_R, y_R, z_R, $\dot{x}_R$, $\dot{y}_R$, $\dot{z}_R$, h_R, $\dot{h}_R$, ψ_P, and ϕ_P. Their definition in terms of SDF-2 variables is as follows:

$$\begin{bmatrix} x_R \\ y_R \\ z_R \end{bmatrix} = \begin{bmatrix} R_{G11} & 0 & R_{G13} \\ 0 & 1 & 0 \\ R_{G31} & 0 & R_{G33} \end{bmatrix} \begin{bmatrix} X_g - R_{gR} \\ Y_g \\ Z_g \end{bmatrix} \tag{318}$$

$$\begin{bmatrix} \dot{x}_R \\ \dot{y}_R \\ \dot{z}_R \end{bmatrix} = \begin{bmatrix} R_{G11} & 0 & R_{G13} \\ 0 & 1 & 0 \\ R_{G31} & 0 & R_{G33} \end{bmatrix} \begin{bmatrix} \dot{X}_g \\ \dot{Y}_g \\ \dot{Z}_g \end{bmatrix} \tag{319}$$

$$h_R = -z_R \tag{320}$$

$$\dot{h}_R = -\dot{z}_R \tag{321}$$

$$\dot{\psi}_p = \frac{1}{\sqrt{1-\ell_2^2}}\,\dot{\ell}_2 \tag{322}$$

$$\dot{\phi}_p = \frac{1}{1+\left(\frac{n_2}{m_2}\right)^2}\left(\frac{n_2}{m_2^2}\,\dot{m}_2 - \frac{\dot{n}_2}{m_2}\right) \tag{323}$$

The variables x_R, $\dot{x}_R$, h_R, and $\dot{h}_R$ are used in the flare maneuver logic (see Section II). The RG matrix (see Equation 111 of Appendix II) is a transformation from the earth coordinate system to the elevated runway coordinate system. The Euler angular rates $\dot{\psi}_p$ and $\dot{\phi}_p$ are used for the yaw and roll autopilots, respectively. They are developed for a pitch-yaw-roll sequence in terms of the direction cosines and direction cosine rates which are available in SDF-2.

SECTION VI

PROBLEM ORGANIZATION

Figure 1 shows the basic autopilot interface with SDF-2. The detailed autopilot interface and the logic organization is shown in Figure 56. A comparison of Figures 26 and 56 shows that the autopilot begins with the auxiliary computation and ends with the control variable response. Several changes were also required internal to SDF-2.

This concludes the formulation of the equations and logic for the autopilot modification to SDF-2.

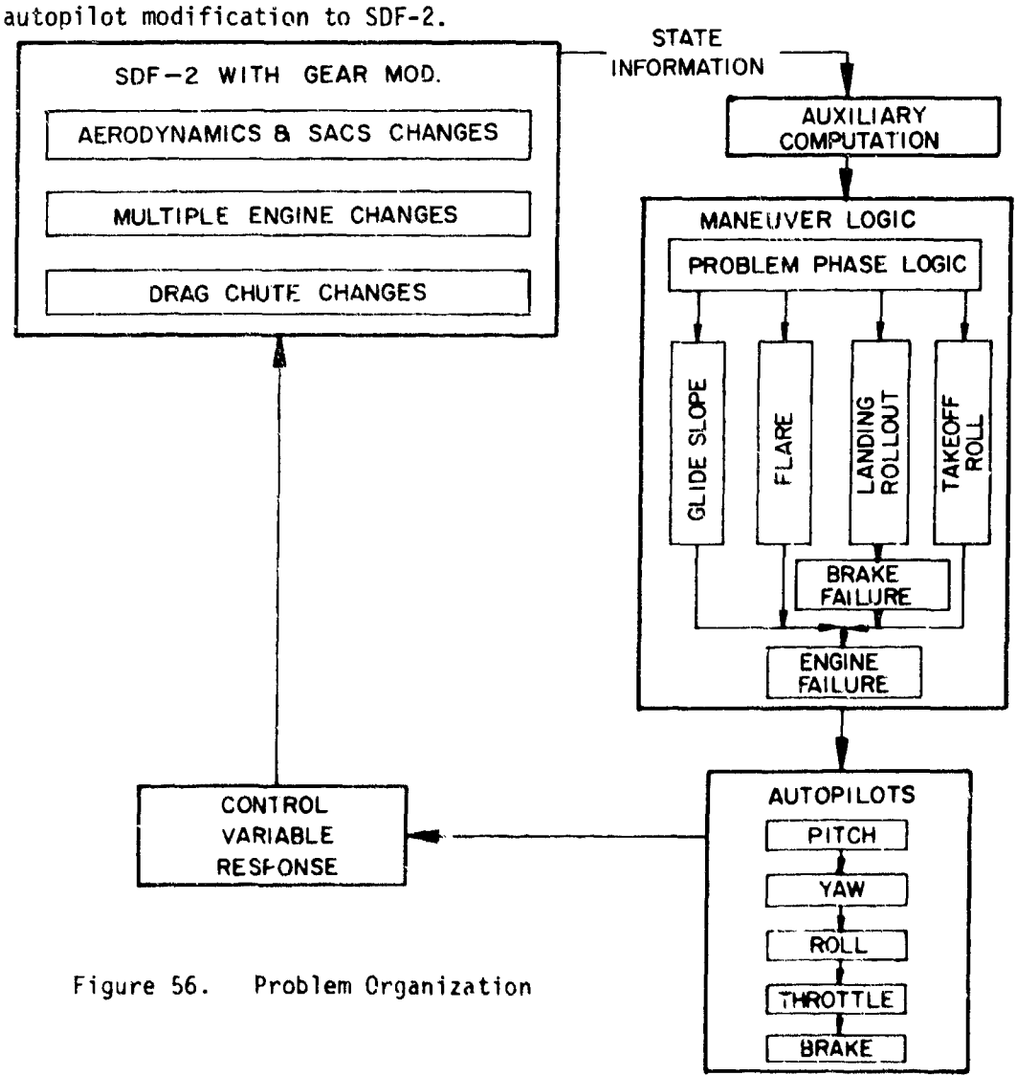

Figure 56. Problem Organization

REFERENCES

1. Brown, Robert C., Brulle, Robert V., Combs, A. E., and Griffin, Gerald D., FDL-TDR-64-1, Part I, Vol 1, "Six-Degree-of-Freedom Flight-Path Study Generalized Computer Program, Problem Formulation," October 1964.

2. Vorwald, R. F., FDL-TDR-64-1, Part II, Vol 1, Six-Degree-of-Freedom Flight Path Study Generalized Computer Program, User's Manual For, Part I, Volume 1, October 1964.

3. Urban H. D. Lynch, Capt, USAF, FDMG TM 68-5, "Derivation of the Equations of Motion for the Landing Gear and Ground Reaction Modification to SDF-2, April 1968.

4. Urban H. D. Lynch, Capt, USAF, FDMC TM 68-11, Autopilot Equations and Logic for the Takeoff and Landing Analysis Modification to SDF-2, October 1968.

5. Urban H. D. Lynch, Capt, USAF, FDMG TM 68-12, Users Manual for the Takeoff and Landing Analysis Computer Program, March 1969.

6. Urban H. D. Lynch, Capt, USAF, AFFDL-TR-68-111, Newtonian Equations of Motion for a Series of Non-Rigid Bodies, September 1968.

7. C. D. Perkins, and R. E. Hage, Airplane Performance Stability and Control, John Wiley & Sons, Inc., New York, 1949, Chapters 10 and 11.

8. BuAer Report AE-61-4, Fundamentals of Design of Piloted Aircraft Flight Control Systems, Vol. II, "Dynamics of the Airframe," February 1953.

9. G. W. Hausner, and D. E. Hudson, Applied Mechanics Dynamics, D. Van Nostrand Company, Inc., New York, 1950.

10. R. A. Becker, Introduction to Theoretical Mechanics, McGraw-Hill Book Co., Inc., New York, 1954.

11. A. G. Webster, The Dynamics of Particles and of Rigid, Elastic, and Fluid Bodies, Hafner Publishing Company, Inc., New York, 1949.

12. J. C. Slater and N. H. Frank, Mechanics, McGraw-Hill Book Co., Inc., 1947.

13. F. B. Seely, and N. E. Ensign, Analytical Mechanics for Engineers, John Wiley & Sons, Inc., New York, 1941, p. 391.

14. Leigh Page, Introduction to Theoretical Physics, D. Van Nostrand Co., Inc., New York.

REFERENCES (Contd)

15. Brian F. Doolin, N. A. C. A. TN 3968, The Application of Matrix Methods to Coordinate Transformation Occurring in Systems Involving Large Motions of Aircraft, May 1957.

16. K. S. W. Champion, R. A. Minzner, and H. T. Pond, AFCRC-TR-59-267, The ARDC Model Atmosphere, 1959, August 1959.

17. R. A. Minzner, and W. S. Ripley, ARCRS-TN-56-204, The ARDC Model Atmosphere, December 1956.

18. Handbook of Geophysics for Air Force Designers, U. S. Air Force Cambridge Research Center, Geophysics Research Directorate, Cambridge, Massachusetts, 1957.

19. Bernard Etkin, Dynamics of Flight/Stability and Control, John Wiley & Sons, Inc. New York, 1959.

20. ASD TDR 62-555, A Rational Method for Predicting Alighting Gear Dynamic Loads, Volume I, "General Methods," December 1963.

21. ESD TDR 64-392, ATC Computational Aid Facility Predicted Paths, May 1964.

22. NA-68-25, Development and Application of a Terminal Spacing Systems, August 1968.

23. NRL-6380, Aircraft Landing Approach Paths with the Rainbow Optical Landing System, June 1966.

24. GCC/EE/65-15, An Investigation of an Automatic Airspeed Control System for the KC-135 Approach and Landing Systems, AFIT Master's Thesis by Eugene Royce Sullivan, June 1965.

25. DDC-TAS-69-54-1, Aircraft Landings, Volume I, "A DDC Bibliography," October 1969.

26. Lockheed Georgia Rpt. LGIUS44-1-7, C-5A Dynamic Landing Analysis, 28 April 1967.